

Ocean Biogeochemistry and the Global Carbon Cycle: An Introduction to the U.S. Joint Global Ocean Flux Study

Ken O. Buesseler

Woods Hole Oceanographic Institution • Woods Hole, Massachusetts USA

In the early 1980s, ocean scientists were increasingly aware of the importance of biologically active elements, such as carbon, nitrogen and oxygen, in the regulation of climate and its effects on the habitability of the planet. As scientists reviewed details of the processes that control ocean carbon cycling and the links among oceanic, atmospheric and sedimentary carbon pools, it was clear that it was “hard to make the numbers add up” (Brewer et al., 1986). Fluxes of carbon into and out of the ocean were only crudely constrained, and little detail existed on the seasonal, regional and global patterns of carbon uptake and export or the flux of carbon between the ocean and its boundaries.

The U.S. Joint Global Ocean Flux Study (JGOFS), a component of the U.S. Global Change Research Program, grew out of the recommendations of a National Academy of Sciences workshop, held in Woods Hole in September 1984. The international program of which it is part was launched three years later under the auspices of the Scientific Committee on Oceanic Research. In 1989, as the first field studies were getting underway, JGOFS became a core project of the International Geosphere-Biosphere Programme.

A major ocean flux program was proposed in the U.S. that would include basin-scale process studies, long-term time-series programs and a global survey of carbon dioxide (CO₂) in the ocean (see *JGOFS Goals* below). Extrapolation of results to the global scale would be assisted by the large-scale data sets emerging from satellite observations. Advances in numerical and ecological modeling and data assimilation would help us predict the global-scale response of oceanic biogeochemical processes to anthropogenic perturbations.


After more than a decade of scientific effort, the success of this study is clearly greater than the sum of its individual parts. With this special issue of *Oceanography*, we hope to highlight a few of the accomplishments of U.S. JGOFS. The authors were asked to bring to The Oceanography Society audience a synthesis of the changing paradigms of ocean biogeochemistry and its contribution to the global carbon cycle.

In this volume, you will see results from the time-series sites near Hawaii and Bermuda, from each of the four major process studies and from the global-scale survey of CO₂, conducted in cooperation with the World Ocean Circulation Experiment. The modeling work discussed in this issue has contributed to advances in our understanding of the controls on upper ocean ecosystems and how these might change with future climate scenarios. An early policy of sharing data and rapid and open distribution via the internet has allowed all scientists access to a consistently high-quality database that will be a long-lasting legacy of U.S. JGOFS.

Advances in methods highlighted in this issue have

led to some key breakthroughs in our ability to understand the dynamics of the dissolved organic carbon pools and particulate fluxes from the upper ocean to the depths. Common protocols and new chemical standards have allowed for accurate comparisons among studies. Within JGOFS and in the future, new technologies will lead to a better understanding of episodic and short-term shifts in ocean biogeochemistry and links among physical forcing, biological responses and chemical fluxes on a range of spatial scales.

As we think about the remaining challenges in ocean biogeochemistry, it is easy to forget how far we have come. After eight years' worth of days at sea, covering almost enough miles to circle the globe 16 times, considerable discussion and hundreds of papers, U.S. JGOFS scientists are confident that we have reduced the uncertainties in our understanding of the global ocean carbon cycle while gaining a new appreciation of the complexity of biogeochemical systems and their variability over time and space. This has been accomplished by many individuals with the help of some true community heroes and with steady support from the National Science Foundation in collaboration with the National Oceanic and Atmospheric Administration, the National Aeronautics and Space Administration, the Department of Energy and the Office of Naval Research. We are pleased to acknowledge the foresight of these agencies in supporting this work.

We appreciate the chance to present U.S. JGOFS through *Oceanography* to our fellow oceanographers and other interested scientists, educators and policymakers. A copy of our new U.S. JGOFS brochure, “A New Wave of Ocean Science,” is included with this issue. Finally, as guest editor, I would like to thank the numerous U.S. JGOFS colleagues who contributed to the scientific insights you are reading about here, the authors of these articles and accompanying highlights, and the staff of the U.S. JGOFS Planning Office in Woods Hole, especially Mardi Bowles and Mary Zawoysky, for shepherding this issue to completion with assistance of the staff of *Oceanography*. 

Reference

Brewer, P.G., K.W. Bruland, R.W. Eppley and J.J. McCarthy, 1986: The Global Ocean Flux Study (GOFS): Status of the U.S. GOFS Program. *EOS*, 67, 44.

JGOFS Goals

- ◆ to determine and understand on a global scale the processes controlling the time-varying fluxes of carbon and associated biogenic elements in the ocean, and to evaluate the related exchanges with the atmosphere, sea floor and continental boundaries;
- ◆ to develop a capacity to predict on a global scale the response of oceanic biogeochemical processes to anthropogenic perturbations, in particular those related to climate change.

Building the Long-term Picture: The U.S. JGOFS Time-series Programs

David M. Karl, John E. Dore and Roger Lukas
University of Hawaii • Honolulu, Hawaii USA

Anthony F. Michaels
University of Southern California • Los Angeles, California USA

Nicholas R. Bates and Anthony Knap
Bermuda Biological Station for Research • Ferry Reach, Bermuda

Introduction

Long-term time-series studies are ideally suited for investigation of the subtle habitat changes, irregularly spaced stochastic events and complex interdependent ecological phenomena that affect biogeochemical cycles in the world ocean. In 1986, during the early planning stages of what would eventually become the U.S. Joint Global Ocean Flux Study (JGOFS), time-series studies were identified as crucial for assessing the baseline or mean states of key parameters in the oceanic carbon cycle and their variability. They were patterned initially after the VERTICAL Transport and EXchange (VERTEX) time-series study then underway in the northeast Pacific Ocean, but the VERTEX field program, which included six cruises and lasted for 18 months, proved to be too short in length and the observations too infrequent to resolve much of the natural variability in open-ocean ecosystems. This discovery presented a scientific and logistical challenge for JGOFS planners.

The process-oriented field studies that took place during JGOFS captured only part of the variability that is characteristic of oceanic biogeochemical processes. They were carried out in specific geographical regions to study important physical-biogeochemical interactions, such as the vernal blooming of the North Atlantic Ocean and the monsoonal forcing of the ecosystems in the surface waters of the Arabian Sea. But capturing the unpredictable, larger-scale and lower-frequency climate variations associated with the El Niño-Southern Oscillation (ENSO), Pacific Decadal Oscillation (PDO) and North Atlantic Oscillation (NAO) was, for the most part, beyond the scope of these process studies. These climate oscillations, which occur irregularly on subseasonal to decadal time scales, may have profound effects on ocean biogeochemistry and on the net balance of carbon between the atmosphere and the ocean. Severe storms, atmospheric deposition, mesoscale features of ocean circulation, volcanic eruptions, extended periods of elevated

precipitation or evaporation, repositioning of large-scale atmospheric circulation features and the warming associated with rising levels of greenhouse gases are among the many ecologically relevant physical forces at work in the coupled ocean-atmosphere system.

Some climatic perturbations lead to increases in turbulent entrainment or upwelling and thus to a redistribution of essential macro- and micronutrients in the upper water column. Increased availability of nutrients leads, in turn, to increases in primary production and, depending on the scale and duration of the disturbance, to changes in populations at higher trophic levels and in the export of dissolved and particulate organic matter. Other perturbations alter near-surface stratification, isolating the upper ocean from the large reservoir of essential nutrients found in the deeper portion of the water column and leading to a variety of ecological consequences. The effects of these processes on ecosystem structure and functioning cannot be observed during any single oceanographic expedition, no matter how well-planned or fortunate. To study these aperiodic events and long-term trends, one must go to sea month after month over many years to observe the natural scales of habitat and ecosystem variability accurately.

Shifting Ecosystem Paradigms: The Marine Microbiological Revolution

When planning for U.S. JGOFS began in the mid 1980s, we thought we had a reasonably comprehensive understanding of the marine carbon cycle. The “Redfield ratio,” which specifies a persistent elemental ratio of carbon to nitrogen to phosphorus in the ocean, was widely accepted (see also Michaels et al., in this issue). Oceanographers had been working with a basic understanding of new versus regenerated organic matter production for two decades (Dugdale and Goering, 1967), and a publication in 1979 (Eppeley and Peterson)

melded new production with the export flux of organic particles in the open ocean. The microbial loop/food-web paradigm was also well established and verified (Pomeroy, 1974; Azam et al., 1983). These concepts guided the design of the JGOFS program.

Our view of plankton dynamics in the sea has changed radically throughout the JGOFS era, however, forcing a reassessment of some of our basic tenets of biological oceanography and marine carbon-cycle research. In the late 1970s, marine scientists discovered the picophytoplankton, tiny floating organisms primarily of the genus *Synechococcus* (Johnson and Sieburth, 1979). Just as the JGOFS field studies were getting underway in 1988, the even more abundant genus *Prochlorococcus* (Chisholm et al., 1988) was discovered. We were faced with the need to accommodate the two most abundant but previously undescribed forms of marine phytoplankton in our ocean carbon-cycle paradigm.

The “marine microbiological revolution” intensified significantly during the 1990s as major technological advances in molecular biology provided new directions for laboratory and field research. In 1992, a new domain of life, the planktonic *Archaea*, was discovered in the ocean (DeLong, 1992). Morphologically similar to *Bacteria*, the *Archaea* are distinctive in their molecular basis for life and, presumably, in their role in the marine carbon cycle. Although they are now recognized as important players in the sea of microbes, little is known about their precise ecological niches.

In 1996, the first full sequencing of the genome of a marine microorganism was completed. With it came the realization that a large percentage of the proteins coded had no readily recognizable function. Researchers hypothesized that this previously undescribed genetic information might be used for survival under variable and sometimes harsh conditions. Recent discoveries of novel biochemical pathways for bacterial photosynthesis (Kolber et al., 2001) and photoheterotrophy (Béjà et al., 2001) in the marine plankton have confirmed the existence of unconventional pathways for carbon and energy flux. There appears to be a large genomic investment in metabolic control and regulation; repressed potential may be unleashed in nature at any time. This new information on the genetic basis for life in the sea has provided exciting clues that help to resolve but also to complicate the carbon-cycle mystery.

Time-series Implementation Strategies

In 1988, two U.S. JGOFS time-series stations were established, one in the North Atlantic near Bermuda (31°45'N, 64°10'W) and the other in the North Pacific near Hawaii (22°45'N, 158°W). The Bermuda Atlantic Time-series (BATS) and the Hawaii Ocean Time-series (HOT) emerged from the planning process to become twin open-ocean programs with similar scientific objectives, research approaches, sampling frequencies, methods of ecosystem interrogation, and nearly identi-

cal suites of core measurements (Figure 1 and Table 1). These core measurements were intended to provide the data sets needed to calibrate, validate and improve biogeochemical models. The proximity of these sites to centers of logistical and intellectual support in Bermuda and Hawaii has been invaluable. Still underway, these programs have yielded data sets that provide a unique and comprehensive picture of oceanic variability and a rich source of testable ecological hypotheses. The BATS and HOT data sets are completely accessible (see sidebars). They and their scientific interpretations (Karl and Michaels, 1996; Siegel et al., 2001) are now part of the U.S. JGOFS legacy.

Ocean time-series observations were not invented by JGOFS. Time-series projects were undertaken in the Baltic and North Seas in the latter portion of the 19th century, and the open-ocean Panulirus Station near Bermuda was initiated in 1954. Until the U.S. JGOFS programs were established, however, there were few multidisciplinary measurement programs focused on the ocean carbon cycle.

Space and time were the primary issues in the initial discussions about establishing time-series sampling programs in JGOFS. Site selection was crucial if the future data sets were to be useful for regional extrapolations or predictions of change. The establishment of JGOFS time-series field studies at sites with previous or ongoing measurement programs at weather ship stations or existing time-series sites had the obvious advantages of an existing archive of data and an historical context. JGOFS planners gained invaluable insights from past and ongoing time-series studies, especially the observations of the seasonal cycle of primary production in the Sargasso Sea made by David Menzel and John Ryther in the late 1950s and the 17-year CLIMAX study conducted in the North Pacific subtropical gyre by John McGowan, Thomas Hayward, Elizabeth Venrick, Richard Eppley and others beginning in the mid-1960s.

Sampling frequency and program duration were also key issues for the planners of the JGOFS time-series programs, who recognized the importance of capturing and interpreting the temporal variability of key biogeochemical processes. Any given time-series data set contains both signal and noise, and signal on one time scale may be noise on another. More frequent data collection and longer time-series records make the separation easier. Monthly shipboard observations over more than a decade have proven effective for documenting subseasonal to interannual variability. But a robust assessment of the decade-scale biogeochemical patterns that are now thought to occur in open ocean ecosystems will probably require a program of at least 30 to 40 years duration and possibly longer.

The JGOFS planners expected the magnitude of variation in carbon stocks and fluxes in response to climate change to be small in comparison with natural variability. The precision and accuracy of measurements, as well as their consistency over time, were cru-

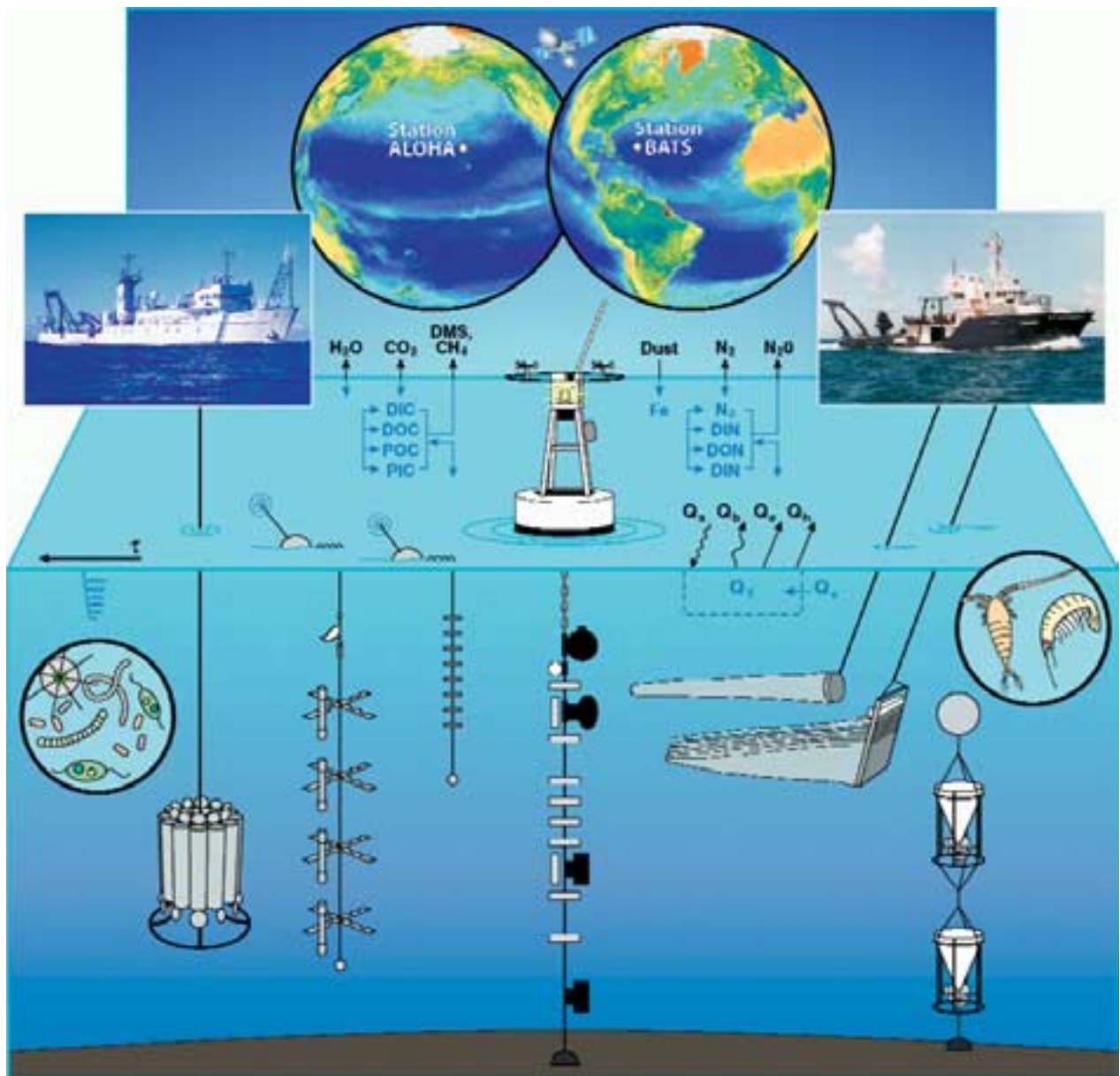


Figure 1. From the macroscope to the microscope, investigations of ocean biogeochemistry at the U.S. JGOFS time-series programs. **(Top)** Satellite view of the global biosphere based on observations from SeaWiFS (September 1997–August 1998), courtesy of NASA Goddard Space Flight Center and the Orbital Sciences Corporation (Gene Feldman, <http://seawifs.gsfc.nasa.gov/SEAWIFS.html>). **(Left-center and right-center)** Research vessels MOANA WAVE and WEATHERBIRD II in the North Pacific and North Atlantic oceans. **(Bottom)** Some of the ship-based and remote-sampling techniques used in BATS and HOT to obtain information on the cycles of carbon and other biogenic elements in the sea. Important components of these cycles, including dissolved and particulate inorganic and organic pools, are shown in center, along with selected air-sea exchanges, including water exchange through evaporation and precipitation and wind forcing. The total heat budget (Q_T) includes the following fluxes: Q_s (solar input), Q_b (long wavelength radiation), Q_c (evaporation), Q_h (conduction) and Q_v (advection). Shown in the enclosed circles are microscopic images of nanoplankton (**left**) and mesozooplankton (**right**).

cial considerations. The comparison and merging of data sets across measurement programs would demand careful, well-structured quality-control and assurance protocols and frequent interlaboratory comparisons (see Dickson and Hansell sidebars, this issue).

The BATS and HOT programs are organized around field expeditions that take place approximately

once a month. Between October 1988, when the field studies began, and the end of December 2000, the two programs have collectively logged approximately 1,300 days at sea and more than 50 person-years of observation and experimentation (Figure 2). Seasonal coverage has been relatively even (Figure 2), a prerequisite for unbiased data and ecological interpretation. At the

Table 1
Common core measurements made at the BATS and HOT open-ocean sites^{1,2,3}

Parameter	Technique/Instrument
<i>Continuous CTD-based Measurements</i>	
Temperature	Thermistor on SeaBird SBE-911 plus
Salinity	Conductivity sensor on SeaBird SBE-911 plus
Depth	Digiquartz pressure sensor on SeaBird SBE-911 plus
Dissolved oxygen	SeaBird Polarographic Oxygen Electrode
Fluorescence	Chelsea Instruments or SeaTech Fluorometer
PAR	Scalar Irradiance Sensor
<i>Discrete Measurements</i>	
Salinity	Conductivity on Guildline Autosol 8400A and IAPSO standard
Oxygen	Winkler Titration, automated photometric (BATS) or potentiometric (HOT) endpoint detection
Total carbon dioxide	Automated coulometric analysis (SOMMA) and A. Dickson standard
Alkalinity	High precision acid titration with potentiometric endpoint detection
Nitrate, Phosphate, Silicate	Technicon Autoanalyzer
Dissolved organic carbon	High-temperature combustion-oxidation
Total dissolved nitrogen	UV oxidation, Autoanalyzer
Particulate carbon	High-temperature combustion, gas analysis
Particulate nitrogen	High-temperature combustion, gas analysis
Particulate biogenic silica	Chemical digestion, colorimetric analysis
Fluorometric chlorophyll a	Acetone extraction, Turner fluorometer
Phytoplankton pigments	HPLC, fluorescence detection
Bacteria	Fluorescence microscopy (BATS) or flow cytometry (HOT)
Zooplankton	Net tows, wet & dry weights, element analysis
<i>Rate Measurements</i>	
Primary production	Trace-metal clean, <i>in situ</i> incubation, ¹⁴ C uptake
Particle fluxes	Free-drifting cylindrical sediment traps (MultiPITs)
Mass	Gravimetric analysis
Total carbon	Particulate carbon (above)
Total nitrogen	Particulate nitrogen (above)

¹ Additional measurements for BATS only include: **(a)** beam attenuation using a SeaTech 25 cm transmissometer, **(b)** bacterial activity using ³H-thymidine incorporation and **(c)** separation of "total" carbon flux into organic and inorganic components by acidification of paired sample and CHN analysis and subsequent calculation of inorganic carbon (Total-organic).

² Additional measurements for HOT only include: **(a)** high sensitivity measurements of nitrate using chemiluminescence and phosphate via magnesium-induced co-precipitation (MAGIC), **(b)** total dissolved phosphorus using UV oxidation and Autoanalyzer, **(c)** particulate phosphorus in water column and sediment traps using high-temperature combustion and colorimetry, **(d)** picophytoplankton enumeration using flow cytometry, **(e)** ATP using fire-fly bioluminescence and **(f)** CTD-dissolved oxygen using the new SeaBird SBE-43 Clark polarographic membrane type sensor.

³ In addition to these measurements, routine meteorological data including wind speed and direction (anemometer), atmospheric pressure (barometer), wet- and dry-bulb air temperature (psychrometer), cloud type and cover, weather and sea state are also collected.

HOT site, a high-frequency CTD profiling program has also resolved internal tides and inertial variability in the region.

Despite the accomplishments of BATS and HOT, we conclude that monthly observations are too infrequent to resolve all of the significant scales of variability in ocean biogeochemistry. For this reason, both time-series programs have deployed moorings with a variety of

instruments and bottom-moored sediment traps for near continuous surveillance (Figure 1). Several satellite-mounted instruments have been providing large-scale data on ocean phenomena during the JGOFS era, including the Topography Experiment (TOPEX/POSEIDON) and Earth Resources Satellite (ERS)-2 altimeters for sea-surface topography, the National Aeronautics and Space Administration (NASA) scatterometer for sea-surface

Bermuda Atlantic Time-series Study (BATS)

Data availability:
<http://www.bior.edu>
 Contact:
 A. Knapp (aknapp@bioz.edu)

Vital BATS statistics, including sea map, key contacts and photo of R/V Weatherbird at her home port at the Bermuda Biological Station for Research.

Hawai'i Ocean Time-series (HOT)

Data availability:
<http://hahana.soest.hawaii.edu>
 Contact:
 D. Karl (dkarl@soest.hawaii.edu)

Vital HOT statistics, including sea map, key contacts and photo of the now retired R/V Moana Wave returning to port after a successful HOT cruise.

winds and the Sea-viewing Wide Field-of-View Sensor (SeaWiFS) ocean-color imager for estimates of sea-surface chlorophyll. (For more information on satellite observations, see Yoder, this issue. For more information on mooring and sensor-based measurements, see Dickey, this issue).

Comparisons Between The BATS and HOT Sites

While the subtropical gyres in which BATS and HOT are located share many ecological characteristics, there are also many fundamental differences. Physical differences are related to the locations of the sampling sites in the subtropical gyres. HOT is within the weak

southward return flow of the eastern gyre, while BATS is within the western gyre recirculation. Thus advective influences are quite different. For example, the thermocline is significantly deeper in the western gyre (BATS) than in the east (HOT). Also, patterns of eddies in the eastern gyre (HOT) show much less energetic variability than in the west (BATS). As a result, chronic oligotrophy characterizes the region around the HOT site, whereas a seasonal, summertime oligotrophy occurs near Bermuda.

The magnitude and duration of the recurrent spring phytoplankton bloom at BATS tracks the depth of winter mixing in the water column, which can vary sub-

Table 2
 Variability in primary production (¹⁴C method), particulate carbon export (measured at 150 m using sediment traps) and the export ratio (e-ratio) for the 11-year BATS and HOT data sets

Parameter	BATS	HOT
Primary Production (mg C m⁻² d⁻¹)		
Mean ± SD	416 ± 178	480 ± 129
Range	111 to 1039	184 to 923
Number of observations	125	94
Particulate Carbon Flux (mg m⁻² d⁻¹)		
Mean ± SD	27.2 ± 13.9	28.3 ± 9.91
Range	8.7 to 76.1	10.7 to 57.0
Number of observations	125	98
Export Ratio		
Mean ± SD	0.072 ± 0.038	0.062 ± 0.026
Range	0.016 to 0.214	0.020 to 0.149
Number of observations	125	89

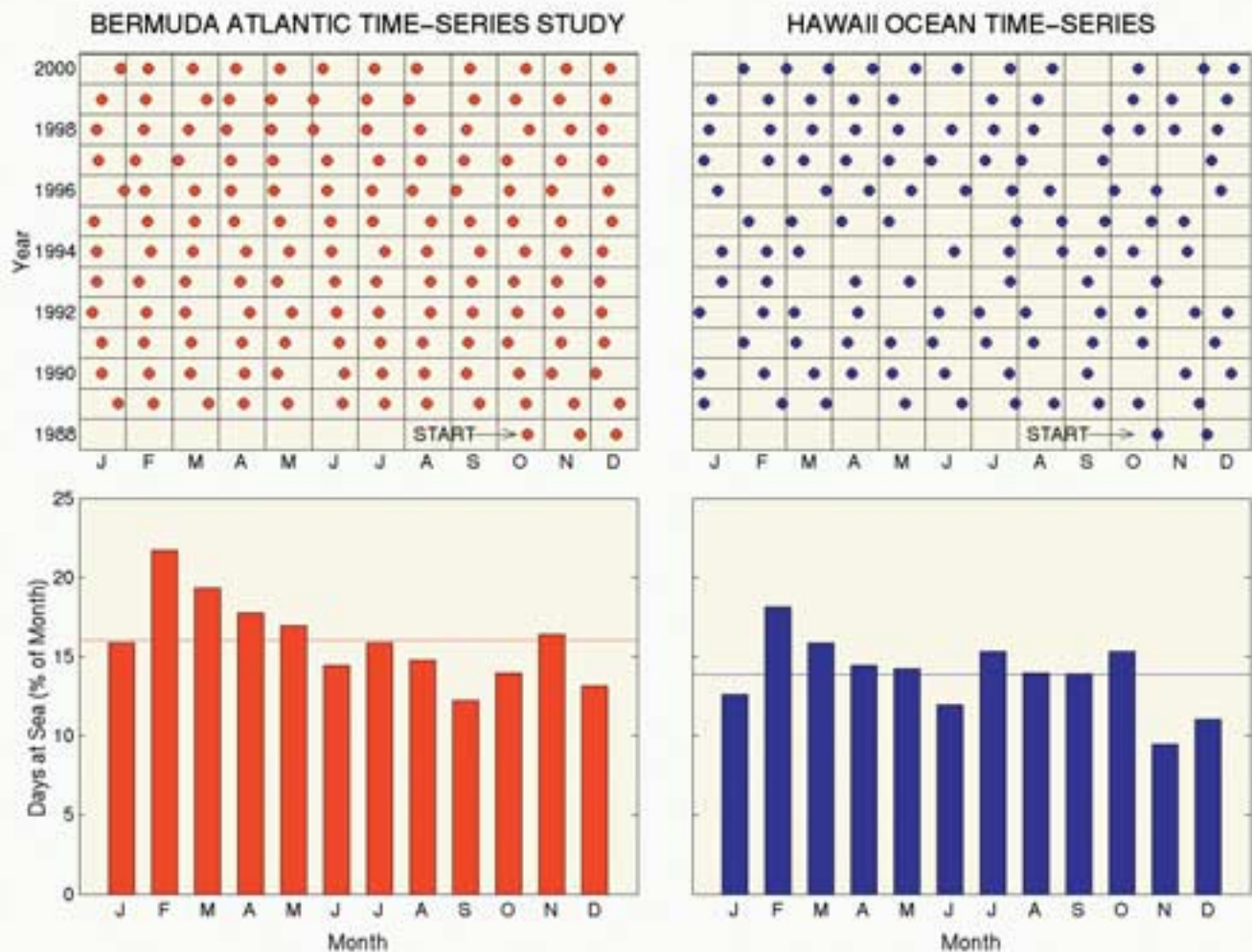


Figure 2. Scientists from the Bermuda Biological Station for Research and the University of Hawaii have gone to sea regularly since October 1988 to observe a broad spectrum of physical and biogeochemical phenomena and to conduct plankton rate experiments. BATS has succeeded in fielding cruises each month over more than 11 years with a total of 701 days at sea. Despite this remarkable achievement, the mean at-sea observation period is only 16% (1 day in 6) of each month. The HOT program has had several gaps in its record, most notably November-December 1993, June-July 1994 and October-November 1997 because of difficulties in scheduling a research vessel. HOT has totaled 606 days at sea, and its mean at-sea observation period is 14% (1 day in 7) of each month.

stantially on both annual and decadal scales (Figure 3) but is generally around 250 to 500 m deep. Conditions near Hawaii are quite stable, on the other hand. At HOT Station ALOHA, wintertime mixed-layer depth rarely exceeds 125 m and is generally much shallower (Figure 3). This difference is linked to the more southerly latitude of HOT relative to the winter storm track and location relative to continental land mass. Surface waters at Station ALOHA receive little in the way of inorganic nutrients from the depths; the result is chronic depletion of nutrients in near-surface waters. As Figure 3 shows, wintertime mixed-layer nitrate concentrations for BATS range between 0.5 and 5 μM , whereas they are less than 0.03 μM and more typically less than 0.01 μM for HOT.

Based on our pre-JGOFS understanding of ocean biogeochemistry, one would predict that the annual

rates of primary production, the total annual export of organic matter and the comparison of exported carbon with total photosynthesis (the so-called export or “e”-ratio) would all be much greater for BATS than for HOT. These biological rates might also be expected to exhibit greater interannual variability at BATS as a result of fluctuations in wintertime nutrient entrainment into the mixed-layer (Figure 3). However, the time-series observations are inconsistent with these simple ecological predictions (Table 2 and Figure 4). Both the climatological mean and range of measured values for primary production, particulate carbon flux and e-ratio, vary unexpectedly at both sites, and the ranges are nearly indistinguishable. Thus, there are basic processes controlling oceanic variability that are outside of our simple paradigms and not resolved by JGOFS sampling approaches. There is still much to be learned about the

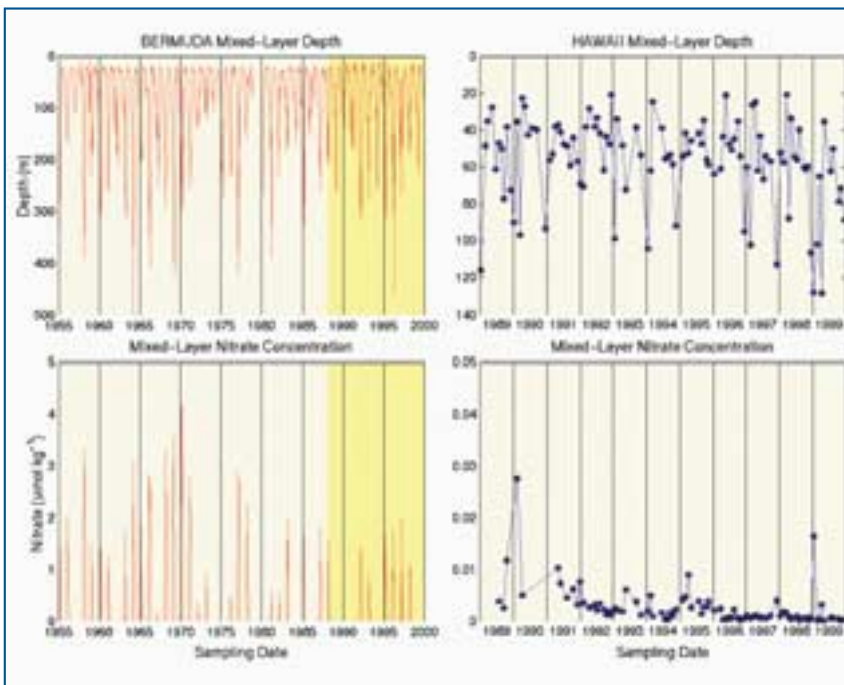


Figure 3. Dynamics of mixed-layer depth (estimated using a 0.125 kg m^{-3} potential density difference criterion) and mixed-layer nitrate concentration for the open ocean near Bermuda (**left**) and Hawaii (**right**). The Bermuda data sets were collected from Hydrostation S from 1955 on and from the BATS station since 1988 (darker shaded portion). The data set from Hawaii is entirely from HOT Station ALOHA. Note changes in scales for both mixed-layer depth (m) and nitrate concentration; values for both these key parameters are much more consistent at the site near Hawaii.

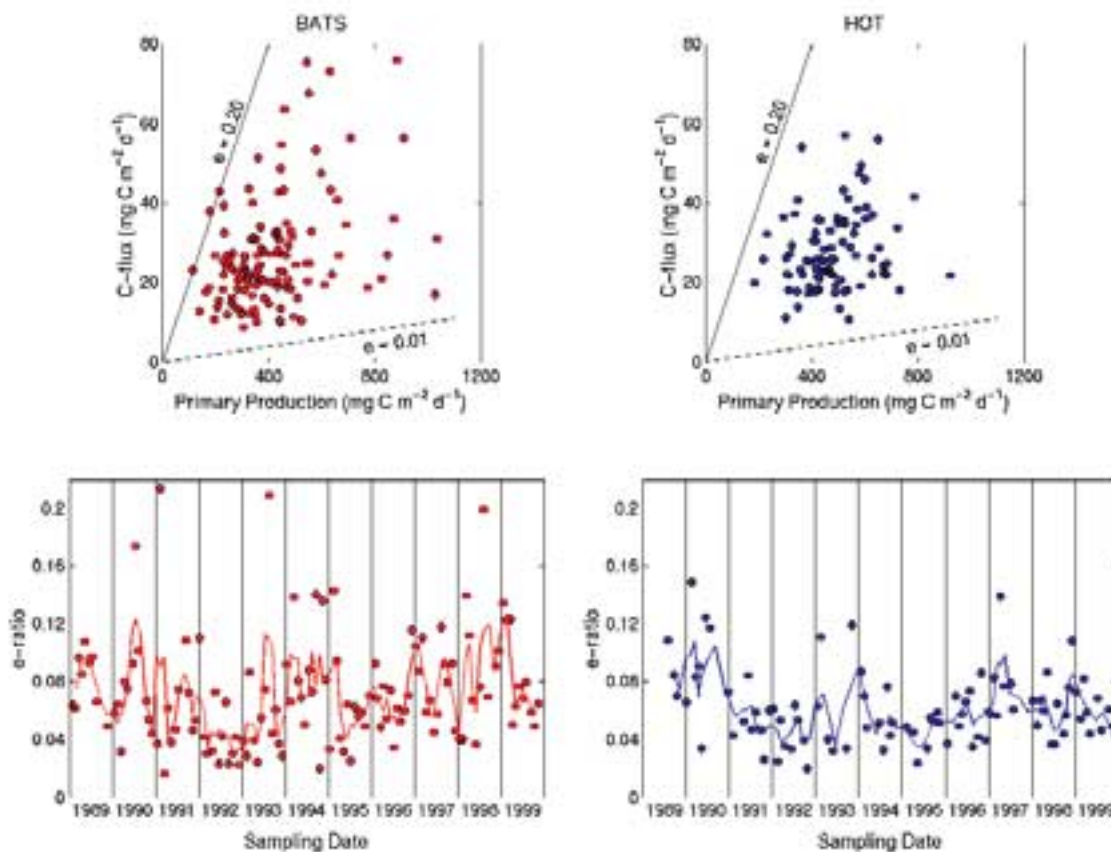


Figure 4. Biological pump dynamics at the U.S. JGOFS time-series sites. (**top**) Primary production (measured by the ^{14}C technique; Table 1) versus particulate carbon flux (measured by free drifting sediment traps; Table 1) at the base of the euphotic zone (C-Flux) for the 11-year observation periods at BATS (left) and HOT (right). The solid lines show constant e -ratio (C-flux \div primary production) values of 0.2 and 0.01 for comparison. Note the poor correlation between these two parameters, which were thought, a priori, to be tightly coupled in the ocean. As shown in the (**bottom**) 11-year export ratio (e -ratio) records for the two sites. Each datum represents the e -ratio for the cruise noted. The solid line is the 3-point running mean e -ratio, shown here to indicate temporal trends in the data sets. A statistical summary of these time-series data is presented in Table 2.

Low-frequency Climate Variability And JGOFS

James Christian
University of Maryland
College Park, Maryland USA

Climate variability exists on a variety of time scales. Interannual modes such as the El Niño-Southern Oscillation (ENSO) and the North Atlantic Oscillation (NAO) coexist and interact with lower-frequency variations that occur over periods of decades to centuries. Upper-ocean temperatures, for example, show variations in the decadal- and interdecadal (15–30 year) ranges. Proxy records such as tree rings also suggest recurrent fluctuations with periods of 50–100 years. In short data records, these lower-frequency signals are indistinguishable from secular trends.

At frequencies lower than those of ENSO cycles, upper-ocean temperature variability is dominated by the interdecadal mode (White and Cayan, 1998), which in the North Pacific corresponds to the “Pacific Decadal Oscillation” (PDO). This mode has a spatial structure somewhat similar to the more familiar ENSO mode; warming of the tropical Pacific coincides with cooling in the northwest Pacific. PDO reversals, expressed as abrupt “regime shifts,” have been documented throughout the 20th century, most recently in 1976. The “phase” of the PDO occasionally reverses itself for a few years in the intervals between these regime shifts, as occurred in 1989–91, coinciding with the first few years of the U.S. JGOFS time-series observations. Thus any short-term ocean observing program may derive a misleading picture of the system under study.

The U.S. JGOFS time-series studies have provided some of the first biogeochemical ocean data that document the effects of interannual-to-interdecadal variability (see Karl et al., this issue). Even after more than a decade, however, these studies have not adequately resolved the dominant climate variability; the interannual ENSO and NAO modes, modulated by lower-frequency variability, have been predominantly in one phase (positive NAO, negative ENSO) throughout the period of observations.

The JGOFS time-series programs have documented significant interannual variability in ocean biogeochemistry. These changes are modulated by lower-frequency climate variability through mechanisms that are poorly understood. Continued high quality, well-calibrated observations are necessary for proper testing of predictive models of ocean biogeochemistry. Even assuming robust representations of the biogeochemical response to changes in physical climate, the modulation of seasonal-to-interannual variability by lower-frequency variability contains nonlinearities and potential surprises. Ecosystem change in response to changing climate creates a significantly more intractable problem, for which current models are almost certainly inadequate.

Low-frequency variability is only beginning to be understood; in fact the evolution of scientific understanding of these processes has occurred largely within the lifetime of JGOFS. Interpretation of the time-series data records in the context of climate variability is thus a subject of ongoing investigation. The time-series studies have shown that observations made on individual cruises are embedded in a complex web of processes that require sustained investigation to understand. Time-series observations have been a critical component of JGOFS and will continue to be essential to the success of future ocean biogeochemistry programs.

Reference

White, W.B. and D.R. Cayan, 1998: Quasi-periodicity and global symmetries in interdecadal upper ocean temperature variability. *J. Geophys. Res.*, 103, 21335–21354.

basic workings of the ocean’s carbon pump (see Ducklow et al., this issue; Berelson, this issue).

The water column between 200 and 1000 m, sandwiched between the sunlit surface waters and the dark abyss, has been termed the “twilight zone.” In this zone, the least studied or understood portion of the water column, inorganic nutrients such as nitrate and phosphate are regenerated from the particulate organic matter that settles from above. The *Bacteria* begin to make way for the *Archaea*. Below approximately 500 m, the *Archaea* equal the heterotrophic bacteria in numbers and biomass (Karner et al., 2001). Unfortunately, none of these twilight zone microorganisms have been cultured as yet, so their physiological characteristics and ecological niches are not yet known.

A comparison of the nitrate versus depth profiles from BATS and HOT shows generally similar trends of increased nitrate with increased depth (Figure 5).

However, closer inspection reveals a much steeper concentration versus depth gradient near Hawaii and a much higher nitrate concentration at any given depth below 200 m (Figure 5). This finding has important implications for our understanding of nitrate transport by advection, diffusion and turbulent mixing.

Perhaps more relevant to the efficient functioning of the biological pump, the molar ratios of nitrate to phosphate (N:P) in the twilight zone vary over time, especially at the BATS site, as well as over depth. At Bermuda the molar ratios of N:P decrease from values >25 to approximately 15 below 200 m. At Hawaii, the N:P molar ratios are more constant for a given depth horizon and exhibit an opposite trend, showing increases with increasing water depth between 200–1000 m (Figure 5). These fundamental differences reflect a complex balance between production and export processes, as well as between particle export

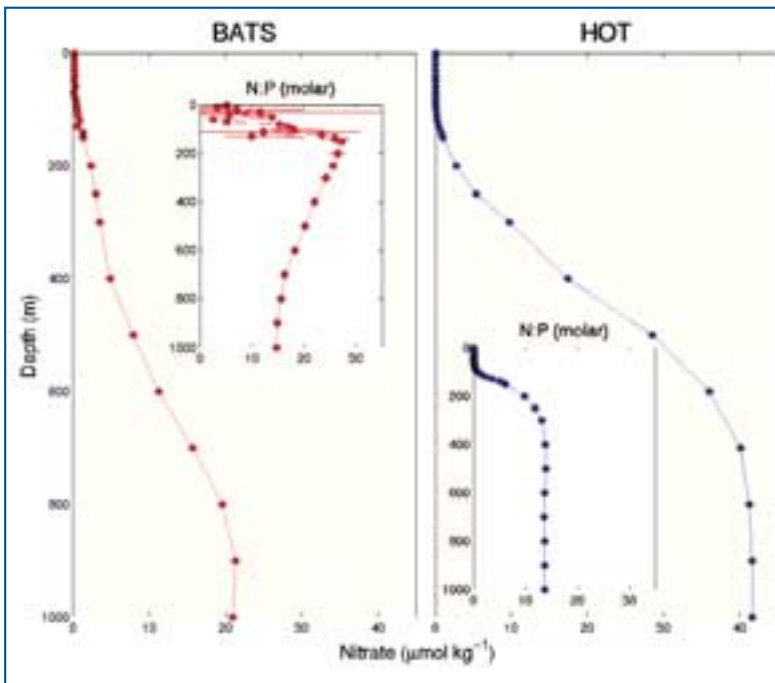


Figure 5. Profiles of nitrate concentration versus depth in the water column for BATS (left) and HOT (right). The data shown are 11-year climatological mean values and 95% confidence intervals. Note that the confidence intervals are smaller than the size of the symbol for the HOT data. Inserts show the depth variation in the dissolved molar nitrate to phosphate ratios (N:P) as mean values with 95% confidence intervals. Note the high variability in the BATS N:P data set in the 0-200 m portion of the water column, which is associated with both seasonal and interannual changes, and the opposing trends in the N:P profiles overall (decreasing for BATS vs. increasing for HOT with increasing water depth).

and remineralization. At N:P ratios below 16, new organic matter production is likely to be nitrogen limited, which favors specialized microorganisms that are able to derive their metabolic nitrogen needs from the relatively inert but inexhaustible supply of dissolved nitrogen gas (see Michaels et al., this issue).

One cannot compare data sets from the upper part of the twilight zone with contemporaneous surface-ocean rates and processes in a straightforward manner, because these mid-water data sets measure signals that

have been integrated over decades. Suffice it to say that these and other comparative data sets from Bermuda and Hawaii suggest that nutrient dynamics in the two major subtropical ocean gyres of the Northern Hemisphere have vastly different biogeochemical processes and ecological controls. Resolution of these differences is a high priority for future research.

Surprises, Riddles and Brain-teasers

Because there were no comparable biogeochemical

Table 3
Inorganic carbon pool dynamics at the U.S. JGOFS BATS and HOT time-series stations¹

Location	Measurement Period	Annual N-DIC Range ² (µmol kg ⁻¹)	Secular N-DIC Change (µmol kg ⁻¹ yr ⁻¹)	Annual fCO ₂ Range (µatm)	Secular fCO ₂ Change (µatm yr ⁻¹)
BATS	10/88 to 12/99 (11 yr)	30-40	+1.23 (+0.61 to +1.85) n = 136	60-120	+1.16 (-0.83 to + 3.16) n = 118
HOT	10/88 to 12/99 (11 yr)	15-20	+1.18 (+0.79 to +1.58) n = 94	25-60	+2.51 (+1.59 to +3.44) n = 86

¹ Data from Bates (2001) and Dore et al. (2001) as well as unpublished results from both time-series programs. Data are presented as the measured range (minima and maxima) or as mean and, in parentheses, 95% confidence intervals, as shown. n = number of observations.

² N-DIC is dissolved inorganic carbon concentration normalized to a constant salinity of 35.0

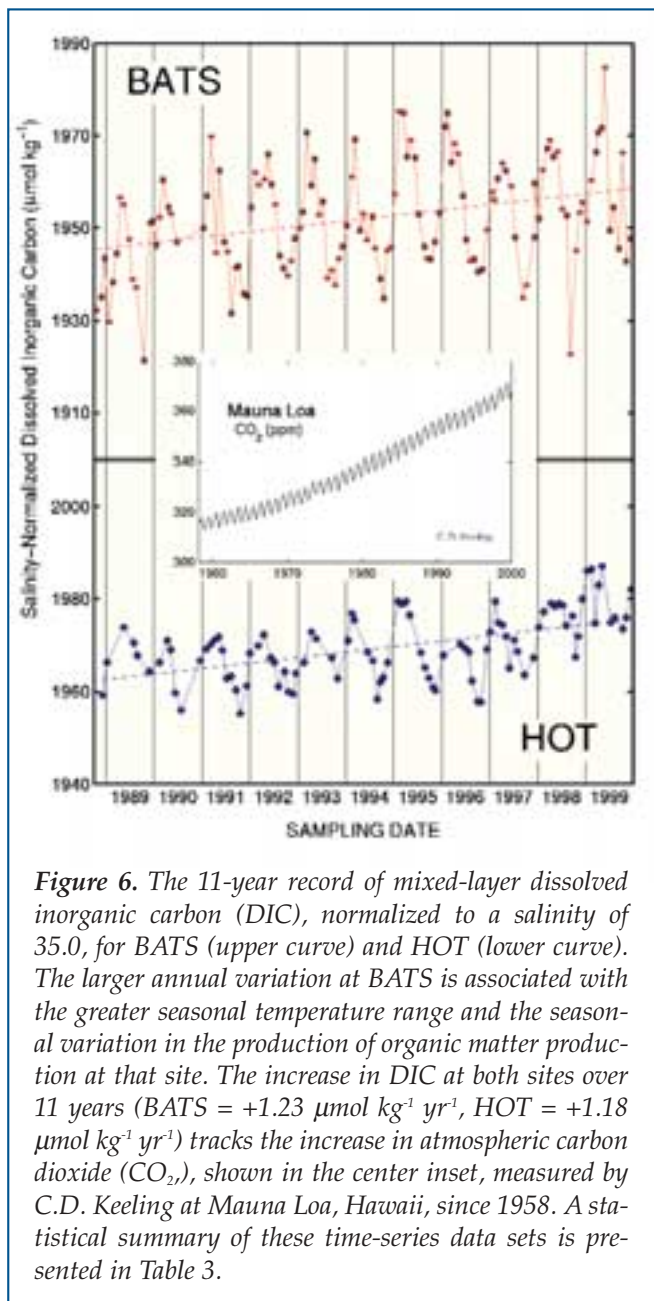


Figure 6. The 11-year record of mixed-layer dissolved inorganic carbon (DIC), normalized to a salinity of 35.0, for BATS (upper curve) and HOT (lower curve). The larger annual variation at BATS is associated with the greater seasonal temperature range and the seasonal variation in the production of organic matter production at that site. The increase in DIC at both sites over 11 years (BATS = $+1.23 \mu\text{mol kg}^{-1} \text{yr}^{-1}$, HOT = $+1.18 \mu\text{mol kg}^{-1} \text{yr}^{-1}$) tracks the increase in atmospheric carbon dioxide (CO_2), shown in the center inset, measured by C.D. Keeling at Mauna Loa, Hawaii, since 1958. A statistical summary of these time-series data sets is presented in Table 3.

data sets gathered on equivalent time scales before the BATS and HOT programs got underway, we had no reliable predictions about what we might find. Although predictions of the ocean's capacity to absorb anthropogenic carbon dioxide could be made on the basis of thermodynamic principles and gas-transfer model calculations, there was no explicit proof that changes in levels of dissolved inorganic carbon (DIC) could actually be detected in the ocean until the BATS and HOT time-series data sets were available (Figure 6). Because natural seasonal and interannual variations in DIC are huge compared to the increase resulting from human activities, accurate and reproducible repeat measurements were required for nearly a decade before we could be certain, as we now are, that the upper water-column inventory of DIC is increasing (Table 3).

Marine scientists working off Bermuda and Hawaii have now observed other previously known but poorly-constrained processes in much greater detail than ever before. To our surprise, and delight, the time-series observations routinely reveal previously undescribed phenomena, including novel ecological pathways and climate-driven biogeochemical connections. This new knowledge and its contribution to the shifting ecological paradigms have made these intensive observational field efforts a labor of love.

One of the major enigmas so far is the apparent uptake and removal of DIC from the water column at both time-series sites during the summer months despite the lack of nitrate, essential for the transformation of inorganic carbon into organic matter. Because any hidden source of nitrate would also contain inorganic carbon, this conundrum cannot be explained in terms of missed nutrient entrainment events. One hypothesis is that the "missing" nitrogen required to sustain these ecosystems may be derived from the metabolic activities of microorganisms that fix nitrogen in the form of N_2 from the atmosphere (Michaels et al., this issue). The evidence for N_2 fixation comes from several independent sources, some based on biological processes reflecting contemporaneous rates and processes and others based on geochemical assessments with integration time scales of years to decades.

Others have hypothesized that N_2 fixation in the ocean may be controlled by the atmospheric deposition of iron, which itself varies in response to changing climate patterns. The transport and distribution of atmospheric dust is also affected by human factors, including population demographics, economic trends and land-use patterns. These complex natural and anthropogenic interactions, with multiple potential feedback loops, affect biogeochemical variability in the otherwise "stable and homogeneous" biomes that we initially sought to monitor and understand. A major scientific challenge is to produce a new ecumenical theory of nutrient dynamics in the sea, one that can be used in a robust conceptual and mathematical framework for accurate prediction of the response of the ocean carbon cycle to climate change and human activities.

We think that wind, heat flux and rainfall changes associated with climate variations have had measurable and significant effects on biogeochemical processes at both BATS and HOT stations. At the BATS site, cold water anomalies in 1992 and 1995 were associated with deeper mixed-layers, higher rates of annual primary production and higher concentrations of near-surface DIC. These events were linked to variations in large-scale climate patterns, specifically NAO and ENSO. At the HOT Station ALOHA, the long-term negative Southern Oscillation Index (SOI) conditions of the 1990s (Figure 7), coupled with an independent extended warm phase of the PDO, have contributed to interdecadal changes in the North Pacific subtropical gyre habitat. These changes, in turn, have encouraged the growth of N_2 -fixing microorganisms, leading to a shift

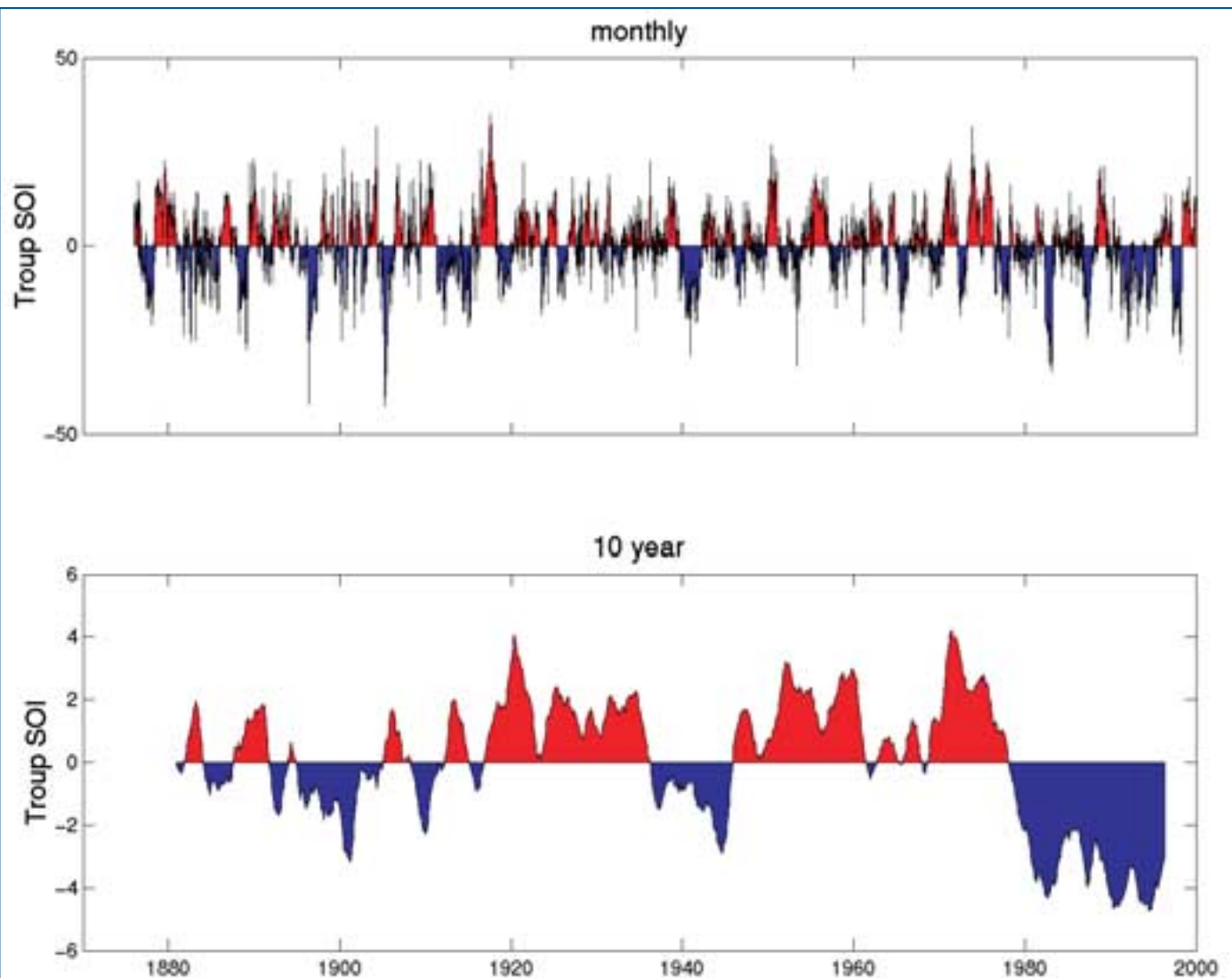


Figure 7. The pulse of the planet's climate system as measured by the Troup Southern Oscillation Index (SOI). Periods characterized by a negative SOI tend to favor El Niño conditions, which have wide-ranging environmental effects, both at sea and on land. The top graph shows the mean monthly Troup SOI record, and the bottom graph presents the 10-year running mean of the same climate record to filter out the high-frequency variations and to focus on the low frequency signals that may be more important for biogeochemical processes and ecological change. There are two key points to consider in the context of JGOFS. The first is that HOT and BATS observations have been made entirely during an extended period with negative SOI values, which are correlated in general with warmer than average sea-surface temperatures in the subtropical northeastern Pacific and elsewhere. The second is that the post-1980 duration of this warm period is unprecedented in the 100-year data set. This finding suggests that ocean conditions during the JGOFS era may not be representative of 20th century mean climatological or ecological conditions.

from the nitrogen-limited ecosystem that prevailed before the 1980s to a phosphorus- or iron-limited system during the JGOFS era (Karl, 1999). These fundamental changes, which have occurred at both sites, have affected local, regional and perhaps global carbon cycle dynamics in the ocean.

The Ocean Carbon Cycle "Universities"

Since the JGOFS time-series programs began, sci-

entists associated with them have created and disseminated knowledge, organized and hosted interdisciplinary workshops and symposia, and facilitated technical training and information exchange. Each site has been the focal point for a large number of related studies that have built on the core research and, in turn, contributed to that common body of understanding. The time-series sites have functioned as ocean carbon cycle "universities," with the time-series "faculty" engaged


in the academic triad of research, teaching and community service.

Among the unique aspects of the JGOFS time-series programs are their roles as facilitators of complementary ocean and atmospheric research and as test-beds for the development and evaluation of novel sensors and other instruments. The extensive and diverse lists of ancillary investigators who have benefited from the core measurement programs testify to the successes of BATS and HOT in these roles. Full and free access to all time-series data in a timely manner is a critical component of both the successful collaboration of these two programs and the widespread use of these data by outside investigators and modelers. The time-series programs have also served as floating classrooms for public education, from kindergarten to elderhostel.

Prospectus For The Future

At the beginning of the JGOFS era, we considered our general understanding of open-ocean subtropical gyres to be nearly complete. These large ecosystems were thought to be stable in time and coherent in space, supporting homogeneous plankton communities that were well-tuned to their habitats and fairly resistant to natural physical forcing. We now recognize these regions as fundamentally different biomes; they are dynamic, variable and poised for ecological opportunity.

BATS and HOT scientists continue to explore the hidden secrets of the marine carbon cycle. Although it is difficult to predict the direction of ocean carbon cycle research, one thing is abundantly clear. Time-series programs need to be preserved, enhanced and expanded to other key sites. These programs and related components of the emerging global ocean observing network will continue to provide opportunities for both basic and applied research well into the future.

At the beginning of the JGOFS era, we had no idea that we would uncover so much biogeochemical variability in the ocean or achieve so many novel insights in connection with the time-series programs. As the data sets grow, new scales of variability will likely become evident. But BATS and HOT are relatively short in length compared to what will be required for a comprehensive understanding of the effects of climate on the ocean's carbon cycle. Extending these field studies over more decades will help us reach firm conclusions that will lead us to accurate ecological predictions. Time to head back to sea. 

Acknowledgments

Sufficient space does not exist to express our collective debt of gratitude to the scientists, technical staff, data managers, students and ship officers and crew who have assisted in the collection, analysis and interpretation of the BATS and HOT data sets. We likewise thank our public and private sector sponsors for their generous financial support, especially the Division of

Ocean Sciences of the National Science Foundation. Since the beginning of JGOFS, the time-series programs have benefited from the oversight of the JGOFS Scientific Steering Committee and from three ad hoc time-series committees chaired by Steve Emerson, Tommy Dickey and Jim McCarthy. Finally, we thank Ken Buesseler, Mardi Bowles and Mary Zawoysky for their efforts in preparing this special issue on the U.S. JGOFS research program. This is U.S. JGOFS Contribution Number 677.

References

- Azam, F., T. Fenchel, J.G. Field, R.A. Meyer-Reil and F. Thingstad, 1983: The ecological role of water column microbes in the sea. *Mar. Ecol. Prog. Ser.*, 10, 257-263.
- Bates, N.R., 2001: Interannual variability of oceanic CO₂ and biogeochemical properties in the Western North Atlantic subtropical gyre. *Deep-Sea Res. II*, 48, 1507-1528.
- Béjà, O., E.N. Spudich, J.L. Spudich, M. LeClerc and E.F. DeLong, 2001: Proteorhodopsin phototrophy in the ocean. *Nature*, 411, 786-789.
- Chisholm, S.W., R.J. Olson, E.R. Zettler, R. Goericke, J.B. Waterbury and N.A. Welschmeyer, 1988: A novel free-living prochlorophyte abundant in the oceanic euphotic zone. *Nature*, 334, 340-343.
- DeLong, E.F., 1992: *Archaea* in coastal marine environments. *Proc. Natl. Acad. Sci. USA*, 89, 5685-5689.
- Dore, J.E., C.J. Carrillo, D.V. Hebel and D.M. Karl, 2001: Carbon cycle observations at the Hawaii Ocean Time-series Station ALOHA. In: *Proceedings of the PICES North Pacific CO₂ data synthesis symposium*. Y. Nojiri and R. Feely, eds., Tsukuba, Japan, October 2000, in press.
- Dugdale R.C. and J.J. Goering, 1967: Uptake of new and regenerated forms of nitrogen in primary productivity. *Limnol. Oceanogr.*, 12, 196-206.
- Eppley, R.W. and B.J. Peterson, 1979: Particulate organic matter flux and planktonic new production in the deep ocean. *Nature*, 282, 677-680.
- Johnson, P.W. and J.McN. Sieburth, 1979: Chroococcoid cyanobacteria in the sea: a ubiquitous and diverse phototrophic biomass. *Limnol. Oceanogr.*, 24, 928-935.
- Karl, D.M., 1999: A sea of change: Biogeochemical variability in the North Pacific subtropical gyre. *Ecosystems*, 2, 181-214.
- Karl, D.M. and A.F. Michaels, eds., 1996: Ocean Time-series: Results from the Hawaii and Bermuda Research Programs. *Deep-Sea Res. II*, Topical Studies in Oceanography, 43.
- Karner, M.B., E.F. DeLong and D.M. Karl, 2001: Archaeal dominance in the mesopelagic zone of the Pacific Ocean. *Nature*, 409, 507-510.
- Kolber, Z.S., F.G. Plumley, A.S. Lang, J.T. Beatty, R.E. Blankenship, C.L. VanDover, C. Vetriani, M. Koblizek, C. Rathgeber and P.G. Falkowski, 2001: Contribution of aerobic photoheterotrophic bacteria to the carbon cycle in the ocean. *Science*, 292, 2492-2495.
- Pomeroy, L.R., 1974: The ocean's food web: A changing paradigm. *BioScience*, 24, 409-504.
- Siegel, D.A., D.M. Karl and A.F. Michaels, eds., 2001: HOT and BATS: Interpretations of Open Ocean Biogeochemical Processes. *Deep-Sea Res. II*, Topical Studies in Oceanography, 48.

Uptake and Storage of Carbon Dioxide in the Ocean: The Global CO₂ Survey

Richard A. Feely

Pacific Marine and Environmental Laboratory

National Oceanic and Atmospheric Administration • Seattle, Washington USA

Christopher L. Sabine

University of Washington • Seattle, Washington USA

Taro Takahashi

Lamont-Doherty Earth Observatory • Palisades, New York USA

Rik Wanninkhof

Atlantic Oceanographic and Meteorological Laboratory

National Oceanic and Atmospheric Administration • Miami, Florida USA

Introduction

Human activity is rapidly changing the composition of the earth's atmosphere, contributing to warming from excess carbon dioxide (CO₂) along with other trace gases such as water vapor, chlorofluorocarbons, methane and nitrous oxide. These anthropogenic "greenhouse gases" play a critical role in controlling the earth's climate because they increase the infrared opacity of the atmosphere, causing the surface of the planet to warm. The release of CO₂ from fossil fuel consumption or the burning of forests for farming or pasture contributes approximately 7 petagrams of carbon (1 Pg C = 1 × 10¹⁵ g C) to the atmosphere each year. Approximately 3 Pg C of this "anthropogenic CO₂" accumulates in the atmosphere annually, and the remaining 4 Pg C is stored in the terrestrial biosphere and the ocean.

Where and how land and ocean regions vary in their uptake of CO₂ from year to year is the subject of much scientific research and debate. Future decisions on regulating emissions of greenhouse gases should be based on more accurate models of the global cycling of carbon and the regional sources and sinks for anthropogenic CO₂, models that have been adequately tested against a well-designed system of measurements. The construction of a believable present-day carbon budget is essential for the reliable prediction of changes in atmospheric CO₂ and global temperatures from available emissions scenarios.

The ocean plays a critical role in the global carbon cycle as a vast reservoir that exchanges carbon rapidly with the atmosphere, and takes up a substantial portion of anthropogenically-released carbon from the

atmosphere. A significant impetus for carbon cycle research over the past several decades has been to achieve a better understanding of the ocean's role as a sink for anthropogenic CO₂. There are only three global reservoirs with exchange rates fast enough to vary significantly on the scale of decades to centuries: the atmosphere, the terrestrial biosphere and the ocean. Approximately 93% of the carbon is located in the ocean, which is able to hold much more carbon than the other reservoirs because most of the CO₂ that diffuses into the oceans reacts with seawater to form carbonic acid and its dissociation products, bicarbonate and carbonate ions (Figure 1).

Our present understanding of the temporal and spatial distribution of net CO₂ flux into or out of the ocean is derived from a combination of field data, which is limited by sparse temporal and spatial coverage, and model results, which are validated by comparisons with the observed distributions of tracers, including natural carbon-14 (¹⁴C), and anthropogenic chlorofluorocarbons, tritium (³H) and bomb ¹⁴C. The latter two radioactive tracers were introduced into the atmosphere-ocean system by atomic testing in the mid 20th century. With additional data from the recent global survey of CO₂ in the ocean (1991–1998), carried out cooperatively as part of the Joint Global Ocean Flux Study (JGOFS) and the World Ocean Circulation Experiment (WOCE) Hydrographic Program, it is now possible to characterize in a quantitative way the regional uptake and release of CO₂ and its transport in the ocean. In this paper, we summarize our present understanding of the exchange of CO₂ across the air-sea

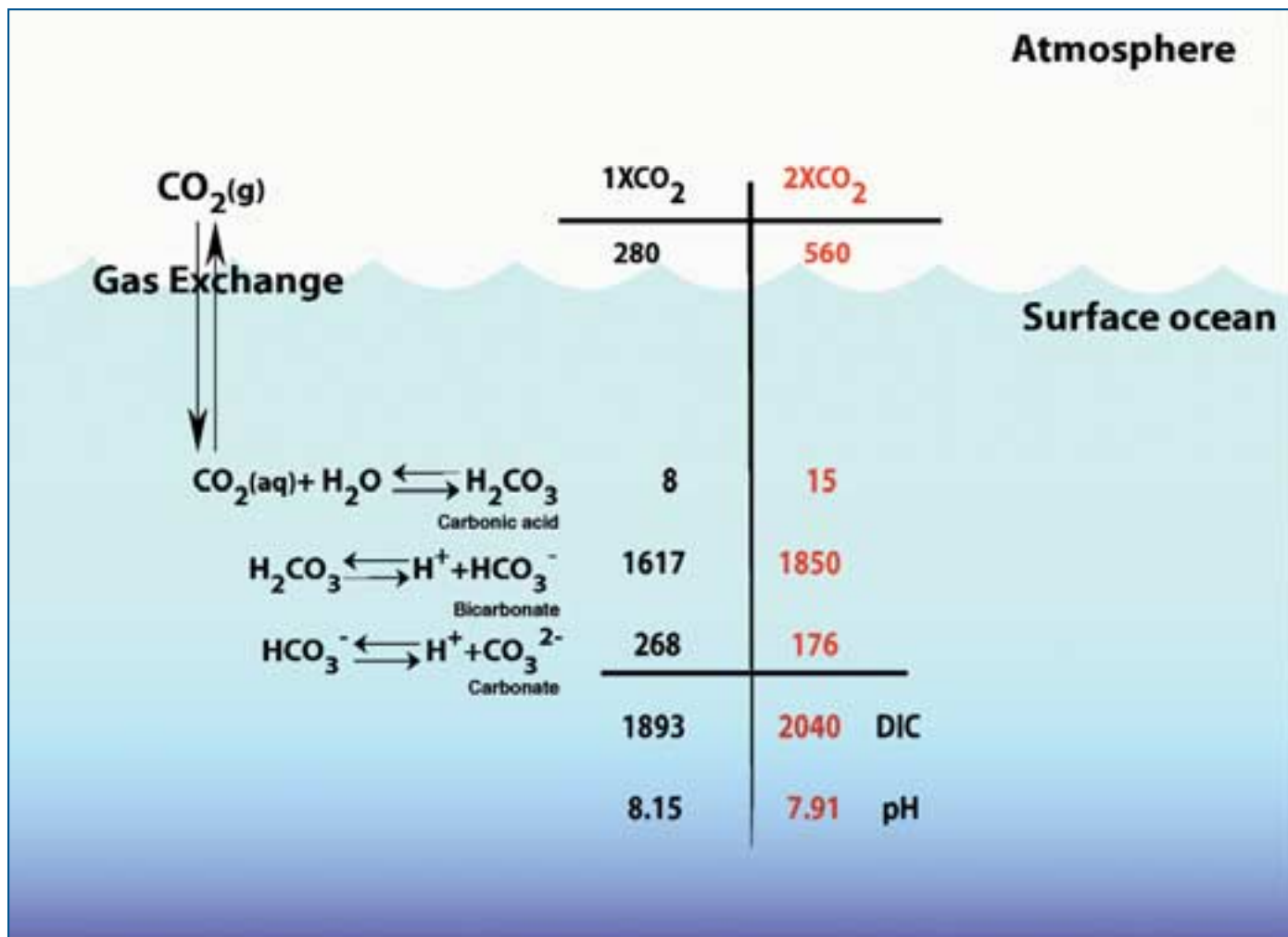


Figure 1. Schematic diagram of the carbon dioxide (CO₂) system in seawater. The 1 x CO₂ concentrations are for a surface ocean in equilibrium with a pre-industrial atmospheric CO₂ level of 280 ppm. The 2 x CO₂ concentrations are for a surface ocean in equilibrium with an atmospheric CO₂ level of 560 ppm. Current model projections indicate that this level could be reached sometime in the second half of this century. The atmospheric values are in units of ppm. The oceanic concentrations, which are for the surface mixed layer, are in units of μmol kg⁻¹.

interface and the storage of natural and anthropogenic CO₂ in the ocean's interior.

Background

The history of large-scale CO₂ observations in the ocean date back to the 1970s and 1980s. Measurements of the partial pressure of CO₂ (pCO₂), total dissolved inorganic carbon (DIC) and total alkalinity (A_T) were made during the global Geochemical Ocean Sections (GEOSECS) expeditions between 1972 and 1978, the Transient Tracers in the Oceans (TTO) North Atlantic and Tropical Atlantic Surveys in 1981–83, the South Atlantic Ventilation Experiment (SAVE) from 1988–1989, the French Southwest Indian Ocean experiment, and numerous other smaller expeditions in the Pacific and Indian Oceans in the 1980s. These studies provided marine chemists with their first view of the carbon system in the global ocean.

These data were collected at a time when no common reference materials or standards were available. As a result, analytical differences between measurement groups were as large as 29 μmol kg⁻¹ for both DIC and A_T, which corresponds to more than 1% of the ambient values. Large adjustments had to be made for each of the data sets based on deepwater comparisons at nearby stations before individual cruise data could be compared. These differences were often nearly as large as the anthropogenic CO₂ signal that investigators were trying to determine (Gruber et al., 1996). Nevertheless, these early data sets made up a component of the surface ocean pCO₂ measurements for a global climatology and also provided researchers with new insights into the distribution of anthropogenic CO₂ in the ocean, particularly in the Atlantic Ocean.

At the onset of the Global Survey of CO₂ in the Ocean (Figure 2), several events took place in the United

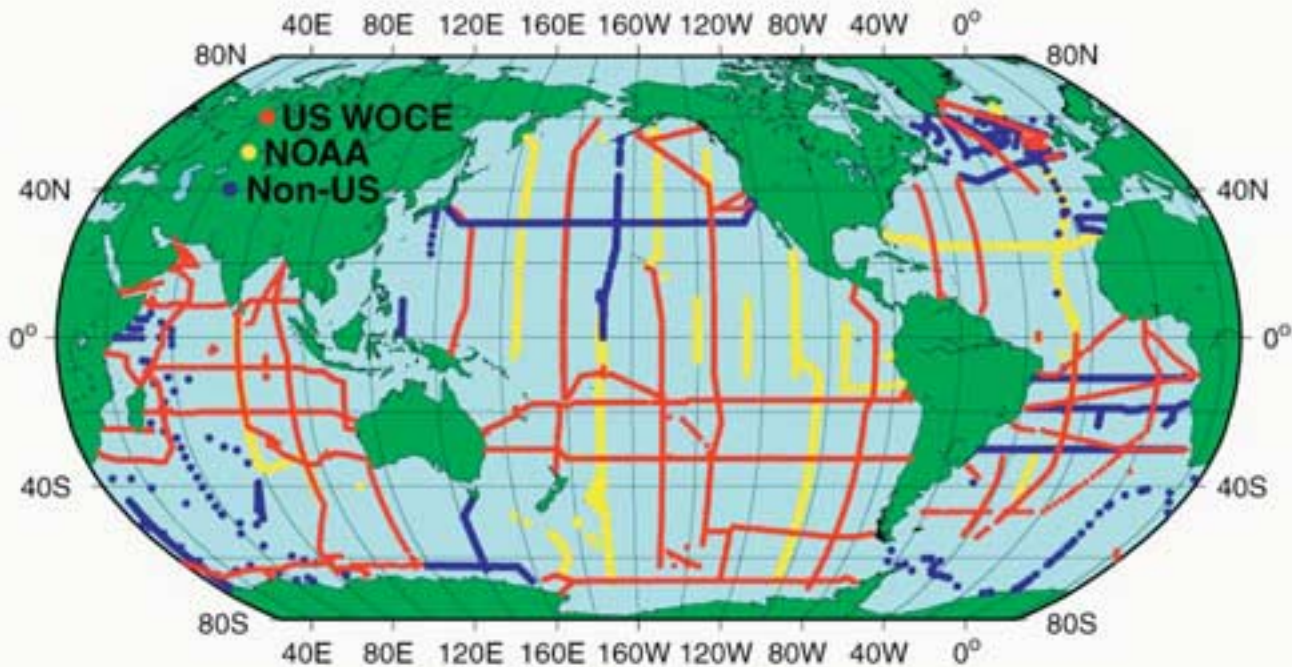


Figure 2. The Global Survey of CO₂ in the Ocean: cruise tracks and stations occupied between 1991 and 1998.

States and in international CO₂ measurement communities that significantly improved the overall precision and accuracy of the large-scale measurements. In the United States, the CO₂ measurement program was co-funded by the Department of Energy (DOE), the National Oceanic and Atmospheric Administration (NOAA) and the National Science Foundation (NSF) under the technical guidance of the U.S. CO₂ Survey Science Team. This group of academic and government scientists adopted and perfected the recently developed coulometric titration method for DIC determination that had demonstrated the capability to meet the required goals for precision and accuracy. They advocated the development and distribution of certified reference materials (CRMs) for DIC, and later for A_T, for international distribution under the direction of Andrew Dickson of Scripps Institution of Oceanography (see sidebar). They also supported a shore-based intercomparison experiment under the direction of Charles Keeling, also of Scripps. Through international efforts, the development of protocols for CO₂ analyses were adopted for the CO₂ survey. The international partnerships fostered by JGOFS resulted in several intercomparison CO₂ exercises hosted by France, Japan, Germany and the United States. Through these and other international collaborative programs, the measurement quality of the CO₂ survey data was well within the measurement goals of $\pm 3 \mu\text{mol kg}^{-1}$ and $\pm 5 \mu\text{mol kg}^{-1}$, respectively, for DIC and A_T.

Several other developments significantly enhanced the quality of the CO₂ data sets during this period. New methods were developed for automated underway and

discrete pCO₂ measurements. An extremely precise method for pH measurements based on spectrophotometry was also developed by Robert Byrne and his colleagues at the University of South Florida. These improvements ensured that the internal consistency of the carbonate system in seawater could be tested in the field whenever more than two components of the carbonate system were measured at the same location and time. This allowed several investigators to test the overall quality of the global CO₂ data set based upon CO₂ system thermodynamics. Laboratories all around the world contributed to a very large and internally consistent global ocean CO₂ data set determined at roughly 100,000 sample locations in the Atlantic, Pacific, Indian and Southern oceans (Figure 2). The data from the CO₂ survey are available through the Carbon Dioxide Information and Analysis Center (CDIAC) at Oak Ridge National Laboratory as Numeric Data Packages and on the World Wide Web (<http://cdiac.esd.ornl.gov/home.html>). Taro Takahashi and his collaborators have also amassed a large database of surface ocean pCO₂ measurements, spanning more than 30 years, into a pCO₂ climatology for the global ocean (Takahashi et al., in press). These data have been used to determine the global and regional fluxes for CO₂ in the ocean.

CO₂ Exchange Across the Air-Sea Interface

In seawater, CO₂ molecules are present in three major forms: the undissociated species in water, [CO₂]aq, and two ionic species, [HCO₃⁻] and [CO₃²⁻] (Figure 1). The concentration of [CO₂]aq depends upon

Reference Materials For Oceanic CO₂ Measurements

Andrew G. Dickson
Scripps Institution of Oceanography
University of California, San Diego,
La Jolla California USA



A 500 ml glass bottle containing certified reference material for oceanic CO₂ measurements.

High-quality measurements of carbon dioxide (CO₂) in the ocean have been an integral part of JGOFS. Despite their importance for understanding the oceanic carbon cycle, measurements made by different groups were rarely comparable in the past. A significant contribution of U.S. JGOFS has been to produce and distribute reference materials for oceanic CO₂ measurements. These materials are stable substances for which one or more properties are established sufficiently well to calibrate a chemical analyzer or to validate a measurement process.

Our laboratory at Scripps Institution of Oceanography (SIO), established in 1989 with U.S. JGOFS support from the National Science Foundation (NSF), has prepared over 50 separate batches of reference material and has distributed more than 25,000 bottles of this material to scientists in 33 laboratories in the U.S. and 58 facilities in 24 other countries. The reference materials have been used both as a basis for collaborative studies and as a means of quality control for at-sea measurements. Although most JGOFS field studies are over, we are still distributing more than 2,000 bottles per year and demand is again growing.

To prepare the reference material, we sterilize a batch of seawater, equilibrate it to a virtually constant partial pressure of CO₂ and deliver it for bottling. For each batch, surface seawater collected on ships of opportunity and stored in our laboratory is pumped into a holding tank using filters and a sterilizing unit to reduce contamination. When the holding tank is nearly full, mercuric chloride is added as a biocide. The seawater is then recirculated for a few days to ensure complete mixing and enable some gas exchange with filtered air that is pumped through the head-space of the tank. Finally, aliquots of the seawater are pumped through an ultraviolet sterilizing unit and a 0.1 µm filter and into clean 500-ml glass bottles. These are sealed with grease and labeled.

Random samples from each batch of reference material are analyzed over a period of 2–3 months for both total dissolved inorganic carbon (C_T) and total alkalinity (A_T), and the results are used to certify the batch before it is distributed. From the start, we used a high-quality method for the determination of C_T in which a weighed amount of seawater is acidified and the CO₂ extracted under vacuum, purified and determined manometrically.

These analyses are carried out in the laboratory of C.D. Keeling at SIO using equipment originally developed for the calibration of gases for atmospheric CO₂ measurements.

By 1996, we had also developed an accurate method for the measurement of A_T using a two-stage potentiometric, open-cell titration with coulometrically analyzed hydrochloric acid. Once this latter method was being employed routinely to certify new batches of reference material, we used it retrospectively to analyze archived samples from earlier batches.

The uncertainties of these analyses used for certification are ± 1.5 µmol kg⁻¹ in C_T and ± 2 mol µkg⁻¹ in A_T, and our reference materials have been shown to be stable for more than 3 years. We are now working on providing pH values on future reference materials, as well as values for δ¹³C.

As part of U.S. JGOFS, the Department of Energy (DOE) supported measurements of



George Anderson filling bottles with sterilized seawater for use as a reference material.

ocean CO₂ system parameters on sections of the WOCE Hydrographic Programme one-time survey. The CO₂ Survey Science Team adopted the use of our reference materials as soon as they were available in early 1991 and continued to use them on subsequent cruises. Measurements made on reference materials while at sea were used to ascertain data quality on these expeditions and are thought to have contributed substantially to the overall high quality of the resultant data set.

A further indication that the use of reference materials has improved oceanographic data quality can be seen by examining the degree of agreement between measurements for deep water masses obtained where two separate cruises intersect. For cruises where reference materials were available, measurements of C_T in deep water now typically agree to within 2 μmol kg⁻¹. This is in sharp contrast to the problems encountered over the years with earlier ocean carbon data sets, where adjustments of as much as 15–20 μmol kg⁻¹ were fairly common. The high-quality data sets now available provide a resource for synthesis and modeling that makes it possible to put together a coherent global view of the oceanic carbon cycle.

Acknowledgements

This work was supported by NSF through grants OCE8800474, OCE9207265, OCE9521976 and OCE-9819007 and by DOE through Pacific Northwest National Laboratory subcontract No. 121945 and grant DEFG0392ER61410. This work was encouraged early on by Neil Andersen, then at NSF, and has benefited from advice from C.D. Keeling, the members of the DOE CO₂ Survey Science Team and colleagues from the National Oceanic and Atmospheric Administration. I should also like to thank Justine Afghan and George Anderson, who carried out most of the technical work involved in this project, as well as Guy Emanuele and Peter Guenther from the Carbon Dioxide Research Group at SIO, who performed the C_T analyses.

the temperature and chemical composition of seawater. The amount of [CO₂]aq is proportional to the partial pressure of CO₂ exerted by seawater. The difference between the pCO₂ in surface seawater and that in the overlying air represents the thermodynamic driving potential for the CO₂ transfer across the sea surface. The pCO₂ in surface seawater is known to vary geographically and seasonally over a range between about 150 μatm and 750 μatm, or about 60% below and 100% above the current atmospheric pCO₂ level of about 370 μatm. Since the variation of pCO₂ in the surface ocean is much greater than the atmospheric pCO₂ seasonal variability of about 20 μatm in remote uncontaminated marine air, the direction and magnitude of the sea-air CO₂ transfer flux are regulated primarily by changes in the oceanic pCO₂. The average pCO₂ of the global ocean is about 7 μatm lower than the atmosphere, which is the primary driving force for uptake by the ocean (see Figure 6 in Karl et al., this issue).

The pCO₂ in mixed-layer waters that exchange CO₂ directly with the atmosphere is affected primarily by temperature, DIC levels and A_T. While the water temperature is regulated by physical processes, including solar energy input, sea-air heat exchanges and mixed-layer thickness, the DIC and A_T are primarily controlled by the biological processes of photosynthesis and respiration and by upwelling of subsurface waters rich in respired CO₂ and nutrients. In a parcel of seawater with constant chemical composition, pCO₂ would increase by a factor of 4 when the water is warmed from polar temperatures of about -1.9 °C to equatorial temperatures of about 30 °C. On the other hand, the DIC in the surface ocean varies from an average value of 2150 μmol kg⁻¹ in polar regions to 1850 μmol kg⁻¹ in the tropics as a result of biological processes. This change should reduce pCO₂ by a factor of 4. On

a global scale, therefore, the magnitude of the effect of biological drawdown on surface water pCO₂ is similar in magnitude to the effect of temperature, but the two effects are often compensating. Accordingly, the distribution of pCO₂ in surface waters in space and time, and therefore the oceanic uptake and release of CO₂, is governed by a balance between the changes in seawater temperature, net biological utilization of CO₂ and the upwelling flux of subsurface waters rich in CO₂.

Database and Methods

Surface-water pCO₂ has been determined with a high precision (±2 μatm) using underway equilibrator-CO₂ analyzer systems over the global ocean since the International Geophysical Year of 1956–59. As a result of recent major oceanographic programs, including the global CO₂ survey and other international field studies, the database for surface-water pCO₂ observations has been improved to about 1 million measurements with several million accompanying measurements of SST, salinity and other necessary parameters such as barometric pressure and atmospheric CO₂ concentrations. Based upon these observations, a global, monthly climatological distribution of surface-water pCO₂ in the ocean was created for a reference year 1995, chosen because it was the median year of pCO₂ observations in the database. The database and the computational method used for interpolation of the data in space and time will be briefly described below.

For the construction of climatological distribution maps, observations made in different years need to be corrected to a single reference year (1995), based on several assumptions explained below (see also Takahashi et al., in press). Surface waters in the subtropical gyres mix vertically at slow rates with subsurface waters because of strong stratification at the base of the mixed

layer. As a result, they are in contact with the atmosphere and can exchange CO₂ for a long time. Consequently, the *p*CO₂ in these warm waters follows the increasing trend of atmospheric CO₂ concentrations, as observed by Inoue et al. (1995) in the western North Pacific, by Feely et al. (1999) in the equatorial Pacific and by Bates (2001) near Bermuda in the western North Atlantic. Accordingly, the *p*CO₂ measured in a given month and year is corrected to the same month in the reference year 1995 using the following atmospheric CO₂ concentration data for the planetary boundary layer: the GLOBALVIEW-CO₂ database (2000) for observations made after 1979 and the Mauna Loa data of Keeling and Whorf (2000) for observations before 1979 (reported in CDIAC NDP-001, revision 7).

In contrast to the waters of the subtropical gyres, surface waters in high-latitude regions are mixed convectively with deep waters during fall and winter, and their CO₂ properties tend to remain unchanged from year to year. They reflect those of the deep waters, in which the effect of increased atmospheric CO₂ over the time span of the observations is diluted to undetectable levels (Takahashi et al., in press). Thus no correction is necessary for the year of measurements.

Distribution Maps for Climatological Mean Sea-air *p*CO₂ Difference

Figure 3 shows the distribution of climatological mean sea-air *p*CO₂ difference ($\Delta p\text{CO}_2$) during February (Figure 3a) and August (Figure 3b) for the reference year 1995. The yellow-red colors indicate oceanic areas where there is a net release of CO₂ to the atmosphere, and the blue-purple colors indicate regions where there is a net uptake of CO₂. The equatorial Pacific is a strong source of CO₂ to the atmosphere throughout the year as a result of the upwelling and vertical mixing of deep waters in the central and eastern regions of the equatorial zone. The intensity of the oceanic release of CO₂ decreases westward in spite of warmer temperatures to the west. High levels of CO₂ are released in parts of the northwestern subarctic Pacific during the northern winter and the Arabian Sea in the Indian Ocean during August. Strong convective mixing that brings up deep waters rich in CO₂ produces the net release of CO₂ in the subarctic Pacific. The effect of increased DIC concentration surpasses the cooling effect on *p*CO₂ in seawater during winter. The high *p*CO₂ in the Arabian Sea water is a result of strong upwelling in response to the southwest monsoon. High *p*CO₂ values in these areas are reduced by the intense primary production that follows the periods of upwelling.

The temperate regions of the North Pacific and Atlantic oceans take up a moderate amount of CO₂ (blue) during the northern winter (Figure 3a) and release a moderate amount (yellow-green) during the northern summer (Figure 3b). This pattern is the result primarily of seasonal temperature changes. Similar seasonal changes are observed in the southern temperate oceans. Intense regions of CO₂ uptake (blue-purple) are seen in the high-latitude northern ocean in summer (Figure 3b)

and in the high-latitude South Atlantic and Southern oceans near Antarctica in austral summer (Figure 3a). The uptake is linked to high biological utilization of CO₂ in thin mixed layers. As the seasons progress, vertical mixing of deep waters eliminates the uptake of CO₂.

These observations point out that the $\Delta p\text{CO}_2$ in high-latitude oceans is governed primarily by deep-water upwelling in winter and biological uptake in spring and summer, whereas in the temperate and subtropical oceans, the $\Delta p\text{CO}_2$ is governed primarily by water temperature. The seawater $\Delta p\text{CO}_2$ is highest during winter in subpolar and polar waters, whereas it is highest during summer in the temperate regions. Thus the seasonal variation of $\Delta p\text{CO}_2$ and therefore the shift between net uptake and release of CO₂ in subpolar and polar regions is about 6 months out of phase with that in the temperate regions.

The $\Delta p\text{CO}_2$ maps are combined with the solubility (*s*) in seawater and the kinetic forcing function, the gas transfer velocity (*k*), to produce the flux:

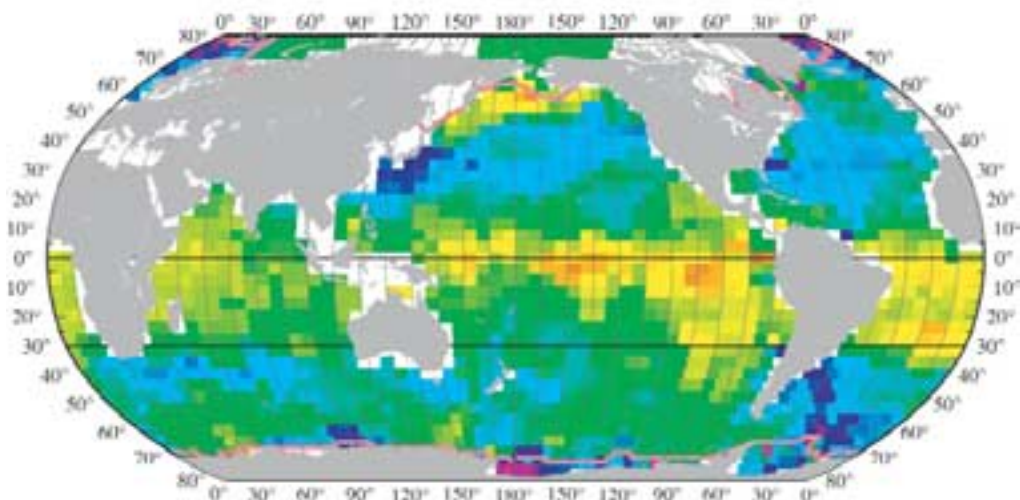
$$F = k \cdot s \cdot \Delta p\text{CO}_2 \quad (1)$$

The gas transfer velocity is controlled by near-surface turbulence in the liquid boundary layer. Laboratory studies in wind-wave tanks have shown that *k* is a strong but non-unique function of wind speed. The results from various wind-wave tank investigations and field studies indicate that factors such as fetch, wave direction, atmospheric boundary layer stability and bubble entrainment influence the rate of gas transfer. Also, surfactants can inhibit gas exchange through their damping effect on waves. Since effects other than wind speed have not been well quantified, the processes controlling gas transfer have been parameterized solely with wind speed, in large part because *k* is strongly dependent on wind, and global and regional wind-speed data are readily available.

Several of the frequently used relationships for the estimation of gas transfer velocity as a function of wind speed are shown in Figure 4 to illustrate their different dependencies. For the Liss and Merlivat (1986) relationship, the slope and intercept of the lower segment was determined from an analytical solution of transfer across a smooth boundary. For the intermediate wind regime, the middle segment was obtained from a field study in a small lake, and results from a wind-wave tank study were used for the high wind regime after applying some adjustments. This relationship is often considered the lower bound of gas transfer-wind speed relationships.

The quadratic relationship of Wanninkhof (1992) was constructed to follow the general shape of curves derived in wind-wave tanks but adjusted so that the global mean transfer velocity corresponds with the long-term global average gas transfer velocity determined from the invasion of bomb ¹⁴C into the ocean. Because the bomb ¹⁴C is also used as a diagnostic or tun-

(a) Calculated $\Delta p\text{CO}_2$ (Seawater - Air) for February 1995



(b) Calculated $\Delta p\text{CO}_2$ (Seawater - Air) for August 1995

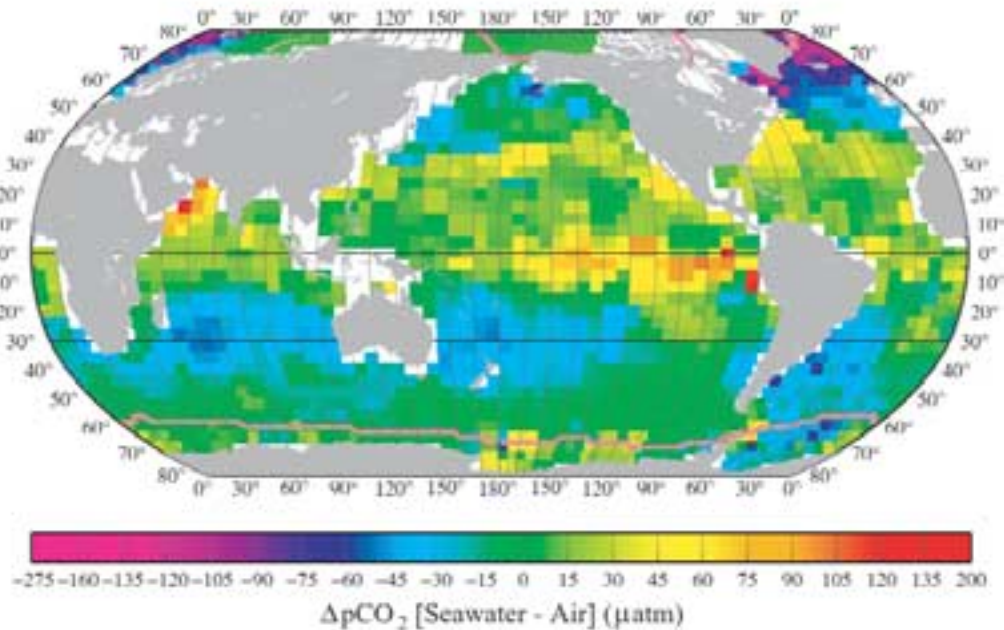


Figure 3. Distribution of climatological mean sea-air $p\text{CO}_2$ difference ($\Delta p\text{CO}_2$) for the reference year 1995 representing non-El Niño conditions in February (a) and August (b). These maps are based on about 940,000 measurements of surface water $p\text{CO}_2$ from 1958 through 2000. The pink lines indicate the edges of ice fields. The yellow-red colors indicate regions with a net release of CO_2 into the atmosphere, and the blue-purple colors indicate regions with a net uptake of CO_2 from the atmosphere. The mean monthly atmospheric $p\text{CO}_2$ value in each pixel in 1995, $(p\text{CO}_2)_{\text{air}}$, is computed using $(p\text{CO}_2)_{\text{air}} = (\text{CO}_2)_{\text{air}} \times (P_{\text{b}} - p\text{H}_2\text{O})$. $(\text{CO}_2)_{\text{air}}$ is the monthly mean atmospheric CO_2 concentration (mole fraction of CO_2 in dry air) from the GLOBALVIEW database (2000); P_{b} is the climatological mean barometric pressure at sea level from the Atlas of Surface Marine Data (1994); and the water vapor pressure, $p\text{H}_2\text{O}$, is computed using the mixed layer water temperature and salinity from the World Ocean Database (1998) of NODC/NOAA. The sea-air $p\text{CO}_2$ difference values in the reference year 1995 have been computed by subtracting the mean monthly atmospheric $p\text{CO}_2$ value from the mean monthly surface ocean water $p\text{CO}_2$ value in each pixel.

Table 1

Global oceanic CO₂ uptake estimates using different gas exchange-wind speed relationships and different wind speed products^a.

Relationship	Equation	Flux (Pg C yr ⁻¹)
Liss & Merlivat [1986]	$k = 0.17 U_{10}$ ($U_{10} < 3.6 \text{ m s}^{-1}$) $k = 2.85 U_{10} - 9.65$ ($3.6 \text{ m s}^{-1} < U_{10} < 13 \text{ m s}^{-1}$) $k = 5.9 U_{10} - 49.3$ ($U_{10} > 13 \text{ m s}^{-1}$)	-1.0
Wanninkhof [1992] [W-92]	$k = 0.39 U_{10}^2$ (long term averaged winds)	-1.8
Wanninkhof & McGillis (1999) [W&M-99]	$k = 1.09 U_{10} - 0.333 U_{10}^2 + 0.078 U_{10}^3$ (long term averaged winds)	-3.0
Nightingale et al. [2000]	$k = 0.333 U_{10} + 0.222 U_{10}^2$	-1.5
NCEP-41 year average winds ^b [W-92]	$k = 0.39 U_{10}^2$ (long term averaged winds)	-2.2
NCEP 6-hour winds ^c	$k = 0.31 U_{10}^2$ (instantaneous winds) [W-92]	-1.7
NCEP 6-hours winds ^c	$k = 0.0283 U_{10}^3$ [W&M-99]	-2.3

- a:** For these calculations the monthly $\Delta p\text{CO}_2$ climatology of Takahashi et al. (in press) was used according to: $F = k (Sc/660)^{1/2} s \Delta p\text{CO}_2$, Sc is the Schmidt number, which is determined for each pixel from climatological SST. The solubility s was determined from standard relationships with SST and salinity. Unless noted, the monthly mean NCEP wind speeds for 1995 were used.
- b:** Using the NCEP 41-year average monthly wind speed product rather than that of 1995.
- c:** Using the NCEP 6-hour wind product. In these cases, the instantaneous wind speed formulations of W-92 and W&M-99 were used.

ing parameter in global ocean biogeochemical circulation models, this parameterization yields internally consistent results when used with these models, making it one of the more favored parameterizations.

Using the same long-term global ¹⁴C constraint but basing the general shape of the curve on recent CO₂ flux observations over the North Atlantic determined using the covariance technique, Wanninkhof and McGillis (1999) proposed a significantly stronger (cubic) dependence with wind speed. This relationship shows a weaker dependence on wind for wind speeds less than 10 ms⁻¹ and a significantly stronger dependence at higher wind speeds. However, the relationship is not well constrained at high wind speeds because of the large scatter in the scarce

observations. Both the U² and U³ relationships fit within the data envelope of the study, but the U³ relationship provides a significantly better fit. Nightingale et al. (2000) determined a gas exchange-wind speed relationship based on the results of a series of experiments utilizing deliberately injected sulfur hexafluoride (SF₆), ³He and non-volatile tracers performed in the last decade.

The global oceanic CO₂ uptake using different wind speed/gas transfer velocity parameterizations differs by a factor of three (Table 1). The wide range of global CO₂ fluxes for the different relationships illustrates the large range of results and assumptions that are used to produce these relationships. Aside from differences in global oceanic CO₂ uptake, there are also significant regional differences. Figure 5 shows that the relationship of W&M-99 yields systematically lower evasion rates in the equatorial region and higher uptake rates at high latitudes compared with W-92, leading to significantly larger global CO₂ uptake estimates.

In addition to the non-unique dependence of gas exchange on wind speed, which causes a large spread in global air-sea CO₂ flux estimates, there are several other factors contributing to biases in the results. Global wind-speed data obtained from shipboard observations, satellites and data assimilation techniques show significant differences on regional and global scales. Because of the non-linearity of the relationships between gas exchange and wind speed, significant biases are introduced in methods of averaging

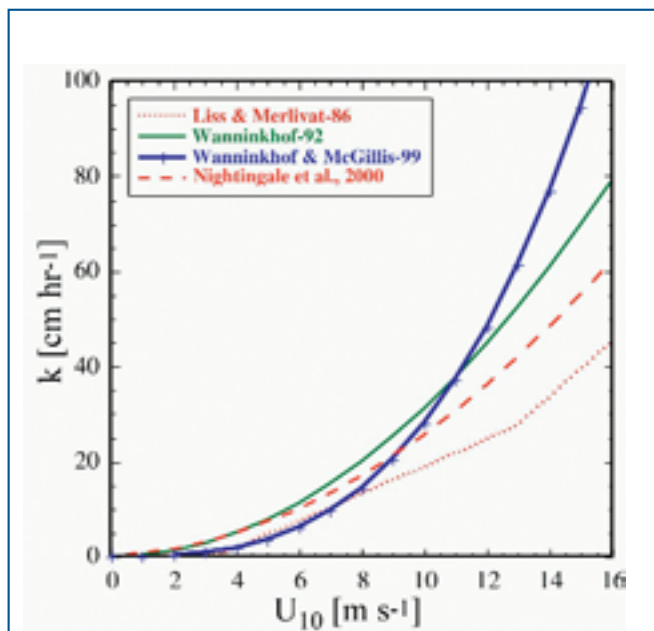


Figure 4. Graph of the different relationships that have been developed for the estimation of the gas transfer velocity, k , as a function of wind speed. The relationships were developed from wind-wave tank experiments, oceanic observations, global constraints and basic theory. The different forms of the relationships are summarized in Table 1. U_{10} is wind speed at 10 m above the sea surface.

Distribution of the Climatological Mean Net Sea-air CO₂ Flux

To illustrate the sensitivity of the gas transfer velocity and thus the sea-air CO₂ flux to wind speed, we have estimated the regional and global net sea-air CO₂ fluxes using two different formulations for the CO₂ gas transfer coefficient across the sea-air interface: the quadratic U² dependence of W-92 and the cubic U³ dependence of W&M-99. In addition, we have demonstrated the effects of wind-speed fields on the computed sea-air CO₂ flux using the National Center for Environmental Prediction (NCEP)-41 mean monthly wind speed and the NCEP-1995 mean monthly wind speed distributions over 4° × 5° pixel areas.

In Table 2 the fluxes computed using the W-92 and the NCEP/National Center for Atmospheric Research (NCAR) 41-year mean wind are listed in the first row for each grouping in column one (for latitudinal bands, oceanic regions and regional flux). The column "Errors in Flux" located at the extreme right of Table 2 lists the deviations from the mean flux that have been determined by adding or subtracting one standard deviation of the wind speed (about ± 2 m sec⁻¹ on the global average) from the mean monthly wind speed in each pixel area. These changes in wind speeds affect the regional and global flux values by about ± 25%. The fluxes computed using the single year mean wind speed data for 1995 are listed in the second line in each column one grouping in the table.

The global ocean uptake estimated using the W-92 and the NCEP 41-yr mean wind speeds is -2.2 ± 0.4 Pg C yr⁻¹. This is consistent with the ocean uptake flux of -2.0 ± 0.6 Pg C yr⁻¹ during the 1990s (Keeling et al., 1996; Battle et al., 2000) estimated from observed changes in the atmospheric CO₂ and oxygen variations.

The wind speeds for 1995 are much lower than the 41-year mean in the northern hemisphere and higher over the Southern Ocean. Accordingly, the northern ocean uptake of CO₂ is weaker than the climatological mean, and the Southern Ocean uptake is stronger. The global mean ocean uptake flux of -1.8 Pg C yr⁻¹ using the NCEP-1995 winds is about 18% below the climatological mean of -2.2 Pg C yr⁻¹, but it is within the ±25% error estimated from the standard deviation of the 41-yr mean wind speed data.

When the cubic wind speed dependence (W&M-99) is used, the CO₂ fluxes in higher latitude areas with strong winds are increased by about 50%, as are the errors associated with wind speed variability. The global ocean uptake flux computed with the 41-year mean wind speed data and the NCEP-1995 wind data is -3.7 Pg C yr⁻¹ and -3.0 Pg C yr⁻¹ respectively, an increase of about 70% over the fluxes computed from the W-92 dependence. These flux values are significantly greater than the flux based on atmospheric CO₂ and oxygen data (Keeling et al., 1996; Battle et al., 2000). However, the relative magnitudes of CO₂ uptake by ocean basins (shown in % in the regional flux grouping in the last four rows of Table 2) remain nearly unaffected by the

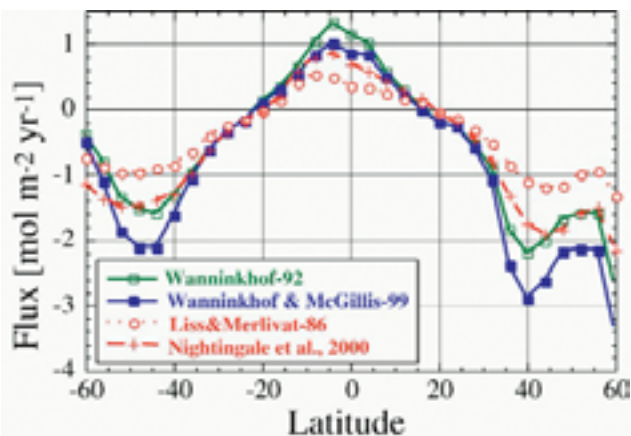


Figure 5. Effects of the various gas transfer/wind speed relationships on the estimated air-sea exchange flux of CO₂ in the ocean as a function of latitude. The global effects on the net air-sea flux are given in Table 1.

the product of gas transfer velocity and wind speed. The common approach of averaging the $\Delta p\text{CO}_2$ and k separately over monthly periods, determining the flux from the product and ignoring the cross product leads to a bias that is about 0.2 to 0.8 Pg C yr⁻¹ lower in the global uptake estimate. This bias shows a regional variation that is dependent on the distribution and magnitude of winds. This issue has been partly rectified in some of the relationships in which a global wind-speed distribution is used to create separate relationships between gas transfer and wind speed for short-term (a day or less) and long-term (a month or more) periods. Since wind-speed distributions are regionally dependent and vary on time scales of hours, this approach is far from perfect.

The groundwork of efforts laid over the past decade and recently improved technologies make the quantification of regional and global CO₂ fluxes a more tractable problem now. Satellites equipped with scatterometers that are used to determine wind speed offer daily global coverage. Moreover, these instruments measure sea-surface roughness that is directly related to gas transfer. This remotely sensed information, along with regional statistics of wind-speed variability on time scales shorter than a day, offers the real possibility that more accurate gas transfer velocities will be obtained. Efforts are underway to increase the coverage of $p\text{CO}_2$ through more frequent measurements and data assimilation techniques, again utilizing remote sensing of parameters such as sea-surface temperature and wind speed. Better quantification of the fluxes will lead to better boundary conditions for models and improved forecasts of atmospheric CO₂ concentrations.

choice of the wind-speed dependence of the gas transfer velocity.

The distribution of winds can also influence the calculated gas transfer velocity. This is because of the non-linear dependence of gas exchange with wind speed; long-term average winds underestimate flux especially for strongly non-linear dependencies. To avoid this bias, the relationships are adjusted by assuming that the global average wind speed is well represented by a Rayleigh distribution function. As noted by Wanninkhof et al. (in press), this overestimates the flux. A more appropriate way to deal with the issue of wind speed variability is to use short-term winds. If the NCEP 6-hour wind products are used, the global flux computed using the W&M-99 cubic wind-speed formulation decreases from -3.7 to -3.0 Pg C yr⁻¹ for the NCEP 41-year winds and from -3.0 to -2.3 Pg C yr⁻¹ for the NCEP 1995 wind data.

The relative importance of the major ocean basins in the ocean uptake of CO₂ may be assessed on the basis of the CO₂ fluxes obtained from our pCO₂ data and W-92 gas transfer velocity (Table 2 and Figure 6). The Atlantic Ocean as a whole, which has 23.5% of the global ocean area, is the region with the strongest net CO₂ uptake (41%). The high-latitude northern North Atlantic, including the Greenland, Iceland and Norwegian seas, is responsible for a substantial amount of this CO₂ uptake while representing only 5% of the global ocean in area. This reflects a combination of two factors: the intense summertime primary production and the low CO₂ concentrations in subsurface waters associated with recent ventilation of North Atlantic subsurface waters. The Pacific Ocean as a whole takes up the smallest amount of CO₂ (18% of the total) in spite of its size (49% of the total ocean area). This is because mid-latitude

uptake (about 1.1 Pg C yr⁻¹) is almost compensated for by the large equatorial release of about 0.7 Pg C yr⁻¹. If the equatorial flux were totally eliminated, as during very strong El Niño conditions, the Pacific would take up CO₂ to an extent comparable to the entire North and South Atlantic Ocean. The southern Indian Ocean is a region of strong uptake in spite of its small area (15% of the total). This may be attributed primarily to the cooling of tropical waters flowing southward in the western South Indian Ocean.

Table 2

The effects of wind speeds and the wind-speed dependence of CO₂ gas transfer velocity on the net sea-air CO₂ flux are shown using the climatological sea-air pCO₂ difference obtained in this work. The flux values have been computed using the (wind speed)² dependence of CO₂ gas transfer velocity by Wanninkhof (1992, W-92) and the (wind speed)³ dependence by Wanninkhof and McGillis (1999, W&M-99) respectively for each of the two sets of wind data: the NCEP/NCAR 41-year (named 41-yr in the table) and 1995 mean monthly wind speeds. Errors in flux (% in the flux) listed in the extreme right column represent the flux changes resulting from + or - one standard deviation (about + 2 m sec⁻¹ on the global average) from the annual mean wind speed in each pixel area. The positive errors in the flux represent an increase in the mean monthly wind speed over each pixel area by one standard deviation; and the negative errors represent a reduction of the mean wind speed by one standard deviation.

Lat. Band	Gas Trans./ Wind Data	Pacific Ocean Pg C yr ⁻¹	Atlantic Ocean Pg C yr ⁻¹	Indian Ocean Pg C yr ⁻¹	Southern Ocean Pg C yr ⁻¹	Global Ocean Pg C yr ⁻¹	Errors in Flux o/o
N of 50°N	W-92/41-yr	+0.01	-0.40	-0.39	+28%,-23%
	W-92/1995	+0.03	-0.18	-0.14	
	W&M-99/41-yr	+0.03	-0.55	-0.52	+44%,-35%
	W&M-99/1995	+0.07	-0.17	-0.10	
14°N-50°N	W-92/41-yr	-0.64	-0.34	+0.07	-0.92	+25%,-23%
	W-92/1995	-0.29	-0.28	+0.03	-0.54	
	W&M-99/41-yr	-0.94	-0.48	+0.10	-1.31	+43%,-32%
	W&M-99/1995	-0.29	-0.38	+0.02	-0.64	
14°N-14°S	W-92/41-yr	+0.74	+0.15	+0.18	+1.07	+29%,-24%
	W-92/1995	+0.61	+0.07	+0.15	+0.83	
	W&M-99/41-yr	+0.67	+0.14	+0.20	+1.00	+43%,-31%
	W&M-99/1995	+0.62	+0.05	+0.12	+0.79	
14°S-50°S	W-92/41-yr	-0.51	-0.33	-0.67	-1.51	+22%,-20%
	W-92/1995	-0.57	-0.31	-0.50	-1.38	
	W&M-99/41-yr	-0.68	-0.51	-0.97	-2.16	+37%,-30%
	W&M-99/1995	-0.88	-0.51	-0.63	-2.02	
S of 50°S	W-92/41-yr	-0.47	-0.47	+26%,-21%
	W-92/1995	-0.58	-0.58	
	W&M-99/41-yr	-0.74	-0.74	+41%,-32%
	W&M-99/1995	-1.02	-1.02	
.....	
Oceanic Regions	W-92/41-yr	-0.40	-0.92	-0.43	-0.47	-2.22	+22%,-19%
	W-92/1995	-0.21	-0.69	-0.33	-0.58	-1.81	
	W&M-99/41-yr	-0.92	-1.39	-0.67	-0.74	-3.72	+40%,-32%
	W&M-99/1995	-0.48	-1.01	-0.48	-1.02	-3.00	
Regional Flux (%)	W-92/41-yr	18	41	19	21	100	
	W-92/1995	12	38	18	32	100	
	W&M-99/41-yr	25	37	18	20	100	
	W&M-99/1995	16	34	16	34	100	

Mean Annual Air-Sea Flux for 1995

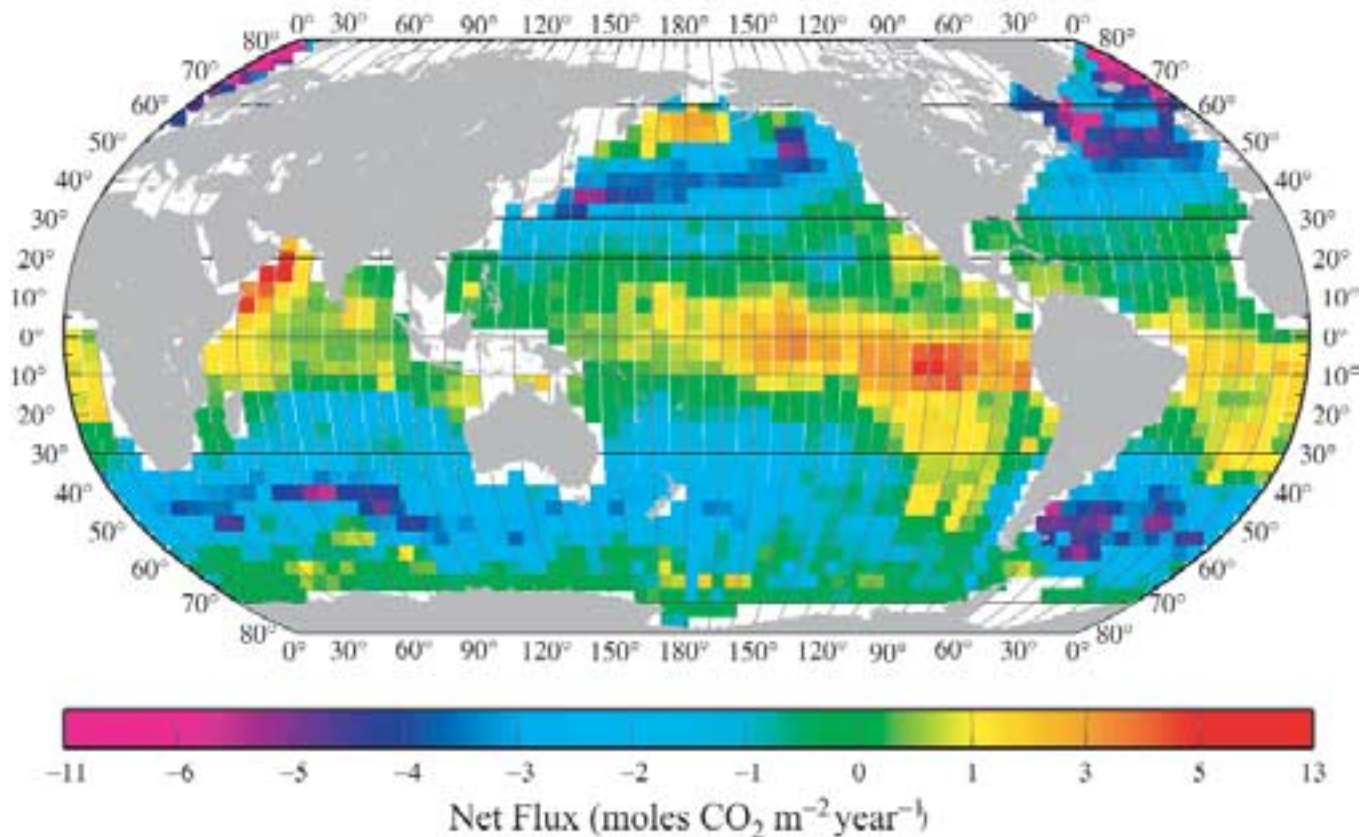


Figure 6. Distribution of the climatological mean annual sea-air CO₂ flux (moles CO₂ m⁻² yr⁻¹) for the reference year 1995 representing non-El Niño conditions. This has been computed using the mean monthly distribution of sea-air pCO₂ difference, the climatological NCEP 41-year mean wind speed and the wind-speed dependence of the CO₂ gas transfer velocity of Wanninkhof (1992). The yellow-red colors indicate a region characterized by a net release of CO₂ to the atmosphere, and the blue-purple colors indicate a region with a net uptake of CO₂ from the atmosphere. This map yields an annual oceanic uptake flux for CO₂ of 2.2 ± 0.4 Pg C yr⁻¹.

Distribution of Anthropogenic CO₂ in the Oceans

To understand the role of the oceans as a sink for anthropogenic CO₂, it is important to determine the distribution of carbon species in the ocean interior and the processes affecting the transport and storage of CO₂ taken up from the atmosphere. Figure 7 shows the typical north-south distribution of DIC in the Atlantic, Indian, and Pacific oceans prior to the introduction of anthropogenic CO₂. In general, DIC is about 10–15% higher in deep waters than at the surface. Concentrations are also generally lower in the Atlantic than the Indian ocean, with the highest concentrations found in the older deep waters of the North Pacific. The two basic mechanisms that control the distribution of carbon in the oceans are the solubility and biological pumps.

The solubility pump is driven by two interrelated factors. First, CO₂ is more than twice as soluble in cold

polar waters than in warm equatorial waters. As western surface boundary currents transport water from the tropics to the poles, the waters are cooled and absorb more CO₂ from the atmosphere. Second, the high-latitude zones are also regions where intermediate and bottom waters are formed. As these waters cool, they become denser and sink into the ocean interior, taking with them the CO₂ accumulated at the surface.

The primary production of marine phytoplankton transforms CO₂ and nutrients from seawater into organic material. Although most of the CO₂ taken up by phytoplankton is recycled near the surface, a substantial fraction, perhaps 30%, sinks into the deeper waters before being converted back into CO₂ by marine bacteria. Only about 0.1% reaches the seafloor to be buried in the sediments. The CO₂ that is recycled at depth is slowly transported over long distances by the large-scale thermohaline circulation. DIC slowly accumulates

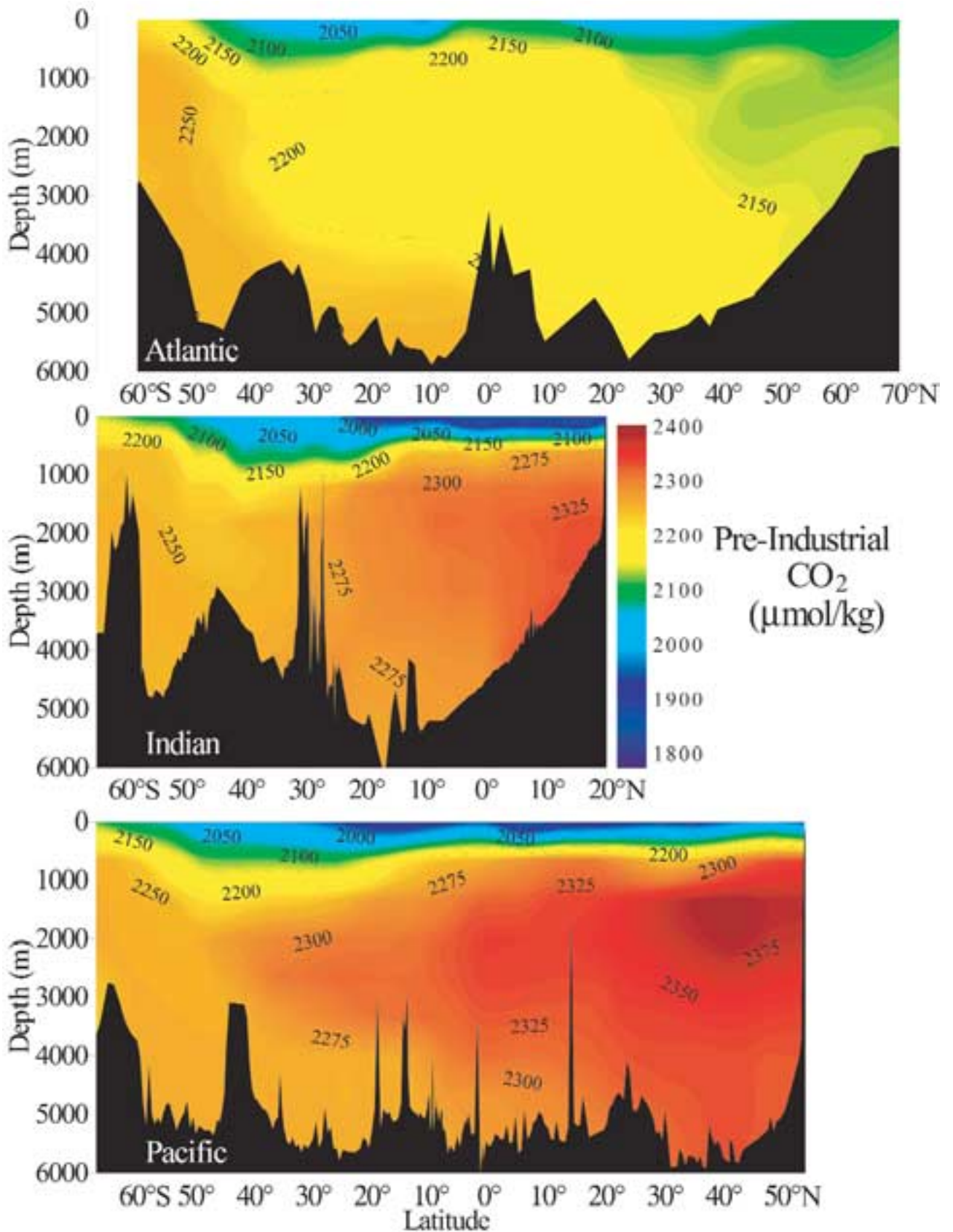


Figure 7. Zonal mean pre-industrial distributions of dissolved inorganic carbon (in units of $\mu\text{mol kg}^{-1}$) along north-south transects in the Atlantic, Indian and Pacific oceans. The Pacific and Indian Ocean data are from the Global CO₂ Survey (this study), and the Atlantic Ocean data are from Gruber (1998).

in the deep waters as they travel from the Atlantic to the Indian and Pacific oceans. Using a 3-D global carbon model, Sarmiento et al. (1995) estimated that the natural solubility pump is responsible for about 20% of the vertical gradient in DIC; the remaining 80% originates from the biological pump.

The approaches for estimating anthropogenic CO₂ in the oceans have taken many turns over the past decade. Siegenthaler and Sarmiento (1993) summarized early approaches for estimating the anthropogenic sink in the oceans, including ocean models of various complexity, atmospheric measurements and transport models used together with pCO₂ measurements and estimates based on changes in oceanic ¹³C and oxygen mass balance. They noted the wide range of ocean uptake estimates (1.6 – 2.3 Pg C yr⁻¹) and concluded that the larger uptake estimates from the models were the most reliable.

The first approaches for using measurements to isolate anthropogenic CO₂ from the large, natural DIC signal were independently proposed by Brewer (1978) and Chen and Millero (1979). Both these approaches were based on the premise that the anthropogenic DIC concentration could be isolated from the measured DIC by subtracting the contributions of the biological pump and the physical processes, including the pre-industrial source water values and the solubility pump.

Gruber et al. (1996) improved the earlier approaches by developing the ΔC* method. This method is based on the premise that the anthropogenic CO₂ concentration (C^{ant}) can be isolated from measured DIC values (C^m) by subtracting the contribution of the biological pumps (ΔC^{bio}), the DIC the waters would have in equilibrium with a preindustrial atmospheric CO₂ concentration of 280 ppm (C^{eq280}), and a term that corrects for the fact that surface waters are not always in equilibrium with the atmosphere (ΔC^{diseq}):

$$C^{\text{ant}} = C^{\text{m}} - \Delta C^{\text{bio}} - C^{\text{eq280}} - C^{\text{diseq}} = \Delta C^* - \Delta C^{\text{diseq}} \quad (2)$$

The three terms to the right of the first equal sign make up ΔC*, which can be explicitly calculated for each sample. The fact that ΔC* is a quasi-conservative tracer helps remedy some of the mixing concerns arising from the earlier techniques (Sabine and Feely, 2001). The ΔC^{diseq} term is evaluated over small isopycnal intervals using a water-mass age tracer such as CFCs.


We have evaluated anthropogenic CO₂ for the Atlantic, Indian, and Pacific oceans using the ΔC* approach. Figure 8 shows representative sections of anthropogenic CO₂ for each of the ocean basins. Surface values range from about 45 to 60 μmol kg⁻¹. The deepest penetrations are observed in areas of deep water formation, such as the North Atlantic, and intermediate water formation, such as 40–50°S. Integrated water column inventories of anthropogenic CO₂ exceed 60 moles m⁻² in the North Atlantic (Figure 9). Areas where older waters are upwelled, like the high-latitude

waters around Antarctica and Equatorial Pacific waters, show relatively shallow penetration. Consequently, anthropogenic CO₂ inventories are all less than 40 moles m⁻² in these regions (Figure 9).

Data-based estimates indicate that the oceans have taken up approximately 105 ± 8 Pg C since the beginning of the industrial era. Current global carbon models generally agree with the total inventory estimates, but discrepancies still exist in the regional distribution of the anthropogenic inventories. Some of these discrepancies stem from deficiencies in the modeled circulation and water mass formation. There are also a number of assumptions in the data-based approaches regarding the use of constant stoichiometric ratios and time-invariant air-sea disequilibria that may be inadequate in some regions. These are all areas of current research. Anthropogenic estimates should continue to converge as both the models and the data-based approaches are improved with time.

Conclusions

As CO₂ continues to increase in the atmosphere, it is important to continue the work begun with the Global Survey of CO₂ in the Ocean. Because CO₂ is an acid gas, the uptake of anthropogenic CO₂ consumes carbonate ions and lowers the pH of the ocean. The carbonate ion concentration of surface seawater in equilibrium with the atmosphere will decrease by about 30% and the hydrogen ion concentration will increase by about 70% with a doubling of atmospheric CO₂ from pre-industrial levels (280 to 560 ppm). As the carbonate ion concentration decreases, the buffering capacity of the ocean and its ability to absorb more CO₂ from the atmosphere is diminished. Over the long term (millennial time scales) the ocean has the potential to absorb as much as 85% of the anthropogenic CO₂ that is released into the atmosphere. Because the lifetime of fossil fuel CO₂ in the atmosphere ranges from decades to centuries, mankind's reliance on fossil fuel for heat and energy will continue to have a significant effect on the chemistry of the earth's atmosphere and oceans and therefore on our climate for many centuries to millennia.

Plans are being formulated in several countries, including the United States, to establish a set of repeat sections to document the increasing anthropogenic inventories in the oceans. Most of these sections will follow the lines occupied during the WOCE Hydrographic Programme on which JGOFS investigators made CO₂ survey measurements. The current synthesis effort will provide an important baseline for assessment of future changes in the carbon system. The spatially extensive information from the repeat sections, together with the temporal records from the time-series stations and the spatial and temporal records available from automated surface pCO₂ measurements on ships of opportunity, will greatly improve our understanding of the ocean carbon system and provide better constraints on potential changes in the future. 

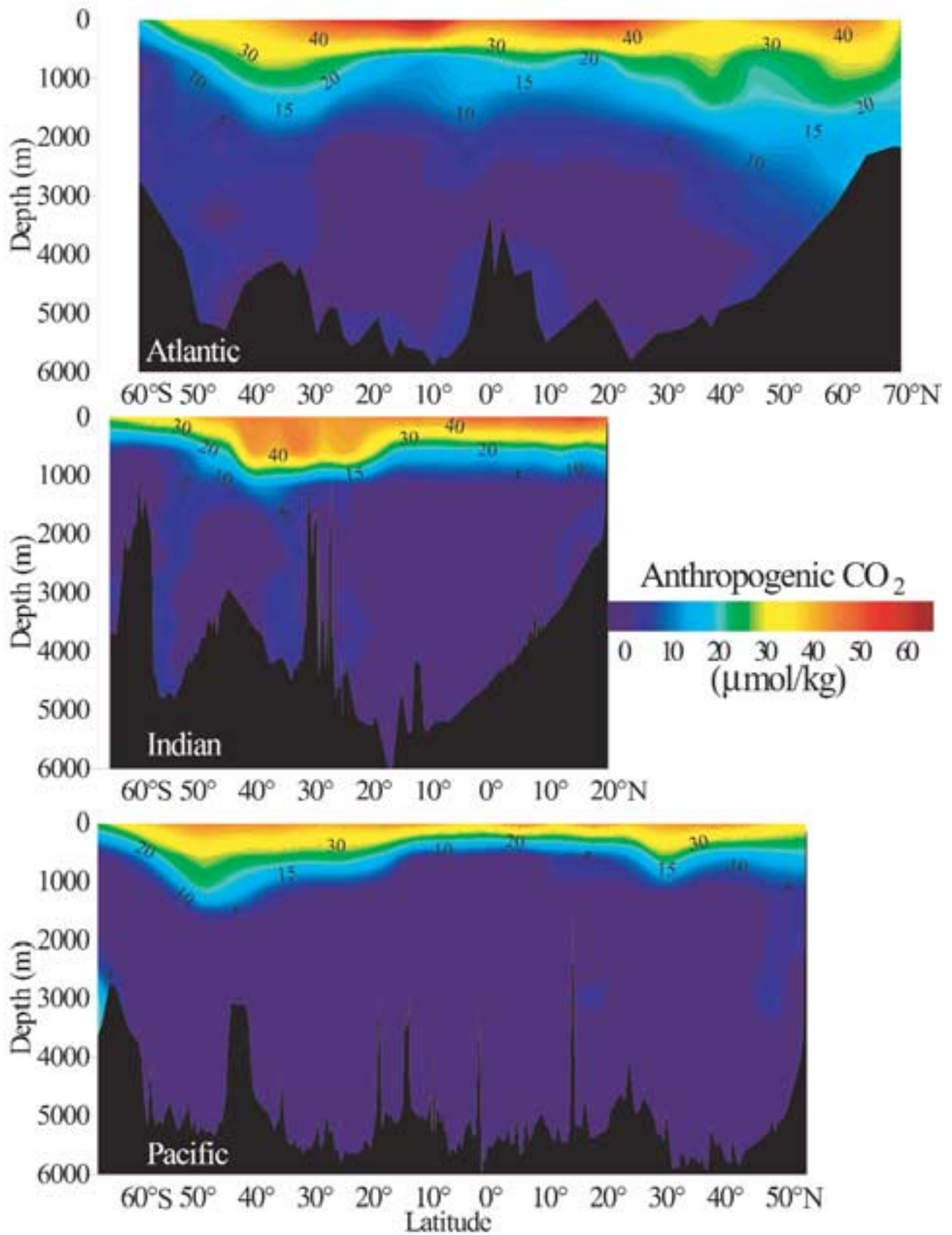


Figure 8. Zonal mean distributions of estimated anthropogenic CO₂ concentrations (in units of μmol kg⁻¹) along north-south transects in the Atlantic, Indian and Pacific oceans. The Pacific and Indian Ocean data are from the Global CO₂ Survey (this study), and the Atlantic Ocean data are from Gruber (1998).

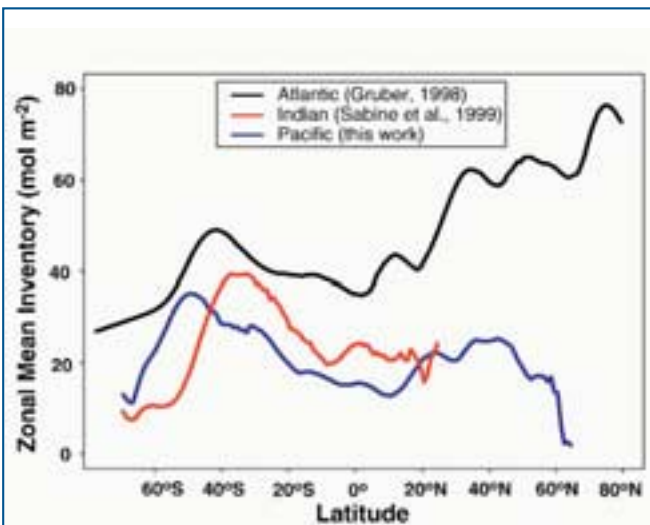


Figure 9. Zonal mean anthropogenic CO₂ inventories (in units of moles m⁻²) in the Atlantic, Indian and Pacific oceans.

Acknowledgements

The authors are grateful to the members of the CO₂ Science Team and the JGOFS and WOCE investigators for making their data available for this work. We thank Lisa Dilling of the National Oceanic and Atmospheric Administration (NOAA) Office of Global Programs, Don Rice of the National Science Foundation and Mike Riches of the Department of Energy (DOE) for their efforts in coordinating this research. This work was supported by DOE and NOAA as a contribution to the U.S. JGOFS Synthesis and Modeling Project (Grant No. GC99-220) and by grants to Taro Takahashi from NSF (OPP-9506684) and NOAA (NA16GP01018). This publication was supported by the Joint Institute for the Study of the Atmosphere and Ocean (JISAO) under NOAA Cooperative Agreement #NA67RJO155, Contribution #832, and #2331 from the NOAA/Pacific Marine Environmental Laboratory. This is U.S. JGOFS Contribution Number 683.

References

Atlas of Surface Marine Data, 1994: CD-ROM NODC-56, Ocean Climate Laboratory, NOAA.

Bates, N.R., 2001: Interannual variability of oceanic CO₂ and biogeochemical properties in the Western North Atlantic subtropical gyre. *Deep-Sea Res. II*, 48(8–9), 1507–1528.

Battle, M., M.L. Bender, P.P. Tans, J.W.C. White, J.T. Ellis, T. Conway and R.J. Francey, 2000: Global carbon sinks and their variability inferred from atmospheric O₂ and δ¹³C. *Science*, 287, 2467–2470.

Brewer, P.G., 1978: Direct observation of oceanic CO₂ increase. *Geophys. Res. Lett.*, 5, 997–1000.

Chen, C.T. and F.J. Millero, 1979: Gradual increase of oceanic CO₂. *Nature*, 277, 205–206.

Feely, R.A., R. Wanninkhof, T. Takahashi and P. Tans, 1999: The influence of the equatorial Pacific contri-

bution to atmospheric CO₂ accumulation. *Nature*, 398, 597–601.

GLOBALVIEW-CO₂: Cooperative Atmospheric Data Integration Project - Carbon Dioxide, 2000. CD-ROM, NOAA CMDL, Boulder, CO. Also available on Internet via anonymous FTP to ftp.cmdl.noaa.gov, Path: ccg/co2/GLOBALVIEW.

Gruber, N., J.L. Sarmiento and T.F. Stocker, 1996: An improved method for detecting anthropogenic CO₂ in the oceans. *Global Biogeochem. Cycles*, 10, 809–837.

Gruber, N., 1998: Anthropogenic CO₂ in the Atlantic Ocean. *Global Biogeochem. Cycles*, 12, 165–191.

Inoue, H.Y., H. Mastueda, M. Ishii, K. Fushimi, M. Hirota, I. Asanuma and Y. Takasugi, 1995: Long-term trend of the partial pressure of carbon dioxide (pCO₂) in surface waters of the western North Pacific 1984–1993. *Tellus*, 47B, 391–413.

Keeling, C.D. and T.P. Whorf, 2000: Atmospheric CO₂ concentrations—Mauna Loa Observatory, Hawaii, <http://cdiac.esd.ornl.gov/npds/npd001.html>, Carbon dioxide Information and Analysis Center, Oak Ridge, TN.

Keeling, R., S.C. Piper and M. Heinmann, 1996: Global and hemispheric CO₂ sinks deduced from changes in atmospheric O₂ concentration. *Nature*, 381, 218–221.

Liss, P.S. and L. Merlivat, 1986: Air-sea gas exchange rates: Introduction and synthesis. In: *The Role of Air-Sea Exchange in Geochemical Cycling*. P. Buat-Menard, ed., Reidel, Boston, 113–129.

Nightingale, P.D., G. Malin, C.S. Law, A.J. Watson, P.S. Liss, M.I. Liddicoat, J. Boutin and R.C. Upstill-Goddard, 2000: *In situ* evaluation of air-sea gas exchange parameterizations using novel conservative and volatile tracers. *Global Biogeochem. Cycles*, 14, 373–387.

Sabine, C.L. and R.A. Feely, 2001: Comparison of recent Indian Ocean anthropogenic CO₂ estimates with a historical approach. *Global Biogeochem. Cycles*, 15(1), 31–42.

Sarmiento, J.L., R. Murnane and C. LeQuere, 1995: Air-sea CO₂ transfer and the carbon budget of the North Atlantic. *Philos. Trans. R. Soc. Lond. (B Biol. Sci.)*, 348, 211–219.

Siegenthaler, U. and J.L. Sarmiento, 1993: Atmospheric carbon dioxide and the ocean. *Nature*, 365, 119–125.

Takahashi, T., S.C. Sutherland, C. Sweeney, A. Poisson, N. Metzl, B. Tillbrook, N. Bates, R. Wanninkhof, R.A. Feely, C. Sabine, J. Olafsson and Y. Nojiri, 2001: Global sea-air CO₂ flux based on climatological surface ocean pCO₂, and seasonal biological and temperature effects, *Deep-Sea Res. I*, in press.

Wanninkhof, R., 1992: Relationship between gas exchange and wind speed over the ocean. *J. Geophys. Res.*, 97, 7373–7381.

Wanninkhof, R. and W.M. McGillis, 1999: A cubic relationship between gas transfer and wind speed. *Geophys. Res. Lett.*, 26, 1889–1893.

Wanninkhof, R., S. Doney, T. Takahashi and W. McGillis: The Effect of Using Time-Averaged Winds on Regional Air-Sea CO₂ Fluxes. In: *Gas Transfer at Water Surfaces*. M. Donelan, W. Drennan, E. Saltzman and R. Wanninkhof, eds., AGU, Washington, in press.

Putting Together the Big Picture: Remote-sensing Observations of Ocean Color

James A. Yoder

National Science Foundation • Arlington, Virginia USA

J. Keith Moore

National Center for Atmospheric Research • Boulder, Colorado USA

Robert N. Swift

EG&G Technical Services, Inc. • Wallops Island, Virginia USA

Introduction

Observations of ocean color from space have been part of the U.S. JGOFS strategy for discerning temporal and spatial variations in upper-ocean productivity on the global scale since the first planning workshops for a U.S. global ocean flux program (National Academy of Sciences, 1984). From the start, remote measurements of near-surface chlorophyll *a* concentrations were envisaged as the major tool for extrapolating upper-ocean chemical and biological measurements in time and space and linking calculations of new and primary production with the flux of particulate material through the water column.

In 1986, researchers at the U.S. National Aeronautics and Space Administration (NASA) Goddard Space Flight Center published the first monthly composite of images from the Nimbus-7 Coastal Zone Color Scanner (CZCS), an ocean color instrument that had been in orbit since 1978. These images showed basin-scale views of phytoplankton chlorophyll distributions for the first time (Esaías et al., 1986). These new images, coupled with the JGOFS requirement for satellite ocean-color measurements, rejuvenated interest at NASA and other space agencies in launching successors to the CZCS.

CZCS stopped operating during 1986. By spring 1988, when the initial planning workshop for the international North Atlantic Bloom Experiment (NABE) was held, it was apparent that data from a new sensor would not be available for the first JGOFS field program, scheduled to begin in the North Atlantic in spring 1989. Because of launch delays and other technical problems, the next ocean-color instrument, the Sea-viewing Wide Field-of-view Sensor (SeaWiFS), was not launched into space until August 1997. Thus satellite ocean-color observations were available only for the Antarctic Environment and Southern Ocean Process Study (AESOPS), the final U.S. JGOFS field program.

Nevertheless, satellite and aircraft ocean-color measurements had an important role in JGOFS. First, retrospective analyses of CZCS chlorophyll images were important for planning all of the U.S. JGOFS process studies (Feldman et al., 1992). Second, aircraft remote-sensing measurements were part of the field studies in the North Atlantic, equatorial Pacific and Arabian Sea. Third, SeaWiFS data collected during AESOPS were used to extrapolate *in situ* measurements made during the field study, making possible a basin-scale calculation of primary production and particulate organic carbon (POC). Finally, data from CZCS, SeaWiFS, the Ocean Color and Temperature Sensor (OCTS), and the Polarization and Directionality of the Earth's Reflectances (POLDER) sensor are contributing substantially to the analyses and modeling studies of the U.S. JGOFS Synthesis and Modeling Project (SMP) (see Doney et al., this issue).

Satellite ocean-color sensors provide the only global ocean measurements on roughly monthly time scales that are directly related to biogeochemical distributions and processes. Thus, new satellite ocean color sensors, such as the Moderate-resolution Imaging Spectroradiometer (MODIS) launched by NASA on the Terra spacecraft in 1999, will play an important and perhaps extended role in future studies of global biogeochemical cycles (Yoder, 2000). Future sensors may be able to provide remote-sensing data on key phytoplankton taxonomic groups, the distribution of POC and chromophoric dissolved organic matter (CDOM) and chlorophyll fluorescence and an index of photosynthetic efficiency.

Background

“Ocean color” is a shorthand term for a specific set of *in situ* measurements from instruments on aircraft or spacecraft used to determine the radiance backscattered

from water and across the air-sea interface at some or many spectral bands. A more formal name for ocean color is ocean spectral reflectance (R) or water-leaving spectral radiance (L_w). Normalized water-leaving radiance (nL_w) and Remote Sensing Reflectance (R_{rs}) are variations of L_w and R that take into account sun angles and atmospheric contributions. Water-leaving radiance is proportional to the backscatter coefficient (bb) and inversely proportional to the absorption coefficient (a) in the equation $L_w @ b_b/a$. The contribution of backscatterers and absorbers are basically additive so that a simple expansion of the basic equation above provides a realistic and useful conceptual and quantitative description of water-leaving radiance.

The principal absorbers at the wavelengths of current satellite sensors are water molecules, phytoplankton pigments, CDOM and particulate detritus. The latter two components have similar absorption properties and are often lumped together. Important backscatterers are water molecules, particularly at comparatively short (blue) wavelengths, phytoplankton and detrital particles, and non-biogenic sediments in coastal waters. Bacteria, viruses, colloids and small bubbles are potentially important components of the backscattering signal; there is much current debate as to their relative contributions.

The U.S. JGOFS Air Corps: Ocean-Color Measurements At Low Altitude

Because satellite ocean-color data were not available at the time, aircraft measurements were used to support some cruise legs during U.S. JGOFS process studies in the North Atlantic, equatorial Pacific and Arabian Sea. Open-ocean field programs are difficult to support with aircraft observations because of the logistical problems posed by the long distances between airports and the study sites. The only aircraft with long-distance capabilities that was routinely available to the JGOFS program was the P-3 operated by the NASA Wallops Flight Facility (Figure 1).

NASA P-3 aircraft flew during portions of the JGOFS pilot study in the North Atlantic in 1989 (NABE), the Equatorial Pacific Process Study (EqPac) in 1992 and the Arabian Sea Process Study in 1994-96. The P-3 flies at low altitude (150 m off the sea surface) and thus below cloud cover. Because of the low altitude, data are collected and displayed along track lines rather than as images.

The primary instrument on the aircraft during the U.S. JGOFS field studies was the NASA Airborne Oceanographic LIDAR (AOL) sensor (Hoge et al., 1986). The AOL is an active sensor that, during the JGOFS overflights, acquired laser-induced fluorescence with excitation at 355 and 532 nm from constituents in the water in contiguous bands 10-nm wide between 390 and 750 nm (Figure 2). The 355 nm laser excites CDOM fluorescence over a broad spectral region centered near 450 nm. The 532 nm laser induces

chlorophyll *a* fluorescence at 685 nm and phycoerythrin fluorescence in bands centered at 560 and 590 nm. To remove effects of variability in attenuation properties in the upper layer of the ocean along the flight path, the fluorescence signals are normalized by the water Raman backscatter resulting from the laser inducing the fluorescence.

In addition to active and passive optical measurements, sea-surface temperature measurements were made with a Heimann infrared radiometer and recorded by the AOL along with the laser-induced fluorescence data. The P-3 also deployed airborne expendable bathythermographs (AXBTs) for vertical temperature profiles.

Data collected during each flight were rapidly processed and results sent by fax, along with a brief report, to oceanographic ships in the study area as well as to other investigators within a few hours of collection. During NABE, AXBT temperature profiles, estimates of chlorophyll *a* concentrations and other data were sent back to a Harvard University ocean modeling group that used the information to set initial conditions for mesoscale models of eddy circulation within the 47°N, 20°W study area (Robinson et al., 1993). In turn, results of model simulations were sent out to the ships and used to help determine and adjust sampling protocols.

In addition to the real-time support for the field studies that the aircraft measurements provided, more extensive analyses of the data helped to demonstrate and quantify the importance of mesoscale variability in the North Atlantic and the close relationship between



Figure 1. During JGOFS-NABE overflights, the U.S. JGOFS Air Corps and the NASA P-3 airplane on the tarmac in Iceland.

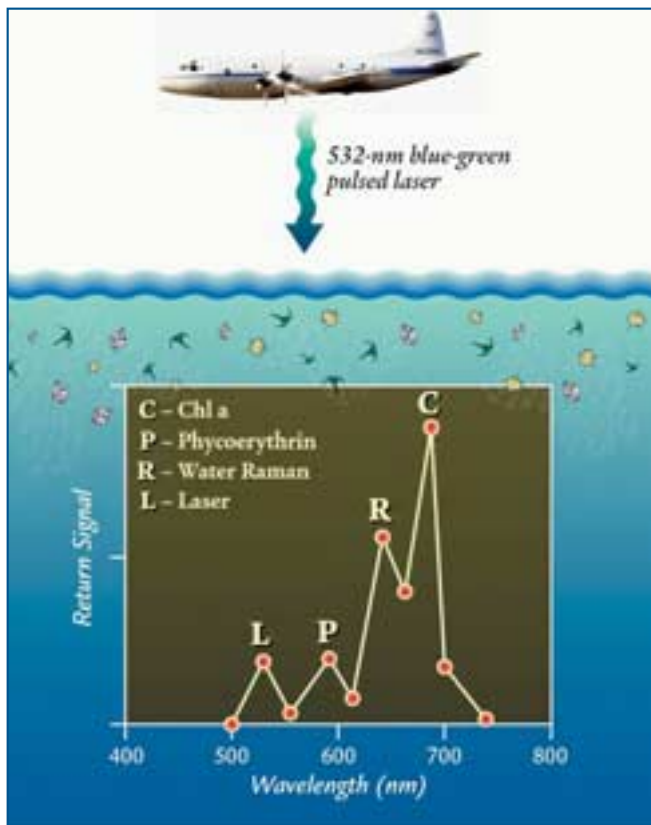


Figure 2. Schematic diagram of the operation of the Airborne Oceanographic Lidar (AOL) and the detected signals (inset). Laser pulses stimulate phytoplankton chlorophyll *a* and phycoerythrin fluorescence (C and P respectively). The on-wavelength laser return signal (L) is used to estimate particle scattering, and the water Raman signal (R) is used to correct for variable laser penetration depths.

temperature and variability in phytoplankton chlorophyll (Robinson et al., 1993). The results were also used to help interpret observations from Marine Light in the Mixed Layer (MLML) moorings south of Iceland that were deployed at the same time as the NABE cruises (see Dickey, this issue). Combining the spatial information from aircraft measurements of surface chlorophyll *a* with the temporal information from the moorings showed that a significant component of the variability at the mooring was caused by advection of phytoplankton patches. These studies in the North Atlantic concluded that there were consistent relationships between the mesoscale patterns of physical parameters and chlorophyll *a* distributions.

Real-time aircraft observations also played an important role during EqPac. Researchers and instruments on P-3 overflights in August 1992 observed very high concentrations of phytoplankton associated with a frontal feature near 2°N, 140°W (Yoder et al., 1994). The observations and positions were radioed from the plane to R/V *Thomas G. Thompson*, which was operat-

ing nearby. The information was used by the oceanographers aboard ship to find and sample this unusual feature.

Ocean-color remote sensing had an interesting and somewhat controversial role in the U.S. JGOFS Arabian Sea study, contributing to a debate over what causes certain patterns observed in the region. CZCS images of the Arabian Sea (Brock and McClain, 1992) suggested that there was a significant area of intense open-ocean upwelling with high concentrations of chlorophyll *a*. One investigation based on analyses of global CZCS imagery (Yoder et al., 1993) referred to the apparently high chlorophyll concentrations following the southwest monsoon in the Arabian Sea as a “major subtropical anomaly.” Although SeaWiFS images show similar patterns, investigators have questioned their interpretation. The question is whether plumes of dust blowing off the nearby desert and over the ocean can lead to inaccurately high results for chlorophyll *a* in remote measurements of ocean color.

Aerosol studies during the Arabian Sea cruises showed that dust concentrations at the ocean surface are not higher during the southwest monsoon than during other seasons (Tindale and Pease, 1999). However, sea-salt aerosol concentrations are exceptionally high because of the strong winds. It is possible that the absorption properties of sea-salt aerosols could produce misleadingly high chlorophyll signals in remote measurements.

Given these data, some investigators have questioned the extent of open-ocean upwelling in the Arabian Sea and the significance of the southwest monsoon period for annual Arabian Sea productivity. Other studies show that open ocean chlorophyll *a* concentrations are at annually high levels during the southwest monsoon (Kinkade et al., 2001), although not as high as inferred from CZCS and SeaWiFS imagery. In summary, satellite ocean-color images of the Arabian Sea may well have overemphasized the significance of the upwelling associated with annual southwest monsoons for annual productivity in the region.

Satellite Observations in the Southern Ocean

Ocean-color data collected over the last two decades has provided key insights into the spatial distribution of phytoplankton blooms and the processes controlling primary production in the Southern Ocean. This information was of material assistance in planning JGOFS field studies in the region. Initial studies using CZCS data and recently more detailed studies using SeaWiFS data (Moore and Abbott, 2000) showed that chlorophyll concentrations are perpetually low over most of the Southern Ocean. The satellite data revealed that phytoplankton blooms are largely restricted to three zones: coastal waters, the marginal ice zone and the major Southern Ocean fronts. Both the European JGOFS transect along 6°W and the AESOPS transect

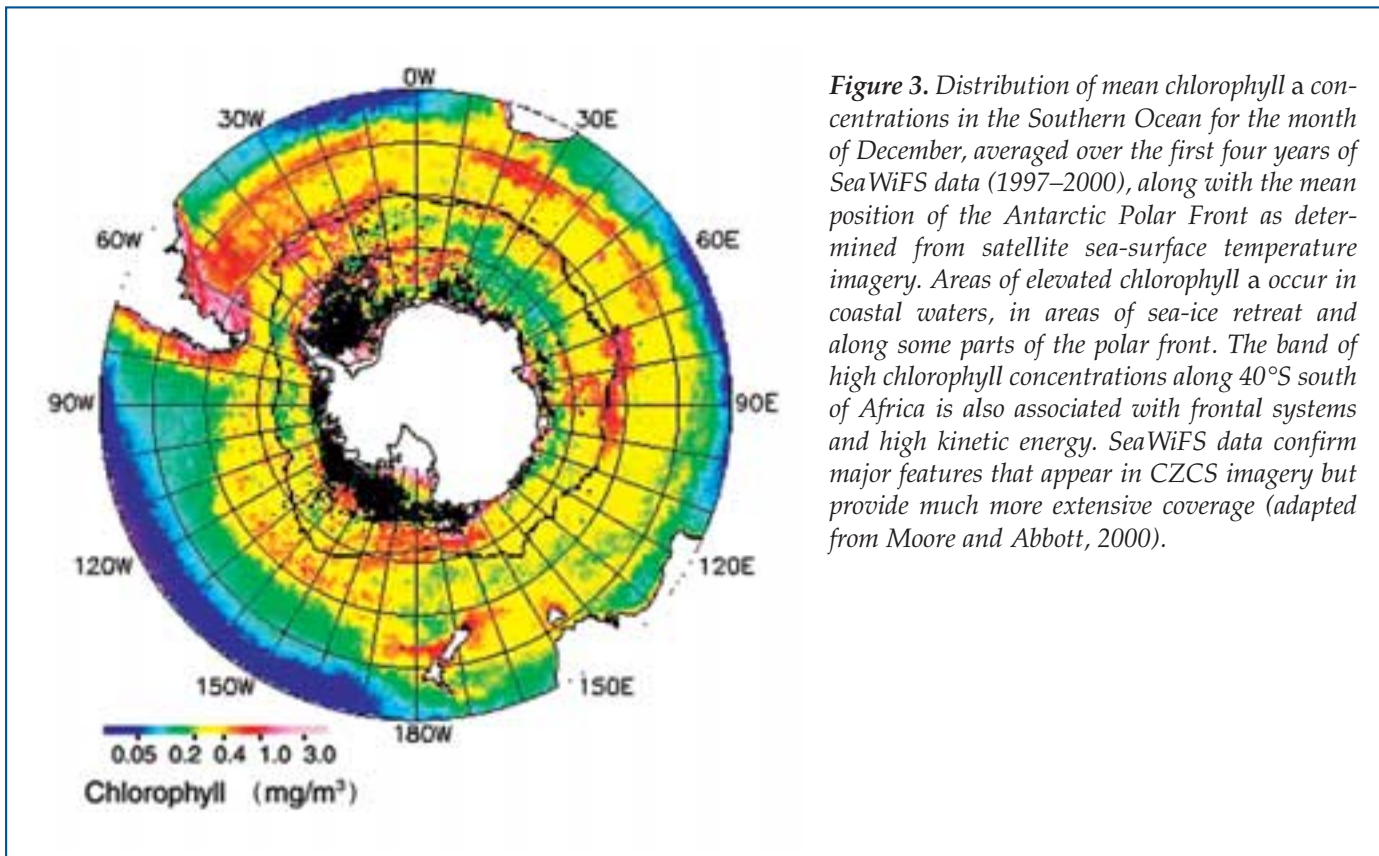


Figure 3. Distribution of mean chlorophyll a concentrations in the Southern Ocean for the month of December, averaged over the first four years of SeaWiFS data (1997–2000), along with the mean position of the Antarctic Polar Front as determined from satellite sea-surface temperature imagery. Areas of elevated chlorophyll a occur in coastal waters, in areas of sea-ice retreat and along some parts of the polar front. The band of high chlorophyll concentrations along 40°S south of Africa is also associated with frontal systems and high kinetic energy. SeaWiFS data confirm major features that appear in CZCS imagery but provide much more extensive coverage (adapted from Moore and Abbott, 2000).

along 170°W took place in regions of frequent phytoplankton blooms associated with the Antarctic Polar Front (Figure 3). The regions where blooms occur are also known to have elevated levels of iron in surface waters. Thus satellite observations have provided indirect evidence supporting the hypothesis that the availability of iron limits phytoplankton growth rates.

Figure 3 depicts the distribution of mean chlorophyll concentrations for the month of December, averaged over the first four years of SeaWiFS data (1997–2000), along with the mean position of the Antarctic Polar Front as determined from satellite sea-surface temperature data. Elevated chlorophyll concentrations are evident in coastal waters, in areas of sea-ice retreat in the Weddell and Ross seas and in some regions along the polar front. The band of high chlorophyll concentrations along 40°S south of Africa is also associated with frontal systems and high eddy kinetic energy. Figure 3 also shows that, in contrast to conditions in the frontal regions, chlorophyll concentrations are generally quite low over the rest of the Southern Ocean.

AESOPS demonstrated the full potential of satellite ocean-color observations as a source of data on the larger spatial context of major field biogeochemical sampling programs and process studies. SeaWiFS images show that the bloom observed from ships at the polar front extended throughout the entire region along the Pacific-Antarctic Ridge, indicating that conditions sam-

pled during the detailed studies conducted along 170°W were representative of a much larger area. The ongoing SeaWiFS mission in conjunction with other current and planned ocean-color sensors provide the best large-scale observations to date for this remote oceanic region and lay the baseline for long-term studies.

U.S. JGOFS Synthesis and Modeling Program (SMP)

SMP investigators and others interested in global biogeochemical cycles are using CZCS, SeaWiFS and other ocean-color sensor imagery to help determine the spatial and temporal variability related to the ocean carbon cycle on a wide variety of scales. The foci of SMP projects (listed at <http://www1.whoi.edu/mzweb/resarea.html>) include mesoscale variability at the Bermuda-Atlantic Time-series Study (BATS) site, upper-ocean productivity in the four major coastal upwelling systems, interannual variability in the North Atlantic related to North Atlantic Oscillation (NAO) cycles and in the equatorial Pacific related to El Niño-Southern Oscillation (ENSO) cycles, CDOM as a potential carbon sink, extrapolation of POC distributions derived from transmissometer measurements, and large-scale patterns in basin and global imagery.

Three examples illustrate the ways in which satellite ocean-color observations are helping investigators synthesize, model and understand biological components of the ocean carbon cycle and their variability.

Remote Sensing Tools For Ocean Biogeochemistry

Mary-Elena Carr
 Jet Propulsion Laboratory
 California Institute of Technology
 Pasadena, California USA

Satellite-borne sensors provide broad spatial and temporal coverage and consistent methodology as well as a powerful capacity for extrapolating, integrating and constraining field observations and modeling results. Repeat coverage allows us to quantify scales of variability otherwise inaccessible outside of process studies. However, remote-sensing measurements are limited in what they can measure, their resolution and their sampling depth, which is usually limited to surface waters in the ocean context. Novel approaches that use both comprehensive comparison of field and satellite observations and new theoretical applications can greatly enrich our use of existing and planned space-based measurements. By assimilating remotely sensed and *in situ* data into circulation models, for example, we can obtain quantitative assessments of relevant ocean parameters, such as subsurface velocity or mixed-layer depth.

What Can We Sense Remotely?

Major oceanographic variables currently measured from space and the sensors designed to measure those variables:

Variable	Sensor
Sea-surface temperature (SST)	AVHRR, MODIS, TMI, ATSR
Sea-surface salinity	(proposed)
Sea-surface height (SSH)	TOPEX/POSEIDON, ERS2
Wind speed and direction	QuickScat, ERS2, SSM/I (speed only)
Chlorophyll concentration	SeaWiFS, MODIS
Fluorescence	MODIS
Aerosols	AVHRR, TOMS, SeaWiFS, MODIS, MISR, ATSR

[Acronyms: Advanced Very High Resolution Radiometer (AVHRR), Moderate Resolution Imaging Spectroradiometer (MODIS), Along-Track Scanning Radiometer (ATSR), Tropical Microwave Imager (TMI), Topography Experiment (TOPEX), European Remote Sensing Satellite (ERS), Special Sensor Microwave Imager (SSM/I), Quick Scatterometer (QuickScat), Sea-viewing Wide Field-of-view Sensor (SeaWiFS), Total Ozone Mapping Spectrometer (TOMS), Multi-angle Imaging Spectro-Radiometer (MISR)]

What Do We Need To Know?

The oceanographic processes and compartments that must be quantified to improve our understanding of ocean biogeochemical cycles are listed below, followed by the pertinent remotely-sensed variable or remote-sensing technique. For highly variable systems, we need platforms that allow higher frequency sampling, such as geostationary platforms.

Oceanographic Process	Variable
Circulation, mixed-layer depth, geostrophic currents	SSH
Air-sea exchange of CO ₂ pCO ₂ of ocean gas exchange coefficient	SST, salinity chlorophyll concentration wind speed surface roughness
Photosynthesis	chlorophyll concentration irradiance, SST, fluorescence
New and export production f-ratio supply of new nutrients new nutrient uptake plankton community structure (N ₂ fixation, calcification)	SST, primary production, NO ₃ chlorophyll concentration heat flux, precipitation oxygen, heat flux heat storage, SST ocean color, compound remote sensing
Carbon species (POC, DOC)	ocean color
Production of radiatively active gases (photochemistry)	ocean color irradiance
Variability, unresolved processes eddies forcing events (storms etc.) coastal processes	variability in SSH, SST, color, wind vector wind vector multispectral ocean color

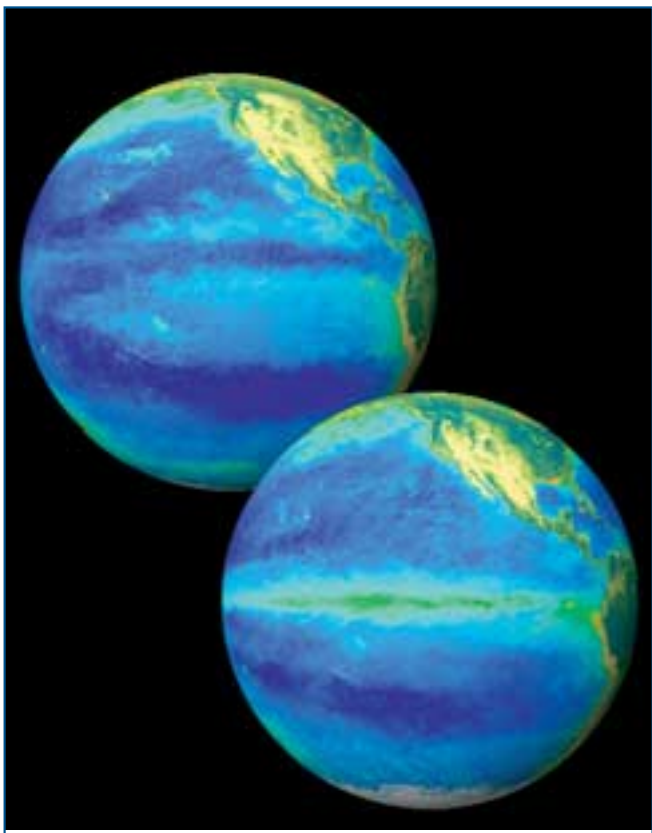


Figure 4. ENSO effects on equatorial Pacific chlorophyll *a* concentrations during January (El Niño) and July (La Niña) of 1998. (Image courtesy of the SeaWiFS Project, NASA Goddard Space Flight Center and ORBIMAGE.)

Investigators have found that the upper ocean in the equatorial Pacific responds dramatically to phases of the ENSO cycle (Figure 4). During the transition from El Niño to La Niña conditions between January and July 1998, SeaWiFS images and *in situ* observations showed a 20-fold increase in surface chlorophyll *a* (from 0.05 to 1.0 mg m⁻³) along the equator in the central Pacific (Chavez et al., 1999). Calculations based on three years of SeaWiFS images indicate that global ocean primary production increased from 54 to 59 petagrams of carbon per year (1 Pg = 10¹⁵ grams) in the period following the 1997–98 El Niño, with higher mean chlorophyll concentrations in the equatorial Pacific providing most of the change (Behrenfeld et al., 2001).

Bio-optical and POC measurements during AESOPS provide a second synthesis example. Shipboard measurements from the Ross Sea and Antarctic Polar Frontal Zone were used to develop a simple empirical algorithm linking water-leaving radiance to upper ocean POC concentrations (Stramski et al., 1999). This relationship and SeaWiFS imagery were then used to estimate the total amount of POC (0.8 Pg C at the December peak in the growing season) within the top 100 meters of the entire Southern Ocean south of 40°S.

As a third example, modelers are learning how to assimilate satellite ocean-color data into numerical models and are using the results to help constrain model parameters and to determine whether a particular model structure is consistent with a given set of observations. In recent assimilation experiments using a marine ecosystem model of the central equatorial Pacific Ocean, similar model parameter values were estimated from assimilation of data from EqPac cruises

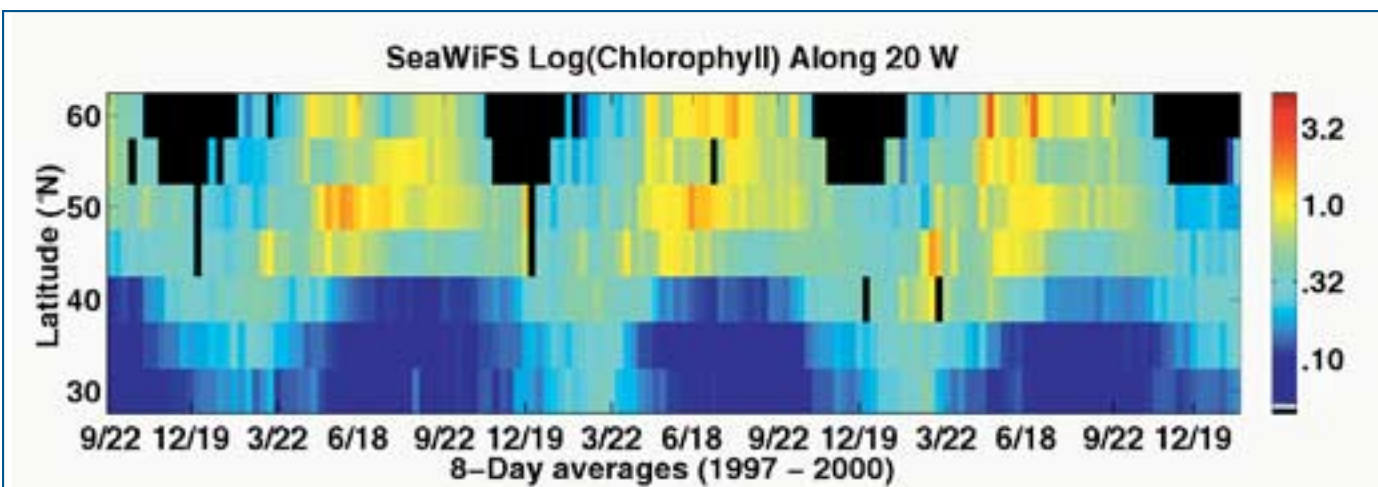


Figure 5. Latitude versus time plot of SeaWiFS chlorophyll (log scale) in the North Atlantic along 20°W longitude. Data are shown in 8-day, 5-degree “bins.” Areas shown in black lack data because of cloud cover and low wintertime sun angles at high latitudes.

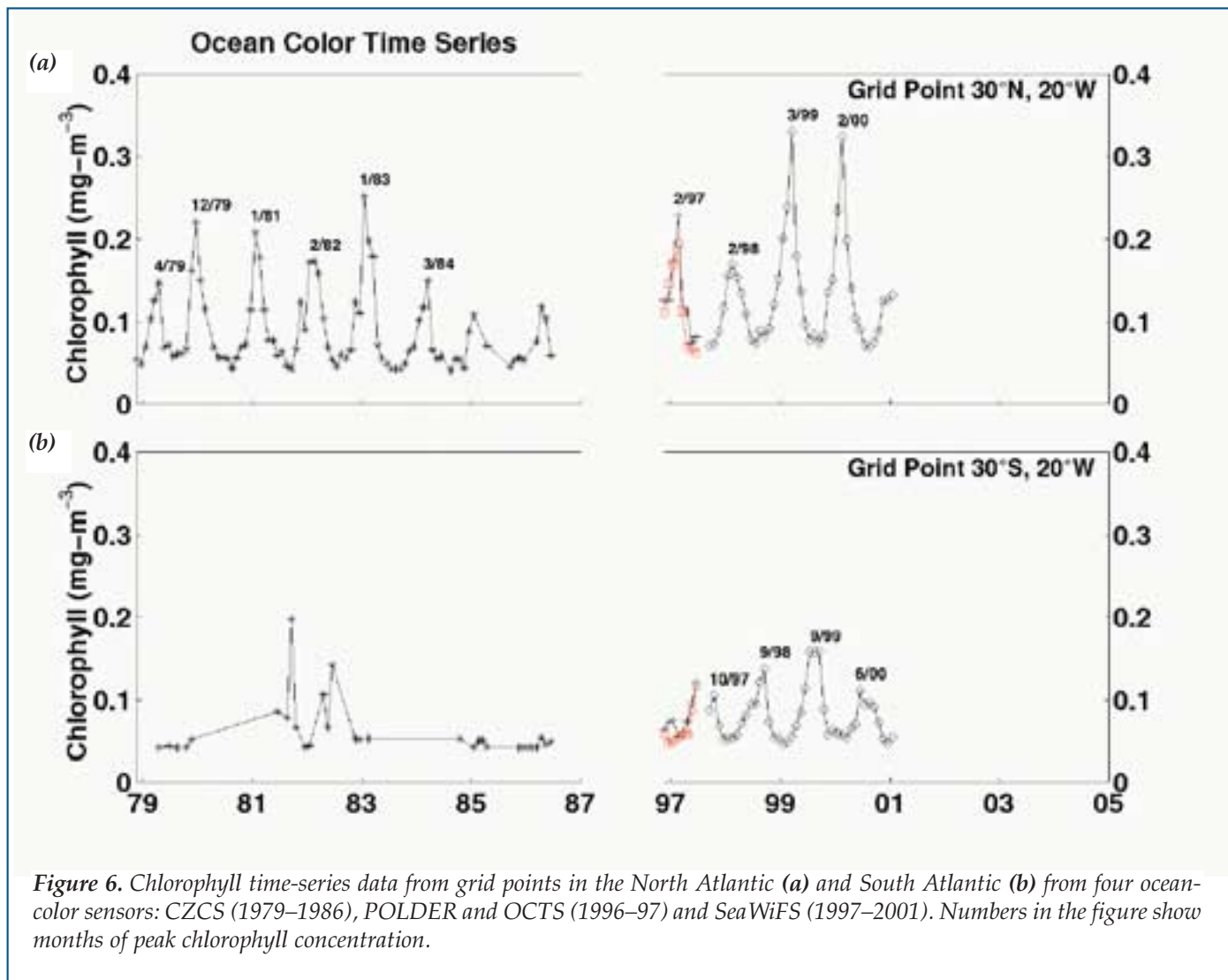


Figure 6. Chlorophyll time-series data from grid points in the North Atlantic (a) and South Atlantic (b) from four ocean-color sensors: CZCS (1979–1986), POLDER and OCTS (1996–97) and SeaWiFS (1997–2001). Numbers in the figure show months of peak chlorophyll concentration.

during the 1991–92 El Niño and from SeaWiFS measurements during the 1997–98 El Niño. Assimilation of SeaWiFS data into the model also helped to identify a period during the 1997–98 El Niño when limitation of phytoplankton productivity switched from macronutrients such as nitrogen to micronutrients such as iron. Finally, the SeaWiFS assimilation experiments showed the importance of matching the temporal scales used in models with those represented in data sets to obtain optimum model parameter values (see Doney et al., this issue).

Future Developments

Remote-sensing measurements of ocean color will play a key role in future ocean carbon cycle studies. Aircraft LIDAR techniques that are under development employ a pump-probe technique, which uses multiple laser pulses to determine phytoplankton fluorescence at different photosystem saturation states, to obtain continuous measurements of the maximum rate of photosynthesis and other photosystem parameters


along flight lines (Chekalyuk et al., 2000). Data obtained with these methods will help refine productivity estimates, identify areas of physiological stress caused by low nutrients and locate transitions in the species composition of phytoplankton communities.

The quality of satellite ocean-color measurements continues to improve with each generation of sensors and with refinements in processing and analysis techniques. New products and capabilities are anticipated within the next few years (Yoder, 2000). For example, data from the new MODIS sensor, which measures chlorophyll fluorescence as well as concentrations, should help investigators identify phytoplankton physiological conditions related to nutrient stress. This information should lead to improved calculations of basin-scale productivity.

Inverse bio-optical models are now able to separate CDOM from chlorophyll; in the future, they may be able to distinguish among types of phytoplankton. Of particular relevance to biogeochemical cycle studies is the possibility of using ocean-color sensors to locate

and map regions containing high abundances of nitrogen-fixing phytoplankton such as *Trichodesmium* (see Michaels et al., this issue). Numerical modelers will learn how to assimilate new data from satellite-mounted sensors into coupled biogeochemical-physical models to improve and extend their descriptive and predictive capabilities.

Finally, multiyear ocean-color data sets will help determine seasonal to interannual variability on ocean basin scales. Figure 5 shows the latitudinal progression of seasonal high chlorophyll concentration during 1998–2000 along the former NABE meridian of 20°W. Future carbon-cycle studies will use data sets of this sort to help focus *in situ* sampling from ships and moorings on key periods and locations as well as to achieve a better understanding of interannual variability.

Figure 6 shows chlorophyll *a* time-series measurements at two grid points in the South and North Atlantic. They contain some interesting features that illustrate how far satellite ocean-color observations have come since the CZCS era. First, a comparison of CZCS and SeaWiFS measurements at the South Atlantic grid point illustrates the improvement in Southern Ocean coverage between CZCS and SeaWiFS. Second, maximum and minimum chlorophyll *a* concentrations derived from POLDER, OCTS and SeaWiFS measurements are comparable, demonstrating that it will be possible to link measurements from different sensors to make decadal or longer data sets. Finally, both the CZCS and SeaWiFS data from the North Atlantic and the SeaWiFS data from the South Atlantic show interannual variability. They indicate that satellite ocean-color measurements may prove useful for determining the effects of climate and regime shifts on ocean productivity and may provide early warning of permanent changes to ocean ecosystems and biogeochemical cycles in response to human-induced climate perturbations. 

Acknowledgements

We thank Maureen Kennelly and Gene Feldman for technical assistance and Ken Buesseler and an anonymous reviewer for their helpful comments. Funding was provided by NASA and NSF. This is U.S. JGOFS Contribution Number 679.

References

- Behrenfeld, M.J., J.T. Randerson, C.R. McClain, G.C. Feldman, S.O. Los, C.J. Tucker, P.G. Falkowski, C.B. Field, R. Frouin, W.E. Esaias, D.D. Kolber and N.H. Pollack, 2001: Biospheric primary production during an ENSO transition. *Science*, 291, 2594–2597.
- Brock, J.C. and C.R. McClain, 1992: Interannual variability in phytoplankton blooms observed in the northwestern Arabian Sea during the southwest monsoon. *J. Geophys. Res.*, 97, 733–750.
- Chavez, F.P., P.G. Strutton, G.E. Friederich, R.A. Feely, G.C. Feldman, D.G. Foley and M.J. McPhaden, 1999: Biological and chemical response of the Equatorial Pacific Ocean to the 1997–1998 El Niño. *Science*, 286, 2126–2131.
- Chekalyuk, A.M., F.E. Hoge, C.W. Wright, R.N. Swift and J.K. Yungel, 2000: Airborne test of laser pump-and-probe technique for assessment of phytoplankton photochemical characteristics. *Photosynth. Res.*, 66, 45–56.
- Esaias, W.E., G.C. Feldman, C.R. McClain and J.A. Elrod, 1986: Monthly satellite-derived phytoplankton pigment distribution for the North Atlantic Ocean Basin. *EOS*, 67, 835–37.
- Feldman, G.C., J.W. Murray and M. Leinen, 1992: Use of the Coastal Zone Color Scanner for EqPac planning. *Oceanography*, 5, 143–145.
- Hoge, F.E., R.E. Berry and R.N. Swift 1986: Active-passive airborne ocean color measurement: 1. Instrumentation. *Appl. Opt.*, 25, 39–47.
- Kinkade, C.S., J. Marra, T.D. Dickey and R.W. Weller, 2001: An annual cycle of phytoplankton biomass in the Arabian Sea, 1994–1995, as determined by moored optical sensors. *Deep-Sea Res. II*, 48, 1285–1301.
- Moore, J.K. and M.R. Abbott, 2000: Phytoplankton chlorophyll distributions and primary production in the Southern Ocean. *J. Geophys. Res.*, 105, 28709–28722.
- National Academy of Sciences, 1984: *Global ocean flux study: Proceedings of a workshop*. National Academy Press, Washington, D.C., 360 pp.
- Robinson, A.R., D.J. McGillicuddy, J. Calman, H.W. Ducklow, M.J.R. Fasham, F.E. Hoge, W.G. Leslie, J.J. McCarthy, S. Podewski, D.L. Porter, G. Saure and J.A. Yoder, 1993: Mesoscale and upper ocean variabilities during the 1989 JGOFS bloom study. *Deep-Sea Res. II*, 40, 9–35.
- Stramski, D., R.A. Reynolds, M. Kahru and B.G. Mitchell, 1999: Estimation of particulate organic carbon in the ocean from satellite remote sensing. *Science*, 285, 239–242.
- Tindale, N.W. and P.P. Pease, 1999: Aerosols over the Arabian Sea: Atmospheric transport pathways and concentrations of dust and sea salt. *Deep-Sea Res. II*, 46, 1577–1595.
- Yoder, J.A., 2000: Terra's View of the Sea. *Science*, 288, 1979–1980.
- Yoder, J.A., C.R. McClain, G.C. Feldman and W.E. Esaias, 1993: Annual cycles of phytoplankton chlorophyll concentrations in the global ocean: A satellite view. *Global Biogeochem. Cycles*, 7, 181–194.
- Yoder, J.A., S.G. Ackleson, R.T. Barber, P. Flament and W.M. Balch, 1994: A line in the sea. *Nature*, 371, 689–692.

Marine Dissolved Organic Matter and the Carbon Cycle

Dennis A. Hansell

University of Miami • Miami, Florida USA

Craig A. Carlson

University of California • Santa Barbara, California USA

Some of our greatest advances in understanding the structure and functioning of natural systems occur when newly developed methods unlock scientific doors. Sometimes these gateways have been barred because of methodological constraints, sometimes because we have lacked reasons to seek them. When scientific necessity and methodology converge, advances in knowledge can be extraordinary. During the Joint Global Ocean Flux Study (JGOFS), such a convergence led to remarkable advances in our understanding of the role of Dissolved Organic Matter (DOM) in the ocean carbon cycle.

Designed to improve our knowledge of the marine carbon cycle, JGOFS depended upon focused studies of the major bioreactive pools of carbon and other elements in the ocean and, as a prerequisite, reliable and accurate methods of measuring these pools. The largest and best understood pool of reactive carbon in the global ocean is Dissolved Inorganic Carbon (DIC), which contains roughly $38,000 \times 10^{15}$ g C (see Feely et al., this volume). We focus in this article on the global reservoir of DOM in the ocean, which contains roughly 685×10^{15} g C, the second largest pool and the least understood at the beginning of JGOFS. DOM contains many biochemically identifiable classes of compounds such as sugars or amino acids, as well as fractions that are more coarsely classified, such as humics. As we consider the cycling of carbon through DOM, it is conceptually useful to isolate the DOM carbon, the fraction scientists term Dissolved Organic Carbon (DOC).

What role does DOM have in the cycling of marine carbon? Numerous publications prior to JGOFS provided insights on how to address this question. Several suggested that the DOM pool is largely old and refractory and thus unavailable for biological consumption. If this characterization is accurate, DOM does not play a central role as a highly reactive reservoir for carbon and could be viewed as unimportant to carbon fluxes and thus to concentrated study in JGOFS. If this characterization is inaccurate or incomplete, DOM requires serious study.

Seminal papers published during the 1980s challenged our long-held views on the role of DOM in the

cycling of the major elements in the ocean (Suzuki et al., 1985; Sugimura and Suzuki, 1988). The then generally accepted and long-held view, as described in Williams and Druffel (1988), was that the biological pump functions primarily through the sinking of biogenic particles. In contrast, results of the experiments of suggested by Sugimura and Suzuki (1988) and Suzuki et al. (1985) suggested that concentrations of DOM were two to four times greater than previously thought, and also that DOC was centrally important to the functioning of the oceanic biological pump. These findings stimulated both alarm and excitement. If true, they would force us to change our long-held belief, and hence were a major reason why JGOFS concentrated on DOM.

In part because of the impetus provided by JGOFS and its core questions, a group of scientists was drafted to test the findings of these provocative papers. The main problem was quickly apparent; the various analytical methods used to measure DOC—including high temperature oxidation, ultra-violet irradiation and persulfate oxidation—were unreliable, and often did not agree. Many new analysts joined the fray, few of whom had experience with DOM measurements. Thus the early analytical results varied widely. Some analysts claimed to find their results in full confirmation of the high DOM concentrations reported by Suzuki et al. (1985) and Sugimura and Suzuki (1988). Those who could not replicate the new measurements had to consider the possibility that their analytical abilities were inferior to those who had verified the high DOC concentrations.

Continuing disagreement among results required scientists to step back from applying them in field studies. Instead a series of intercomparison exercises were organized that proved invaluable for evaluating the methods, however vexingly slow. While investigators interested in DOC were wrestling with questions of methodology, U.S. JGOFS field studies proceeded without reliable techniques for measuring one of the largest carbon pools in the ocean. The pressure to solve the analytical uncertainties increased.

While the full story of how the DOC methods were

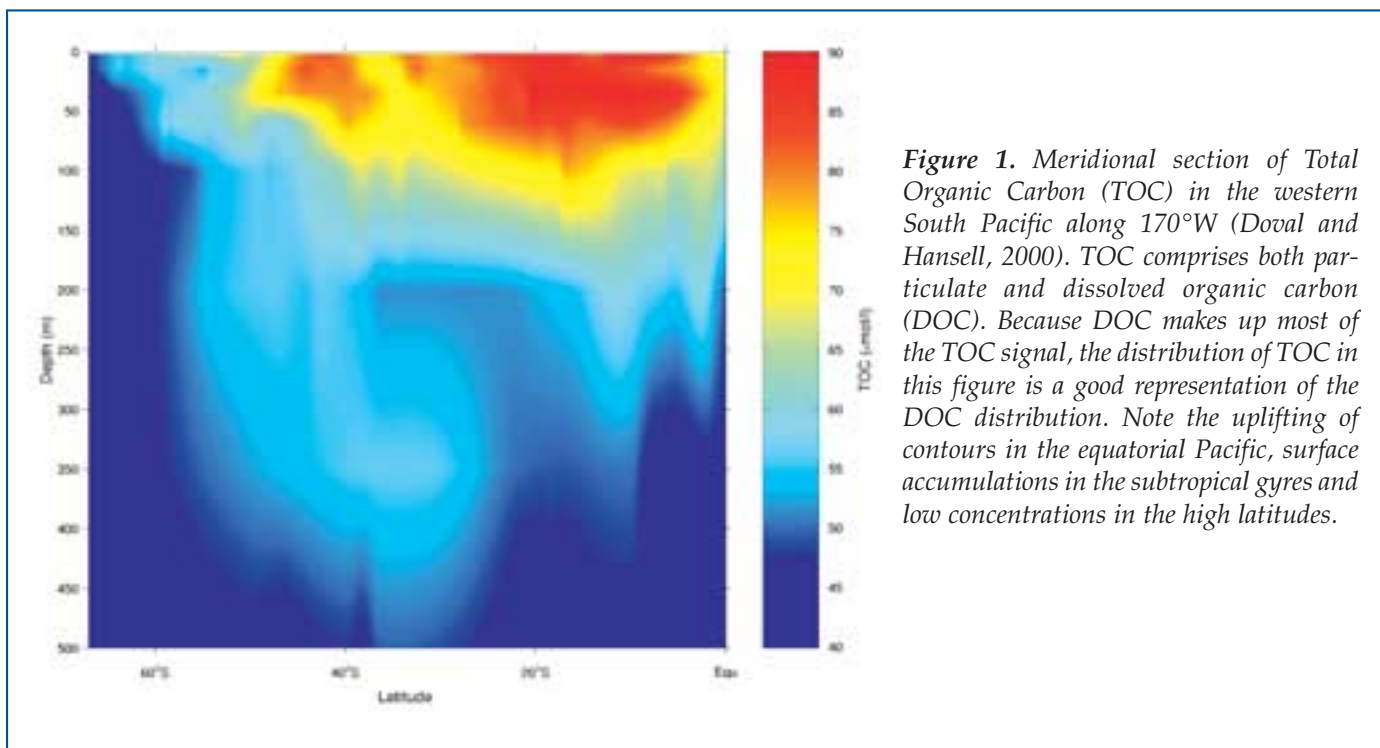


Figure 1. Meridional section of Total Organic Carbon (TOC) in the western South Pacific along 170°W (Doval and Hansell, 2000). TOC comprises both particulate and dissolved organic carbon (DOC). Because DOC makes up most of the TOC signal, the distribution of TOC in this figure is a good representation of the DOC distribution. Note the uplifting of contours in the equatorial Pacific, surface accumulations in the subtropical gyres and low concentrations in the high latitudes.

evaluated is too long for full treatment here, we will provide brief historical highlights. For more details on methodology and history, refer to the forthcoming book entitled *Biogeochemistry of Marine Dissolved Organic Matter* (Academic Press), edited by D.A. Hansell and C.A. Carlson.

Community-wide DOC method intercomparison exercises were inaugurated in 1991 at a workshop in Seattle, organized by John Hedges and John Farrington. Jonathan Sharp led further intercomparisons throughout the 1990s. These exercises were used to evaluate the various methods and to establish protocols for achieving agreement among laboratories. The intercomparison efforts evolved, with U.S. JGOFS encouragement, into a sustained reference material program (see sidebar) that currently provides water samples with agreed-upon DOC concentrations to analysts throughout the world.

The method intercomparisons provided two salient results. One, that the high DOC concentrations reported by Sugimura and Suzuki (1988) were not repeatable and therefore not valid. Two, the role of DOC in the carbon cycle remained enigmatic.

JGOFS investigators still faced certain critical questions: What is the true spatial and temporal variability of DOC in the ocean? What role does DOC have as a reservoir for carbon fixed during primary (and new) production? What role does DOC have in the biological pump? What aspects of its composition and character are important with regard to carbon cycling? Our best answers to these questions, reflecting the progress made to date, form the balance of this article.

We do not attempt a comprehensive review of recent findings on the role of DOM in ocean processes

but focus instead on aspects of DOC that are most relevant to JGOFS questions. New areas and topics that we cannot cover here include the optical properties and biochemical composition of DOM, inclusion of DOM in models, the biological and chemical reactivity of DOM, and characteristics of DOM cycling in specific marine environments such as sediments, continental shelves, high latitudes and upwelling zones. Chapters in the forthcoming book mentioned above provide much greater detail on these topics.

The Role of DOC in the Carbon Cycle

Drawing on observations made at the U.S. JGOFS field study sites, we begin with an evaluation of the spatial distribution of DOC at regional and basin scales in both the surface and deep ocean. Next, we evaluate the temporal variability of DOC, focusing on seasonal variation in both high and low latitudes. Following this assessment of variability, we examine net community production, focusing on DOC that accumulates over time periods of biogeochemical relevance. In the section that follows, we evaluate the contribution of DOC to the biological pump by examining the mechanisms and locations of DOC export, and attempt to develop an understanding of the controls on export. We close providing some examples of how ideas about DOC have changed and discuss the significance of DOC's quality and character.

Spatial Variability of DOC

DOC is produced by biological processes in the upper ocean and mixed downward and diluted by physical processes. The upper-ocean distribution of DOC reflects the balance between these processes.

Determining Dissolved Organic Carbon In The Ocean

Dennis A. Hansell
University of Miami
Miami, Florida USA

Dissolved organic matter in the ocean contains roughly the same amount of carbon as is present in the atmosphere in the form of carbon dioxide (CO₂). Ocean scientists from many nations are now studying the production, consumption, composition and distribution of this large pool of carbon with the aim of understanding its role in the ocean carbon cycle. Marine DOC measurements are made at more than 100 laboratories in the United States and many more elsewhere.

As the number of laboratories measuring dissolved organic carbon (DOC) began to increase in the early 1990s, it quickly became evident that poor agreement existed among the methods. The primary problem was the lack of commonly available seawater standards that could be employed for intercomparison of methods and results. To overcome this obstacle, the National Science Foundation (NSF) in 1998 began support for development of a reference material program for DOC analyses, administered by the Bermuda Biological Station for Research. The project has subsequently moved to the University of Miami.

Two forms of reference material have been developed for DOC analysis. One is deep ocean water (44–46 μM DOC and 21.5 μM total nitrogen), collected at a depth of 2600 meters in the Sargasso Sea and containing biologically refractory DOC. The other is low carbon water, containing DOC at a level of roughly 2 μM. DOC concentrations for both materials are determined through the consensus of a group of independent investigators. Current participants are: James Bauer of Virginia Institute for Marine Science, Ronald Benner of the University of South Carolina, Yngve Børsheim of the Norwegian Institute of Science and Technology, Gus Cauwet of the Laboratoire Arago, France, Robert Chen of the University of Massachusetts, Boston, Dennis Hansell and Wenhao Chen of the University of Miami, Charles Hopkinson of the Marine Biological Laboratory, Ken Mopper and Jianguo Qian of Old Dominion University, and Hiroshi Ogawa of the University of Tokyo.

To date, some 45 laboratories in 18 nations have received more than 13,000 ampoules of these materials. Although the analytical protocols of these analysts vary greatly, their laboratories are now better able to achieve comparable results, a concrete step forward for ocean carbon-cycle research. Comparability extends and amplifies the value of all our individual efforts.

Concentrations are relatively high year round in the subtropical gyres (Figure 1). At high latitudes, where deep ocean water containing little DOC refreshes the surface layer in winter, DOC concentrations can be quite low. In coastal regions and along the equator, DOC values at the surface are normally relatively low where upwelling is strongest.

In the central equatorial Pacific, DOC is depressed at the surface because of upwelling (see the upward doming of the subsurface DOC contours at the equator [Figure 1]). The Equatorial Undercurrent, near 200 m west of the international dateline, has a DOC concentration around 55 μM. This water is transported eastward, shoaling to near surface levels in the central and eastern equatorial Pacific and bringing with it low DOC water (Figure 2). The return flow of surface water to the west shows an increase in DOC to roughly 65 μM as a result of the biological processing of carbon.

The highest DOC concentrations (>70 μM) are found in the Western Pacific Warm Pool west of 165°W in the upper 100 m (Figure 2). The position of the front separating the DOC-enriched warm pool to the west and the recently upwelled water to the east varies with the state

of the El Niño-Southern Oscillation (ENSO) cycle. The DOC-enriched water is found further to the east during El Niño conditions.

The effect of upwelling on DOC concentrations is similar at coastal upwelling sites. Strong upwelling occurs along the coast of Oman in the Arabian Sea, driven by the intense winds of the Southwest Monsoon (Hansell and Peltzer, 1998). Low surface-water DOC concentrations are present during upwelling even when primary productivity is quite high, showing the effect of dilution from below.

Reports on the distribution and variability of DOC in the deep ocean have varied greatly over the years. Some authors have reported a complete absence of DOC gradients in the deep ocean; others have found small to very large gradients in concentration. In an effort to narrow the uncertainty, we surveyed representative sites in the deep ocean (Hansell and Carlson 1998a). As Figure 3 shows, we found a 29% decrease in DOC concentration from the northern North Atlantic (48 μM in the Greenland Sea) to the northern North Pacific (34 μM in the Gulf of Alaska). This gradient reflects the export of formerly subtropical water

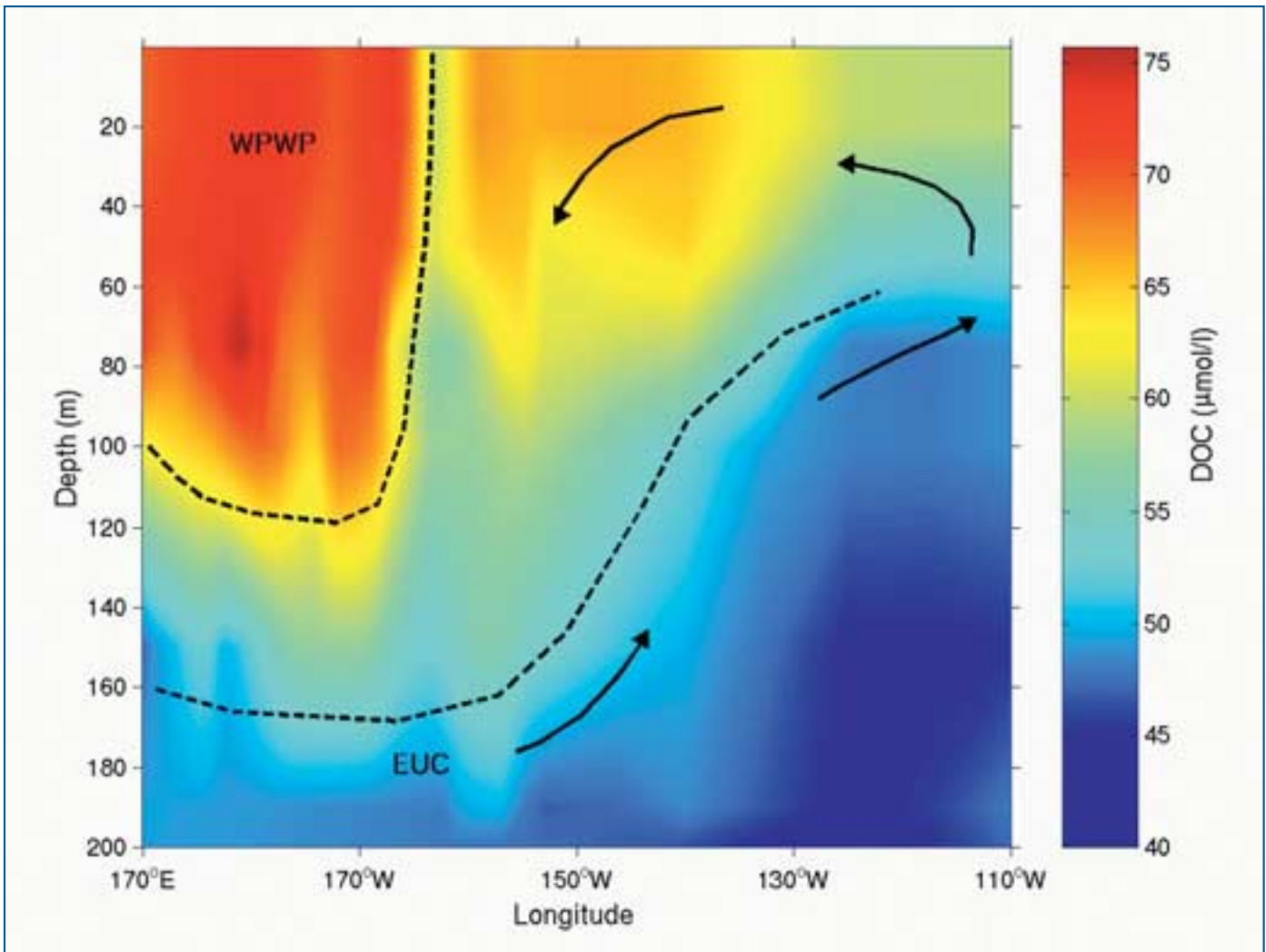


Figure 2. Zonal section of DOC along the equator in the Pacific Ocean. The data represent a compilation of measurements made in autumn 1992 (Peltzer and Hayward, 1996; 110°W to 140°W) and in autumn 1994 (Hansell et al., 1997; 150°W to 170°E), during similar stages of the El Niño-Southern Oscillation cycle. Note the shoaling of Equatorial Undercurrent (EUC) water low in DOC concentration to the east. The high DOC concentrations west of the dateline are associated with the Western Pacific Warm Pool (WPWP). The dashed lines delineate the various water masses described; arrows indicate the general direction of relevant currents.

enriched in DOC, as North Atlantic Deep Water (NADW) is formed, and a decrease in DOC through microbial remineralization and mixing along the path of deep ocean circulation away from the North Atlantic. The formation of Antarctic Bottom Water (AABW) does not introduce significant additional DOC into the deep ocean; thus the concentrations remain low in the deep water near sites where AABW is formed.

Temporal Variability of DOC

Strong seasonal increases in DOC concentrations associated with phytoplankton blooms appear to be characteristic of systems that receive high inputs of new nutrients over winter periods. The waters of the Ross Sea polynya, for example, undergo deep mixing

over the winter, with nitrate concentrations in excess of 30 μM at the surface prior to the spring bloom. DOC concentrations increase in the surface layer from winter lows of 42 μM to summer highs of 65–70 μM (Carlson et al., 2000). DOC concentrations in the Ross Sea increase by 15–30 μM where the blooms of *Phaeocystis* and diatoms are particularly strong. Because DOC accumulation is concentrated within the upper 30 to 50 m in the Ross Sea, the change in integrated stocks of DOC in the upper 150 m is modest relative to the magnitude of primary production (up to 6 g C m⁻² d⁻¹). Where phytoplankton blooms are weak because of deep mixing or iron limitation, DOC concentrations remain low.

At the site of the U.S. JGOFS Bermuda Atlantic Time-series Study (BATS), located at 31°50'N, 64°10'W

in the Sargasso Sea, convective overturning during winter introduces small amounts of new nutrients into the euphotic zone, followed by small phytoplankton blooms (see Karl et al., this issue). Adequate light is present in this subtropical region throughout the period when overturning occurs. Subsurface water low in DOC is mixed upward during the period of highest primary productivity, thereby reducing DOC concentrations in surface waters (Figure 4). Once stratification reasserts itself with the warming of the surface ocean and the bloom ends, DOC concentrations rebuild to normal summer levels. The change in concentration from the annual low to the annual high is only 3 to 6 μM , small in comparison with the change in high-latitude systems. However, the bloom still supports a net production of as much as 1.5 moles m^{-2} of DOC over the upper 250 m (Carlson et al., 1994; Hansell and Carlson, 2001). Surprisingly, the annual increase in DOC stock is as large as in the much more productive Ross Sea (Carlson et al., 2000), but the increase in DOC concentration is less because the material is mixed more deeply into the water column during the period of net production.

DOC and bloom dynamics in the Arabian Sea during the Northeast Monsoon are similar to those of the Sargasso Sea. Convective overturn in the Arabian Sea, forced by cool dry winds off the Tibetan Plateau, mixes moderate amounts of nutrients into the euphotic zone. Similarly to the Sargasso Sea, changes in DOC concentration are not large during the bloom because of deep

vertical mixing, but the DOC stock increases by 2 moles C m^{-2} during the growing season (Hansell and Peltzer, 1998). Likewise, similar changes in DOC stock are characteristic of the Ross Sea.

Low-latitude systems do not experience winter freshening of the surface layer, nor exhibit seasonality in DOC concentrations. One example is the Hawaii Ocean Time-series (HOT) study site, located at 22°45'N, 158°W in the North Pacific subtropical gyre. Variability in DOC occurs on interannual time scales at this location, but there is no recurring trend with seasons. Church et al. (2001) report interannual net accumulation from 1993 to 1999 of a DOM pool enriched in carbon and nitrogen relative to phosphorus. This long-term change may be a manifestation of the broad, ecosystem-wide shift from nitrogen to phosphorus limitation described by Karl et al. (this issue) for the region around the HOT site. On the other hand, only small shifts in DOM concentration have been noted in the Sargasso Sea.

Net Community Production of DOC

DOC is produced on a daily basis as part of primary and secondary production in the surface ocean. Most of the DOC released is remineralized by microorganisms on time scales of hours to days. For DOC to play a role in the ocean carbon cycle beyond serving as substrate for surface ocean microbes, it must act as a reservoir for carbon on the time scales of ocean circulation. The fundamental question is how much carbon fixed by primary producers accumulates each day or season in the DOC pool.

Seasonal increases of DOC stocks in the Ross Sea indicate that 8–20% of net community production (NCP) in the polynya accumulates each growing season as DOC (Carlson et al., 2000; Hansell and Carlson, 1998b). The balance of NCP is lost to the deep ocean as sinking biogenic particles, mostly in the form of the colonial phytoplankton *Phaeocystis antarctica* or diatoms. Average annual rates of NCP in the Ross Sea polynya range between 6 and 10 moles C m^{-2} ; thus a maximal net DOC production of 1.2 to 2 moles C m^{-2} occurs over the growing season. The rate of DOC production in the Ross Sea, normalized to NCP, is similar to that found in the equatorial Pacific. Estimates of net DOC production as a percentage of NCP in the central equatorial Pacific range from 6 to 40%, with most estimates near the 20% level.

Net DOC production in the Ross Sea and the equatorial Pacific occurs when the conditions are right for net autotrophy. In the Ross Sea, these conditions are present when adequate vertical stability and light are available, while in the equatorial Pacific light becomes available following upwelling. At these sites, the vertical stability of the upper water column is relatively strong during the periods of net production.

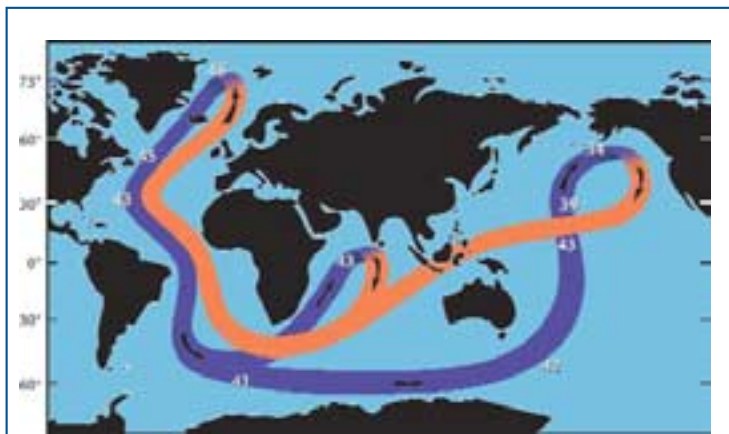


Figure 3. A global map of DOC concentrations in the deep ocean associated with the formation of deep water in the North Atlantic (orange arrows), its transport and distribution throughout the ocean (blue ribbon) and its return to the upper ocean (orange arrows). The North Atlantic near-surface concentration is assumed to be 60 μM prior to overturning. Mixing and remineralization reduce DOC concentrations along the path of deep-water flow from 48 μM in the Greenland Sea to a low of 34 μM in the Gulf of Alaska. The cause of the large and abrupt decrease in DOC concentrations in the deep Pacific Ocean between the equator and the Gulf of Alaska is unknown.

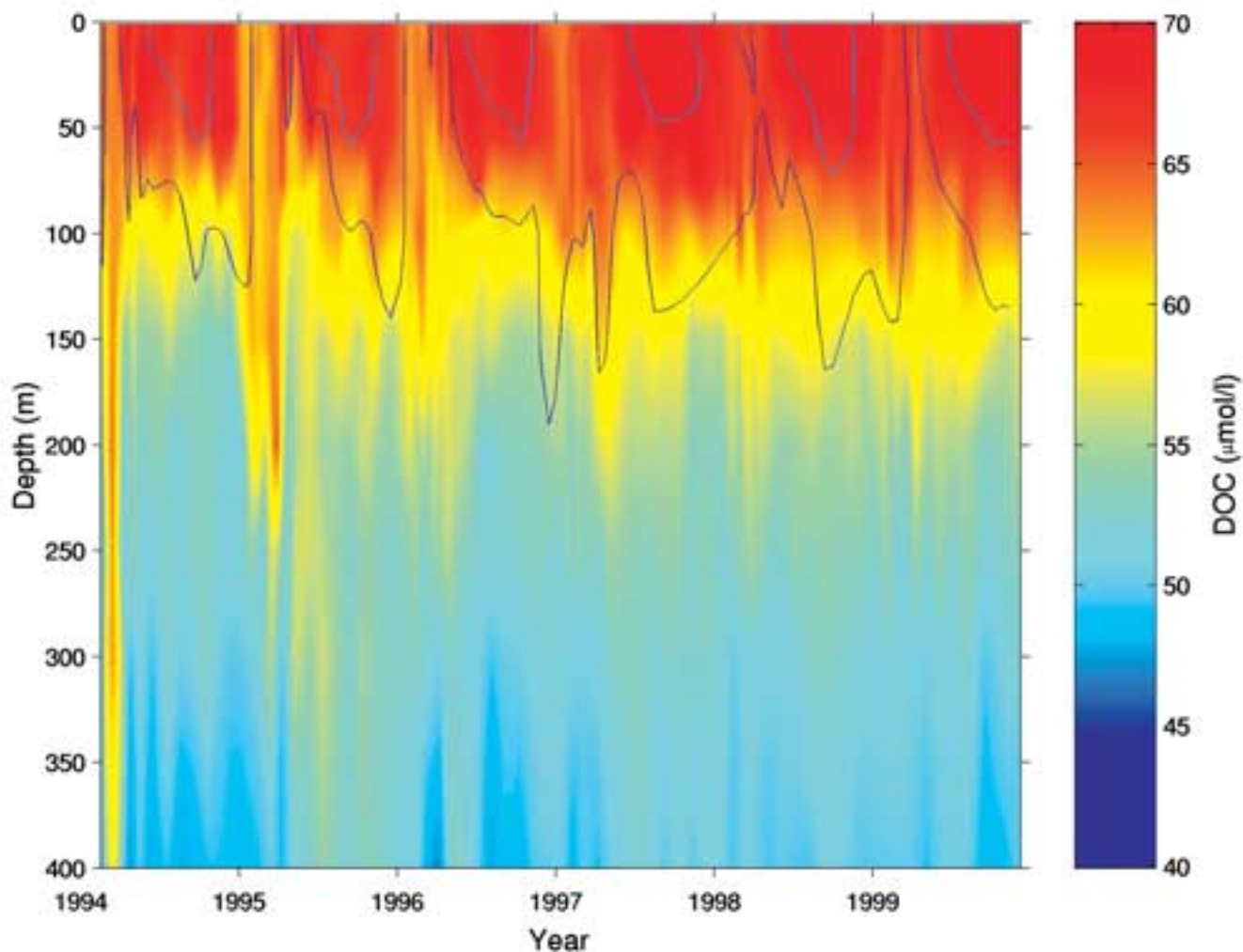


Figure 4. Time-series data on DOC concentrations in the western Sargasso Sea near Bermuda at the BATS site. Seasonality is evident in both the DOC and temperature contours (shallow contour is 24°C; deeper contour is 20°C). Note the decrease in surface DOC concentrations at the time of convective overturning. While concentrations decrease with this vertical mixing, the integrated stocks of DOC actually increase as a result of new primary production.

The Sargasso Sea presents a stark contrast. Light is adequate year round but nutrients are not, so that a reduction in vertical stability with convective overturn of the water column and entrainment of nutrients is required for net autotrophy to occur. In winter 1995 at the BATS site, the DOC stock increased by 1.4 moles C m⁻² in response to maximum mixing depths of 260 m (Figure 4). In subsequent years with mixed layer depths of less than 220 m, DOC stocks increased by less than 0.7 moles C m⁻² during overturning events (Hansell and Carlson, 2001). During the 1995 spring bloom, net DOC production was estimated to be 59–70% of the NCP (Hansell and Carlson, 1998b). This value declines to 8% when the period of evaluation is extended from the seasonal spring bloom to the entire year.

One benefit of normalizing DOC accumulation rates to NCP is that we have a lot of data on NCP. We

can use the findings on net DOC production, along with existing estimates for new (nitrate-based) production in various ocean regions, to estimate annual rates of DOC accumulation (Hansell and Carlson, 1998b). As one would expect, the regions of highest new production, such as equatorial and coastal upwelling areas, contribute the most to net DOC production globally. The weakest sites for the entrainment of nitrate to the surface, such as the subtropical gyres, contribute the least to net DOC production. About 17% of global new production each year ends up as net DOC production. If global new production is roughly 7×10^{15} g C yr⁻¹, we calculate that net DOC production in the global ocean should be about 1.2×10^{15} g C yr⁻¹.

The Contribution of DOC to the Biological Pump

The vertical export of organic matter from the surface ocean into deeper waters, often referred to as the

“biological pump”, is a central process in the ocean carbon cycle (see Ducklow et al., this issue). The export of sinking biogenic particles drives respiration in the ocean interior and helps to maintain the strong vertical gradient of inorganic carbon in the ocean. Prior to the JGOF years, the role of DOC as a component of export received little analysis beyond speculative modeling. DOC arguably plays its most important role in the ocean carbon cycle if and when it contributes to the biological pump.

DOC export in the ocean is a result of accumulation in the surface ocean (Figure 1), redistribution with the wind-driven circulation, and eventual transport to depth with overturning (thermohaline) circulation at high latitudes and subduction in the subtropical gyres. DOC export with the ventilation of the ocean occurs when there is a vertical gradient in DOC concentrations at the onset of overturning. When vertical DOC gradients are weak or absent, there is little net downward movement of DOC with overturning.

Establishing the contribution of DOC to the export of carbon from the surface ocean is best undertaken by normalizing the gradients in DOC concentrations to the gradients in Apparent Oxygen Utilization (AOU). AOU is associated with the remineralization of sinking biogenic particles and subducted DOC and reflects the total oxidation of biogenic carbon along specific density layers. In the isopycnal surfaces between 23.5 and 27.0 sigma- θ (a unit of density) along 170°W in the South Pacific, 21% to 47% of the AOU is driven by the oxidation of DOC (Doval and Hansell, 2000). DOC oxidation along 170°W is largely restricted to the upper 500 m. At greater depths, only biologically refractory DOC remains in the water column; thus oxidation of sinking organic particles alone drives AOU at these depths.

Carbon fixed in DOC is sequestered from exchange with the atmosphere for the longest periods of time when export is associated with the formation of deep and bottom water. The strong meridional gradient in deep water DOC, along the proximal path of the deep western boundary current, provides evidence for the export of DOC with NADW formation (Figure 3; Hansell and Carlson, 1998a). NADW, with an initial DOC concentration of 48 μM in the deep Greenland Sea, overrides and entrains northward flowing AABW with a DOC concentration of 41 μM . The mixing of these two source waters, along with microbial degradation of the labile DOC fractions, produces a concentration gradient in the Atlantic Ocean (Figure 3).

AABW forms in the cyclonic gyres that develop south of the Antarctic Circumpolar Current, particularly those in the Weddell and Ross Seas. The contribution of AABW formation to DOC export appears to be very small. Studies in the Ross Sea during the 1997 austral summer season showed that DOC concentrations in the surface 50 m rose more than 20 μM above background levels in certain areas (Carlson et al., 2000). By the time winter overturning began in the fall, reminer-

alization of the DOC reduced mean concentrations to less than 5 μM above background. The vertical export of this material, if any remains after overturning is complete, would contribute only 2% of the total annual export of particulate plus dissolved organic carbon in the Ross Sea. Remineralization of the DOC prior to overturning prevents it from making a major contribution to export in this system.

In order for DOC export to occur, its concentration must be higher at the surface than in deeper waters. The excess DOC in surface waters consists of fractions that are resistant to rapid microbial degradation. We use the term “exportable DOC” to refer to DOC in surface waters during overturning that is in excess of concentrations at the depth to which vertical mixing takes place. Because the lifetime of exportable DOC is longer than the season of production, it is available for transport via surface currents to sites where water masses are formed.

DOC is produced primarily in the equatorial and coastal upwelling regions, and secondarily in the subtropical gyres (Hansell and Carlson, 1998b). We hypothesize that the DOC produced at these sites accumulates in the subtropical gyres (Figure 5). Wind-driven circulation patterns in the surface ocean dictate the transport and distribution of the accumulated DOC. When DOC-enriched surface waters from the gyres are transported to higher latitudes, DOC is exported with overturning circulation.

The high-latitude regions replenished by subtropical gyre waters via western boundary currents, such as the northern North Pacific and northern North Atlantic, contain exportable DOC during the times when overturning takes place. DOC export occurs in high-density water masses, such as the NADW, the North Pacific Intermediate Water and probably the Labrador Sea Intermediate Water; water masses that are formed in high northern latitudes and fed by subtropical water.

The Southern Ocean, on the other hand, does not appear to contain significant amounts of exportable DOC. Sharp fronts in a variety of properties separate the Antarctic Circumpolar Current System (ACCS) from the DOC-enriched subtropical gyres (Figure 5), as evidenced by the abrupt shifts in DOC concentrations south of the gyres shown in Figure 1. Locally produced exportable DOC is absent as well (Carlson et al., 2000). Thus DOC export in high-density water masses formed in the high latitudes of the Southern Hemisphere is relatively weak.

Changing Ideas on DOC and the Carbon Cycle

One axiom of our understanding about DOC has been that nutrient depletion drives high rates of net production. This perception is based on numerous batch phytoplankton culture experiments, where nutrients were allowed to run out. When nutrients were present and the phytoplankton were in exponential growth phase, DOC release was very small. When

nutrients were depleted and the plants went into stationary phase, carbon fixation exceeded the nitrogen stocks available to support biomass growth and carbon-rich DOM was released. Because of these results, the assumption has been that nutrient depletion forces high levels of DOC production everywhere in the ocean. It would follow that high levels of DOC would be present in oligotrophic systems because of nutrient limitation.

This argument concerning oligotrophic systems can be tested against BATS time-series data from the Sargasso Sea (Figure 4). Net DOC production takes place primarily when rates of primary production are highest during the spring bloom period. During summers, when nutrients are most depleted, no further accumulation of DOC takes place. Nor is there a major increase in bacterial respiration rates relative to primary productivity to indicate an increased release of labile DOC.

The data from the Sargasso Sea indicate that nutrient depletion alone does not drive high rates of DOC production. Once nutrient depletion is sustained in natural systems, a new equilibrium state is eventually achieved with a different plankton community structure. Perhaps it is the rapid switch in nutrient levels from abundance to depletion that triggers rapid DOC production in experimental cultures. If this is the case, transient events should be the most important for rapid DOC production.

Because of the role of stratification in maintaining elevated DOC levels in the surface ocean, a positive correlation between DOC concentration and primary productivity is absent for much of the oligotrophic ocean. In the highly stratified portions of the open ocean, DOC is instead positively correlated with temperature, another sign of the importance of physical controls on ecosystem processes. In contrast, at higher latitudes where DOC concentrations are depressed during the winter, increases in DOC do indeed accompany the springtime rise in primary productivity (Carlson et al., 2000). In these high-latitude systems, increased water column stability favors both phytoplankton growth and DOC accumulation in the upper ocean.

The Effect of DOC Quality on Carbon Export

Over the last decade, investigators have made great advances in understanding the significance of DOM lability (bio-

logical availability) and how it varies in space and time. By combining information on the age of DOC from ¹⁴C measurements with data from utilization experiments and accurate determinations of distribution, we have gained insights into the partitioning of the bulk DOC pool into various fractions defined by their lability.

Ocean ecosystems below the euphotic zone are characterized by net heterotrophy. Biologically labile DOC delivered to these depths by diffusion, turbulent mixing or the dissolution of sinking particles is utilized

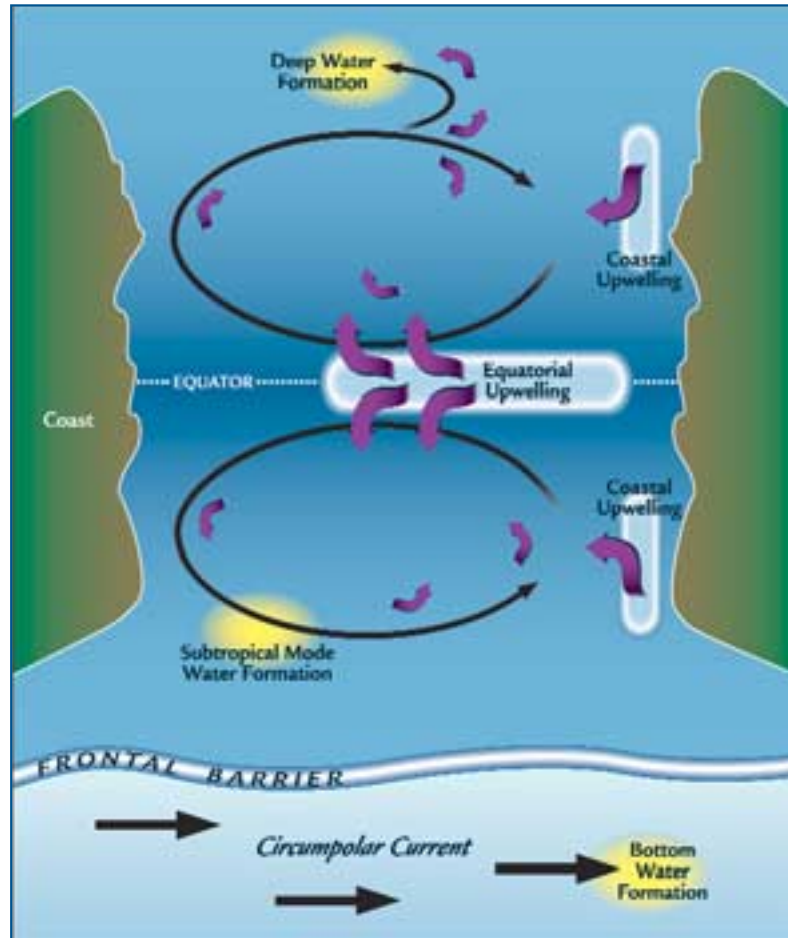



Figure 5. DOC net production, transport and export in the ocean. Regions of significant net DOC production (broad arrows) include coastal and equatorial upwelling regions that support much of the global new production. DOC is transported into and around the subtropical gyres with the wind-driven surface circulation. Export takes place if exportable DOC (elevated concentrations indicated by dark blue fields) is present during overturning of the water column. Such is the case when DOC-enriched subtropical water serves as a precursor for deep and intermediate water mass formation. DOC is also exported with subduction in the gyres. In regions where DOC-enriched subtropical water is prevented by polar frontal systems from serving as a precursor for overturning circulation (such as at the sites of Antarctic Bottom Water formation in the Southern Ocean) DOC export is a weak component of the biological pump. Waters south of the Antarctic Polar Front lack significant exportable DOC (depicted by light blue field) during winter.

by microbes, leaving behind an increasingly refractory remnant. The refractory pool of DOC is best represented by the deep ocean stocks (>1000 m) with apparent mean ages of 4000 to 6000 years in the North Atlantic and the North Central Pacific oceans (Bauer et al., 1992). Because the mean age of the deep DOC is much greater than the time scale of thermohaline circulation, refractory DOC is reintroduced into surface waters via ocean circulation.

Upper ocean stocks of DOM in excess of the deep refractory pool are composed of “labile” and “semi-labile” fractions. Labile compounds, such as neutral sugars and amino acids, fuel rapid microbial production turnover on time scales of minutes to days; they are generally present at nanomolar concentrations. Because labile compounds represent a very small fraction of bulk DOM in the open ocean (0–6%), the vertical gradient of the bulk DOM observed in thermally stratified systems mostly comprises semi-labile DOM. The semi-labile fraction is made up of polysaccharides (Benner et al., 1992) and is biologically reactive over months to years. Thus it accumulates in surface waters and generates the vertical gradients of DOC that we observe. This fraction, referred to above as exportable DOC, contributes to export if it escapes microbial degradation in the surface waters long enough to be mixed into the depths during winter overturning (Carlson et al., 1994).

Conclusions

JGOFS brought new and exciting questions to ocean biogeochemistry, and the scientific community responded with persistence and zeal. Advancing our understanding of the marine carbon cycle required significant improvements in our methodologies and protocols. We relearned the value of reference materials, intercomparisons and coordinated efforts for attacking large and difficult questions.

Investigators interested in DOC have made a good deal of progress during the JGOFS years. As with all good science, much has been learned, however many new questions have also been generated. We have more to learn about what limits the amount of DOC in the ocean, what controls its production and lifetime, and what DOC is composed of. The amount of carbon residing in the pool of DOC in the ocean is equivalent to the amount in the pool of atmospheric CO₂. Thus a small change in the size of the DOC pool could have a major effect on the air-sea exchange of carbon. A fuller understanding of the role of DOC in the ocean carbon cycle and how it might respond to environmental perturbation is essential to our ability to predict the effects of changing climate on the global ocean. 

This is U.S. JGOFS Contribution Number 681.

References

- Bauer, J.E., P.M. Williams and E.R.M. Druffel, 1992: ¹⁴C activity of dissolved organic carbon fractions in the north-central Pacific and Sargasso Sea. *Nature*, 357, 667–670.
- Benner, R., J.D. Pakulski, M. McCarthy, J.I. Hedges and P.G. Hatcher, 1992: Bulk chemical characteristics of dissolved organic matter in the ocean. *Science*, 255, 1561–1564.
- Carlson, C.A., H.W. Ducklow and A.F. Michaels, 1994: Annual flux of dissolved organic carbon from the euphotic zone in the northwestern Sargasso Sea. *Nature*, 371, 405–408.
- Carlson, C.A., D.A. Hansell, E.T. Peltzer and W.O. Smith, Jr., 2000: Stocks and dynamics of dissolved and particulate organic matter in the southern Ross Sea, Antarctica. *Deep-Sea Res. II*, 47, 3201–3225.
- Church, M.J., H.W. Ducklow and D.M. Karl, 2002: Decade-scale secular increase in dissolved organic carbon and nitrogen inventories in the North Pacific subtropical gyre. *Limn. and Oceano.*, 47[1], 1–10.
- Doval, M. and D.A. Hansell, 2000: Organic carbon and apparent oxygen utilization in the western South Pacific and central Indian Oceans. *Marine Chemistry*, 68, 249–264.
- Hansell, D.A., C.A. Carlson, N. Bates and A. Poisson, 1997: Horizontal and vertical removal of organic carbon in the equatorial Pacific Ocean: A mass balance assessment. *Deep-Sea Res. II*, 44, 2115–2130.
- Hansell, D.A. and C.A. Carlson, 1998a: Deep ocean gradients in dissolved organic carbon concentrations. *Nature*, 395, 263–266.
- Hansell, D.A. and C.A. Carlson, 1998b: Net community production of dissolved organic carbon. *Global Biogeochem. Cycles*, 12, 443–453.
- Hansell, D.A. and C.A. Carlson, 2001: Biogeochemistry of total organic carbon and nitrogen in the Sargasso Sea: Control by convective overturn. *Deep-Sea Res. II*, 48, 1649–1667.
- Hansell, D.A. and E.T. Peltzer, 1998: Spatial and temporal variations of total organic carbon in the Arabian Sea. *Deep-Sea Res. II*, 45, 2171–2193.
- Peltzer, E.T. and N.A. Hayward, 1996: Spatial and temporal variability of total organic carbon along 140°W in the equatorial Pacific Ocean in 1992. *Deep-Sea Res. II*, 43, 1155–1180.
- Sugimura, Y. and Y. Suzuki, 1988: A high-temperature catalytic oxidation method for the determination of non-volatile dissolved organic carbon in seawater by direct injection of a liquid sample. *Mar. Chem.*, 24, 105–131.
- Suzuki, Y., Y. Sugimura and T. Itoh, 1985: A catalytic oxidation method for the determination of total nitrogen dissolved in seawater. *Mar. Chem.*, 16, 83–97.
- Williams, P.M. and E.R.M. Druffel, 1988: Dissolved organic matter in the ocean: Comments on a controversy. *Oceanography*, 1, 14–17.

Upper Ocean Carbon Export and the Biological Pump

Hugh W. Ducklow, Deborah K. Steinberg
College of William & Mary • Gloucester Point, Virginia USA

Ken O. Buesseler
Woods Hole Oceanographic Institution • Woods Hole, Massachusetts USA

Introduction

Biology, physics and gravity interact to pump organic carbon into the deep sea. The processes of fixation of inorganic carbon in organic matter during photosynthesis, its transformation by foodweb processes (trophodynamics), physical mixing, transport and gravitational settling are referred to collectively as the “biological pump” (Figure 1). When the Global Ocean Flux Study (GOFS) began in 1984 in the U.S., followed in 1987 by the international Joint Global Ocean Flux Study (JGOFS), several ideas about the functioning of the biological pump formed the conceptual core of the fledgling program:

- ◆ The biological and physical processes in the ocean that control the air-sea carbon dioxide (CO₂) balance are key factors in the planetary climate system.
- ◆ The efficiency of the biological pump, expressed as the amount of carbon exported from the surface layer divided by the total amount produced through photosynthesis, is determined by foodweb processes.
- ◆ Pump efficiency and export processes can be monitored and understood through a global network of sediment traps and satellite sensors, informed by process studies and models.

In this article, we review the antecedents of JGOFS thought on the relationship between biological processes and carbon export and highlight some JGOFS achievements. We then look ahead to suggest where the field is headed and what the major problems are now, after more than a decade of multidisciplinary research in JGOFS.

Historical And Theoretical Background

In 1979, Richard Eppley, a biological oceanographer, and Bruce Peterson, a limnologist, published in *Nature* a synthesis of estimates of primary production

and new production rates from several locations in the coastal and open Pacific Ocean. They also demonstrated that the flux of particles out of the surface layer, as measured by sediment traps, generally approximated the large-scale rate of new production. In 1967, Richard Dugdale and John Goering had defined new production as the fraction of the overall net primary production that was supported by external, or “new” inputs of nutrients. They focused on nitrate in deep ocean water supplied to the euphotic zone by vertical mixing and upwelling as the principal new nutrient, but they did explicitly identify N₂ fixation as a potential source of new nitrogen (see Michaels et al., this issue). They also highlighted sinking particles as the major pathway for export in the oceanic nitrogen budget. But it was Eppley and Peterson (1979) who articulated the paradigm that came to govern ocean flux studies over the coming decades:

We estimate the sinking flux of POC [Particulate Organic Carbon] in the deep ocean by assuming that new production, as defined by Dugdale and Goering, is quantitatively equivalent to the organic matter that can be exported from the total production in the euphotic zone without the production system running down (Eppley and Peterson, 1979, p. 679).

Eppley and Peterson also defined the ratio of new to total production as the f-ratio and showed that f was an asymptotic function of the magnitude of total production. This relationship provided an explicit link between remotely-sensed primary production rates and the ocean carbon cycle. If total production could be estimated from remotely-sensed properties, one could apply the Eppley-Peterson algorithm and calculate the export rates as functions of time and space. The f-ratio thus provided both a means to define the efficiency of the biological pump quantitatively and a step toward quantifying the functioning of the pump on a global scale.

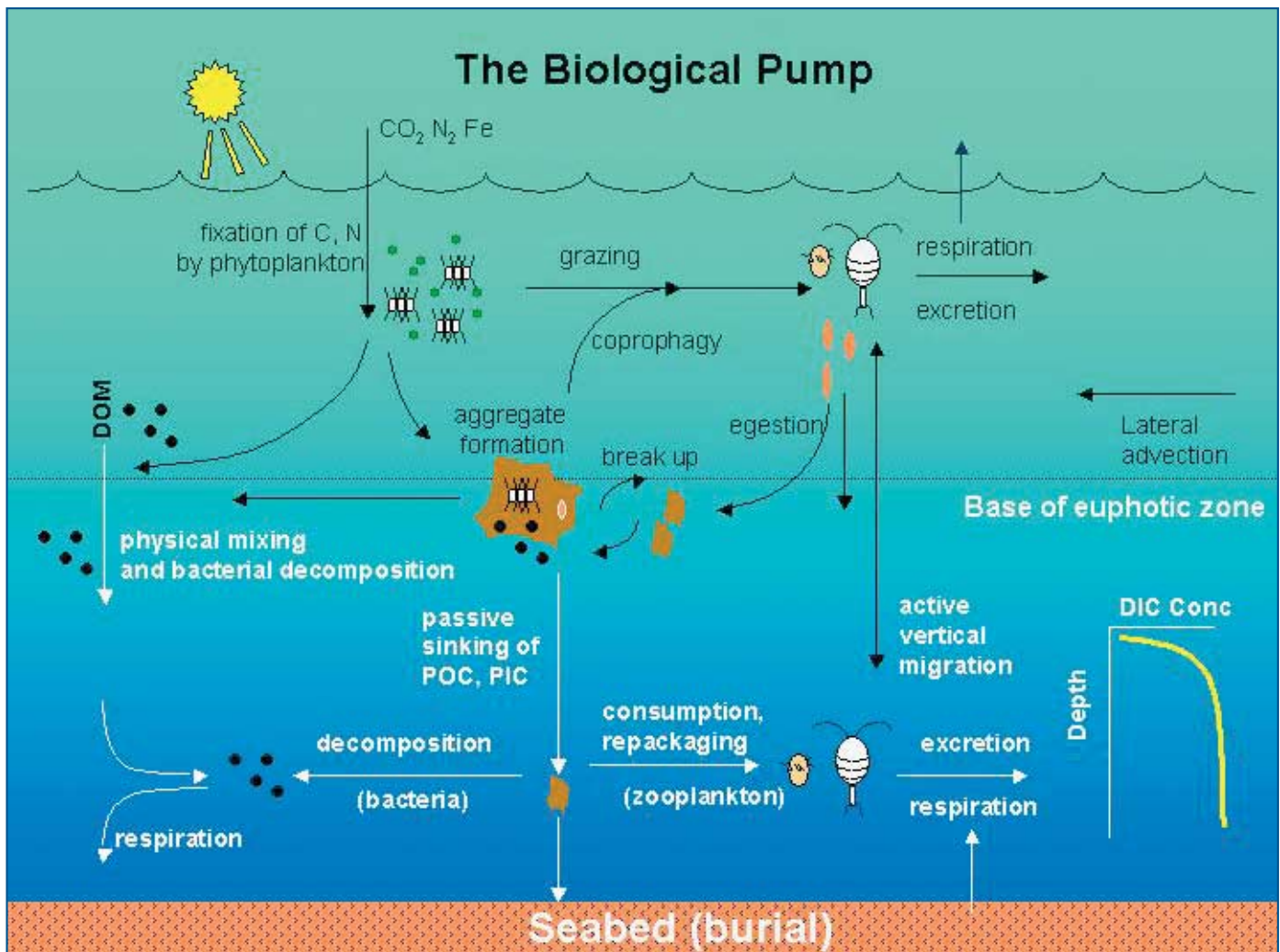


Figure 1. Components of the “biological pump” are responsible for transforming Dissolved Inorganic Carbon (DIC) into organic biomass and pumping it in particulate or dissolved form into the deep ocean. Inorganic nutrients and Carbon Dioxide (CO_2) are fixed during photosynthesis by phytoplankton, which both release Dissolved Organic Matter (DOM) and are consumed by herbivorous zooplankton. Larger zooplankton—such as copepods, egest fecal pellets—which can be reingested, and sink or collect with other organic detritus into larger, more-rapidly-sinking aggregates. DOM is partially consumed by bacteria (black dots) and respired; the remaining refractory DOM is advected and mixed into the deep sea. DOM and aggregates exported into the deep water are consumed and respired, thus returning organic carbon into the enormous deep ocean reservoir of DIC. About 1% of the particles leaving the surface ocean reach the seabed and are consumed, respired, or buried in the sediments. There, carbon is stored for millions of years. The net effect of these processes is to remove carbon in organic form from the surface and return it to DIC at greater depths, maintaining the surface-to-deep ocean gradient of DIC (inset graph at lower right). Thermohaline circulation returns deep-ocean DIC to the atmosphere on millennial timescales.

At the kick-off GOFS workshop sponsored by the U.S. National Academy of Sciences, Bruce Frost (1984) gave a seminal talk showing how foodweb structure and processes could influence the amount and fraction of production exported - in other words, how foodweb structure governed the f-ratio. Using a simple, steady-state model (Figure 2) and making simple assumptions about the partitioning of primary production between dissolved and particulate matter and among various size classes of grazers, Frost showed how the f-ratio and e-ratio (ratio of sinking flux to primary produc-

tion) varied as functions of the pathways by which nitrogen flowed among different organisms—phytoplankton, large and small grazers and bacteria.

Frost’s “simple” model was unique at the time because it included dissolved organic matter flows (see Hansell and Carlson, this issue) and bacteria. It also pointed out the importance of the recycling of detrital materials in the efficiency of the pump. Finally, his model showed how the sometimes vague term “foodweb structure” could be described quantitatively in a system of linear equations. Another important lesson

learned from this type of model was that the magnitude of export in quasi steady-state systems is set by the level of new production and by physics, rather than by the foodweb *per se* (Figure 2).

These two early contributions provided important core concepts that JGOFS has depended upon right up to the present: a quantitative relationship between new and total production and the linkages among foodweb structure, biological pump efficiency and export.

Limiting Nutrients And Large Cells

An interesting example of the role of foodweb structure is provided by the case of the diatoms. A second look at Frost's diagram shows that this model emphasizes the microbial "background state" of planktonic systems, the near steady-state assemblage of small-celled plankton kept in check by small, rapidly growing micrograzers. But phytoplankton blooms are often dominated by larger-celled organisms whose growth is stimulated by inputs of new nutrients. In addition to the familiar blooms each spring in the temperate zone and those caused by coastal upwelling, blooms are also triggered by aeolian inputs of iron, as shown in recent dramatic iron-fertilization experiments (Coale et al., 1996). Most plankton variability appears to be driven by diatom blooms, which are limited by inputs of silicon rather than nitrogen. Diatoms are important for several reasons. With mineralized, siliceous shells, they sink like rocks. Because they are large, they support the growth of larger zooplankton. For example, the massive diatom blooms in the ice edge surrounding Antarctica contribute to pulsed export events in that region (Figure 3).

Measuring the Strength of the Biological Pump

At the beginning of JGOFS, Eppley (1989) summarized four general approaches to measuring new production and its

equivalent, export production. One common method mentioned was bottle incubation experiments using compounds labeled with the ¹⁵N isotope as a tracer for estimating new production, introduced by Dugdale and Goering (1967). Another was the use of upper-ocean sediment traps to measure particle flux or export production, widely applied by John Martin and his colleagues in the Vertical Transport and Exchange (VERT-TEX) program of the 1980s. An alternative approach

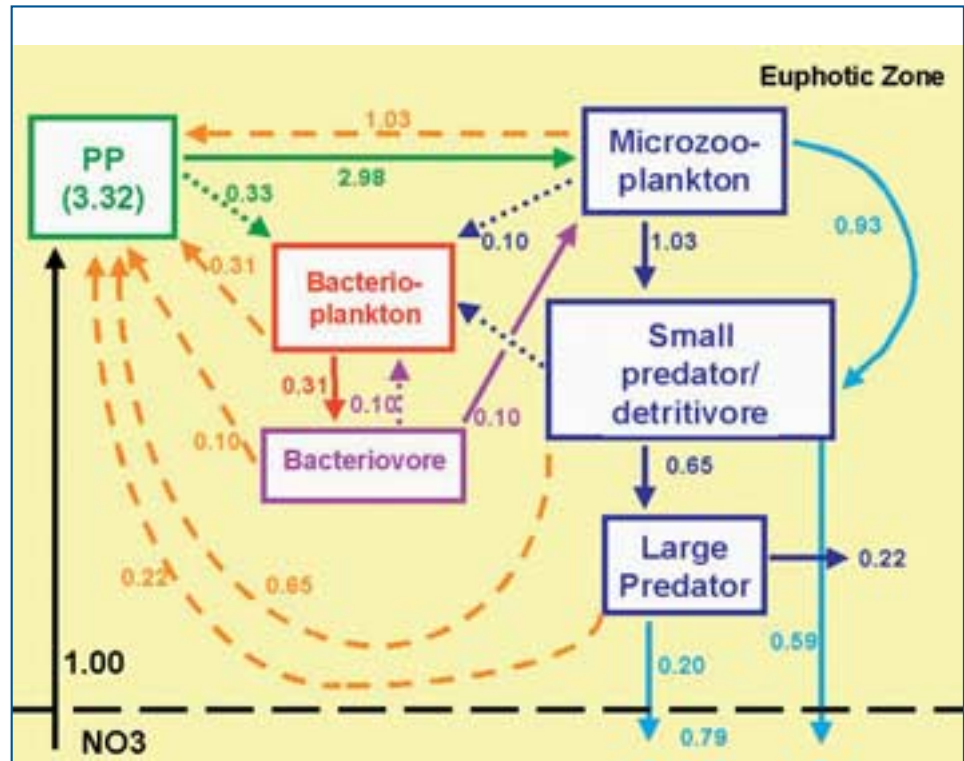


Figure 2. Foodweb model from Frost (1984) showing the influence of foodweb structure on export efficiency (proportion of export to total production). This represents Frost's Scenario 2, in which phytoplankton, dominated by small cells, release 10% of the photosynthesized material as Dissolved Organic Matter (DOM); the rest is consumed by microzooplankton. Solid arrows represent particulate fluxes; dashed orange arrows, flows of ammonium; and dotted arrows, flows of DOM. The numbers show flows resulting from a unit input of new nitrogen (nitrate or NO₃) at steady state. No DOM export is included in this model. The f-ratio is 1/3.32, or 0.3. The particle export balancing the NO₃ input includes sinking particles plus emigration or harvest of the large predator production (0.22). Changing the proportion of primary production (PP) released as DOM from 10/90 to 50/50 increases the total primary production 50% to 5.1 and reduces the e-ratio by 35% to 0.15. This is because total export stays constant while total PP increases. Changing the DOM supply merely alters the relative amounts of bacteria and bacteriovores consumed by microzooplankton, while their total consumption stays the same. Assuming that all herbivory is accomplished by the small predators reduces the total PP to 2.1 and increases the f-ratio and e-ratio to 0.47 and 0.37 respectively. The sinking term stays constant. The only way to increase the absolute amount of export at a steady state is to increase the new production, which is usually controlled by physical factors. The maximum f-ratio for this system is attained when there is no DOM release by phytoplankton and all PP is eaten by the small predators. (This diagram includes the effects of recycling, neglected in Frost's original model).

was to use seasonal changes in oxygen or nutrient stocks to examine regional trends in geochemical balances, from which one could draw inferences about net fluxes into or out of the surface ocean. These geochemical balance methods integrated over all forms of carbon transport, including particle settling, active zooplankton migration and the physical mixing of Particulate and Dissolved Organic Carbon (POC and DOC).

The fourth method for measuring the strength of the biological pump involved the use of a naturally occurring particle-reactive radionuclide, thorium-234, as a tracer for sinking particles. Thorium-234 (^{234}Th) has a half-life of 24 days and is produced at a constant rate from its soluble parent uranium-238 (^{238}U). Lower ^{234}Th activity in surface waters was found to be associated with higher rates of ^{234}Th loss via sinking particles. As summarized by Eppley, POC export could be calculated by multiplying the particulate ^{234}Th residence time by the stocks of POC, assuming equal particle residence times, an assumption that was not supported by further field studies.

The first JGOFS pilot study in the North Atlantic in 1989 included a new ^{234}Th approach (Buesseler et al., 1992). With this new method, the calculation of the ^{234}Th flux was based on the measured total disequilibrium between ^{234}Th and ^{238}U , as in prior studies. The resulting flux was then multiplied by the empirically measured ratio of POC to ^{234}Th or Particulate Organic Nitrogen (PON) to ^{234}Th on particles to determine flux in carbon or nitrogen units.

In theory, the ^{234}Th methods should yield particulate flux values equivalent to those derived from trap measurements if they are integrated over the same space and time scales, as both should be when quantifying gravitational settling rates. The apparent discrepancy between ^{234}Th values derived from water-column measurements and the ^{234}Th levels measured in trap fluxes stimulated controversy early in the JGOFS decade. Investigators are still debating the extent of biases in shallow-trap measurements, and it is not certain whether a calibration derived from ^{234}Th measurements can be applied to all particle classes. We still do not know under what conditions and particle regimes traps are accurate, and whether sediment trap biases

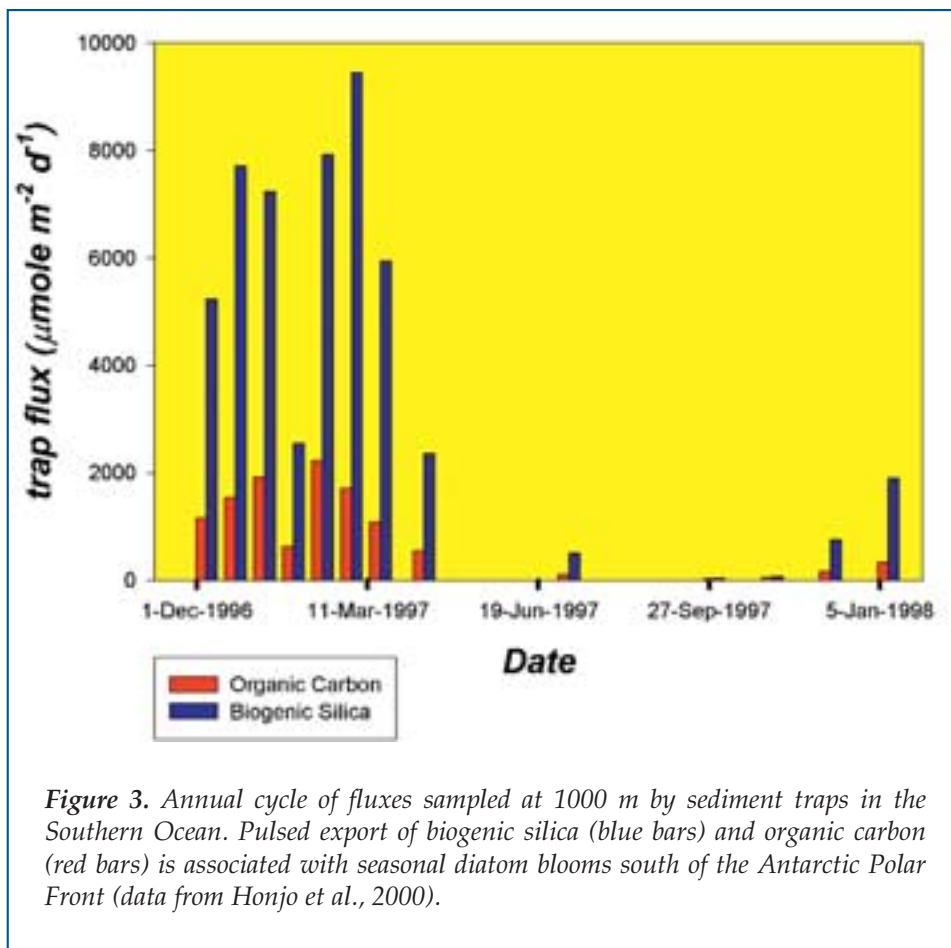


Figure 3. Annual cycle of fluxes sampled at 1000 m by sediment traps in the Southern Ocean. Pulsed export of biogenic silica (blue bars) and organic carbon (red bars) is associated with seasonal diatom blooms south of the Antarctic Polar Front (data from Honjo et al., 2000).

are primarily the result of the flow of water over, in and out of the trap mouth; sample preservation problems; or the collection of “swimmers”, zooplankton that swim into the traps and die.

JGOFS provided a forum for discussion of these issues in two publications, one U.S. and one international (Knauer and Asper, 1989; Gardner, 2000). The ^{234}Th method is limited primarily by its use of empirical ratios of POC to ^{234}Th in samples collected on filters that may or may not reflect the majority of particles responsible for gravitational settling losses. The strongest evidence in support of the new ^{234}Th method is the consistency between ^{234}Th -derived export numbers and other estimates of new and export production (Buesseler, 1998). With improvements over the years, this approach has been used in every U.S. JGOFS time-series and process study.

When comparing methods for ascertaining new and export production, it is important to keep issues of time and space scales in mind. For example, incubations last for 24 hours, but traps are deployed for a number of days or weeks. One must also bear in mind the differences in the processes that each method actually measures, whether gravitational settling, nutrient uptake or DOC transport. A review of new production methods suggested that differences of less than a factor of two are difficult to resolve in general (Ducklow,

POC flux vs. primary production

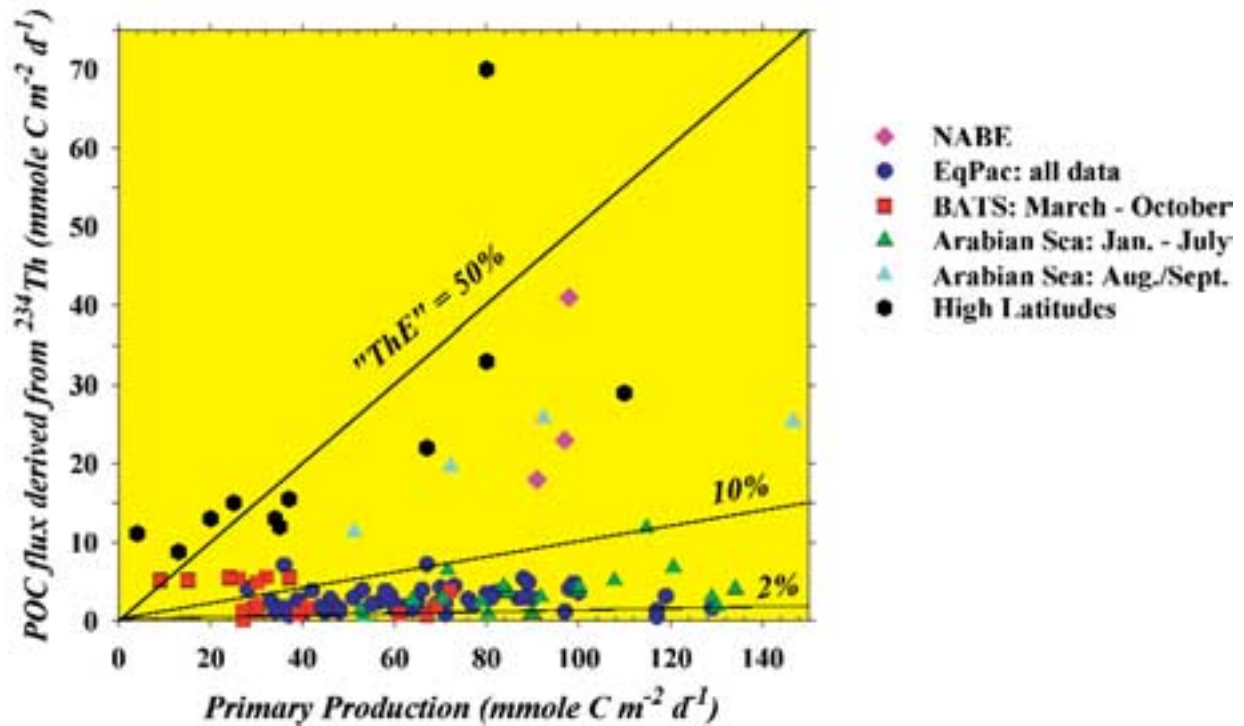


Figure 4. Summary plot of primary production (determined by standard ¹⁴C methods) vs. Particulate Organic Carbon (POC) flux from the upper ocean (100 or 150 m fluxes determined using ²³⁴Th methods). Ratios of POC flux to primary production ("ThE" ratio) for 50%, 10% and 2% are shown. (Figure updated from Buesseler, 1998).

1995). Future studies will benefit from improvements in trap design, tracer methods such as ²³⁴Th and optical methods that quantify particle abundance and composition. With improved compilations of global ocean data sets, mean annual estimates of new production using seasonal oxygen and nutrient changes can be computed more reliably.

Efficiency of the Biological Pump

An early goal of JGOFS was to understand both seasonal and regional variability and the controls on the efficiency of the biological pump. Pre-JGOFS studies suggested some universal or at least regional relationships in the ratios of new or export production to primary production. But U.S. JGOFS data from the time-series programs near Bermuda and Hawaii and the process studies provided evidence that the efficiency of the biological pump was not easily parameterized and varied considerably between sites and within seasons at any one site. Data from the time-series sites suggest that primary production and sediment-trap fluxes are poorly or even negatively correlated. At Hawaii, David Karl and his coworkers observed an order of magnitude variability in their 150 m sediment trap record, plus unexpected decoupling of primary

production and export. Their data show a three-year decrease in POC flux that coincides with a steady rise in primary production within the normal range of seasonal variability at the Hawaii Ocean Time-series (HOT) study site. They suggest that transient biological processes such as diatom blooms and a major ecosystem change from nitrogen to phosphorus limitation may be responsible for changes in the export/production ratio (see Karl et al., this issue).

The existing ²³⁴Th-based flux data suggest that while much of the ocean is characterized by low relative ratios of export to production, the locations and times of high export coincide with locations and times of large phytoplankton blooms—diatoms in particular (Figure 4). One example suggesting that diatom blooms control export comes from the Arabian Sea, where the POC flux remains relatively low, except in late summer during the annual southwest (SW) monsoon (Figure 5a). Measurements throughout the year suggest a positive relationship between export flux and the abundance of diatoms, as measured by levels of the pigment fucoxanthin (Figure 5b). The shift towards higher POC flux during the late SW monsoon corresponds to a change in the relationship between export rates and pigment concentrations. The efficiency of the biological

pump appears to increase, as evidenced by the higher export rates for a given diatom pigment concentration. Also, in the Arabian Sea, the seasonal data show delays greater than a month between the onset of production at the start of the monsoon and export.

The time lag between the uptake of nutrients and subsequent export is one characteristic of plankton blooms that must be considered in ecosystem models and in balancing local estimates of new and export production. Our Arabian Sea data support the hypothesis that large cells control the efficiency of the biological pump in this context, but they do not provide a universal “calibration” that can be used to extrapolate to other areas and times in which this simple relationship is not seen. Such data alone do not tell us whether the export flux is controlled by zooplankton grazing pressures or by nutrient limitation followed by aggregation and settling. While we know from sediment trap data that particle fluxes decrease rapidly with depth between the euphotic zone and 500–1000 m, we have little knowledge of the processes that control this remineralization pattern (see Berelson, this issue). Microbial decomposition, zooplankton consumption and chemical dissolution are all likely to alter the local efficiency of the biological pump.

The Role of Zooplankton

Zooplankton play a well-documented role in the biological pump by feeding in surface waters and producing sinking fecal pellets. Vertically migrating zooplankton and nekton also play an important role in transport by consuming organic particles in the surface waters at night and metabolizing the ingested food below the mixed layer during the day. One significant contribution of the JGOFS program is an increase in our understanding of how passive sinking of fecal pellets and active transport via diel vertical migration affect patterns and magnitude of fluxes of carbon and associated elements from the surface to the deep ocean.

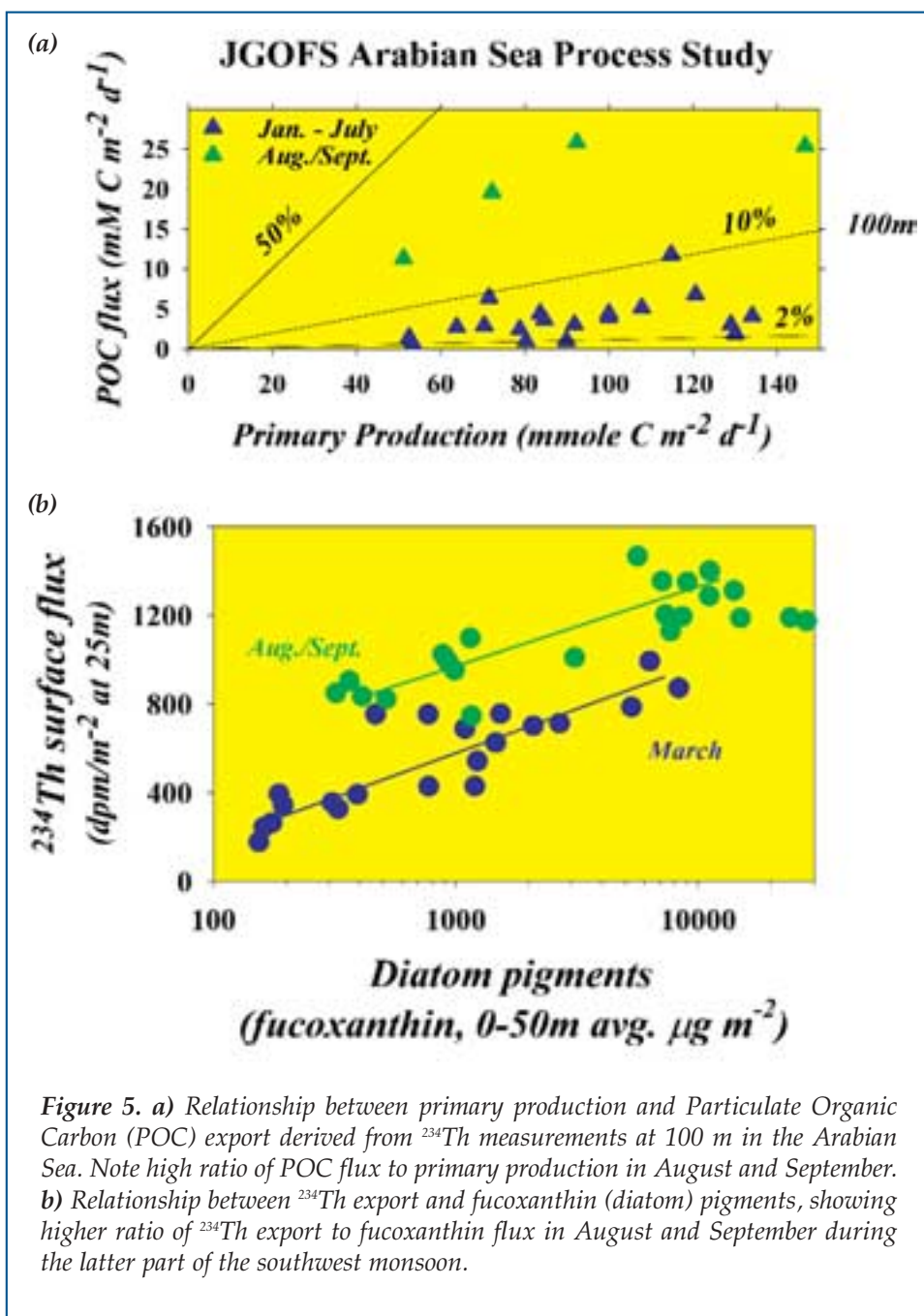


Figure 5. *a*) Relationship between primary production and Particulate Organic Carbon (POC) export derived from ^{234}Th measurements at 100 m in the Arabian Sea. Note high ratio of POC flux to primary production in August and September. *b*) Relationship between ^{234}Th export and fucoxanthin (diatom) pigments, showing higher ratio of ^{234}Th export to fucoxanthin flux in August and September during the latter part of the southwest monsoon.

Passive Sinking of Fecal Pellets

While it is clear that much of the carbon in the ocean is recycled through the microbial food web, potentially leaving little energy in the form of food for metazoa, larger organisms are more important than small for export because of the high sinking rates of large cells and the short food chains that produce large sinking particles. Thus the zooplankton play an integral role in the flux of material out of the euphotic zone by consuming the larger phytoplankton and producing sinking fecal pellets.

Changes in zooplankton biomass and composition can dramatically affect the composition and sedimenta-

tion rate of fecal pellets and thus the export of organic material to the deep ocean. Results from JGOFS show differences in the importance of fecal pellet flux from one ocean basin or season to another. In the Arabian Sea, the grazing of mesozooplankton is significant, and the fecal pellet flux averages 12% of primary production. This high proportion is linked to high zooplankton biomass, an abundance of large diatoms, and warm temperatures that lead to high zooplankton growth rates (Roman et al., 2000). Estimated fecal flux during the northeast (NE) monsoon and intermonsoon is higher than the measured export flux, indicating some recycling in the surface waters, but makes a smaller contribution during the SW monsoon, when uneaten phytoplankton cells contribute more to the flux.

In the equatorial Pacific, comparisons of data collected in the subtropical oligotrophic gyre and in the mesotrophic High Nutrient-Low Chlorophyll (HNLC) equatorial region show that mesozooplankton biomass is on average 2.5 times higher, and fecal pellet production is roughly 2 times higher in the HNLC region. This contrast indicates a comparatively larger contribution of fecal pellets to the sinking flux in the HNLC equatorial Pacific (Le Borgne and Rodier, 1997). Estimates indicate that mesozooplankton fecal pellets contribute up to 100% of the sinking POC flux in this region (Dam et al., 1995). Comparisons of data collected at the U.S. JGOFS HOT and the Bermuda Atlantic Time-series (BATS) sites, both located in oligotrophic regions, show on average, a higher annual contribution of fecal pellets to total flux at the HOT site than at the BATS site. This difference is probably associated with the higher mesozooplankton biomass and growth rates at the HOT site (Roman et al., in press).

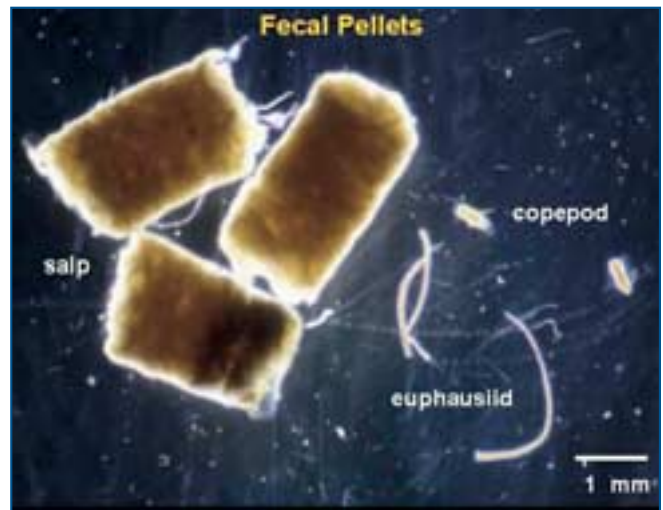


Figure 7. Size comparison of salp fecal pellets with those of other common zooplankton taxa.

Zooplankton biomass alone is not necessarily a good predictor of flux; the species composition of the resident community can have a dramatic effect on the efficiency of the biological pump. For example, there is a positive but weak relationship between monthly zooplankton biomass and organic carbon flux at the BATS site (Figure 6). Analysis of the bloom dynamics of salps (large gelatinous pelagic tunicates) in the 10-year BATS record indicates that salps consume on average 4% of the primary production, but that fecal pellets from salps can constitute an average of 33% (with a maximum of 100%) of the sediment trap flux at 150 m.

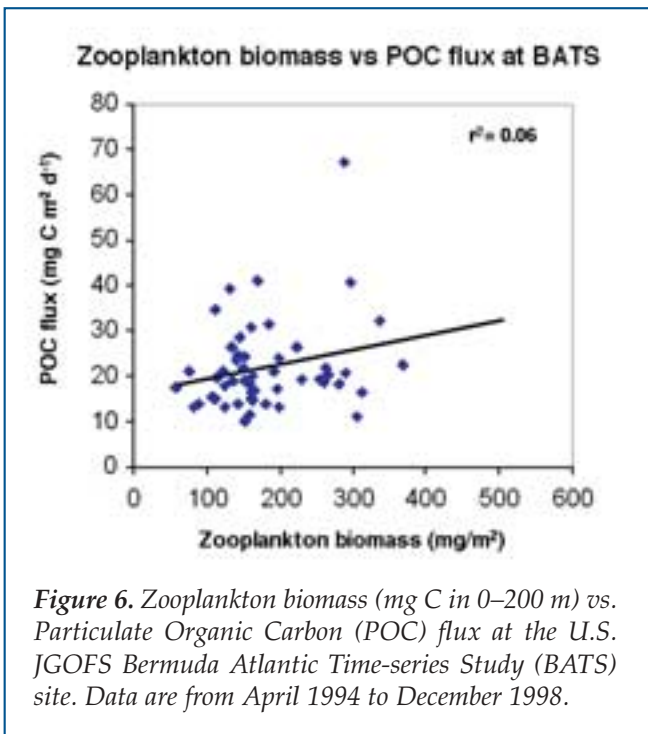


Figure 6. Zooplankton biomass (mg C in 0–200 m) vs. Particulate Organic Carbon (POC) flux at the U.S. JGOFS Bermuda Atlantic Time-series Study (BATS) site. Data are from April 1994 to December 1998.



Figure 8. Common vertically migrating zooplankton and micronekton at the U.S. JGOFS Bermuda Atlantic Time-series Study (BATS) site. a) Copepod *Pleuromamma xiphias*; b) Amphipod *Anchylomera blossevillie*; c) Euphausiid *Thysanopoda aequalis*; and d) Sergestid shrimp *Sergestes Atlanticus*.

Although salps are ubiquitous in the global ocean at generally low densities, periodic blooms give rise to dense populations. Due to the high filtration rates of salps and the wide range of suspended particles they are able to consume, salps effectively package small particles into large. As a result, the large and heavier particles or fecal pellets sink rapidly (Figure 7). In the southern ocean, large blooms of *Salpa thompsoni* exert grazing pressure orders of magnitude higher than the resident copepod populations; this grazing is high enough to prevent the buildup of phytoplankton blooms (Dubischar and Bathmann, 1997). Thus, changes in the relative abundance of zooplankton species, not only increase in biomass alone, may dramatically affect: the amount of primary production consumed; the composition and sedimentation rate of

sinking particles; and the flux of organic material to the deep ocean.

Active Export Via Zooplankton Vertical Migration

Many species of zooplankton that live below the euphotic zone during the day, travel up into the surface waters at night to feed, and then descend again before dawn (Figure 8). Zooplankton can actively increase the magnitude of the export of organic material by transporting surface-ingested material in their guts to deep waters, where this material is then metabolized. Zooplankton molting or mortality from predation also contributes to the transportation of assimilated organic biomass into the deep waters. Initial studies by Alan Longhurst and colleagues (1990) called attention to the

potential importance of this process. Since then, JGOFS and other studies have concluded that calculations of export to deep waters should include vertical migration. Including the active transport of carbon and nitrogen through vertical migration increases our estimates of new production by increasing estimates of export.

By viewing Table 1, you will see why vertical migration can increase estimates of export. Table 1 shows the studies of active transport to date, most of which have been carried out through JGOFS. These observations demonstrate that vertically migrating zooplankton can transport a significant amount of carbon to deep water.

While active transport of carbon is on average only 4% to 34% of the sinking particulate organic carbon flux measured by sediment traps, it can be as high as 70% (Table 1). The relative importance of migration versus other fluxes, such as the physical mixing of dissolved organic matter or the passive sedimentation of organic particles, differs with the biomass of

Table 1

Studies to date measuring the ratio of downward transport of carbon by diel migrating zooplankton to gravitational particulate organic carbon (POC) fluxes measured by sediment traps (updated from Steinberg et al. 2000). Migrating biomass is the integrated night minus day zooplankton biomass in the surface 150 meters. Migratory flux is the amount of dissolved C respired or excreted by migrating zooplankton below 150 m or the depth of the euphotic zone. % of mean POC flux = (migratory flux/sediment trap flux at 150 m or the depth of euphotic zone) X 100%. Mean, and range (given in parentheses). Flux due to mortality at depth is not included here, although it is estimated in some studies. Data not listed here were not provided, or unclear, in reference

Location of study and time of year	Migrating biomass (mgC m ⁻²)	Migratory flux (mgC m ⁻² day ⁻¹)	% of mean POC flux	Reference
Subtropical & tropical Atlantic-several stations (September)	5.5 (2.8-8.8)	6 (4-14)	1
BATS (March/April)	191 (82-536)	14.5 (6.2-40.6)	34 (18-70)	2
Equatorial Pacific: (March/April)	96	4.2	18	3
(October)	155	7.3	25	
Equatorial Pacific: oligotrophic HNLC area (September/October)	47 53	3.8 7.9	8 4	4,5
North Atlantic (NABE)	(5-480)	(19-40)	6
BATS (year-round)	50 (0-123)	2.0 (0-9.9)	8 (0-39)	7
HOT (year-round)	142	3.6 (1.0-9.2)	15 (6-25)	8

References: ¹Longhurst et al. (1990) *Deep-Sea Research*, 37(4): 685-694, ²Dam et al. (1995) *Deep-Sea Research*, 42(7): 1187-1197, ³Zhang and Dam (1997) *Deep-Sea Research II*, 44: 2191-2202., ⁴LeBorgne and Rodier (1997) *Deep-Sea Research II*, 44: 2003-2023, ⁵Rodier and Le Borgne (1997), *Deep-Sea Research II*, 44: 2085-2113, ⁶Morales (1999) *Journal of Plankton Research*, 21: 1799-1808, ⁷Steinberg et al. (2000) *Deep-Sea Research I*, 47: 137-158, ⁸Al-Mutairi and Landry (2001) *Deep-Sea Research II*, 48: 2083-2103.


the migrating organisms, the study location and the season. Although one might expect migrant flux to be more important in oligotrophic regions where a high proportion of zooplankton migrate and particle fluxes are relatively low, this is not always the case. Active flux at the oligotrophic BATS and HOT sites is generally lower or similar to fluxes in more mesotrophic regimes such as the equatorial Pacific. Comparison of the HOT and BATS data sets reveals higher active flux at HOT, in part because of higher migrating biomass at that site and in part because of differences in metabolite rate calculations (Table 1).

We conclude that the relative importance of migration versus other fluxes appears to be more closely tied to the biomass of the migrating community than to the magnitude of gravitational flux. Thus, active flux is likely to be important in systems with a high migrating biomass. While there are a number of studies of inorganic carbon and nitrogen transport by migrators, there are only a handful that have included other kinds of active transport. When forms of transport such as organic excretion, defecation, mortality and molting are considered, estimates of active transport may be more than double the current estimates. These processes are not well known and need attention in future studies.

Conclusions, Models And Prospects

The simple relationships among production rates, sedimentation and foodweb structure that helped to stimulate the creation of the JGOFS program now look simplistic and naïve. The algorithms relating productivity and export, used in global and cross-system comparisons, break down when one attempts to make predictions within regions and systems. Intensive observations at the U.S. JGOFS time-series and process-study sites revealed the dependency of these relationships on scale and the strong role foodweb structure plays in the magnitude of flux and pump efficiency. The effects of food webs on export fluxes are mediated through conditions that select for the emergence of large organisms—such as diatoms, *Trichodesmium*, krill and salps—out of the microbial background. These conditions are still crudely formulated in carbon cycle models. In order to represent the regional and temporal variability of export and its composition accurately, models need new levels of ecological complexity, including parameterization of individual keystone species populations.

New appreciation of the role of foodweb structure and functioning is linked to new radioisotopic approaches and new tools developed during JGOFS, used to sample surface fluxes at finer spatial resolutions and at higher frequencies, than can be achieved with sediment traps alone. The example of export variability illustrates once again that a key JGOFS achievement has been the multidisciplinary cooperation by geochemists, microbiologists and ecologists to attack

problems of carbon flux together—across a spectrum of ocean ecosystems. 

This is U.S. JGOFS Contribution Number 684.

References

- Buesseler, K.O., 1998: The de-coupling of production and particulate export in the surface ocean. *Global Biogeochemical Cycles*, 12(2), 297–310.
- Buesseler, K.O., M.P. Bacon, J.K. Cochran and H.D. Livingston, 1992: Carbon and nitrogen export during the JGOFS North Atlantic Bloom Experiment estimated from ²³⁴Th:²³⁸U disequilibria. *Deep-Sea Res. I*, 39(7–8), 1115–1137.
- Coale, K. H., K. S. Johnson, S. E. Fitzwater, R. M. Gordon, S. Tanner, F. P. Chavez, L. Ferioli, C. Sakamoto, P. Rogers, F. Millero, P. Steinberg, P. Nightingale, D. Cooper, W. P. Cochlan, M. R. Landry, J. Constantinou, G. Rollwagen, A. Trasvina and R. Kudela, 1996: A massive phytoplankton bloom induced by an ecosystem-scale iron fertilization experiment in the equatorial Pacific Ocean. *Nature*, 383, 495–501.
- Dam, H.G., X. Zhang, M. Butler and M.R. Roman, 1995: Mesozooplankton grazing and metabolism at the equator in the central Pacific: Implications for carbon and nitrogen fluxes. *Deep-Sea Res. II*, 42(2–3), 735–756.
- Dubischar, C.D. and U.V. Bathmann, 1997: Grazing impact of copepods and salps on phytoplankton in the Atlantic sector of the Southern Ocean. *Deep-Sea Res. II*, 44(1–2), 415–433.
- Ducklow, H.W., 1995: Ocean biogeochemical fluxes: New production and export of organic matter from the upper ocean. *Reviews of Geophysics Suppl.* (U.S. Natl. report to IUGG, Contributions in Ocean Sciences), 1271–1276.
- Dugdale, R.C. and J.J. Goering, 1967: Uptake of new and regenerated forms of nitrogen in primary productivity. *Limnol. Oceanogr.*, 12, 196–206.
- Eppley, R.W., 1989: New production: history, methods, problems. In: *Productivity of the Ocean: Present and Past*. W.H. Berger, V.S. Smetacek and G. Wefer, eds., Wiley & Sons, New York, 85–97.
- Eppley, R.W. and B.J. Peterson, 1979: Particulate organic matter flux and planktonic new production in the deep ocean. *Nature*, 282, 677–680.
- Frost, B.W., 1984: Utilization of phytoplankton production in the surface layer. In: *Global Ocean Flux Study: Proceedings of a Workshop, September 10–14, 1984, Woods Hole, Massachusetts*. National Academy Press, Washington, D.C., 125–135.
- Gardner, W.D., 2000: Sediment trap sampling in surface waters. In: *The Changing Ocean Carbon Cycle: A Midterm Synthesis of the Joint Global Ocean Flux Study*. R.B. Hanson, H.W. Ducklow, and J.G. Field, eds., Cambridge University Press, Cambridge, 240–284.
- Honjo, S., R. François, S. Manganini, J. Dymond and R. Collier, 2000: Particle fluxes to the interior of the Southern Ocean in the Western Pacific sector along 170°W. *Deep-Sea Res. II*, 47(15–16), 3521–3548.
- Knauer, G. and V. Asper, 1989: *Sediment Trap Technology and Sampling: Report of the U.S. GOFS Working Group on Sediment Trap Technology and Sampling*. U.S. GOFS Planning Report No. 10, 94 pp.
- Le Borgne, R. and M. Rodier, 1997: Net zooplankton and the biological pump: a comparison between the oligotrophic and mesotrophic equatorial Pacific. *Deep-Sea Res. II*, 44, 2003–2023.
- Longhurst, A.R., A.W. Bedo, W.G. Harrison, E.J.H. Head and D.D. Sameoto, 1990: Vertical flux of respiratory carbon by oceanic diel migrant biota. *Deep-Sea Res.*, 37(4), 685–694.
- Roman, M., S. Smith, K. Wishner, X. Zhang, and M. Gowing, 2000: Mesozooplankton production and grazing in the Arabian Sea. *Deep Sea Res. II*, 47, 1423–1450.
- Roman, M.R., H.A. Adolf, M.R. Landry, L.P. Madin, D.K. Steinberg and X. Zhang., in press: Estimates of oceanic mesozooplankton production: A comparison between the Bermuda and Hawaii time-series data. *Deep-Sea Res. II*.
- Steinberg, D.K., C.A. Carlson, N.R. Bates, R.J. Johnson, A.F. Michaels and A.H. Knap, 2001: Overview of the U.S. JGOFS Bermuda Atlantic Time-series Study (BATS): a decade-scale look at ocean biology and biogeochemistry. *Deep-Sea Res. II*, 48, 1405–1447.

The Flux of Particulate Organic Carbon Into the Ocean Interior: A Comparison of Four U.S. JGOFS Regional Studies

William M. Berelson

University of Southern California • Los Angeles, California USA

Introduction

The delivery of nutrients to the sunlit surface ocean spurs phytoplankton growth and the production of particulate organic carbon (POC). As organisms die or are consumed and excreted, some of these particles settle and are exported deep into the ocean interior before remineralization occurs; this process is a component of what is commonly called the “biological pump” (see Ducklow et al., this issue). Equations that generalize the relationship between the amount of carbon produced and the amount exported from the surface ocean, as well as the relationship between the export flux and ocean depth, are key components of models that seek to predict the distribution of CO₂ in the ocean in time and space.

This paper represents a summary of carbon budgets, an assimilation of U.S. JGOFS data related to the production and export of POC from the surface ocean to the deep sea floor. Two major concerns arise in the assembly of such budgets. One is whether or not particles settle vertically from the spot where formation occurs to a spot on the sea floor. We know that this does not happen to all particles, yet there is evidence in budget calculations and in the sedimentary record suggesting that there must be some major component of the particulate “rain” that falls essentially vertically (Berelson et al., 1997; Lee et al., 1998; Nelson et al., 2001).

Another major concern in constructing the vertical flux budgets is that various types of measurements made by various individuals and groups, at different times and different locations, are assembled and presented as a uniform picture when, in fact, they are a melange of many techniques, sites and timescales. One of the accomplishments of the U.S. JGOFS field program was that many POC flux measurements were made using consistent protocols, by many of the same investigators, at the same locations and during the same times.

In this paper we present 17 POC budgets for U.S. JGOFS sites in the North Atlantic, equatorial Pacific, Arabian Sea and the Southern Ocean. One budget is from the North Atlantic Bloom Experiment (NABE) site at 48°N, 21°W; seven are from the Equatorial Pacific Process Study (EqPac) between 9°N and 12°S at approx-

imately 140°W; five are from the Arabian Sea (AS) from 10°N to 19°N and 57°E to 65°E, and four are from the Pacific sector of the Southern Ocean (SO) from 55°S to 68°S at approximately 170°W.

We are primarily considering four types of flux determinations: the production of POC during primary productivity (PP) in the surface ocean as determined through the carbon-14 (¹⁴C) method; the export of POC from the upper few hundred meters of the water column as determined by thorium isotope budgets (Figure 1a); measurement of the rain of POC at a variety of depths with sediment traps (Figure 1b) and the sum of sea-floor remineralization rates determined using benthic landers (Figure 1c) and pore water measurements plus POC burial rates. Although the budgets presented in this paper integrate measurements made, with a few exceptions, during the same time intervals (Table 1), it is noteworthy that each measurement records fluxes on a different timescale. Productivity measurements, for example, can be considered a snapshot of carbon production over a few hours, whereas burial-rate measurements integrate hundreds to thousands of years.

The primary goal of this paper is to assemble POC budgets for various oceanic regions and to compare the relationships between primary productivity and export and export versus depth between regions. We have a choice in constructing these budgets as to what space and time frames to include. By including the longest time interval over which measurements were made, we are more likely to smooth and average out spurious data in favor of a more generalized picture. Sites were identified by the presence of a sediment-trap mooring. For the EqPac region, we show how grouping stations may influence budget interpretations. Measurement methodologies used for various studies are described in the papers referenced in Table 1.

Results

The logarithmic scale used in Figures 2 and 3 tends to emphasize the two orders of magnitude difference between PP and particulate rain below 2000 m and to minimize the changes in POC flux below this depth. The between-site range in PP and rain below 2000 m

varies by an order of magnitude. However, there are differences of approximately 2 orders of magnitude in estimates of POC export at 100 m, reflecting variability both in this parameter and in our ability to quantify export. As a general rule, roughly 1% of the POC produced in the surface ocean is exported to depths below 2000 m, although there are systematic differences between regions. Another general observation is that POC rain between 2000 m and 5000 m shows little change.

We compare three models relating POC export to PP with observed data (Figure 4). These models vary in the way they formulate the relationship between PP and POC flux, but they are all based on data. It is apparent that the models overestimate POC export. We examine this relationship further in the summary presented in Figure 5, where export flux at 1000 m and 3000 m at all sites is compared to the flux predicted in the models. In constructing these plots, we used a linear interpolation of export flux at the target depth for sites where flux data existed within 500 m of this horizon. At three depth horizons, there were not enough data to make the interpolation.

We also compare POC flux profiles to a function describing flux vs. depth as a power law. This function, known as the Martin equation (Martin et al., 1987), has the following form:

$$\text{POC flux at depth } z = \text{POC flux at } 100 \text{ m} * (z/100)^b \quad (1)$$

In this equation, z represents depth in meters and b is a unitless fitting parameter. Solution of this equation requires knowledge of the POC flux at 100 m. The data presented in this paper were fitted with this equation after we determined an average flux value for export at 100 m. We used values supplied by Lee et al. (1998) for the Arabian Sea and values from Nelson et al. (2001) for the Southern Ocean sites.

For EqPac and NABE, POC flux at 100 m was determined as the simple average of all estimates of export; these included estimates of export at depths between 75 m and 150 m that were grouped into a single export value. For EqPac, we only used flux estimates

that incorporated results from both study seasons.

It may be argued that an average value for POC export at 100 m should not be derived by combining estimates based on different measurement techniques (floating traps vs. thorium, for example). With few exceptions, the various methods, when applied at the same location and during the same time period, yield flux estimates that agree within a factor of three or better. The plots in Figure 2 show the fit of Equation 1 to the observed data and the calculated value of b .

Discussion

The assemblage of primary productivity and POC export data from the U.S. JGOFS process studies in the North Atlantic, equatorial Pacific, Arabian Sea and Southern Ocean permits comparison among the regions (Figures 2-5). Several regional trends are apparent. At sites in the Arabian Sea and the equatorial Pacific where PP values are comparable, the export of POC from 100 m is greater in the Arabian Sea. Southern Ocean POC export rates are comparable to export fluxes at other

Table 1
Identification of Data References

Depth	North Atlantic	Equatorial Pacific	Arabian Sea	Southern Ocean
Euphotic (PP)	Martin et al. (1993) DSR, 40	Barber et al. (1996) DSR II, 43	Lee et al. (1998) DSR II, 45	Nelson et al. (2001) DSR II (in press)
75-850 m (Export)	Buesseler et al. (1992) DSR, 39 Martin et al. (1993) DSR, 40	Buesseler et al. (1995) DSR II, 42 Luo et al. (1995) DSR II, 42 Murray et al. (1996) DSR II, 43 Bacon et al. (1996) DSR II, 43 Wakeham et al. (1997) DSR II, 44	Lee et al. (1998) DSR II, 45	Nelson et al. (2001) DSR II (in press)
Deep Traps	Honjo & Manganini (1993) DSR, 40 Martin et al. (1993) DSR, 40	Honjo et al. (1995) DSR II, 42 Wakeham et al. (1997) DSR II, 44	Lee et al. (1998) DSR II, 45	Honjo et al. (2000) DSR II, 47
Benthic Recycling	Pfannkuche (1993) DSR, 40	Hammond et al. (1996) DSR II, 43 Berelson et al. (1997) DSR II, 44		Nelson et al. (2001) DSR, in press

North Atlantic (NABE): Late April-early June 1989.

Equatorial Pacific (EqPac): Spring and fall 1992. One field season took place during El Niño conditions, and the other during non-El Niño conditions.

Arabian Sea (AS): November 1994-December 1995, covering both monsoon and inter-monsoon seasons.

Southern Ocean (SO): October 1997-March 1998. Sediment trap measurements were not made beyond January 1998. Thus trap fluxes for December 1996 to March 1997 and October 1997 to February 1998 were combined to compute POC rain rates representative of the time when water column measurements were made.

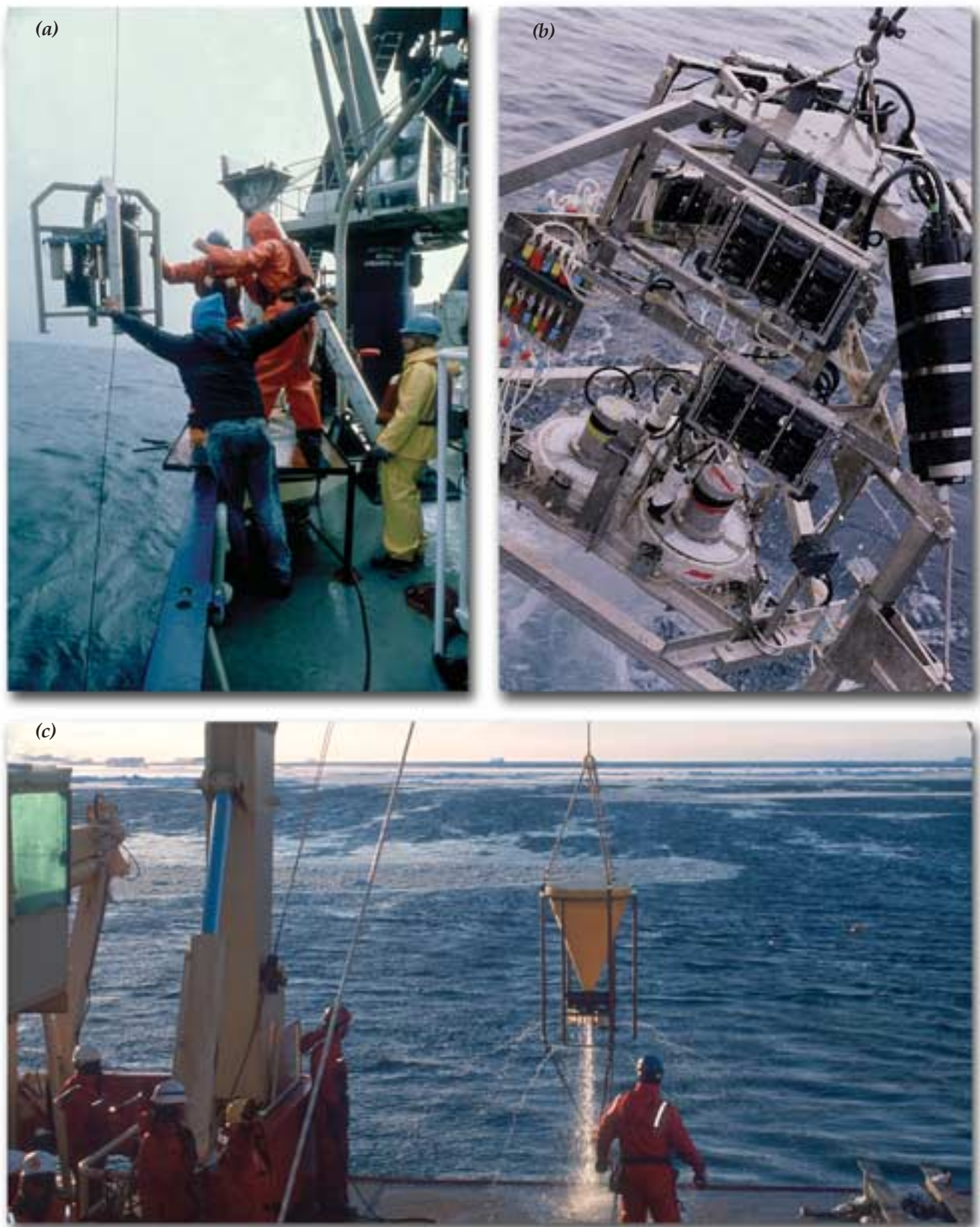


Figure 1. *a) Large-volume in situ pump used for collecting thorium-234 samples, photo courtesy of Ken Buesseler. b) Recovery of benthic lander, photo courtesy of William Berelson. c) Recovery of deep sediment trap in Southern Ocean, photo courtesy of Susumu Honjo.*

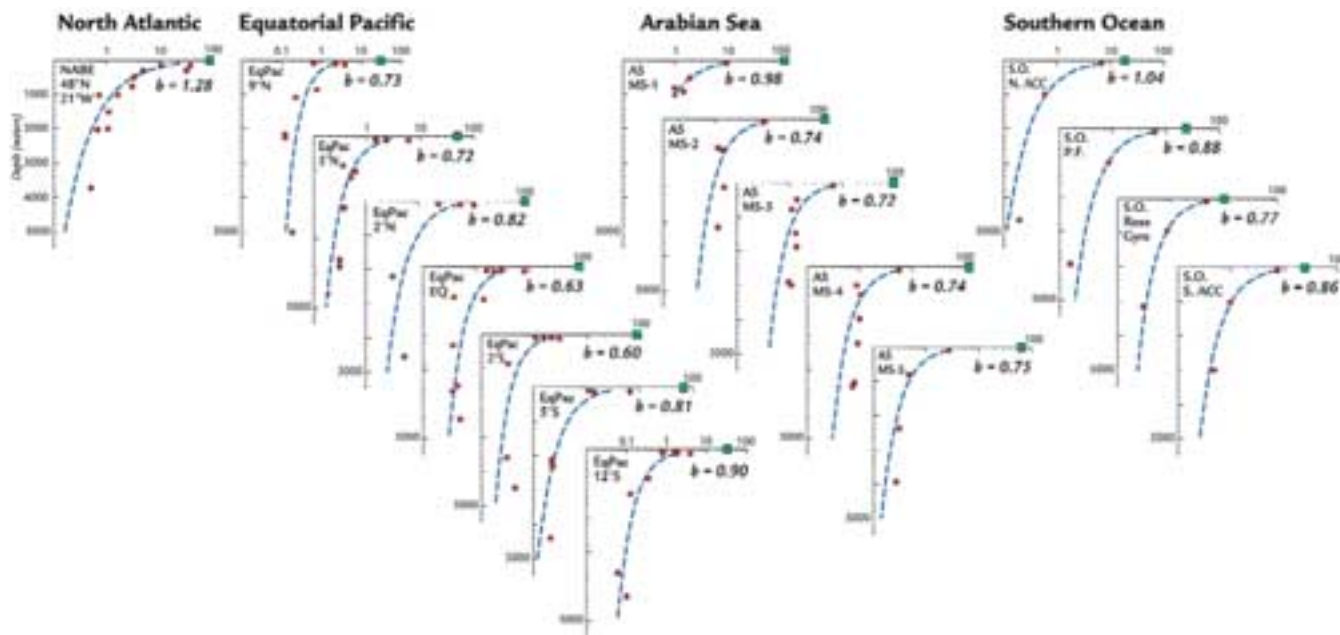


Figure 2. Plots of POC flux vs. depth for all 17 stations in the U.S. JGOFS regional studies conducted in the North Atlantic, equatorial Pacific, Arabian Sea and Southern Ocean. Squares identify estimates of primary productivity, and solid circles are estimated flux values at various depths. The deepest points for EqPac, SO and NABE are defined by benthic recycling and sediment burial fluxes. Note the log scale for the flux ($\text{mmol C m}^{-2} \text{d}^{-1}$) and some variability in this scale. Depth scale is in meters. An average value of POC flux at 100 m was determined, and that value was used as an anchor point in defining the best fit given by the Martin equation (Equation 1). We show equation fits to all the observed data for each of the study sites and the calculated fitting parameter b , described in the text.

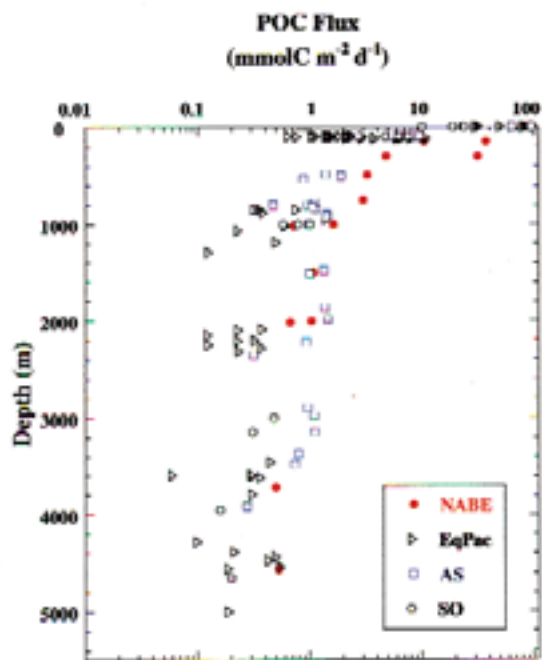


Figure 3. Summary plot of POC flux vs. depth. Points plotted on the depth = 0 axis represent estimates of primary productivity.

sites even though PP in the Southern Ocean is significantly lower. In the Arabian Sea, 1% of primary production reaches a depth of 2000 m; in the equatorial Pacific, this value is closer to 0.6%, and in the Southern Ocean, 1–2%. Finally, the Martin function tends toward a systematic underprediction of POC fluxes at depths greater than 3000 m.

We find that previously published models overestimate the amount of POC reaching 1000 m by a factor of 2 to 5 when primary productivity values are greater than $40 \text{ mmol C m}^{-2} \text{d}^{-1}$ (Figure 5). Model-estimated flux is greater than the measured flux at 3000 m as well, although the “Pace model” (Pace et al., 1987) shows a trend that is similar to the data trend and overestimates flux by less than a factor of two. It is notable that the Southern Ocean data are in reasonable agreement with all the model estimates, both at 1000 m and at 3000 m. The offset between the U.S. JGOFS data and the earlier models could be explained if earlier estimates of PP were low because of trace-metal contamination effects (Martin et al., 1993).

The assembled U.S. JGOFS data define a trend in primary production vs. POC rain that is roughly linear through an order of magnitude change in primary production. The Southern Ocean data add considerable scatter to such a trend. As POC export is positively correlated

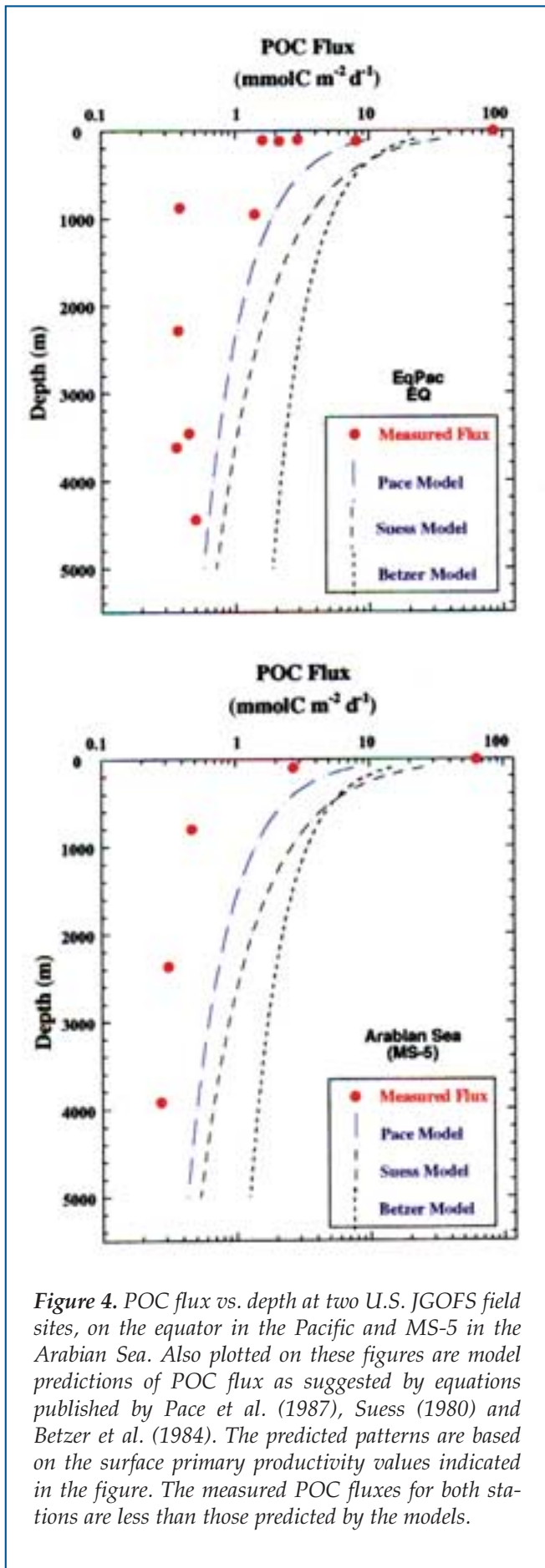


Figure 4. POC flux vs. depth at two U.S. JGOFS field sites, on the equator in the Pacific and MS-5 in the Arabian Sea. Also plotted on these figures are model predictions of POC flux as suggested by equations published by Pace et al. (1987), Suess (1980) and Betzer et al. (1984). The predicted patterns are based on the surface primary productivity values indicated in the figure. The measured POC fluxes for both stations are less than those predicted by the models.

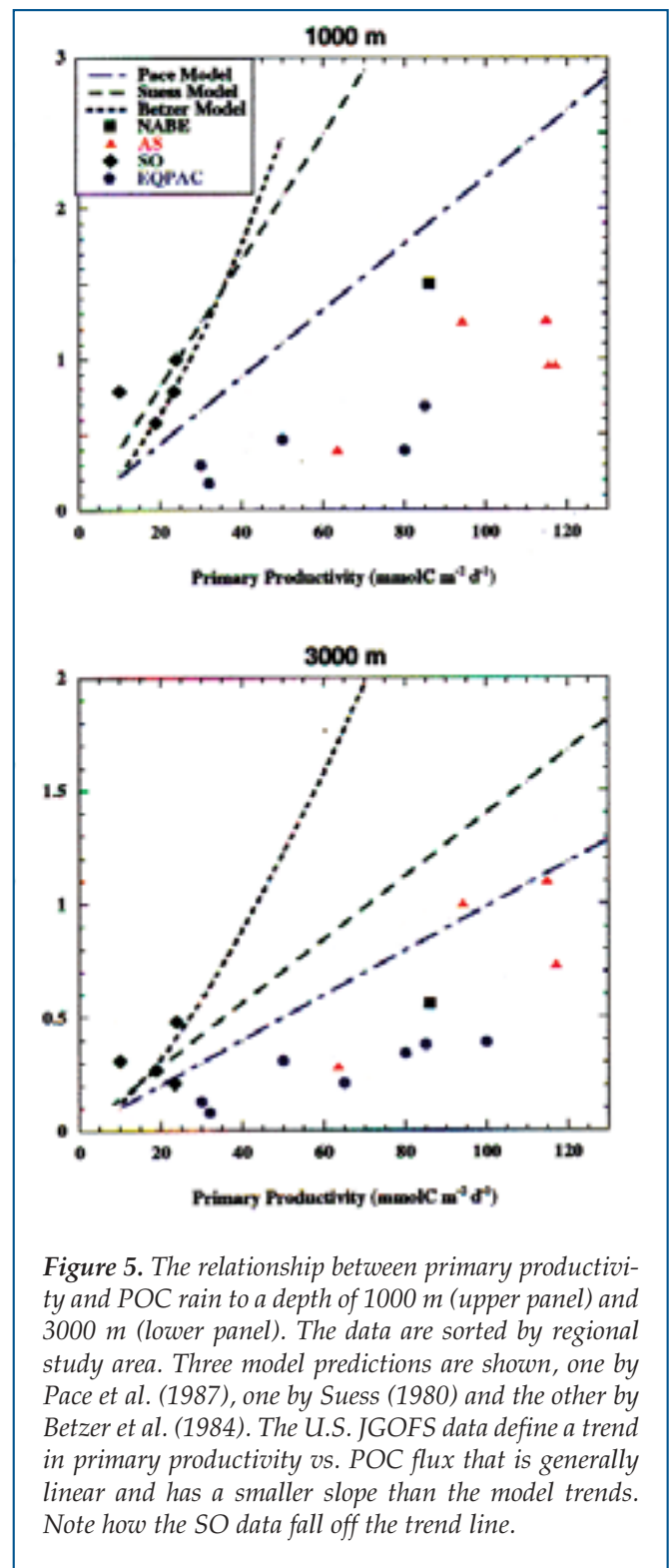


Figure 5. The relationship between primary productivity and POC rain to a depth of 1000 m (upper panel) and 3000 m (lower panel). The data are sorted by regional study area. Three model predictions are shown, one by Pace et al. (1987), one by Suess (1980) and the other by Betzer et al. (1984). The U.S. JGOFS data define a trend in primary productivity vs. POC flux that is generally linear and has a smaller slope than the model trends. Note how the SO data fall off the trend line.

with PP, a linear fit suggests that PP can account for about 70% of the variability in export of POC at 1000 m and about 80% of the variability in POC export at 3000 m. A linear fit between PP and POC export that passes through the origin defines a slope of approximately 120:1 ($\text{mmol C m}^{-2} \text{d}^{-1} / \text{mmol C m}^{-2} \text{d}^{-1}$) at 1000 m and approximately 150:1 at 3000 m. However, these slopes misrepresent the Southern Ocean data.

The Martin equation (Equation 1) is a commonly used parameterization in global biogeochemical models. In our analysis of this fitting equation, we find that the value chosen to represent POC export at 100 m is very important to the evaluation of the curve fit and the curve-fitting exponent b . For all 17 sites described, the total range of b values varied by a factor of 2, between 0.59 and 1.28. The greater the value of this parameter, the sharper the curvature in POC rain vs. depth. The distribution of b values shows some regional differences: for NABE, $b = 1.28 \pm 0.06$; for SO, $b = 0.88 \pm 0.12$; for AS, $b = 0.79 \pm 0.11$; and for EqPac, $b = 0.74 \pm 0.11$. The NABE export value at 100 m was derived from an average of estimates from thorium and floating-trap data and is larger than the floating-trap estimate alone; therefore the b value determined in this paper is greater than the value (0.946) reported by Martin et al. (1993), which considers only the trap data.

The shape of the Martin curve for sites from the U.S. JGOFS process studies is not significantly different from the curve fit for data from the time-series stations in the subtropical gyres. The fitting exponent b equals 0.81 for the Hawaii Ocean Time-series (HOT) site and ranges from 0.61 to 0.95 for the Bermuda Atlantic Time-series Study (BATS) site.

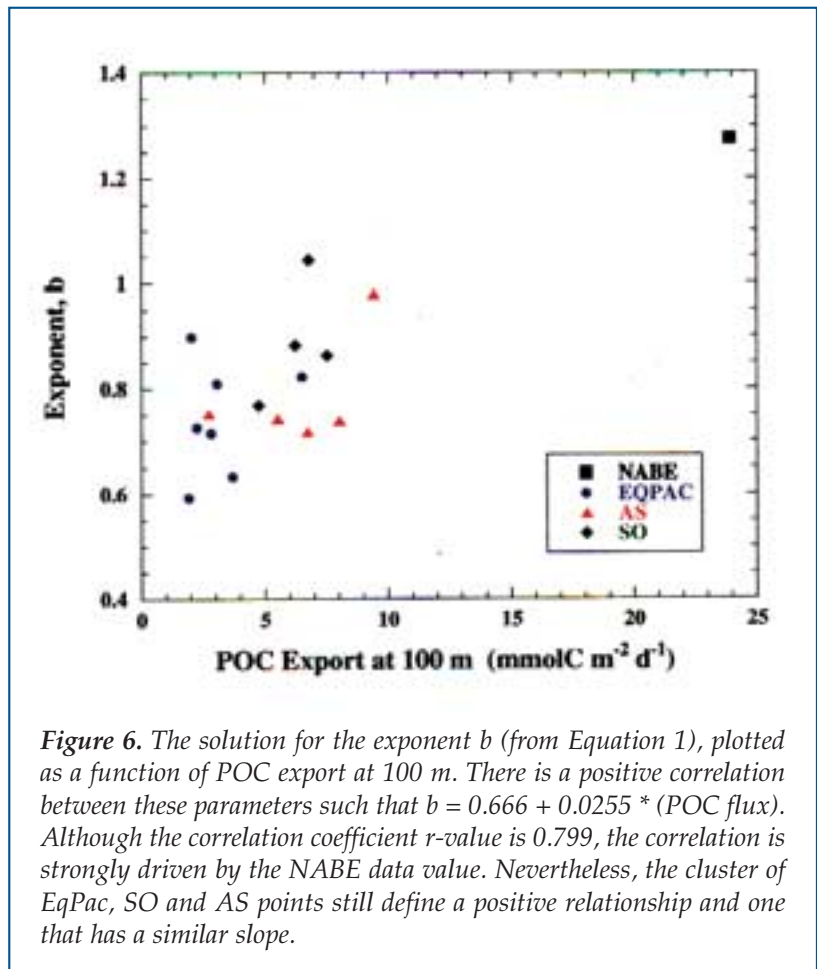
The uncertainty (\pm one standard deviation) in the regional value of b is large relative to the difference between regions. As a test of the sensitivity of this formulation, we fitted data from the equatorial Pacific, grouping all data within the latitudinal zones 2°N, equator and 2°S. Three different estimates of POC export at 100 m were fitted to the deep trap and sediment recycling data. Each method yields a different value of POC export at 100 m: 2.5 mmol C m⁻² d⁻¹ (Buesseler et al., 1995); 7.3 mmol C m⁻² d⁻¹ (Murray et al., 1996), and 3.1 mmol C m⁻² d⁻¹ (Wakeham et al., 1997). These different export values predict b values of 0.53, 0.97 and 0.61, respectively. Clearly, curvature in the Martin function is sensitive to the value chosen to represent export at 100 m, and a factor of 3 difference in flux at 100 m can affect the value of b by a factor of 2.

The fact that b values for Southern Ocean and North Atlantic sites are greater than b values for Arabian Sea and equatorial Pacific sites suggests that there may be some control on POC degradation vs. depth that is regionally specific. Although it seems counterintuitive, at sites where export below 100 m is high, degradation within the upper 1000 m occurs at an especially high rate. This relationship is shown by the positive correlation between the amount of POC export from 100 m and

the b value (Figure 6). Although this trend is defined by the cumulative data set and is manifested only within the Southern Ocean regional data, the relationship between POC export and intensity of shallow degradation warrants further consideration.

There are numerous possible explanations for the correlation described above. The rate constant for POC degradation may vary regionally in association with some inherent differences in molecular composition; kinetic effects influenced by temperature structure, oxygen concentration or mineral associations may play a role. Various sites may simply develop different microbial and heterotrophic communities capable of processing POC with a greater or lesser efficiency. One might hypothesize that settling velocity is related to b , such that high b values are indicative of more slowly settling POC. We propose these hypotheses as a means of promoting further thought about the significance of the Martin equation and its application in various global models, as well as the significance of processes occurring in the “twilight zone,” the region of the water column between 100 m and 1500 m where particles undergo intense remineralization.

An average of all 17 U.S. JGOFS sites yields a mean value of $b = 0.82 \pm 0.16$ (one standard deviation), remarkably close to the mean value defined by Martin



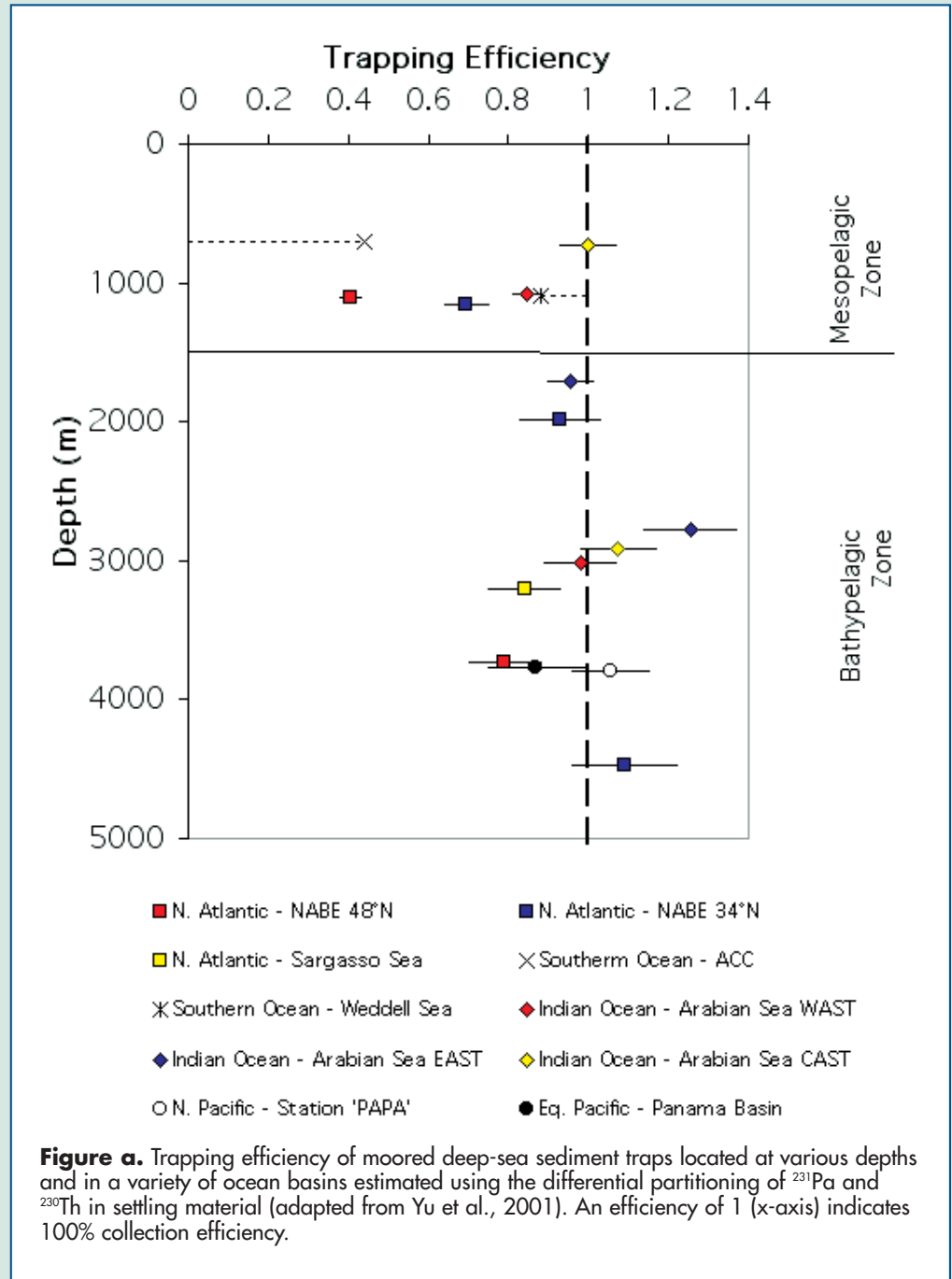
Catching The Rain Of Particles: How Accurate Are Deep-Sea Moored Sediment Traps?

Roger François, Susumu Honjo and Michael P. Bacon
 Woods Hole Oceanographic Institution
 Woods Hole, Massachusetts USA

The deployment of sediment traps moored to the seafloor has been an integral part of all JGOFS programs (Honjo, 1996). Developed initially in the 1970s, moored sediment traps are still our primary means for sampling and quantifying the settling flux of particles to the deep sea, one of the key factors that regulate the global carbon cycle.

Although moored sediment traps are widely used, questions have been raised as to whether they record the vertical flux of particles accurately. The interactions between fragile particles settling through a moving fluid and intercepting conical funnels, the sediment-trap receptacle most often used for deep-sea deployments, are very complex. Controlled laboratory and field experiments have demonstrated that sediment traps may significantly under- or overestimate the vertical flux of particles, depending on their shape, size and density, the shape of the intercepting receptacle and the velocity and eddy fields surrounding it.

Two natural radionuclides (^{230}Th and ^{231}Pa) produced by radioactive decay of uranium dissolved in seawater provide an *in situ* means of assessing the efficiency of sediment traps. Uranium concentration in seawater is essentially constant. Therefore the rate of formation of ^{230}Th and ^{231}Pa is uniform throughout the water column and accurately known. Both nuclides are particle-reactive and rapidly removed from seawater by adsorption on settling particles. The two isotopes differ slightly in particle reactivity, with ^{230}Th being removed by settling particles faster than ^{231}Pa and the latter being more effectively transported laterally by eddy diffusion and advection toward regions of higher particle flux. This differential partitioning during the removal of two nuclides with identical source function can be used to predict the vertical flux of ^{230}Th from the ratio of ^{231}Pa to ^{230}Th in the intercepted settling mate-



rial and estimates of the lateral ^{231}Pa : ^{230}Th transport ratio.

Using this approach, Yu et al. (2001) have estimated the trapping efficiency of deep-sea moored sediment traps deployed in different oceanic regions (Figure a). The results show that when the traps are deployed in the bathypelagic zone (at depths >1500 m), E is approximately 1 (0.98 ± 0.14 ; $n = 10$, 1σ), indicating that the sediment traps intercept the vertical flux of particles accurately. At shallower depths, however, trapping efficiencies are sometimes low.

Using a slightly different approach, Scholten et al. (2001) reached a similar conclusion. The reasons for the more erratic behavior of sediment traps in the mesopelagic zone are not yet clear. The low trapping efficiencies are not uniquely associated with higher current velocities, although that is a likely contributing factor. The nature and hydrodynamic properties of the settling particles, which appear to change with depth as particles lose organic matter and become more consolidated through cycles of aggregation and disaggregation, could also be an important factor.

From these results, we conclude that deep-sea moored sediment traps (in contrast to the conventional shallow surface-tethered floating traps) accurately measure the vertical flux of particles when deployed in the bathypelagic zone of the ocean. When they are deployed at intermediate depths, however, or at any depth in regions with high current velocity (typically $> 10 \text{ cm s}^{-1}$), significant undertrapping may occur. It is thus advisable that ^{230}Th and ^{231}Pa be measured routinely with every sediment trap deployment. Once trapping efficiency is estimated, it can be used to correct the measured settling flux of important biogeochemical constituents.

Deep-sea moored sediment traps have been a very important tool and contributor to the success of JGOFS. Combining their use with radiochemical analysis will further enhance their usefulness in future programs.

References

- Honjo, S., 1996: Fluxes of Particles to the Interior of the Open Oceans. In: *Particle Flux in the Ocean*. SCOPE vol. 57, John Wiley & Sons, New York, 91–154.
- Scholten, J.C., J. Fietzke, S. Vogler, M.M.R. Rutgers van der Loeff, A. Mangini, W. Koeve, J. Waniek, P. Stoffers, A. Antia and J. Kuss, 2001: Trapping efficiencies of sediment traps from the deep Eastern North Atlantic: the ^{230}Th calibration. *Deep-Sea Res. II*, 48, 2383–2408.
- Yu, E.-F., R. François, M.P. Bacon, S. Honjo, A.P. Fleer, S.J. Manganini, M.M. Rutgers van der Loeff and V. Ittekkot, 2001: Trapping efficiency of bottom-tethered sediment traps estimated from the intercepted fluxes of ^{230}Th and ^{231}Pa . *Deep-Sea Res. I*, 48, 865–889.

et al. (1987) of 0.86. The similarity in these values suggests great flexibility in the application of the Martin equation. However, as it is arbitrary to define export flux as beginning at 100 m, the use of a universally defined export and decay equation is also arbitrary. The U.S. JGOFS data shown here demonstrate that the fitting parameter b is not a global constant and is in many cases significantly greater or less than 0.86.

This analysis leaves many other major questions for future consideration. One is whether the sediment trap data are accurate. Work by Yu et al. (2000) indicate that some traps, especially those located at depths less than 1500 m, tend to undertrap the rain of particles (see sidebar by François, this issue). The correction of such a systematic error would shift b toward a lower value. Another uncertainty in the trap data involves the contribution of “swimmers,” especially in the shallower traps. The development and use of indented rotating sphere traps (Peterson et al., 1993) and the good agreement between these and other trap data (Lee et al., 1998) suggest that many of the “swimmer” problems can be greatly reduced. Sediment recycling rates provide an excellent check for deep trap flux values.


Although these rates depend on assumptions about diagenetic reaction stoichiometries and transport mechanisms, these two approaches converge in defining the POC rain into the deep sea.

Summary

The picture of POC transport through the entire water column has sharpened as a direct result of U.S. JGOFS research. Although carbon export into the deep water is positively correlated with primary productivity, the relationship we see may be regionally dependent. Small changes in PP result in greater differences in POC flux into the ocean interior in the Southern Ocean than occurs in temperate and tropical regions.

The Martin equation, a function that describes the flux of POC below 100 m, has been applied to data assembled from 17 locations. This formulation is very sensitive to the value assigned to POC export at 100 m. While one of the virtues of the data set discussed in this paper is that at most sites the same methods were used to determine POC export, great uncertainty still exists about how best to quantify export at 100 m. Therefore great uncertainty exists about the significance of the Martin equation fit.

Regions with greater export from 100 m have larger values for the curve-fitting exponent b (Figure 6).

Many global circulation models rely on equations describing the respiration of POC as a function of depth. This process is particularly important in the upper 1000 m of the water column. Thus the formulation and mechanistic explanation of the Martin equation will require the analysis of more regional data than has been attempted thus far. Although the b value of 0.86 that was defined by Martin et al. (1987) is very close to the average value for all the U.S. JGOFS regional sites considered ($b = 0.82$), there is a factor of 2 in the range of this parameter, from 0.6 to 1.3. The global average value hides important differences in controls of b , and the U.S. JGOFS regional studies have opened a door to the further examination of these differences. 

Acknowledgements

I would like to acknowledge the accessibility of U.S. JGOFS data, particularly the data made available by sediment trap investigators Susumu Honjo, Jack Dymond and Robert Collier. I acknowledge two excellent synthesis papers authored by Cindy Lee and David Nelson. This paper benefited from the critical review of Anthony Michaels, Douglas Hammond, Roger François and Ken Buesseler. This is U.S. JGOFS Contribution Number 685.

References

Berelson, W., R. Anderson, J. Dymond, D. DeMaster, D. Hammond, R. Collier, S. Honjo, M. Leinen, J. McManus, R. Pope, C. Smith and M. Stephens, 1997: Biogenic budgets of particle rain, benthic remineralization and sediment accumulation in the Equatorial Pacific. *Deep-Sea Res. II*, 44, 2251–2282.

Betzer, P.R., W.J. Showers, E.A. Laws, C.D. Winn, G.R. DiTullio and P.M. Kroopnick, 1984: Primary productivity and particle fluxes on a transect of the equator at 153°W in the Pacific Ocean. *Deep-Sea Res.*, 31, 1–11.

Buesseler, K. O., M. P. Bacon, J. K. Cochran and H. D. Livingston (1992). Carbon and nitrogen export during the JGOFS North Atlantic bloom experiment estimated from ^{234}Th : ^{238}U disequilibria. *Deep-Sea Res.*, 39(7/8), 1115–1137.

Buesseler, K.O., J.A. Andrews, M.C. Hartman, R. Belastock and F. Chai, 1995: Regional estimates of the export flux of particulate organic carbon derived from Th^{234} during the JGOFS EqPac program. *Deep-Sea Res. II*, 42, 777–804.

Lee, C., D.W. Murray, R.T. Barber, K.O. Buesseler, J. Dymond, J. Hedges, S. Honjo, S.J. Manganini, J. Marra, C. Moser, M.L. Peterson, W.L. Prell and S. Wakeham, 1998: Particulate organic carbon fluxes: compilation of results from the 1995 U.S. JGOFS Arabian Sea Process Study. *Deep-Sea Res. II*, 45, 2489–2501.

Martin, J.H., S.E. Fitzwater, R.M. Gordon, C.N. Hunter

and S. Tanner, 1993: Iron, primary production and carbon-nitrogen flux studies during the JGOFS North Atlantic Bloom Experiment. *Deep-Sea Res.*, 40, 115–134.

Martin, J.H., G.A. Knauer, D.M. Karl and W.W. Broenkow, 1987: VERTEX: carbon cycling in the NE Pacific. *Deep-Sea Res.*, 34, 267–285.

Murray, J.W., J. Young, J. Newton, J. Dunne, T. Chapin, B. Paul and J.J. McCarthy, 1996: Export flux of particulate organic carbon from the central equatorial Pacific determined using a combined drifting trap- ^{234}Th approach. *Deep-Sea Res. II*, 43, 1095–1132.

Nelson, D.M., R.F. Anderson, R.T. Barber, M.A. Brzezinski, K.O. Buesseler, Z. Chase, R.W. Collier, M.L. Dickson, R. Francois, M.R. Hiscock, S. Honjo, J. Marra, W.R. Martin, R.N. Sambrotto, F.L. Sayles and D.E. Sigmon, 2001: Vertical budgets for organic carbon and biogenic silica in the Pacific Sector of the Southern Ocean, 1996–1998. *Deep-Sea Res. II*, in press.

Pace, M.L., G.A. Knauer, D.M. Karl and J.H. Martin, 1987: Primary production, new production and vertical flux in the eastern Pacific Ocean. *Nature*, 325, 803–804.

Peterson, M.L., P. Hernes, D. Thoreson, J. Hedges, C. Lee and S. Wakeham, 1993: Field evaluation of a valved sediment trap. *Limnol. Oceanog.*, 38, 1741–1761.

Suess, E., 1980: Particulate organic carbon flux in the oceans: Surface productivity and oxygen utilization. *Nature*, 288, 260–263.

Wakeham, S.G., J.I. Hedges, C. Lee, M.L. Peterson and P.J. Hernes, 1997: Compositions and transport of lipid biomarkers through the water column and surficial sediments of the equatorial Pacific Ocean. *Deep-Sea Res. II*, 44, 2131–2162.

Yu, E.-F., R. Francois, M.P. Bacon, S. Honjo, A.P. Flier, S.J. Manganini, M.M. Rutgers van der Loeff and V. Ittekkot, 2000: Trapping efficiency of bottom-tethered sediment traps estimated from the intercepted fluxes of ^{230}Th and ^{231}Pa . *Deep-Sea Res. I*, 48, 865–889.



Element Stoichiometry, New Production and Nitrogen Fixation

Anthony F. Michaels

University of Southern California • Los Angeles, California USA

David M. Karl

University of Hawaii • Honolulu, Hawaii USA

Douglas G. Capone

University of Southern California • Los Angeles, California USA

Introduction

Over the decade and a half since planning for the Joint Global Ocean Flux Study (JGOFS) began, a number of shifts, both subtle and profound, have occurred in certain paradigms of biological and chemical oceanography. Nowhere have greater changes taken place than in the way we view the stoichiometry of elements in the ocean and the processes that influence these patterns. We started this era with a conception of new production that focused on nitrate, linked to other elements in a simple, generally stable ratio in the ocean. We now know that elemental ratios vary more than we thought. We also know far more about the importance of iron as a limiting nutrient and its effects on elemental stoichiometry. Assumptions about systems in steady state have given way to the recognition that nothing is constant except change. Relationships between nutrient fluxes and climate conditions over a broad spectrum of time scales have become apparent.

These changes in our perceptions accord biological processes a more significant role in the exchange of carbon between oceanic and atmospheric pools and open the door to the evaluation of possible options for the active sequestration of carbon dioxide (CO₂). They also provide a springboard for research in the post-JGOFS era that can elucidate these processes and predict their role in the future behavior of ocean ecosystems and elemental cycles.

Marine nitrogen and phosphorus cycles are inextricably linked to the carbon cycle in the ocean. Pioneering research efforts by Hildebrand W. Harvey, L.H.N. Cooper and Alfred C. Redfield established a robust quantitative ratio of carbon to nitrogen to phosphorus (C:N:P) in the cells of phytoplankton and particulate matter in the laboratory and in both surface and deep ocean waters. It became known as the

“Redfield Ratio,” specifying 106 moles C to 16 moles N to 1 mole P. The observed biochemical, molecular and enzymatic similarities of most planktonic organisms led Redfield and his colleagues to a unifying theory that, while it has greatly simplified efforts to model the complex dynamics of nutrient fluxes in the sea, may have inadvertently stifled the examination and explanation of non-conforming evidence.

The Geochemical Ocean Sections (GEOSECS) field program in the 1970s produced the first high-quality global data on nutrient and transient tracer distributions. Analysis of these data sets confirmed the global distribution of relatively constant nutrient ratios. Although absolute ratios often varied from the canonical Redfield values, changes in nutrient levels along isopycnal or neutral density surfaces in the deep sea usually retained ratios near those specified by Redfield (Anderson and Sarmiento, 1994). Because of the apparent consistency of the Redfield ratio throughout the ocean, knowledge of one element allowed investigators to calculate the concentration of other elements, and by inference, the processes that controlled them.

Another paradigm that governed ways of thinking about nutrient fluxes when JGOFS began was the “new production hypothesis.” Introduced by Dugdale and Goering (1967), this formulation distinguished between the recycling of a limiting nutrient within a system and its introduction from outside the system. For nitrogen in the euphotic zone, this approach was used to distinguish between the recycling of ammonium and the uptake of nitrate, introduced through upwelling from deep waters (Figure 1a). Eppley and Peterson (1979) extended this conceptual analysis to show the balance between imports and exports in a steady-state ocean and to begin to identify regional patterns in the pro-

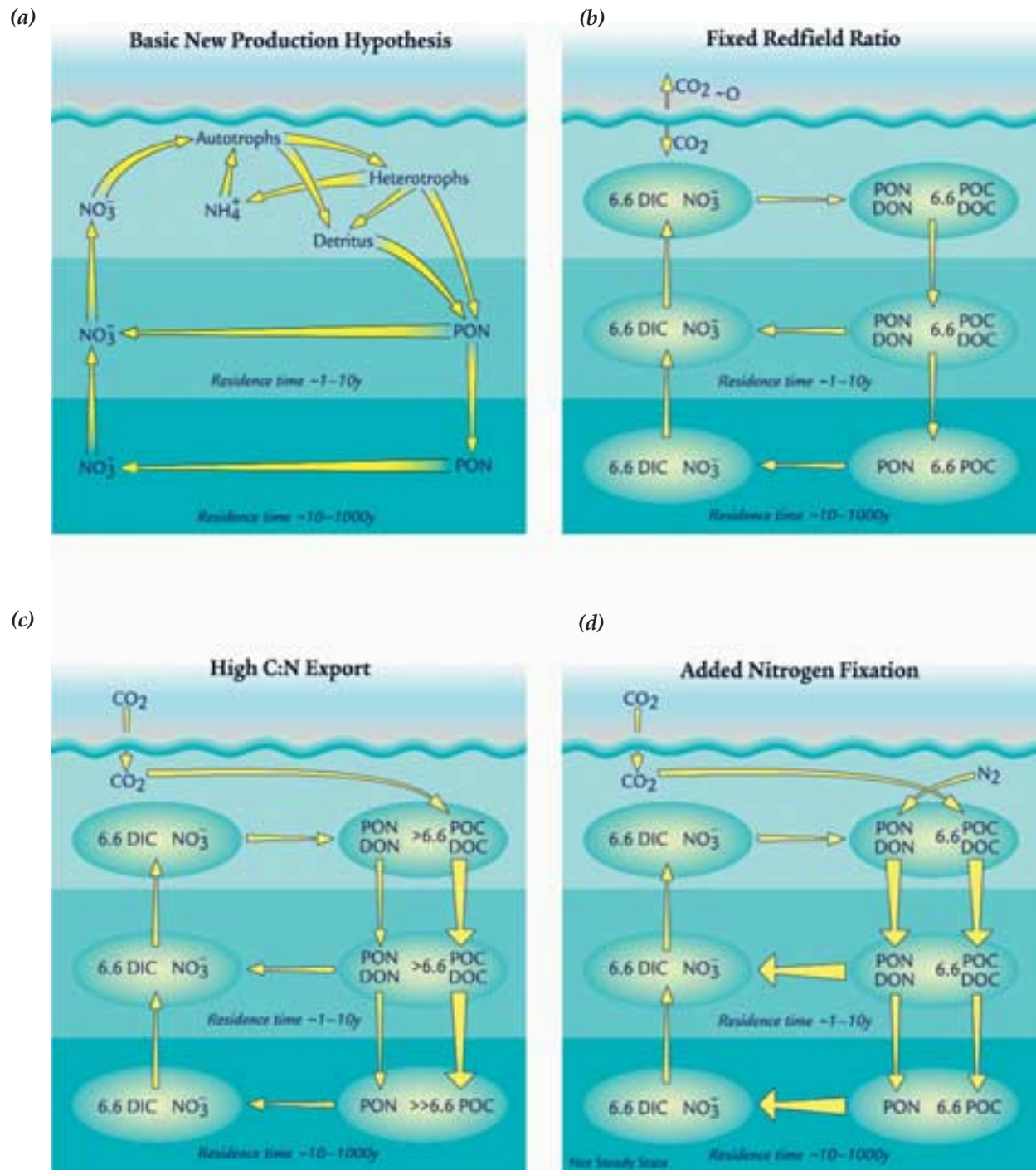


Figure 1. Coupling between the carbon and nitrogen cycles in the upper ocean. **a)** A simplified version of the “new production hypothesis.” It compares growth based on exogenous “new” nutrients that enter the euphotic zone from above or below with that based on “regenerated” nutrients supplied by respiration within the euphotic zone. **b)** Conceptual figure of the linkage between the nitrogen and carbon cycles under the assumption of a fixed C:N ratio of 6.6 moles:1 mole. **c)** A modified version of the coupled carbon and nitrogen cycles to illustrate the effect on CO_2 uptake in the ocean of elevated C:N ratios in sinking particles or preferential loss of nitrogen during remineralization. In this model, the nitrogen cycle can remain at a steady state, but the carbon can build up in the deep sea on time scales shorter than the ventilation of the ocean. **d)** A modified version of the coupled carbon and nitrogen cycles to illustrate the effect of nitrogen fixation on the air-sea exchange of CO_2 . Increases in nitrogen fixation increase the total nitrate stock of the sea and the vertical gradient of CO_2 , as well as maintaining a lower surface $p\text{CO}_2$. This system is not at steady state for either carbon or nitrogen. Increases in denitrification have an opposite effect, leading to net outgassing as the water returns to the surface with less nitrate, thus maintaining a weaker vertical gradient of CO_2 .

portion of the total production that is based on exogenous nitrogen. Both articles mentioned the fixation of atmospheric nitrogen (N_2) and atmospheric deposition as sources of nitrogen for the upper ocean but, in line with the understanding at the time, treated them as negligible components of the exogenous flux that could be ignored in most first-order analyses.

Contributions From JGOFS

The discovery of elemental stoichiometry in the ocean that does not conform to the Redfield ratio was an unexpected consequence of the interdisciplinary and collaborative research fostered by JGOFS and other ocean programs such as the World Ocean Circulation Experiment (WOCE). In 1988, U.S. JGOFS established time-series programs in the subtropical gyres of the North Atlantic and the North Pacific with stations located near Bermuda and Hawaii respectively (see Karl et al., this issue). Repeated observations at the Bermuda-Atlantic Time-series Study (BATS) and Hawaii Ocean Time-series (HOT) sites over more than a decade have yielded recurrent, unexpected patterns that cannot be ignored as “one-off” anomalies but have to be considered as results of a basic set of processes that unfold through time.

During the first of the JGOFS process studies, the North Atlantic Bloom Experiment of 1989, key questions about element ratios were raised as investigators observed that the draw-down of inorganic nutrients during bloom conditions did not appear to obey the biogeochemical “rules” (Sambrotto et al., 1993). Carbon continued to disappear after the major nutrients were gone. At that time, the importance of dissolved organic phosphorus, nitrogen and carbon was not yet appreciated as the relevant analytical methods had just begun to be refined (see Hansell and Carlson, this issue). Thus uncertainties could still be regarded as associated with the unmeasured pool of dissolved organic matter (DOM) or ascribed to short time-scale measurements or horizontal processes unresolved by the sampling program.

Sediment trap measurements also raised questions about elemental stoichiometries. Nitrogen appeared to be remineralized over shallower depths than carbon (Martin et al., 1987). This observation made sense as the relative lability of these two elements is influenced by the biological needs of heterotrophic communities in deeper waters. The cells of bacteria and protozoa contain more nitrogen and phosphorus than the sinking detritus does. The difference in elemental composition suggests that these organisms work harder to mobilize and assimilate nutrients than they do carbon. However, this fractionation cannot be sustained if elements are constantly remineralized in mid-water in accordance with the Redfield ratio, a pattern clearly shown in most deep ocean waters.

Data from the first five years of measurements at the U.S. JGOFS time-series sites near Hawaii and Bermuda expanded the scale of questions about ele-

ment ratios and required the formulation of hypotheses to explain anomalies that occurred year after year or showed a consistent trend over time. The time-series stations were also the first sites at which a wide variety of measurements were made in the same place and over the same time periods. They also attracted investigators from a variety of disciplines, increasing the opportunity to explore novel solutions.

In the Bermuda study, anomalous patterns showed up both in the elemental ratios observed and in efforts to use mass-balance approaches to understand the overall carbon cycle of the region (Michaels et al., 1994). Bermuda, located in the Sargasso Sea, is far enough north that the seasonal cycle involves relatively deep winter mixing followed by stratification in summer and fall. Each year this seasonal cycle homogenizes carbon and other nutrients in the upper ocean. Following the late spring stratification, biological and physical processes create vertical gradients in nutrients and carbon. Winter mixing introduces nitrate into the surface ocean that is quickly removed through primary productivity and export. However, the total dissolved inorganic carbon (DIC) continues to decline throughout the late spring and summer in the absence of new nitrate (Figure 2).

Were nitrate to be added by mixing through eddies or other processes, additional DIC would be introduced as well. Thus simple enhancements of the nitrate-driven new production cannot produce the observed results. Patterns in the concentrations of dissolved organic matter (DOM) and gas exchange also cannot explain the loss of DIC (Michaels et al., 1994). Results from regional cruises show that horizontal advection is unlikely to cause the continued decline of DIC each summer; the gradients are small and the seasonal pattern widespread. Where is this carbon going, how and why?

The Sargasso Sea is characterized by another nutrient anomaly as well. Ratios of nitrate to phosphate in the upper 1000 m of this basin are much higher than in most other parts of the ocean, even when corrected for asymmetries resulting from analytical errors at low concentrations. This implies either that the remineralization of nitrate occurs much faster than that of phosphate, the opposite of what one would expect from the relative lability of the nutrients, or that export from the euphotic zone includes more nitrogen than the Redfield ratio predicts. Further, the transition from a well-mixed layer 250 m deep in the spring to a stratified water column in the fall is accompanied by gradients in DIC and nutrients over this depth range, the result of productivity in the surface waters and remineralization below. The remineralization ratio of C:N:P that results from a comparison of these gradients is approximately 377:24:1, very different from the Redfield ratio (Table 1).

The ratio of nitrate to phosphate can be reformulated as a nitrate anomaly, often referred to as N^* (Michaels et al., 1996; Gruber and Sarmiento, 1997), by subtracting a scaled phosphate concentration from the

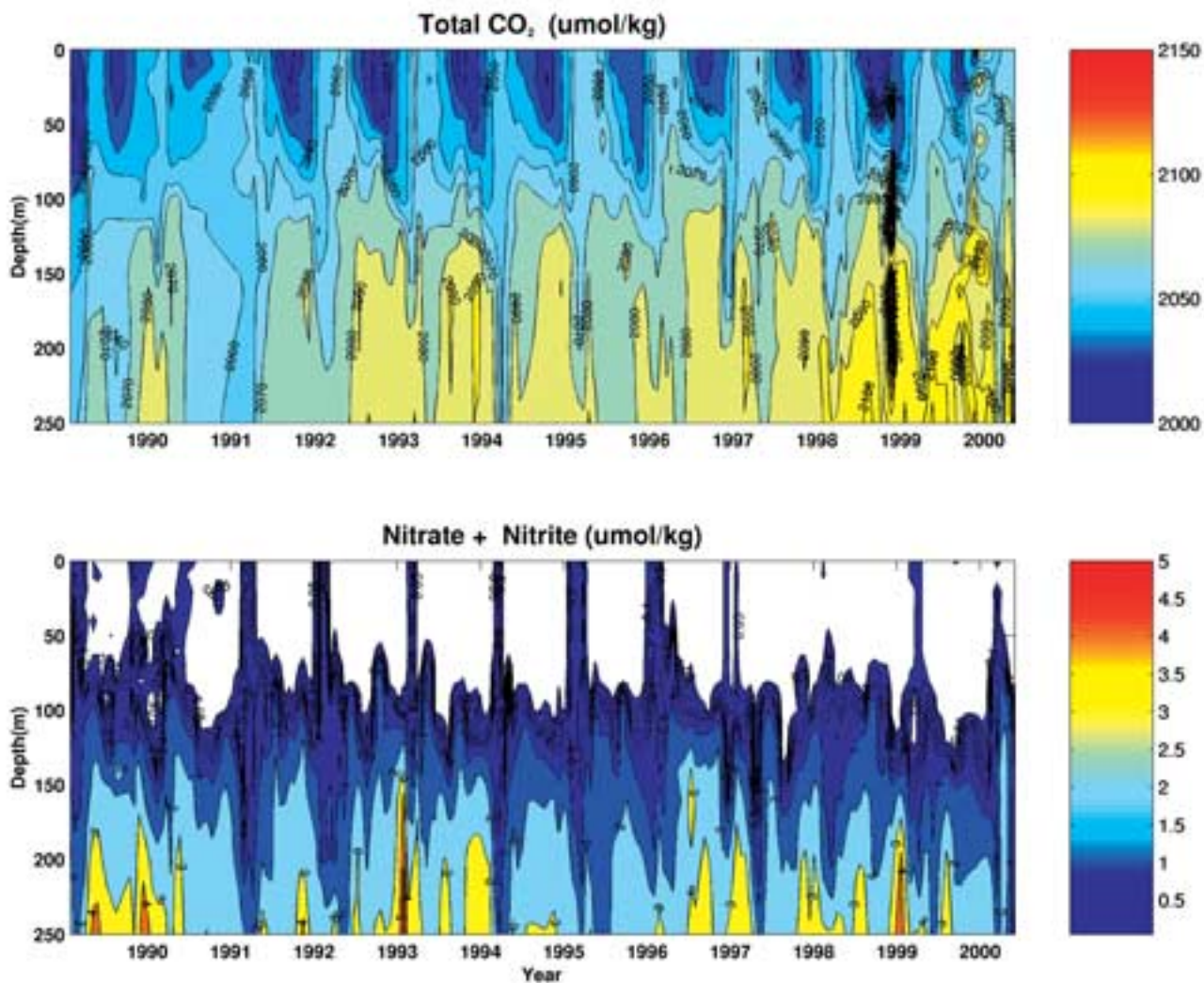


Figure 2. Decadal patterns of dissolved inorganic carbon (DIC) and nitrate at the Bermuda Atlantic Time-series Study (BATS). DIC in the upper 100 m declines steadily through the summer while the nitrate, briefly present in the early spring, is generally absent the rest of the year. Dissolved organic carbon (not shown here) also declines or changes little through the summer (Michaels et al., 1994).

measured nitrate value ($\text{NO}_3\text{-}16^*\text{PO}_4$ or some variant thereof). N^* will be higher when high N:P organic matter is exported and subsequently remineralized or when nitrogen is preferentially remineralized from exported dissolved and particulate organic matter. The current balance of evidence indicates that N_2 fixation in surface waters can be a source of high N:P organic matter. N^* will be lower when nitrate is removed in denitrification or when phosphate is preferentially remineralized from exported dissolved and particulate organic matter. In the Sargasso Sea, N^* data can be used to infer the rate of creation of the excess nitrate. Values for the region range from 28 to 90 Tg N/y ($\text{Tg} = 10^{12}$ grams), dramatically higher than previous estimates of oceanic nitrogen fixation worldwide (Michaels et al., 1996, Gruber and Sarmiento, 1997).

Gruber and Sarmiento (1997) applied the N^*

approach on the global scale and concluded that the patterns of positive and negative N^* are associated with the balance between denitrification and this putative nitrogen fixation. Strong cross-basin patterns of N^* suggest the creation of nitrate in the surface waters of the gyres and the loss of nitrate in the well-developed oxygen minima under the equatorial and eastern boundary current upwelling zones. The spatial correspondence between strong positive N^* anomalies and aeolian dust flux is particularly striking (Figure 3). Both the data from the Sargasso Sea and the global analyses suggest that iron in these aeolian dust inputs may serve as a control on nitrogen fixation, an hypothesis that requires further research.

At the Hawaii Ocean Time-series (HOT) station, investigators with a more biological orientation came to similar conclusions about N_2 fixation and further

Table 1

Comparison of the mean concentration of inorganic carbon, nitrate and phosphate in upper 100 m with that between 150 and 250 m. Data from the Bermuda Atlantic Time-Series Station in the September-October period when mixed-layer depths are still less than 100 m. If we assume that the spring mixing to 250 m homogenizes the water column, the fall comparison may indicate net remineralization stoichiometries from the previous summer.

	DIC	Nitrate	Phosphate
0–100 m mean (μM)	2043	0.08	0.02
150–250 m mean (μM)	2084	2.67	0.13
Difference (μM)	41	2.59	0.11
D DIC: D Nitrate = 15.9 (mole/mole) D DIC: D Phosphate = 377 (mole/mole) D Nitrate: D Phosphate = 23.6 (mole/mole)			

redefined our sense of the instability of ocean nutrient stoichiometry over time. Several lines of evidence from HOT Station ALOHA, located at 22°45'N, 158°W, suggest that N₂ fixation has been an important source of new nitrogen for the pelagic ecosystem of the North Pacific subtropical gyre since the early 1990s. The evidence includes measurements of the abundance of *Trichodesmium*, cyanobacteria species that fix N₂ in the open ocean, and estimates of the potential rate at which N₂ fixation takes place; assessment of the molar N:P stoichiometries of surface-ocean dissolved and particulate matter pools and development of a one-dimensional model to calculate mass balances for nitrogen and phosphorus; measurements of seasonal variations in the natural abundance of ¹⁵N, an isotope of nitrogen, in particulate matter exported to the deep sea, and observations of secular changes in soluble reactive phosphorus (SRP), soluble nonreactive phosphorus (SNP) and dissolved organic nitrogen (DON) pools during the period of increased rates of N₂ fixation (Karl et al., 1997).

Budget estimates suggest that N₂ fixation is currently supplying up to half of the nitrogen required to sustain the observed export of particulate matter from the euphotic zone at Station ALOHA. But observations also suggest that this relatively high level of N₂-supported production may represent a transient state of the ecosystem. This state may be simply a phase in a long-term cycle, or it may represent a shift in response to well-documented decade-long changes in climate in the North Pacific (Karl et al., this issue). Our changing perspective on biogeochemical dynamics in the gyre is likely to have a profound influence on how we model ecosystem processes, including the potential effects of natural or anthropogenic environmental change and their relationship to carbon sequestration in the ocean.

Results from the two JGOFS time-series programs tell us that the ocean's major nutrient cycles are dynamic rather than static (Karl et al., this issue). They

vary significantly on time scales ranging from diel to decadal and probably longer. Although measurements of N₂ fixation were not explicitly part of the research program of the U.S. JGOFS regional process studies, results from the Arabian Sea Process Study show that, even in systems dominated by seasonal upwelling of nutrients, dense populations and spatially extensive surface blooms of *Trichodesmium* can occur throughout the central basin and do contribute directly and substantially to the nitrogen budget (Capone et al., 1998).

Should We Be Surprised?

Some would argue that the discovery of anomalous stoichiometries and the reassessment of the significance of N₂ fixation as a source of nitrogen in ocean systems should not come as surprises. Geochemists have argued for years that N₂ fixation should make up the deficit in ocean nitrogen budgets. Redfield himself observed in 1958 that "nitrogen fixation is so active that there is no difficulty in assuming that it might serve in adjusting the phosphorus-nitrogen ratio in the sea."

Certain fundamental limits on elemental composition in organisms are set by phosphate requirements for nucleotides, nucleic acids and membranes, the nitrogen requirements of proteins and varying iron requirements as a factor in specific enzymes of metabolism (Falkowski, 2000). However, there are many ways that organisms can make use of nutrient resources to grow and reproduce, even in the face of what appear at first to be exogenous limits. Thus some prokaryotic organisms can satisfy their need for one of the basic nutrients by fixing nitrogen from the nearly inexhaustible supply of dissolved N₂ gas.

The biological literature is replete with studies that show large and flexible ranges in elemental stoichiometry for microorganisms growing under various light and nutrient regimes (Karl et al., 2001). The uptake of excess or "luxury" nutrients, especially phosphorus and iron, and the formation of carbon-rich storage products such

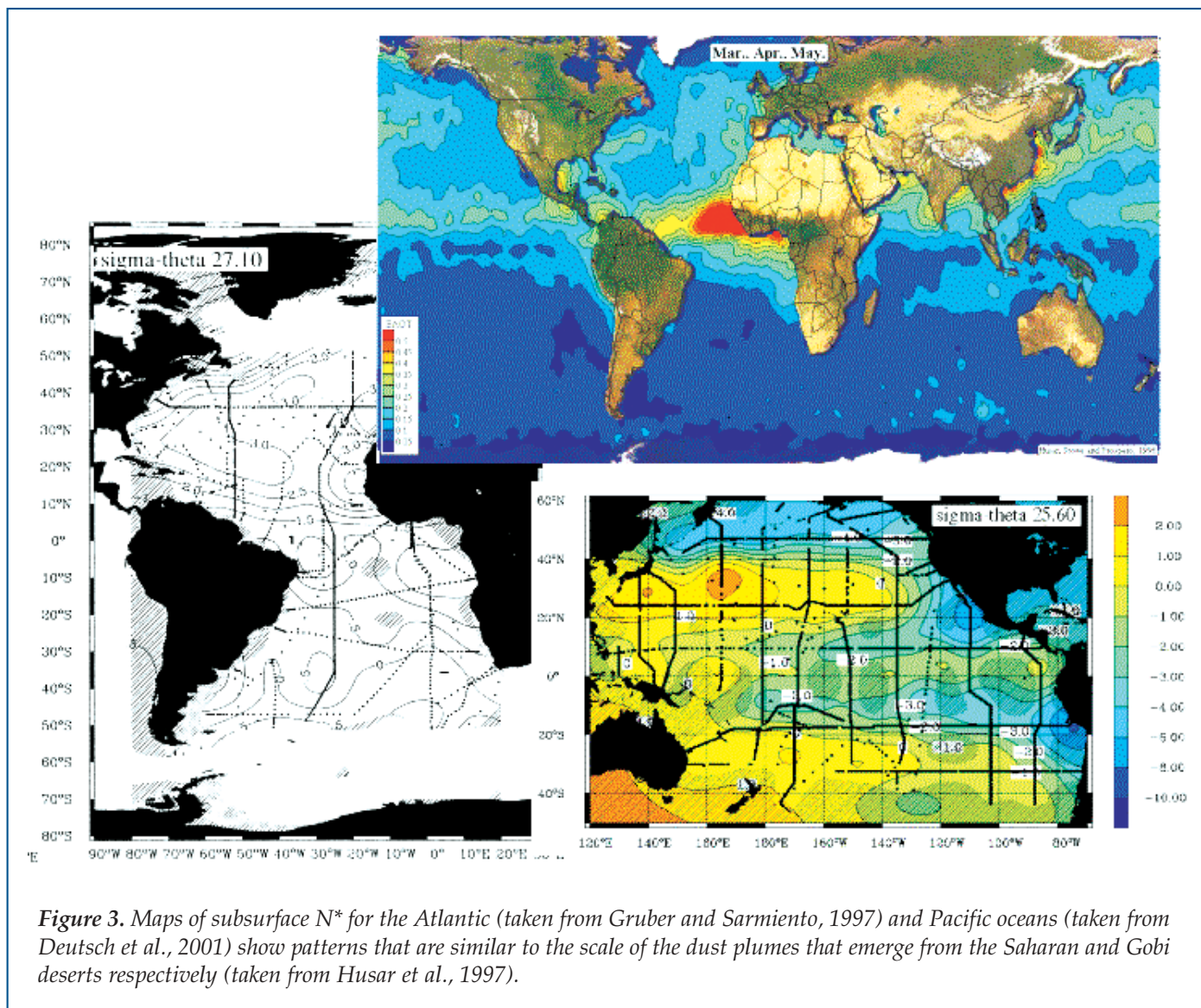


Figure 3. Maps of subsurface N^* for the Atlantic (taken from Gruber and Sarmiento, 1997) and Pacific oceans (taken from Deutsch et al., 2001) show patterns that are similar to the scale of the dust plumes that emerge from the Saharan and Gobi deserts respectively (taken from Husar et al., 1997).

as lipids or polyhydroxybutyrate are commonplace in the microbial world. In freshwater systems, these organism-level processes yield a wide range of elemental ratios in the water or the ecosystem (Elser et al., 1996). No limnologist would accept the idea of a fixed and constant elemental stoichiometry in lakes. Perhaps our view of the ocean is affected by its enormous size and the long residence time of nutrients within it. But these facts should not constrain our thinking.

Implications For Modeling The Ocean Carbon Cycle

JGOFS is nearing the final stage of a synthesis and modeling effort to incorporate the discoveries of the field studies into a coherent set of predictive ocean carbon-cycle models. These models must, among other things, be able to describe current temporal and spatial patterns in the ocean uptake of CO_2 and predict changes that might occur in the future. To do this, they must include all of the processes that can influence the partial pressure of CO_2 ($p\text{CO}_2$) in surface waters. Physical con-

straints, such as the effects of temperature and wind speed on $p\text{CO}_2$ and the exchange of gases across the air-sea interface, have always been part of the thermodynamic calculations of these models. However, biological processes are less well understood and more difficult to describe. In the initial effort to incorporate biological and chemical processes into models of the carbon cycle, the Redfield ratio was a powerful tool for assessing the ability of the models to reproduce the basic biogeochemical patterns of the sea. When we turn to the need to predict oceanic responses to changing environmental conditions, we run up against its limitations.

The fixed stoichiometry of the Redfield ratio implies that nutrient uptake only removes a fixed amount of DIC from the surface water and that all of the carbon in the organic material formed is remineralized with the nutrients. Thus the introduction of nutrients into the surface ocean through upwelling brings with it sufficient DIC for the primary production that these nutrients fuel. Biological processes can contribute little net carbon sequestration in an ocean governed

strictly by the Redfield ratio, regardless of the magnitude of the export flux or the size of the export ratio, unless changes occur in the High Nutrient—Low Chlorophyll (HNLC) areas where nutrients are underutilized (Figure 1b). A change in the rate of new production based on nitrate may affect the amount of material that is cycled, but it will have little effect on the DIC flux as long as nutrient removal is either complete or unchanging.

The assumption of a constant element ratio, when applied in the construction of a model, does not allow most biological processes any effect on the flux of carbon between atmosphere and ocean, except in systems where nutrients are not completely consumed. If this is how the ocean functions, we can ignore most biological processes and properties in creating our models. If, as we think, the stoichiometry of elements in the ocean is not always in line with that described by the Redfield ratio, then we have to understand the full implications of the different stoichiometries and include the appropriate processes in models in order to predict the effect of the living ocean on the flux of carbon between the ocean and the atmosphere.

If Redfield ratio assumptions are relaxed in a non-steady-state world, the work of modeling carbon dynamics becomes more interesting (Figures 1c and 1d). The C:N ratio of exported materials is generally higher than the ratio of elements taken up in primary productivity. In this situation (Figure 1c), an increase in export flux causes a net transfer of carbon from the surface ocean to the deep sea on the time-scales involved in the ventilation of deep water masses (centuries to millennia). A decrease in export has the opposite effect. The same thing can occur if carbon is remineralized over a greater depth interval, on average, than nitrogen. On centennial to millennial time scales, the extra carbon in the deep sea will return to the surface. On interannual and decadal time scales, however, the uncoupling of the remineralization of nitrogen from the remineralization of carbon means that changes in the rates of biological processes, export in particular, can have a net effect on the atmospheric carbon concentration.

Another obvious modification of the fixed-ratio assumption that should be made is the inclusion of gas phases and the air-sea exchange of gases on the delivery side of the nitrogen cycle. Nitrogen is introduced into the ocean from the atmosphere, or from dissolved gases in the water that are ultimately equilibrated with the atmosphere, during deposition of nitrate and N_2 fixation (Figure 1d). On a global scale, the deposition of reactive nitrogen plays a modest, though increasing role (Galloway et al., 1995), but oceanic N_2 fixation appears to be more significant than previously thought (Capone, 2001).

The global rate of oceanic N_2 fixation is now estimated to exceed 100-150 Tg N/y, and global denitrification rate estimates are even higher (Capone, 2001). On glacial-interglacial time scales, the balance of these

processes changes the total amount of nitrate in the ocean within the permissible bounds set by the variability of N:P ratios in organisms. The balance of these two rates may also influence the sequestration of atmospheric CO_2 in the ocean directly by providing new nitrogen to the upper ocean. Accumulating evidence indicates that iron availability may be one of the key factors regulating the growth of planktonic marine diazotrophs (organisms that fix N_2) and thereby the relative amounts of N_2 fixation versus denitrification. The primary pathway for the delivery of iron to the open ocean is through dust deposition.

Perhaps the most exciting implication of our improved understanding of the role of the diazotrophs is that N_2 fixation may be directly involved in the global coupling between ocean biogeochemistry and the climate system. Consider the following set of linked hypotheses that emerge from this new understanding: The rate of N_2 fixation in the global ocean may affect the concentration of CO_2 in the atmosphere on time scales of decades (variability in surface biogeochemistry) to millennia (changes in the total stock of nitrate from the balance of N_2 fixation and denitrification). Carbon dioxide concentrations in the atmosphere may influence climate. The climate system, in turn, may influence the rate of N_2 fixation in the ocean by controlling the supply of iron in the form of dust derived from climate-sensitive deserts ashore and by influencing the stratification of the upper ocean.

It is intriguing to speculate that the circular nature of these influences may constitute a feedback system, particularly on longer time-scales (Figure 4). Further, there are possible internal feedback dynamics within the ocean as changes in the total nitrate stock may, in turn, influence the rates of denitrification and N_2 fixation. In addition, human activity may have a role in the current manifestation of this feedback cycle through agricultural practices on the margins of deserts that affect dust production as well as through the release of CO_2 into the atmosphere from fossil fuel consumption and deforestation.

The key point is that the assumptions about simple and fully coupled nitrogen dynamics and rate processes in the upper ocean that arise from the traditional conceptualizations of element ratios and new production are not sufficient to explain what we observe or to predict change in ocean ecosystems. We need to understand how the deviations from our assumptions affect the links between elements. One of the most important lessons from the time-series programs and other JGOFS investigations is that intensive, long-term studies have revealed processes that are at odds with the assumptions based on our traditional paradigms. When we include newly examined pathways in our mental and numerical models, we conclude that air-sea carbon dynamics differ from the patterns indicated by these simplifying assumptions. Thus we have to look explicitly for these pathways to understand their effects.

Modeling Biogeochemical Cycles In The Post-JGØFS Era

Raleigh R. Hood
University of Maryland Center for Environmental Science
Cambridge, Maryland USA

Modelers and field researchers alike have come to appreciate the importance of trace metals, silica and phosphorus in natural cycles as well as the evidence for elemental stoichiometry that varies from the relationships described by Alfred Redfield and his colleagues half a century ago. It is clear that if we want to model the more subtle aspects of elemental cycles in the ocean, which could be important in determining net carbon export on a variety of time scales, we will have to include multiple nutrients in our models and allow them to deviate from Redfield proportions. These realizations have emerged relatively recently, thanks in good part to measurements made at the Hawaii Ocean Time-series (HOT) and Bermuda Atlantic Time-series Study (BATS) sites over the last decade (see Michaels et al., this issue; Karl et al., this issue).

The focus of most modeling studies since the early 1990s, however, has been on incorporating more realistic food-web structures into models. Examples include efforts at explicit representation of the microbial loop and multiple size classes of phytoplankton and zooplankton. This focus stems from the fact that food-web structure has a profound effect upon export of material from the euphotic zone. Considerable progress has been made, and numerous models now reproduce observed shifts in ecosystem structure and export flux in response to perturbations in nutrients and light.

With some level of success behind us, modelers are beginning to turn their attention to the role of multiple limiting nutrients and non-Redfield element cycling. Several recently developed regional and global models allow for multiple elements and differences in elemental composition among food-web components. But these models are becoming increasingly complicated, and we may have reached the limits of our ability to understand, validate and run them. Continued progress will require advances in our understanding of *in situ* elemental cycles and our ability to analyze and understand the dynamics of complicated model systems, as well as advances in computing power. At the same time we must avoid the temptation to build complicated "models of everything" that cannot be validated, have limited scientific usefulness and are nearly as difficult to understand as the systems we are trying to model.

The primary motivation for developing large-scale biogeochemical models is our hope of predicting how the ocean uptake of carbon dioxide will respond to anthropogenic perturbations and global warming. This is one scientific application where a "model of everything" is, perhaps, appropriate, because we seek to predict general and currently unknown biogeochemical responses to perturbations that may exceed anything we have observed before. However, there is no guarantee that complex models will be able to generate the correct ecosystem responses.

The truth is that we are "flying blind" in our efforts to predict the future with these models. Unlike our colleagues in physical oceanography, we have no underlying theoretical foundation to guide us. We do not have a complete system of equations that can be systematically studied and simplified for different applications with known limitations. One thing we do know is that a full set of equations capable of describing the functioning of biogeochemical cycles in the ocean is going to be incredibly complex.

The Redfield ratio provides one of the few general principles that we have. We know that, on average, the uptake and release of elements in the ocean tend to occur in specific proportions. The general explanatory power and robustness of the Redfield ratio suggests that it captures some fundamental aspect of elemental stoichiometry in ecosystems that is governed by physiological laws. The fact that models based upon the Redfield ratio fail to predict the details and subtleties of elemental cycles should come as no surprise. They fail because they do not include second- and third-order terms. The problem we face is that these terms are clearly important on short time and space scales, and they may be important when we integrate model results over longer time and space scales as well.

Perhaps biogeochemical models based upon the Redfield ratio are analogous to the geostrophic approximation in physics, and what we seek now is something more akin to primitive equations with multiple elements and variable stoichiometries. But the realization that elemental cycles in the ocean are often more complicated than a simple fixed ratio predicts in no way diminishes the Redfield ratio as an overarching principle in the study of biogeochemical cycles. Nor does it diminish its usefulness as a simplifying assumption in models, as long as the assumption is made with care.

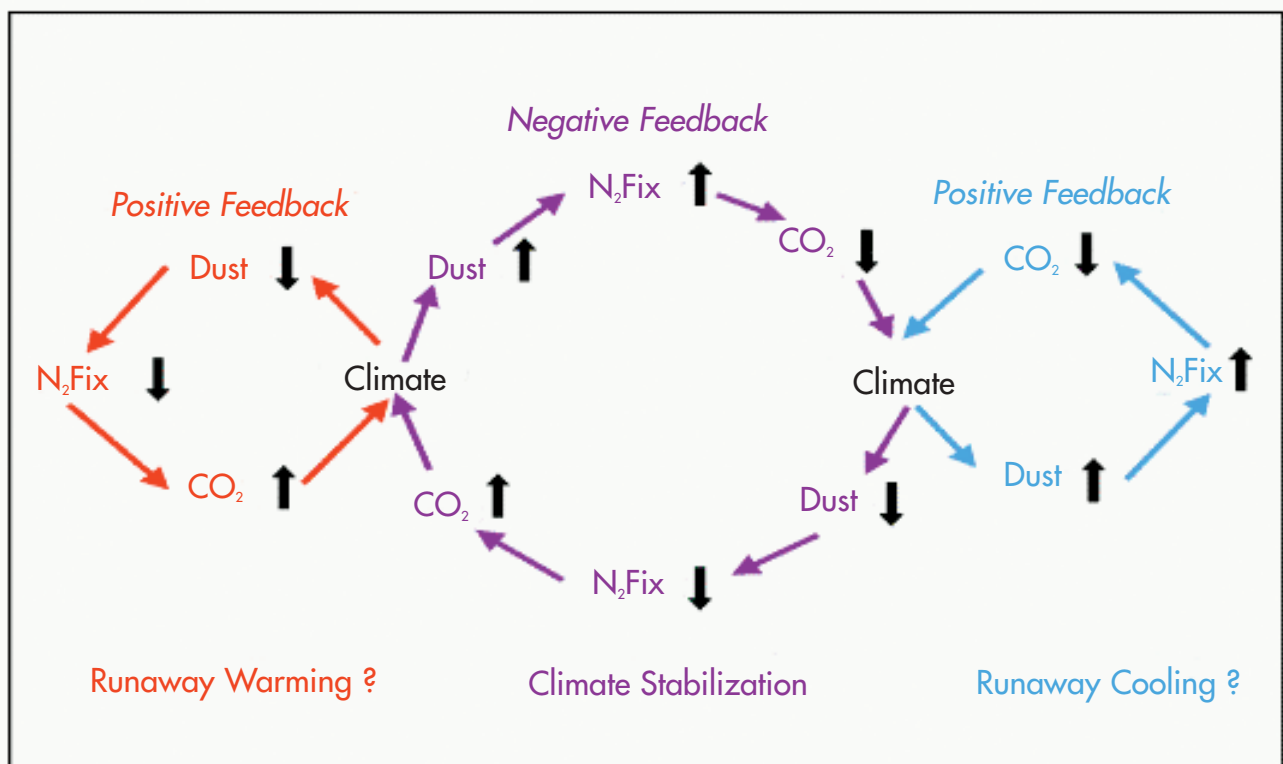



Figure 4. A hypothesis presented by the authors for a climate-based feedback cycle that involves nitrogen fixation, dust deposition and climate. The sign of the feedback is critically determined by the relationship between climate change and the supply of dust to the oligotrophic ocean gyres. If a warmer climate delivers more dust (and vice versa), then the cycle is stabilizing. If a warmer and perhaps wetter climate delivers less dust to a specific area, then the cycles could lead to runaway warming or cooling. The cycles are further bounded by the interaction of oceanic nitrate stocks on the rates of nitrogen fixation and denitrification, by the direct effects of climate on these rates and by the uncertain fate of iron in midwater.

Conclusion

In their treatise on nutrient dynamics in the sea, Dugdale and Goering (1967) were careful to emphasize that there were several potential sources of new nitrogen for the euphotic zone, each of equal value but with potentially different ecological consequences. As there were few data on N_2 fixation rates when their original paper was published, importation of nitrate from below the euphotic zone was considered to provide most of the new nitrogen in the sea.

Thirty years after the new production concept was introduced, there is increasing evidence that rates of oceanic N_2 fixation may have been systematically underestimated. More recently, application of modern molecular methods to detect the presence and composition of N_2 -fixing microorganisms at the U.S. JGOFS time-series sites has revealed a broad spectrum of previously uncharacterized gene sequences (Zehr et al., 2000). Yet-to-be-cultured microorganisms may hold the key to further understanding of carbon cycle dynamics (Capone, 2001).

We conclude that ecosystem models and biogeochemical extrapolations should be carefully reconsidered to determine the effects of traditional simplifying assumptions on their dynamics. The fact that the Redfield ratio paradigm has been with us so long, like the new versus recycled production conceptualization of nutrient dynamics, reflects our history of undersampling, a previously limited set of technical approaches and less than complete understanding of biological dynamics in the sea. It also reflects the power of early generalizations in structuring great advances in our field. The challenge is knowing when to use these simplifying assumptions and when to move on.

We submit that the time has come for a careful and complete reconsideration of the Redfield ratio and the new/export production paradigms. The new information gained during JGOFS field programs should be used to help develop a new and expanded conceptual framework for nutrient dynamics in the sea. This ecumenical theory should also leave room for the additional discoveries that are likely to emerge. 

Acknowledgements

We thank the many technicians and scientists who have contributed to the success of the two U.S. JGOFS time-series programs and of elemental cycling research in other parts of JGOFS. We thank the National Science Foundation (NSF) and the other federal agencies for their financial support. We particularly thank NSF for support of the time-series stations and of nitrogen fixation research in the Biocomplexity Program. This is U.S. JGOFS Contribution Number 678.

References

- Anderson, L. and J. Sarmiento, 1994: Redfield ratios of remineralization determined by nutrient data analysis. *Global Biogeochem. Cycles*, 8, 65–80.
- Capone, D.G., 2001: Marine nitrogen fixation: What's the fuss? *Current Opinions in Microbiology*, 4, 341–348.
- Capone, D.G., A. Subramaniam, J. Montoya, M. Voss, C. Humborg, A. Johansen, R. Siefert and E.J. Carpenter, 1998: An extensive bloom of the N₂-fixing cyanobacterium, *Trichodesmium erythraeum*, in the central Arabian Sea. *Mar. Ecol. Progress Series*, 172, 281–292.
- Deutsch, C., N. Gruber, R.M. Key, J.L. Sarmiento and A. Ganachaud, 2001: Denitrification and N₂ fixation in the Pacific Ocean. *Global Biogeochemical Cycles*, 15, 483–506.
- Dugdale, R.C. and J.J. Goering, 1967: Uptake of new and regenerated forms of nitrogen in primary productivity. *Limnol. and Oceanog.*, 12, 196–206.
- Elser, J.J., D.R. Dodderfuhr, N.A. MacKay and J.H. Schampel, 1996: Organism size, life history, and N:P stoichiometry. *BioScience*, 46, 674–684.
- Eppley, R.W. and B.J. Peterson, 1979: Particulate organic matter flux and planktonic new production in the deep ocean. *Nature*, 282, 677–680.
- Falkowski, P., 2000: Rationalizing elemental ratios in unicellular algae. *Journal of Phycology*, 36, 3–6.
- Galloway, J.N., W.H. Schlesinger, H. Levy II, A. Michaels and J.L. Schnoor, 1995: Nitrogen fixation: Anthropogenic enhancement—environmental response. *Global Biogeochem. Cycles*, 9, 235–252.
- Gruber, N. and J. Sarmiento, 1997: Global patterns of marine nitrogen fixation and denitrification. *Global Biogeochem. Cycles*, 11, 235–266.
- Husar, R., J. Prospero and L. Stowe, 1997: Characterization of tropospheric aerosols over the oceans with the NOAA advanced very high resolution radiometer optical thickness operational product. *Journal of Geophys. Res. Atmosph.*, 102, 16889–16909.
- Karl, D., R. Letelier, L. Tupas, J. Dore, J. Christian and D. Hebel, 1997: The role of nitrogen fixation in biogeochemical cycling in the subtropical north Pacific ocean. *Nature*, 386, 533–538.
- Karl, D.M., K.M. Bjorkman, J.E. Dore, L. Fujieka, D.V. Hebel, T. Houlihan, R.M. Letelier and L.M. Tupas, 2001: Ecological nitrogen-to-phosphorus stoichiometry at Station ALOHA. *Deep-Sea Res. II*, in press.
- Martin, J.H., G.A. Knauer, D.M. Karl and W.W. Broenkow, 1987: VERTEX: carbon cycling in the northeast Pacific. *Deep-Sea Res.*, 34, 267–85.
- Michaels, A.F., N.R. Bates, K.O. Buesseler, C.A. Carlson and A.H. Knap, 1994: Carbon-cycle imbalances in the Sargasso sea. *Nature*, 372, 537–540.
- Michaels, A.F., D. Olson, J.L. Sarmiento, J.W. Ammerman, K. Fanning, R. Jahnke, A.H. Knap, F. Lipschultz and J.M. Prospero, 1996: Inputs, losses and transformations of nitrogen and phosphorus in the pelagic north Atlantic ocean. *Biogeochemistry*, 35, 181–226.
- Redfield, A.C., 1958: The biological control of chemical factors in the environment. *Am. Sci.*, 46, 205–221.
- Sambrotto, R.N., G. Savidge, C. Robinson, P. Boyd, T. Takahashi, D.M. Karl, C. Langdon, D. Chipman, J. Marra and L. Codispoti, 1993: Elevated consumption of carbon relative to nitrogen in the surface ocean. *Nature*, 36, 248–50.
- Zehr, J.P., E.J. Carpenter and T.A. Villareal, 2000: New perspectives on nitrogen-fixing microorganisms in subtropical and tropical open oceans. *Trends in Microbiology*, 8, 68–73.



The Internal Weather of the Sea and Its Influences on Ocean Biogeochemistry

Dennis J. McGillicuddy, Jr.

Woods Hole Oceanographic Institution • Woods Hole, Massachusetts USA

Introduction

Interconnections between the physical, biological and chemical processes that regulate carbon cycling in the ocean span a tremendous range of space and time scales. For example, regional to global-scale variations in the biogeochemical constituents of the water column are closely linked with the general circulation of the ocean. At finer scales, such relationships are just as striking, if not more so. A particularly strong manifestation of these linkages occurs at the oceanic mesoscale, sometimes referred to as the “internal weather of the sea.” Highly energetic currents, fronts and eddies are ubiquitous features of ocean circulation, with characteristic spatial scales of 10–100 km and temporal scales of weeks to months. Their space scales are thus smaller and time scales longer than their counterparts in atmospheric weather, but the dynamics of the two systems are in many ways analogous. Both are characterized by large-amplitude departures from mean conditions on relatively small spatial scales, over relatively short periods of time.

Mesoscale phenomena include a diverse set of physical, chemical and biological interactions that influence the distribution and variability of the biogeochemical constituents of the water column. Complex yet highly organized flows continually deform and rearrange the hydrographic structure of the near-surface waters in which plankton reside. These motions affect biogeochemical cycling in two major ways: they alter distributions via the movement of water masses, and they modulate the rates of chemical and biological processes. Common manifestations of the second factor are associated with vertical transport, which can affect the availability of both nutrients and light to phytoplankton and therefore the rate of primary production. The dynamics of mesoscale and sub-mesoscale flows are replete with mechanisms that can produce vertical motions, thereby modulating the efficacy of the biological pump.

In essence, there are two aspects of mesoscale physical-biogeochemical coupling that have major implications for the study of global ocean fluxes. First, unless observations are specifically designed to deal

with mesoscale variability, spatial variations propagating through an area can be mistaken for temporal variability in that area. Second, mesoscale dynamic processes themselves can drive significant fluxes that affect local, regional and basin-scale biogeochemical budgets. Examples of both issues will be highlighted in the following brief overview of the U.S. Joint Global Ocean Flux Study (JGOFS) process studies and time-series programs.

The North Atlantic Bloom Experiment

The spring bloom in the North Atlantic is one of the most salient seasonal events that affect the global distribution of surface ocean phytoplankton biomass (Figure 1). The basic mechanism controlling this basin-scale phenomenon was established by Harald Sverdrup, Gordon Riley and others in the first half of the 20th century. Vigorous winter mixing sets the stage by bringing nutrient-rich deep water into the surface layer. As the mixed layer shoals with the onset of stratification in the spring, the abundance of both light and nutrients stimulates a massive proliferation of phytoplankton. The international North Atlantic Bloom Experiment (NABE), carried out in 1989 as a pilot study for JGOFS, was designed to quantify the fluxes of carbon associated with this annual event and to assess its effectiveness in fueling the biological pump.

JGOFS investigators observed dynamics of the bloom that were generally consistent with the Sverdrup model; the onset of stratification clearly led to a phytoplankton bloom. However, the presence of mesoscale variability complicated interpretation of the measurements in a number of ways. The field of eddies around the sampling site at 47°N, 20°W was mapped in real time during the study. Three cyclonic eddy features (referred to as “big,” “standard” and “small”) were identified with a combination of satellite altimetry and hydrographic observations (Figure 2a). Significant variability in chlorophyll fluorescence associated with these features was evident in Airborne Oceanographic LIDAR surveys of the region. The vertical structure of these cyclones is such that isopycnal surfaces in their

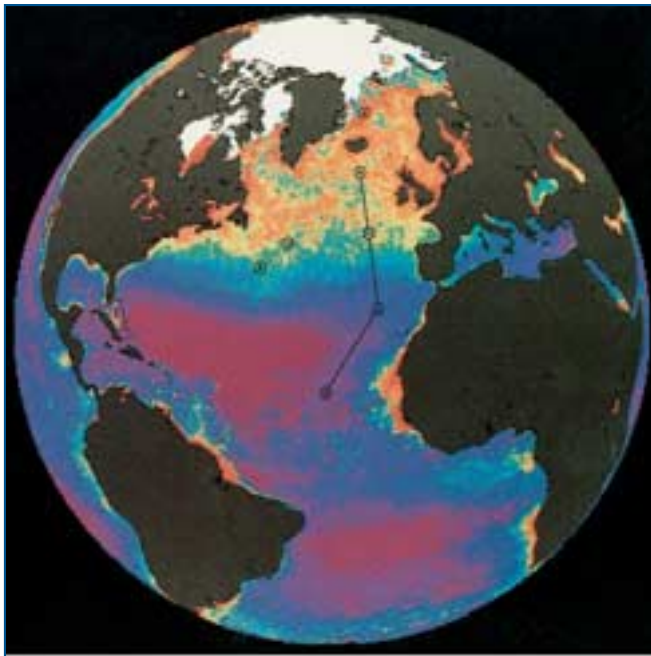


Figure 1. Composite of April–June period for 1979–1986 from the NIMBUS-7 Coastal Zone Color Scanner data showing phytoplankton pigment in the surface ocean. Purple represents lowest pigment levels ($<0.1 \text{ mg m}^{-3}$), and red represents the highest ($>3 \text{ mg m}^{-3}$). Areas of the most intensive studies during the 1989 North Atlantic Bloom experiment are indicated by circles; high-resolution transect work was undertaken along the line roughly following the 20°W meridian. (Image by Gene Feldman, NASA Goddard Space Flight Center.)

interiors are domed upward in the water column. Therefore near-surface waters in these features tend to be colder, denser and richer in nutrients than the surrounding ocean.

NABE investigators sampled a mixture of water masses from the mesoscale environment during two time-series studies. Starting near 47°N , 20°W , the first set of time-series measurements began outside the small eddy and finished inside it two weeks later. The second set of time-series measurements, made over a period of 10 days, were entirely inside the small eddy. What are the ramifications of starting a series of measurements outside the eddy and finishing it inside? Spatial variability can be mistaken for temporal variability; moving from outside to inside causes an apparent sink of heat and source of nitrate in the observations.

This effect can be quantified with the help of a three-dimensional coupled physical-biogeochemical model. For example, sampling simulated mixed-layer nitrate fields in space and time along the first time-series cruise track (Figure 2b & c) produces results (black line) that match the data (green squares). For comparison, the red and blue lines in Figure 2c show

the results of one-dimensional simulations at the center and outside of the eddy respectively. Attributing spatial variability in the data to changes over time can significantly affect conclusions regarding the functioning of the system. Moving from outside to inside the eddy results in underestimation of biological utilization related to the apparent source of nitrate. This causes the ratio of new to total production (f-ratio) computed from measurements of primary production and changes in nutrient inventories during the first set of time-series measurements (days 115–128) to be almost a factor of two lower (0.37) than that computed from samples taken from a single water mass (0.64) in the numerical model (Figure 2d).

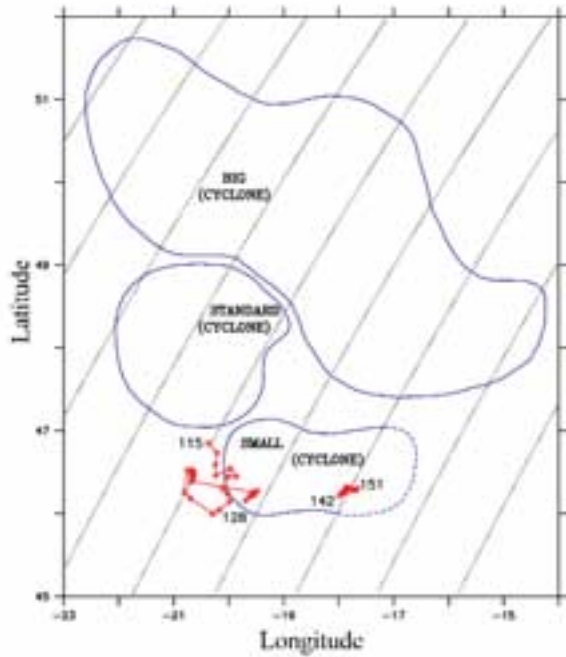
Although the predominant influence of eddies on the bloom itself appears to be the heterogeneity they bring to the initial conditions for the event, their effect may be even more dramatic after the bloom. Although few NABE samples were taken during the post-bloom period at 47°N , model simulations indicate that three-dimensional dynamic effects associated with interactions among eddies are responsible for most of the new production after the bloom. According to the model, the three cyclonic eddies in the area evolved and interacted very strongly during the two months following the bloom. Simulations indicate that intense vertical motions associated with these interactions cause significant fluxes of nutrients into the euphotic zone. The upwelling caused by eddy interactions substantially increases simulated plant and animal production for periods of weeks. Whether by supplying heterogeneity to the initial conditions of the bloom or through dynamic effects during the post-bloom period, eddies appear to exert a significant influence on the export of biogenic material from the euphotic zone in the North Atlantic sampled during NABE. For example, Newton et al. (1994) document strong mesoscale variability in particle flux to the deep sea in this region. Nonetheless, details of the mechanistic linkage between eddy-driven processes and export to the deep ocean remain largely unknown.

The Equatorial Pacific Process Study

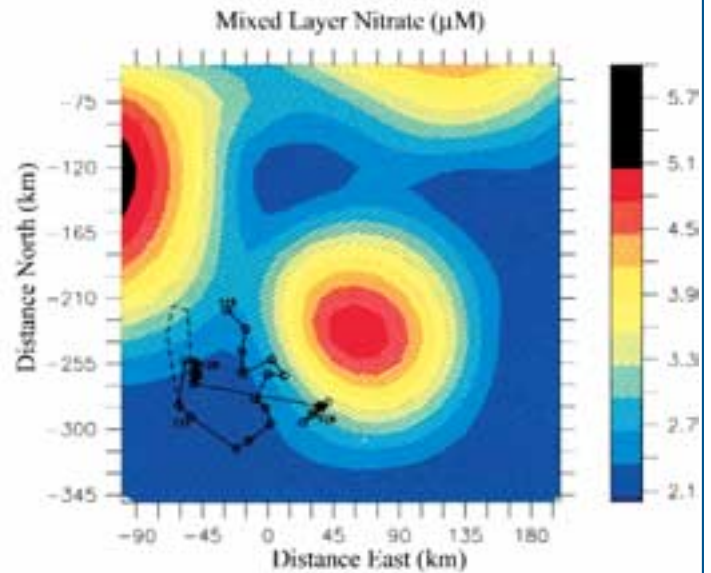
The equatorial Pacific is home to some of the most striking regional-scale structure and low-frequency variability in carbon cycling anywhere in the world ocean (Murray et al., 1994). Wind-driven upwelling at the equator brings deep water rich in dissolved inorganic carbon to the surface, the source of roughly 1.0 Gt C yr^{-1} ($1 \text{ Gt} = 10^9 \text{ tonnes}$) that is released into the atmosphere as carbon dioxide (CO_2). Outgassing in this region, the largest natural net source of CO_2 to the atmosphere, is subject to large fluctuations associated with El Niño–Southern Oscillation (ENSO) cycles. For example, deepening of the thermocline during 1991–1992 El Niño conditions appears to have reduced the outgassing of CO_2 to 0.3 Gt C yr^{-1} , roughly one third of its mean value.

Upwelling at the equator also transports large

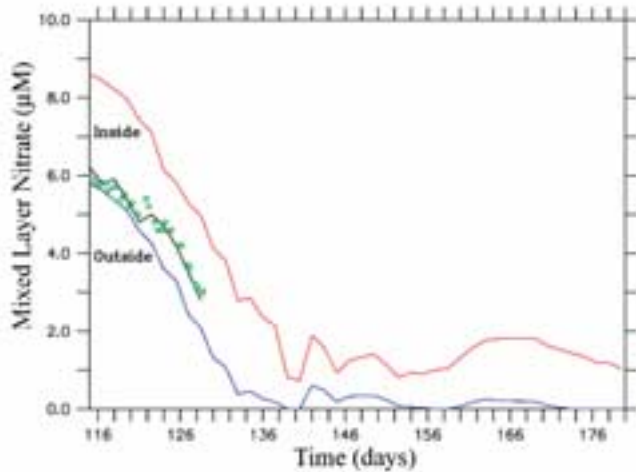
(a)



(b)



(c)



(d)

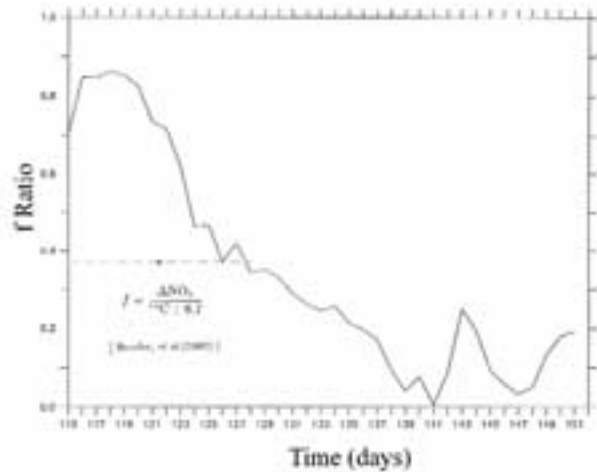


Figure 2. **a)** Map of a mesoscale eddy field around 47°N, 20°W for May 8–24, 1989. Ground tracks of GEOSAT altimetric data used in the analysis are indicated by dotted lines. Two U.S. JGOFS time-series cruise tracks are shown in red. Year days are indicated at the beginning and end of each time-series track. **b)** Track of the first time-series cruise superimposed on a field of mixed-layer nitrate simulated with a three-dimensional coupled physical-biogeochemical model. **c)** Mixed-layer nitrate concentrations in μM (green squares) and values extracted from the coupled model along the cruise track (solid black line). Red and blue lines indicate the model solutions for inside and outside the eddy respectively. **d)** Simulated time-series record of depth-integrated f-ratio outside the “standard” eddy (black line); an observational estimate of the f-ratio during this time period (from Bender et al., 1992) is indicated with an open circle. The dashed line indicates the temporal extent of the data used to compute this average value. Panel a adapted from Robinson et al., 1993; panels b, c and d adapted from McGillicuddy et al., 1995.

quantities of inorganic nutrients into surface waters, fueling new production of approximately 1.0 Gt C yr^{-1} , a significant fraction of the global total. The fact that the upwelled nutrients are not fully utilized by phytoplankton leads to the enigmatic persistence of the high-nutrient, low-chlorophyll (HNLC) conditions characteristic of this region. A variety of mechanisms have been proposed to explain this phenomenon, from “bottom-up” regulation through the supply of micronutrients such as iron to “top-down” control through zooplankton grazing. Idealized box-models that explicitly represent the joint effects of bottom-up control on large phytoplankton (silica limitation on diatoms) and top-down control on small phytoplankton (microzooplankton grazing on picoplankton) predict new and export production comparable to measured values (Dugdale and Wilkerson, 1998). Various aspects of this diverse set of controls have been incorporated into three-dimensional circulation models that show some success in simulating the large-scale mean characteristics of the nutrient and chlorophyll distributions of the region (Figure 3).

What are the detailed processes responsible for regulating biogeochemical cycling in the equatorial Pacific? Thirteen months’ worth of continuous time-series observations from moored bio-optical instruments deployed during the U.S. JGOFS Equatorial Pacific Process Study (EqPac) in the early 1990s documented vigorous variability on time scales ranging from days to seasons (see Dickey, this issue). Much of the energy in higher-frequency fluctuations observed in such fixed-point records is associated with wavelike disturbances propagating through the region, including Kelvin waves and tropical instability waves (TIWs).

A spectacular manifestation of the effect of a TIW on surface ocean physical and biogeochemical properties was observed during an EqPac cruise in August 1992 (Figure 4). Although the characteristic wavelength of such features is quite large (on the order of 1000 km), the frontal boundary along the leading edge can be extraordinarily sharp (less than 1 km). The front associated with this TIW produced a “line in the sea” visible to astronauts flying overhead on the space shuttle *Atlantis* as well as to those on board ship (Figure 4a).

Shipboard observations revealed an extraordinary abundance of the buoyant diatom *Rhizosolenia castracanei*. Concentrations of this organism were sufficient to discolor the water, giving it a brown appearance on the warm side of the front. A few meters away on the cold side of the front, surface waters were a more characteristic blue (Figure 4b). Analysis of elemental budgets in the observed velocity field (Figure 4c) suggests that the very high diatom concentrations observed at the front were predominantly a result of accumulation rather than local photosynthesis. Convergence at the front, in concert with the upward motion of the buoyant organisms through the water, concentrated them in regions of strongest downwelling.

The extraordinary aggregation of diatoms at the line

in the sea appears to be only the surface manifestation of the dramatic effect of the TIW on upper-ocean ecosystem structure. Shipboard measurements show that total chlorophyll increased by about a factor of two as such waves passed. Moreover, the diatom contribution to total chlorophyll increased three- to four-fold (Bidigare and Ondrusek, 1996). EqPac investigators found that the periods of strongest TIW activity coincided with peaks in the flux of organic carbon and biogenic silica to the deep sea (Honjo et al., 1995). However, the peaks in these fluxes did not occur near the equator where the line in the sea was observed, but farther north and south at 5°N , 2°S and 5°S . Although vigorous meridional velocities on the order of 100 cm s^{-1} associated with TIWs are sufficient to explain this poleward displacement by horizontal advection, existing data are not sufficient to confirm or reject this hypothesis.

Mechanistic links between the activity of various types of waves and upper ocean biogeochemical response have been investigated in the context of numerical models. For example, Friedrichs and Hofmann (2001) explicitly included the effects of wave-induced motions in a one-dimensional coupled physical-biological model, using vertical velocities diagnosed from measurements made by instruments on the Tropical Atmosphere Ocean (TAO) mooring array. Their simulations suggest that the increase in chlorophyll and change in species composition associated with TIWs observed during EqPac cruises resulted from the combination of two factors: enhanced growth stimulated by the vertical advection of iron and accumulation of buoyant diatoms in the convergence at the leading edge of the front.

Friedrichs and Hofmann also found that the large-amplitude equatorially-trapped internal gravity waves characteristic of this region can also stimulate phytoplankton growth locally through the vertical advection of iron into the euphotic zone. Because the time scale for iron utilization by rapidly growing picoplankton is short compared to the period of these internal gravity waves (6–8 days), this mechanism can result in a large net flux of iron into the euphotic zone—perhaps 30% or more of the mean flux resulting from wind-driven upwelling alone. However, detailed partitioning of the fluxes among all of the processes active in the equatorial Pacific is made difficult by the convolution of variability present in the observations; relevant time scales range from interannual (El Niño) to weeks (TIWs) to days (internal gravity waves).

The Arabian Sea Process Study

The Arabian Sea is a highly productive region with sediments that are rich in organic carbon. It is one of the few areas of the world ocean with a mid-depth oxygen minimum zone, which contributes to its distinct biogeochemical character. The region is also subject to a regular oscillation in powerful monsoonal winds, which have a dramatic effect on the structure of the upper water column. The 1994–1996 Arabian Sea Process

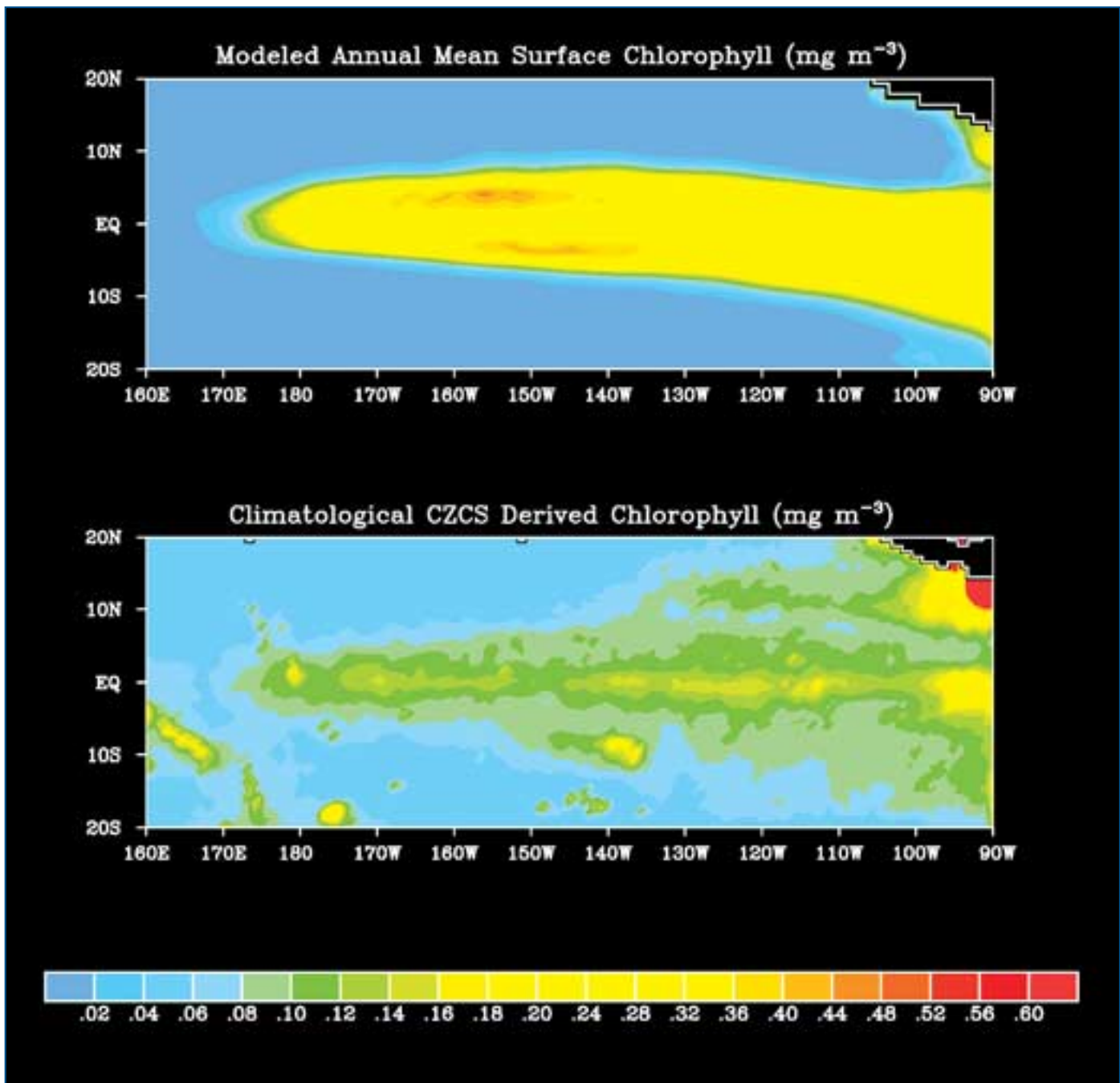


Figure 3. Comparison of modeled annual mean surface chlorophyll from Chai et al., 1996 (**top panel**) with chlorophyll derived from Coastal Zone Color Scanner (CZCS) data (**bottom panel**). Although the overall simulated pattern agrees with the CZCS data with respect to the positions of the maximum zonal and meridional gradients, there are several notable discrepancies. First, the modeled chlorophyll along the equator is about a factor of two higher than the CZCS estimates. In-situ chlorophyll measurements reveal that the mean surface chlorophyll is generally closer to the simulated values, suggesting that the CZCS underestimated chlorophyll concentrations in the equatorial Pacific. Second, the modeled surface chlorophyll maxima occur at 3°N and 3°S, whereas the CZCS data show a maximum right on the equator. In-situ observations appear to be more consistent with the simulation (Bidigare and Ondrusek, 1996). The discrepancy may be a result of temporal and spatial averaging of the CZCS data.

Study (ASPS) provided an opportunity for detailed investigation of biogeochemical responses to this strong atmospheric forcing.

The processes that regulate the biogeochemical

effects of monsoonal forcing are complex. During the summer months, the warm, moist air of the southwest monsoon flows in a strong jet along the western portion of the basin (Figure 5a). This results in vertical motion

(a)



(b)



(c)

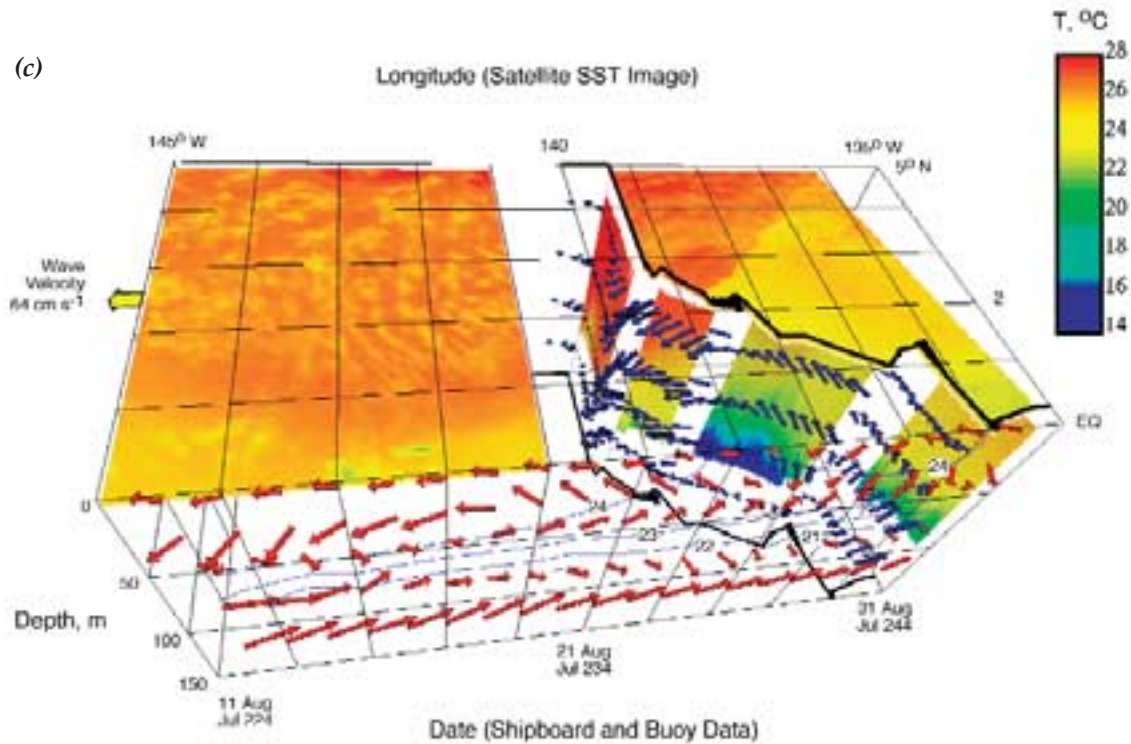


Figure 4. *a*) View from the space shuttle Atlantis. *b*) Photograph from the deck of R/V Thomas G. Thompson showing the sharp boundary at which surface waters were discolored by high concentrations of *Rhizosolenia castracanei*. *c*) Physical structure of the tropical instability wave. A sea-surface temperature (SST) swath from the NOAA AVHRR satellite is cut away to reveal subsurface detail from shipboard and moored observations. The satellite image was taken on Aug. 21, when the ship was at 5°N. To correct for the westward propagation of the wave, the shipboard and moored data have been transposed to the east at a rate of 0.5° per day. The convergent front is evident in the diagonal line in SST, reaching from about 140°W at the equator to 5°N, 135°W. Subsurface temperatures from the surface to approximately 100 m depth were observed with an undulating oceanographic recorder. Horizontal velocity estimates come from shipboard and moored acoustic Doppler current profiler (ADCP) data. A vector length of one degree (squares on surface) corresponds to a velocity of 333 cm s⁻¹. North of the front, the water flows parallel to the front towards the southwest. Just south of the front, the water flows into the front, subducting to the northwest. Near the equator, surface water flows to the west and the equatorial undercurrent to the east. Panels *a* and *b* are from Yoder et al., 1994; panel *c* is from Archer et al., 1997.

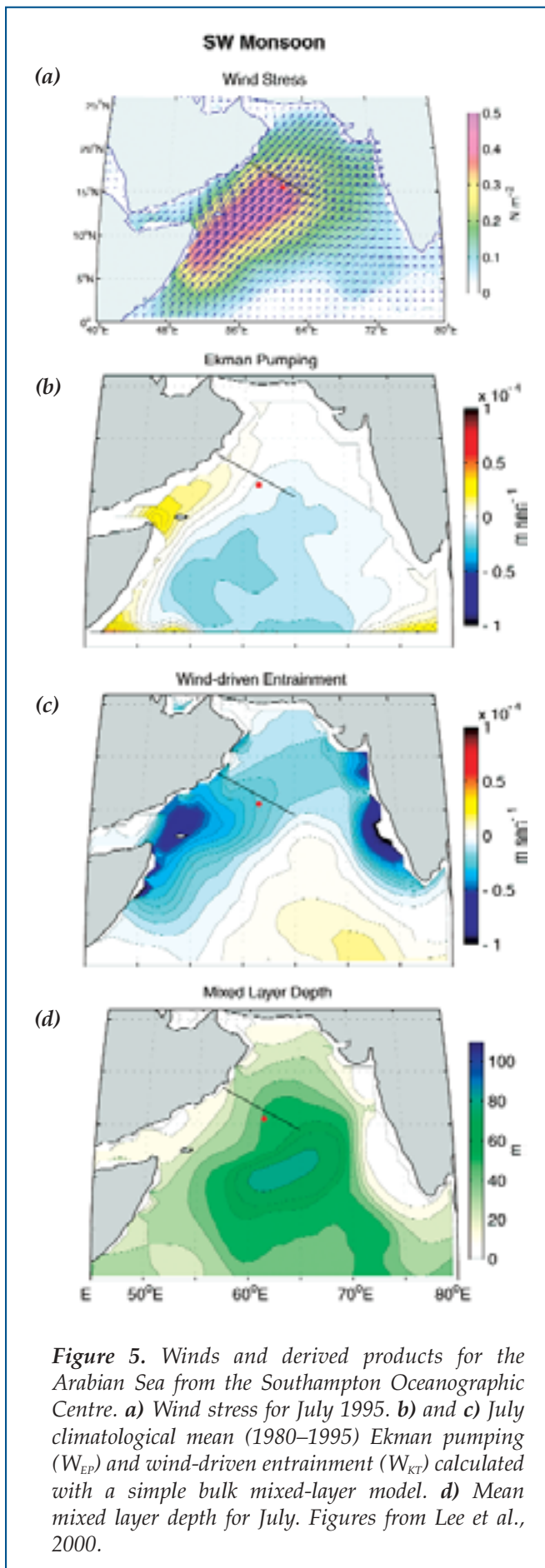


Figure 5. Winds and derived products for the Arabian Sea from the Southampton Oceanographic Centre. **a)** Wind stress for July 1995. **b)** and **c)** July climatological mean (1980–1995) Ekman pumping (W_{EP}) and wind-driven entrainment (W_{KT}) calculated with a simple bulk mixed-layer model. **d)** Mean mixed layer depth for July. Figures from Lee et al., 2000.

associated with wind-stress curl anomalies on either side of the jet (Figure 5b): downwelling along its southeastern flank and upwelling on its northwestern side. This particular wind-driven upwelling phenomenon occurs well offshore from the continental shelf. The winds themselves also enhance vertical mixing through direct input of turbulent energy (Figure 5c). The combination of these upwelling/downwelling phenomena and wind-driven turbulence generate significant spatial gradients in the depth of mixing (Figure 5d) and therefore entrainment of nutrients and other elements from below the mixed layer.

This analysis demonstrates that a complex mixture of open-ocean processes affect vertical exchanges in the Arabian Sea. However, one of the most striking findings of the ASPS was the degree to which coastal processes and associated filaments and eddies could contribute to biogeochemical cycling in the open ocean (Smith, 2001). The southwest monsoon wind pattern is favorable for coastal upwelling along the western edge of the basin. Just as in other regions of coastal upwelling, mesoscale filaments can transport upwelled waters large distances from the coast.

Detailed SeaSoar surveys, satellite data and acoustic Doppler current profiler (ADCP) observations clearly documented the penetration of an upwelling-derived coastal filament well into the interior of the basin during the summer of 1995 (Figure 6). The biogeochemical signature of this filament was unmistakable during ASPS cruises. One encounter with this feature some 723 km off the coast in July revealed the highest biomass and productivity observed during the late southwest monsoon period (Barber et al., 2001). Pigment analysis showed a dramatic shift in the phytoplankton community, with diatoms constituting a large fraction of the total chlorophyll (Latasa and Bidigare, 1998). Observed depletion of silicic acid relative to nitrate is consistent with a diatom bloom within the filament. Time-series measurements of biogenic silica in deep sediment traps suggest that such shifts in species composition appear to be related to large exports of organic carbon in this region, which are clearly affected by coastal filaments (Honjo et al., 1999).

The relative importance of coastal and open-ocean upwelling in supplying the nutrients that drive the Arabian Sea's vigorous biological pump remain uncertain. Observations during ASPS suggested the dominance of coastal upwelling, eddies and filaments during the southwest monsoon and convectively driven mixing during the northeast monsoon (Smith, 2001). Surprisingly, spatially averaged productivity during these two time periods was approximately equal (Barber et al., 2001).

Coastal upwelling filaments were by no means the only type of mesoscale feature observed during the ASPS. Mesoscale eddies were prominent in the velocity field measured by shipboard ADCP (Kim et al., 2001). Eddy events were clearly discernible in moored time-series measurements of physical and bio-optical vari-

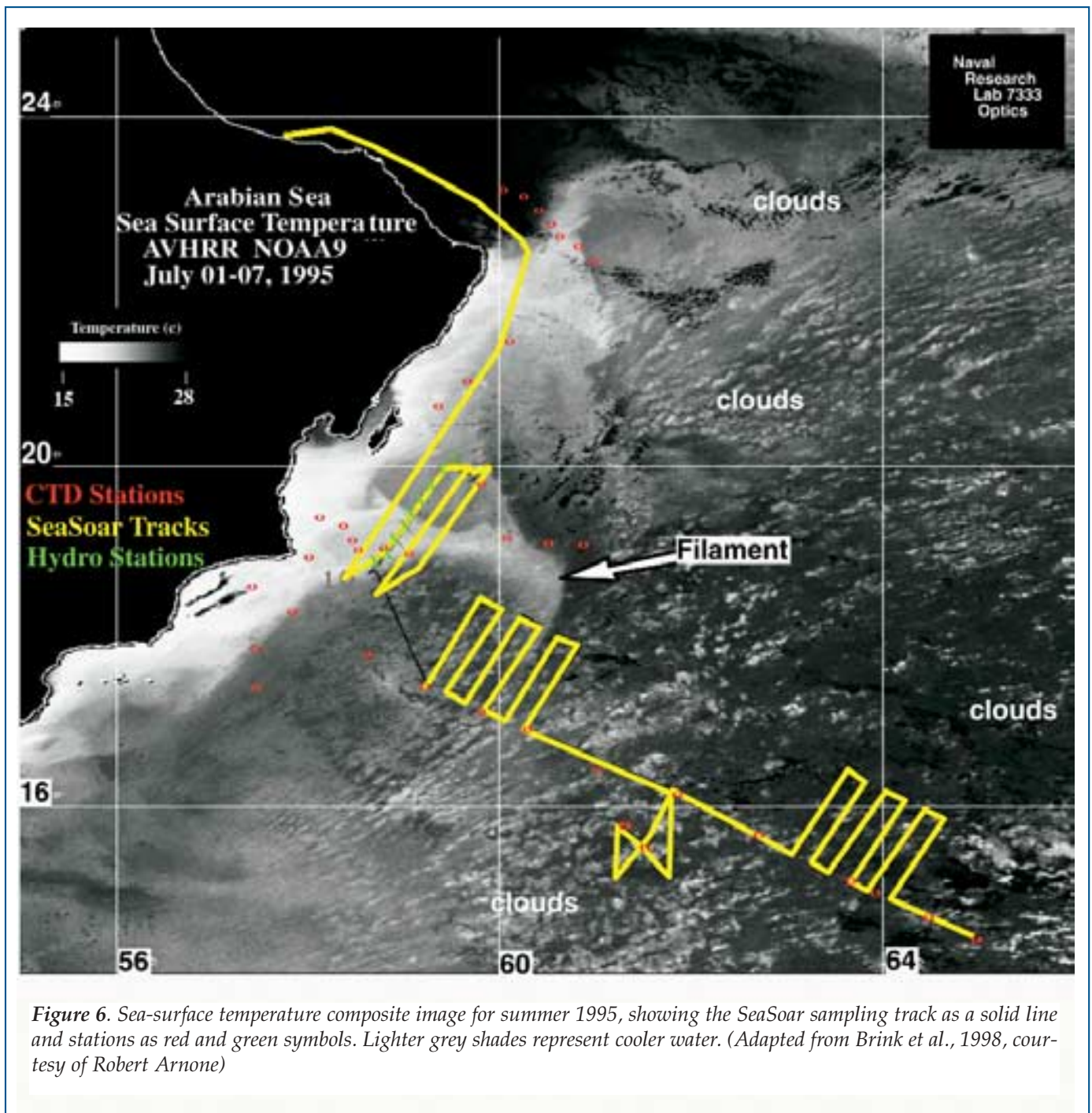


Figure 6. Sea-surface temperature composite image for summer 1995, showing the SeaSoar sampling track as a solid line and stations as red and green symbols. Lighter grey shades represent cooler water. (Adapted from Brink et al., 1998, courtesy of Robert Arnone)

ables as well (see Dickey, this issue). Comparison of deep sediment-trap data with the mooring records suggests that the timing of several, but not all, of the largest export events coincides with the appearance of mesoscale features in the upper ocean (Honjo et al., 1999).

Eddy variability may exert some control on large-scale biogeochemical distributions as well. Kim et al. (2001) note that the geographic extent of the mid-depth oxygen minimum zone in the northeast-central portion of the basin coincides with a minimum in eddy kinetic energy observed in the TOPEX/Poseidon altimetric

record. Nevertheless, despite this set of intriguing observations, it is still difficult to quantify the integrated effect of mesoscale processes on biogeochemical cycling in the Arabian Sea. Although three-dimensional coupled models of this region are advanced, they have tended to focus on physical-biogeochemical interactions that occur on larger scales. More explicit treatment of the highly energetic mesoscale variability observed during the ASPs will certainly help to quantify the effect of these phenomena on the overall functioning of the system.

The Antarctic Environment and Southern Ocean Process Study

The Southern Ocean is the largest HNLC region in the world ocean. Although chlorophyll concentrations are generally low throughout, elevated pigment biomass is found in three different regimes: coastal and continental shelf waters, areas of seasonal sea ice retreat and in the vicinity of major fronts (Figure 7). Despite the relatively low levels of chlorophyll in surface waters, particle fluxes to the ocean interior are high. Organic carbon fluxes measured from the Antarctic Polar Front (APF) southward during the U.S. JGOFS Antarctic Environment and Southern Ocean Process Study (AESOPS) in 1996-98 were approximately twice the ocean-wide average of $1 \text{ g C m}^{-2} \text{ yr}^{-1}$, and biogenic silica fluxes were among the highest measured in the entire JGOFS program (Honjo et al., 2000). Lithogenic fluxes to the deep sea were among the lowest measured in the open ocean, consistent with low dust input and associated iron limitation of phytoplankton production. It has been suggested that much of the global oceanic uptake of CO_2 occurs in the Southern Ocean, and coupled atmosphere-ocean models indicate that uptake in this region may be very sensitive to climate change (Sarmiento et al., 1998). Thus the need to understand carbon fluxes in this region is particularly compelling (Smith et al., 2000).

AESOPS comprised studies in two different regions: the APF and the Ross Sea. Mesoscale processes were evident in both areas; Ross Sea processes are described in the accompanying sidebar by Hales et al., and processes in the APF are treated here. Observational approaches to resolving mesoscale fluctuations in the vicinity of the APF took several forms, including an array of bio-optical moorings, clusters of bio-optical drifters and high-resolution SeaSoar surveys (Barth et al., 2001). All three techniques revealed mesoscale and submesoscale variability that would be extremely difficult to resolve using traditional hydrographic measurements.

SeaSoar observations in the APF documented highly organized structure in the chlorophyll field, with a large peak in chlorophyll situated at a meander crest (Figure 8). Analysis of two surveys

conducted approximately one week apart demonstrated the persistence of this chlorophyll feature at the meander crest. This finding is particularly intriguing given the fact that advection by a strong, narrow current in the meander displaces water parcels by 100–200 km over this time interval. Thus it appears that the peak in chlorophyll is a response to an upstream perturbation that persists for time scales of at least one week.

What processes could be responsible for such a perturbation? Woods (1988) suggests that intense vertical motion associated with a meandering front could give rise to mesoscale variations in phytoplankton productivity and biomass. The internal dynamics of mesoscale currents is such that changes in curvature give rise to submesoscale regions of upwelling and downwelling oriented within the crest and trough structure. Thus a fluid parcel moving through the current experiences

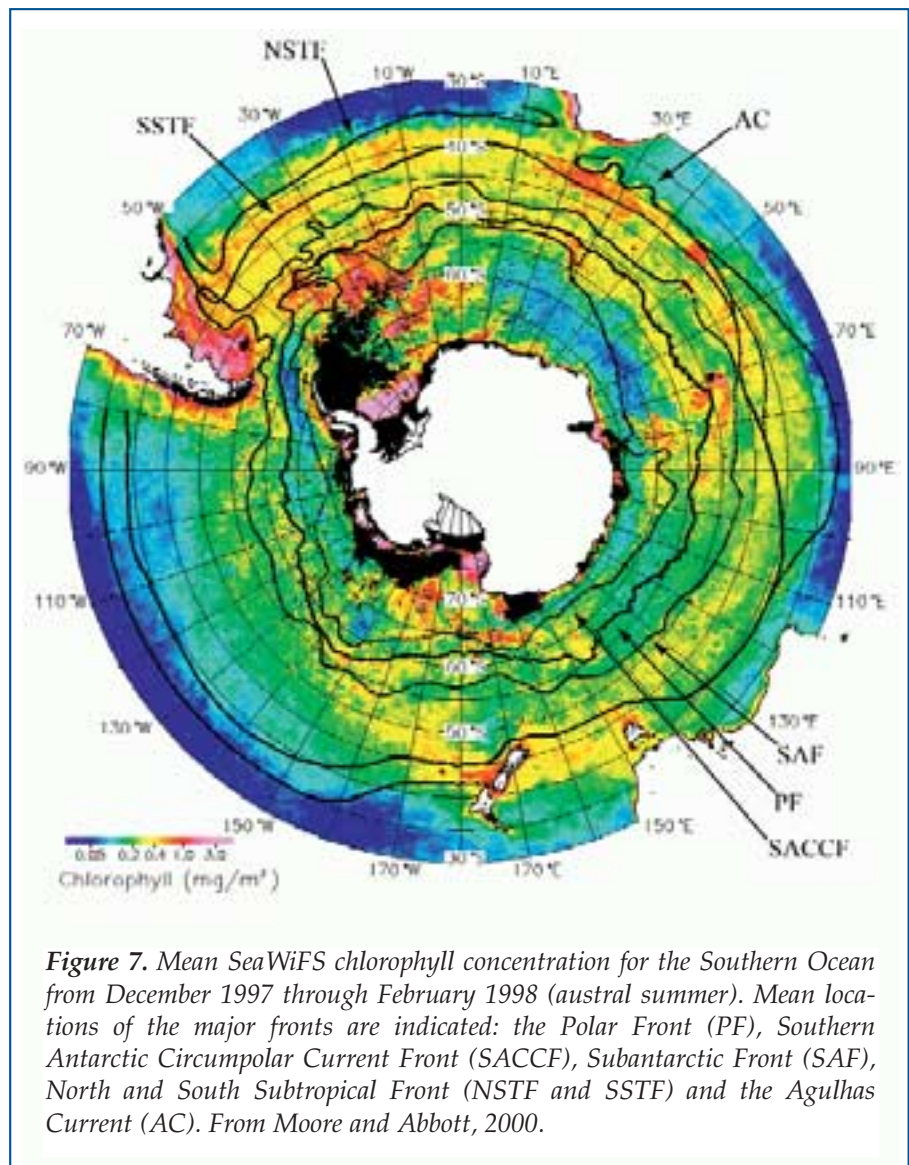


Figure 7. Mean SeaWiFS chlorophyll concentration for the Southern Ocean from December 1997 through February 1998 (austral summer). Mean locations of the major fronts are indicated: the Polar Front (PF), Southern Antarctic Circumpolar Current Front (SACCF), Subantarctic Front (SAF), North and South Subtropical Front (NSTF and SSTE) and the Agulhas Current (AC). From Moore and Abbott, 2000.

alternating bouts of upwelling and downwelling on a time scale set by its advective characteristics.

Based on growth rate calculations and the observed velocity field, Barth et al. (2001) infer that the observed chlorophyll peak was actually a response to upwelling of nutrients and/or trace metals in the preceding meander, located approximately 200 km upstream. What is the net effect of these motions on upper ocean biota, and how do they work together to create the elevated levels of biomass at the front that are shown in Figure 7? A complex mixture of horizontal advection, vertical advection and vertical mixing is clearly involved. However, the detailed dynamic balances are yet to be fully understood.

The Time-series Programs

Interpretation of time-series observations at fixed locations in the ocean is often complicated by the presence of spatial heterogeneity that changes over time. The phenomena to which this statement applies span a tremendous range of spatial and temporal scales, from microscale patchiness to decadal fluctuations in the general circulation. Ultimately, the utility of time-series measurements for understanding oceanic processes depends on our ability to differentiate between spatial and temporal variability.

U.S. JGOFS has produced two of the highest quality biogeochemical time-series programs to date: the Hawaiian Ocean Time-series (HOT) and the Bermuda Atlantic Time-series Study (BATS). Typical sampling intervals of one month resolve the seasonal cycle, and interannual trends are clearly evident (see Karl et al., this issue). Superimposed on these signals are higher frequency variations with amplitudes sometimes comparable to the explicitly resolved time scales. In attempting to develop a mechanistic understanding from the time-series records, it is relevant to inquire about the nature of the unresolved phenomena and their net effect on the overall characteristics of the system.

One aspect of biogeochemical cycling in which mesoscale processes may play a significant role is nutrient supply to the upper ocean. We have known for some time that geochemical estimates of new production in the main subtropical gyres of both the Atlantic and Pacific far surpass levels that can be sustained by traditional mechanisms of nutrient supply (e.g. Jenkins and Goldman, 1985). Several different lines of evidence emerging from both time-series sites now suggest that eddy-induced upwelling may provide a significant fraction of the “missing” nutrients.

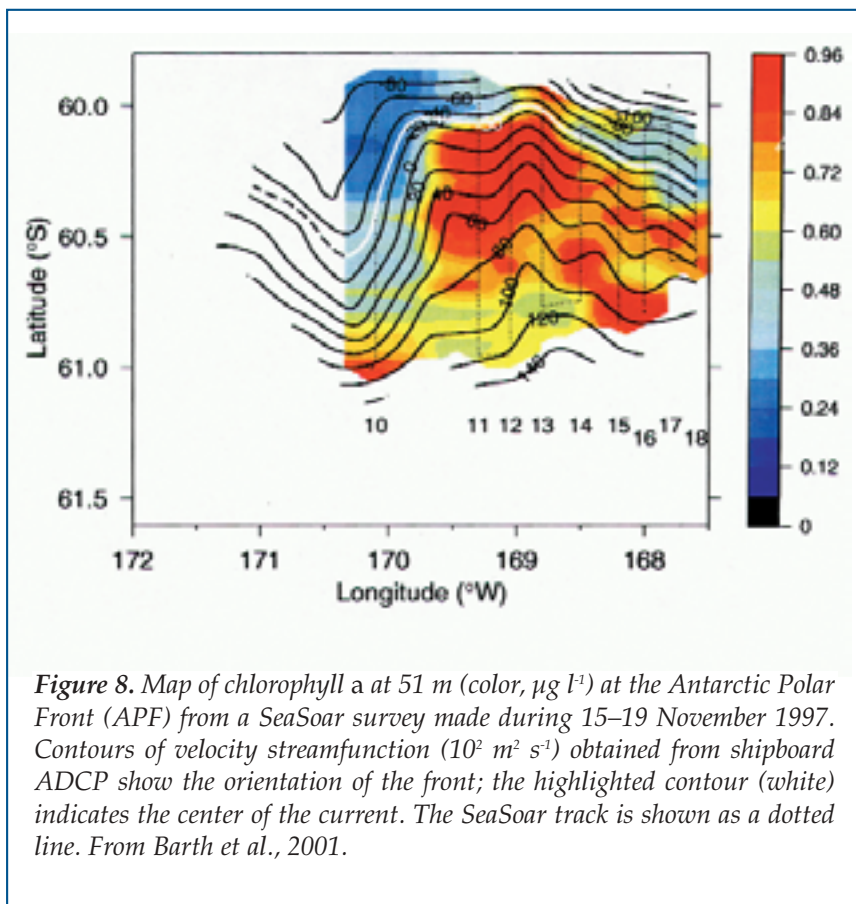


Figure 8. Map of chlorophyll a at 51 m (color, $\mu\text{g l}^{-1}$) at the Antarctic Polar Front (APF) from a SeaSoar survey made during 15–19 November 1997. Contours of velocity streamfunction ($10^3 \text{ m}^2 \text{ s}^{-1}$) obtained from shipboard ADCP show the orientation of the front; the highlighted contour (white) indicates the center of the current. The SeaSoar track is shown as a dotted line. From Barth et al., 2001.

Letelier et al. (2000) synthesized a variety of data from the shipboard measurements, moored sensors and satellite-based instruments to describe the passage of a mesoscale feature at the HOT site during the spring of 1997 (Figure 9). That event resulted in a three-fold increase in chlorophyll concentrations in the top 25 m of the water column and an increase in the inventory of nitrate plus nitrite of more than four orders of magnitude in the top 100 m. In addition, this feature had a dramatic effect on community structure. Pigment analysis suggests that the relative contribution of diatoms to the standing stock of chlorophyll *a* increased twofold in the interior of the eddy.

Investigators have observed similar events near Bermuda. Comparison of two nutrient profiles, taken one month apart in the summer of 1986 at nearby Station S before BATS began, suggested an eddy-driven nutrient injection event that could account for 20–30% of the annual new production (Jenkins, 1988). Since that time, the advent of moored biogeochemical measurement systems has provided the opportunity for much higher resolution of such phenomena in a time-series mode.

Data from the Bermuda Testbed Mooring program have revealed a number of mesoscale events at the BATS site (see Dickey, this issue). For example, in July 1995 a nutrient pulse and associated increase in chlorophyll and particulate material was associated with the passage of a mode-water eddy (Figure 10). This feature

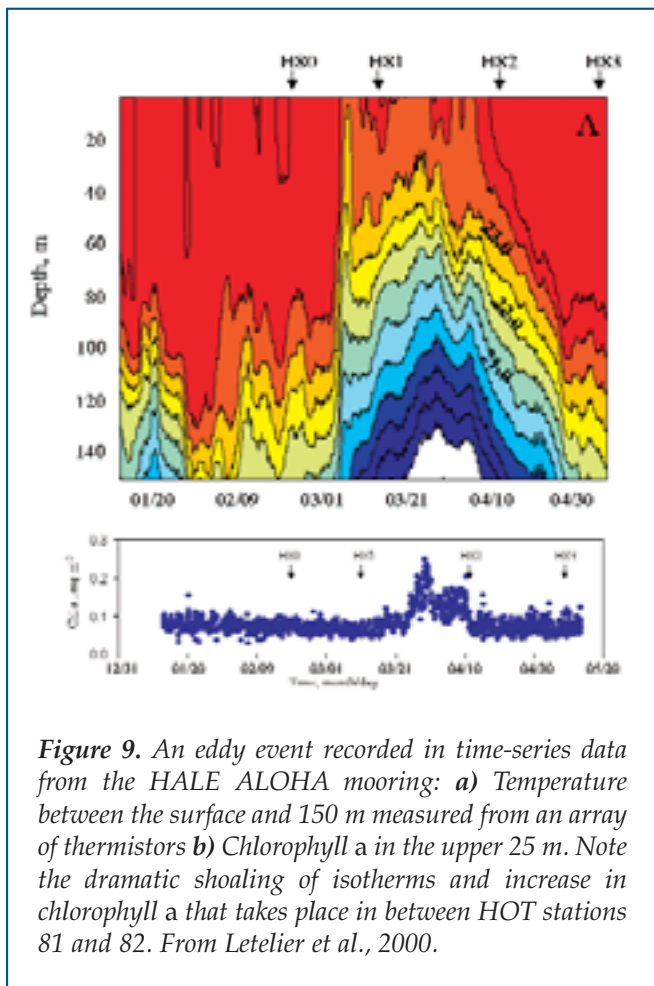


Figure 9. An eddy event recorded in time-series data from the HALE ALOHA mooring: **a)** Temperature between the surface and 150 m measured from an array of thermistors **b)** Chlorophyll a in the upper 25 m. Note the dramatic shoaling of isotherms and increase in chlorophyll a that takes place in between HOT stations 81 and 82. From Letelier et al., 2000.

was clearly visible as a positive sea-level anomaly in satellite altimetry (Figure 11; also see <http://science.whoi.edu/users/mcgillic/tpd/tpd.html>). BATS observations during this period document a depletion in silicic acid together with dramatic changes in pigment composition, suggesting that a bloom of diatoms occurred within the eddy.

Although fixed-point time-series measurements are indispensable, spatial information is essential to put them in context. Mesoscale biogeochemical surveys carried out as part of the BATS validation cruises demonstrate that eddy-induced upward displacement of density surfaces can inject nutrients into the euphotic zone, bringing about the accumulation of biomass in the overlying waters (McGillicuddy et al., 1998). Satellite data show correlated variation in mesoscale ocean color and sea-surface temperature patterns in the Sargasso Sea that is consistent with these results.

Although this diverse set of observations provides a phenomenological basis for description of the effects of mesoscale processes on the biogeochemical properties of ocean systems, models are necessary to get at the statistics. Some evidence suggests that mesoscale eddies supply a significant portion of the annual nutrient budget. Regional numerical simulations indicate that eddy-induced upwelling causes intermittent flux-

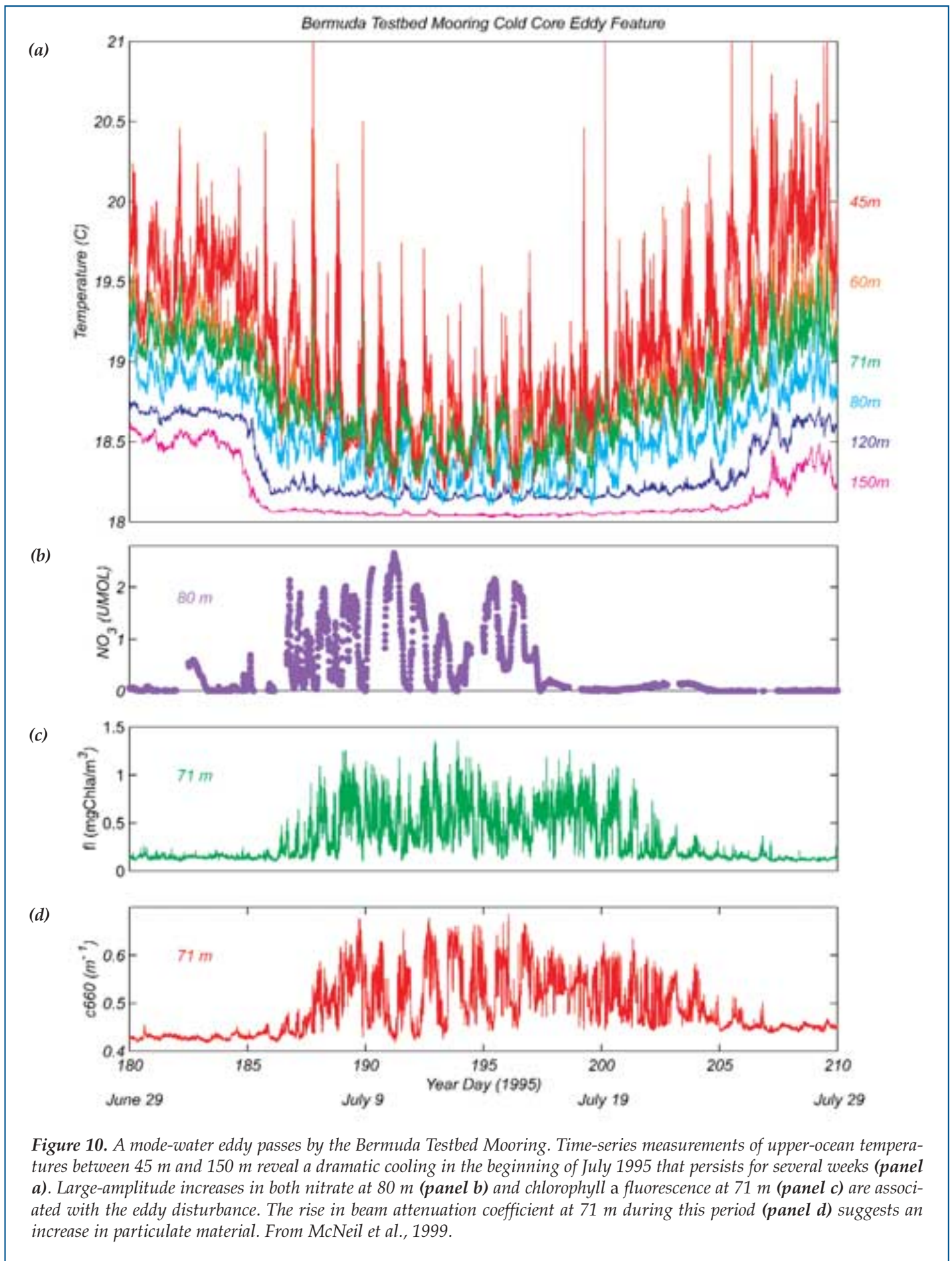
es of nitrate into the euphotic zone in amounts sufficient to balance the nutrient demand implied by geochemical estimates of new production. Nitrate flux calculations based on satellite altimetry and a statistical model linking sea-level anomalies to subsurface isopycnal displacements provide estimates of a comparable order (Siegel et al., 1999).

Conclusions

These examples from the U.S. JGOFS field studies demonstrate the striking relationships between physical and biogeochemical properties that occur at the oceanic mesoscale. There are several important ramifications with respect to global ocean fluxes. First, mesoscale motions create spatial heterogeneity that makes discrete measurements difficult to interpret. These difficulties can be overcome by spatio-temporal averaging over a suitably large number of observations. However, practical constraints associated with existing technology generally preclude such an approach in process studies and time-series programs. Thus we are faced with the problem of extracting large-scale signals from observations that are strongly affected by the mesoscale environment. Fortunately, remote sensing measurements, advanced *in situ* measurement techniques and numerical modeling help to diagnose the signature of mesoscale effects in biogeochemical data sets, thereby ameliorating the sampling problem to some degree.

It is also clear that the relevance of mesoscale physical-biogeochemical interactions runs much deeper than the sampling issue. At least for some areas of the world ocean, there is substantial evidence to indicate that eddies play a significant role in driving biogeochemical budgets. Given that mesoscale phenomena are ubiquitous and particularly energetic features of ocean circulation, it is possible that this finding may have general applicability. However, the nature of mesoscale physical-biogeochemical linkages has yet to be elucidated fully. Several examples cited above suggest that mesoscale physical disturbances cause shifts in planktonic species assemblages that then lead to large fluctuations in export. Among these phenomena are tropical instability waves in the equatorial Pacific, coastal filaments in the Arabian Sea and mid-ocean eddies at the HOT and BATS sites. Thus complex and highly nonlinear biological processes may regulate the biogeochemical ramifications of mesoscale perturbations.

How will we make progress on this complex and interdisciplinary problem? Rapidly developing measurement technologies (see Dickey, this issue) are leading to significant advances in our ability to sample biogeochemical quantities on space and time scales previously resolved only for physical properties. Despite these promising developments, it will not be practical to resolve all space and time scales of interest with observations alone; the union between observations and models is critical. Coupled physical-bioge-



Small-scale Variability In The Ross Sea

Burke Hales
Oregon State University
Corvallis, Oregon USA

Colm Sweeney and Taro Takahashi
Lamont-Doherty Earth Observatory
Palisades, New York USA

U.S. JGOFS studies of meso- and sub-mesoscale processes and variability in the Ross Sea were carried out with four one-day deployments of the Lamont Pumping SeaSoar (LPS) from RVIB *Nathaniel B. Palmer* during November and December 1997. Three of these were conducted along 76.5°S, and the fourth was a three-dimensional survey of a 60 km² grid centered on 76.5°S between 172°E and 174°E and selected because of high chlorophyll levels observed by satellite-mounted sensors and relayed to the ship.

The LPS is modified to pump water samples back to the ship for analysis with a suite of new, high-speed chemical systems. With this system, nutrient and carbonate chemistry fields can now be resolved with spatial resolutions approaching those attainable with *in situ* physical and bio-optical sensors.

During these brief surveys, we found physical variability on horizontal scales of 10–15 km. We also found that spatial variability in chemical species occurs on similar scales, and that there are no simple correlations between physical, bio-optical and chemical parameters, which would alleviate the need to sample them all in high spatial resolution.

Figure A shows some of the results obtained during the three-dimensional survey between 172°E and 174°E. Warming of surface waters from above is evident from distributions of temperature, as are several intrusions of warmer modified circumpolar deep water at depths of 80–120 m in the western sections. Temperatures range from -1.9°C to -0.8°C. The horizontal scale of variability is small; several prominent features appear to have north-south dimensions of only a few kilometers. East-west dimensions are also small, as seen by the lack of clear continuity between adjacent north-south track lines.

The partial pressure of carbon dioxide (pCO₂), measured continuously at a frequency of 0.5 Hz in the sample stream delivered to the shipboard laboratory, shows the effects of water mass origin and biological productivity. The former was highest in the warm subsurface modified circumpolar deepwater, and the latter was lowest in areas of high chlorophyll and nitrate depletion. Unlike temperature, variability in pCO₂ is large. It ranges from 450 μatm (nearly 100 μatm above atmospheric saturation) to less than 250 μatm (more than 100 μatm below

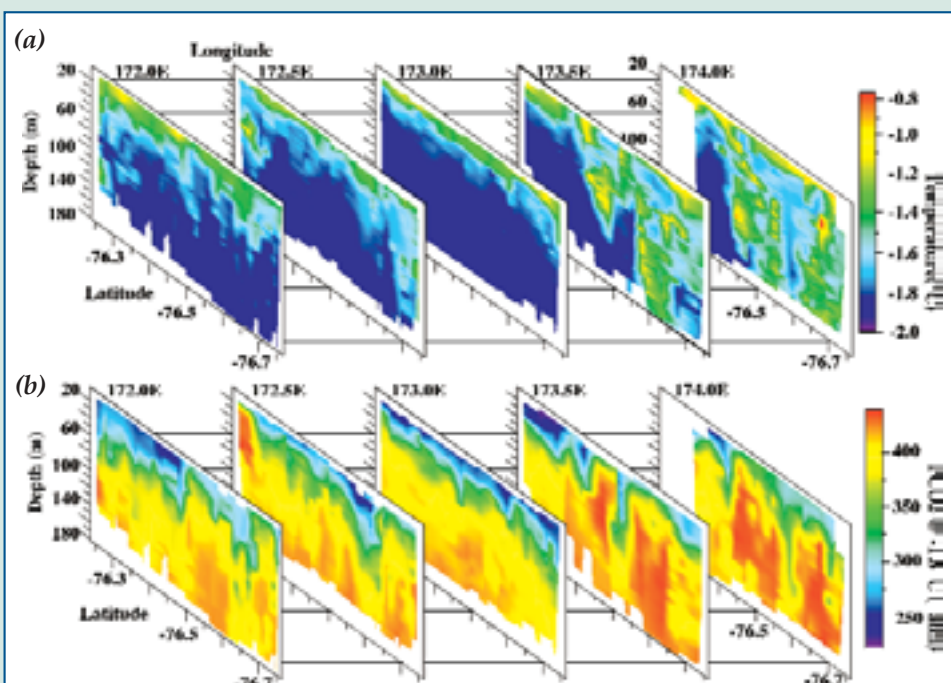


Figure A. Distributions of temperature **(a)** and pCO₂ **(b)** in a 60 km² grid in the Ross Sea, surveyed over a 20-hour period in December 1997 with the Lamont Pumping Seasoar (LPS). Temperature was measured with *in situ* sensors aboard the LPS; pCO₂ was measured with a high-speed equilibration system aboard the ship in a sample seawater stream pumped back to the ship from the LPS. Both fields show patterns of modified circumpolar deep water at depth, identified as warm water with high pCO₂ levels at depths of about 100 m. At the surface, they show the effects of two different factors: warming from insolation, which elevates surface temperatures, and uptake of carbon during photosynthesis, which lowers surface pCO₂. Both fields exhibit small horizontal scales of variability; many prominent features have horizontal dimensions of only about 10 km.


atmospheric saturation). As with temperature, this variability occurs over small horizontal scales, frequently 10 km or less.

Most of this variability would be missed by traditional hydrostation sampling. A quantitative analysis of the errors in predicting the true distributions of temperature and $p\text{CO}_2$ by interpolation of coarse sampling indicates that resolution as fine as 15 km misses two-thirds of the total variability in well-resolved fields. While there are similarities in the apparent horizontal scale of $p\text{CO}_2$ and temperature variability, one cannot be used as a proxy for the other. At greater depths, high temperatures and high $p\text{CO}_2$ levels coincide; at the surface, low temperatures coincide with low $p\text{CO}_2$. Therefore chemical fields that vary greatly in space cannot be simply estimated from well-resolved physical fields. Both must be measured with adequate resolution.

We are only beginning to speculate about the processes that could lead to such small horizontal-scale variability in the Ross Sea. The vertical stratification was weak in the study area. Thus narrow bands of surface waters that have experienced some warming or biological productivity could be mixed down to greater depths periodically, giving rise to some of the structure seen in Figure 1.

We do not know what causes such downward mixing. Winds were minimal during the two weeks over which the LPS surveys were carried out, and other surface phenomena, such as increased warming and sea-ice melting, should lead to enhanced stratification rather than downward convection. We also have no simple explanation as to why photosynthetic activity should be so variable in a region with abundant nutrients and light availability.

Further study is needed to unravel these relationships. We need to look with a keen eye at small horizontal-scale physical processes, using acoustic Doppler current profiler or microstructure-based measurements of physical transport, and phytoplankton physiology, employing optical measurements of photosynthetic efficiency and absorbance cross section or measurements of pigment distributions.

chemical models are maturing rapidly, as is their linking to observations through data assimilation (see Doney, this issue). If future research efforts are to develop a mechanistic understanding of ocean carbon cycling that is sound enough to facilitate skillful prediction, it will be essential to deal explicitly with the issues of physical-biogeochemical interactions at the scales on which these mechanisms operate. JGOFS experience suggests there is a great deal of biogeochemical activity associated with the internal weather of the sea. 

Acknowledgments

The author gratefully acknowledges support from the National Science Foundation, the National Aeronautics and Space Administration and the Jet Propulsion Laboratory. Thanks go to Larry Anderson, David Archer, Bob Arnone, Jack Barth, Will Berelson, Ken Brink, Ken Buesseler, Fei Chai, Tommy Dickey, Gene Feldman, Marjy Friedrichs, Valery Kosnyrev, Craig Lee, Ricardo Letelier, Keith Moore, Sharon Smith, Colm Sweeney and Jim Yoder for contributing constructive critiques, ideas and figures to this effort. The author would like to thank the SeaWiFS Project and the Distributed Active Archive Center at Goddard Space Flight Center for production and distribution of the ocean color data used in this article. These activities are sponsored by NASA's Mission to Planet Earth.

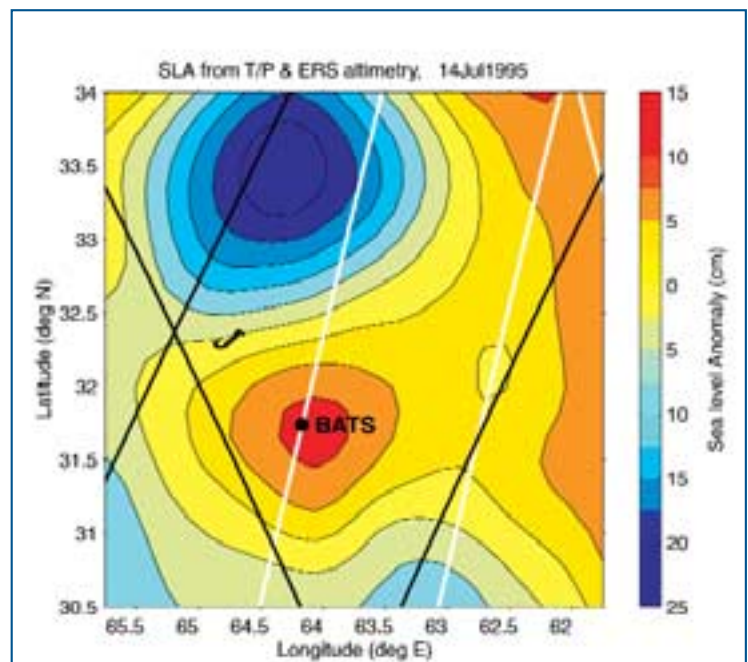


Figure 11. Objectively analyzed sea-level anomaly in the vicinity of the BATS site for July 14, 1995. Black and white lines show satellite ground tracks. The eddy feature observed in the Bermuda Testbed Mooring record in Figure 10 is clearly visible as a positive sea-level anomaly.

Special thanks go to Anita Norton and Mardi Bowles for their help in preparation of the manuscript and editorial revision. This is WHOI contribution 10503 and U.S. JGOFS Contribution Number 671.

See

<http://science.whoi.edu/users/mcgillic/papers/tos-jgofs.pdf> for a version of this paper that includes full references.

References

- Archer, D., J. Aiken, W. Balch, R. Barber, J. Dunne, P. Flament, W. Gardner, C. Garside, C. Goyet, E. Johnson, D. Kirchman, M. McPhaden, J. Newton, E. Peltzer, L. Welling, J. White and J. Yoder, 1997: A meeting place of great ocean currents: shipboard observations of a convergent front at 2°N in the Pacific. *Deep-Sea Res. II*, 44, 1827–1849.
- Barber, R., J. Marra, R. Bidigare, L. Codispoti, D. Halpern, Z. Johnson, M. Latasa, R. Goericke and S. Smith, 2001: Primary productivity and its regulation in the Arabian Sea during 1995. *Deep-Sea Res. II*, 48, 1127–1172.
- Barth, J., T. Cowles and S. Pierce, 2001: Mesoscale physical and bio-optical structure of the Antarctic Polar Front near 170°W during austral spring. *J. Geophys. Res.*, in press.
- Bender, M., H. Ducklow, J. Kiddon, J. Marra and J. Martin, 1992: The carbon balance during the 1989 spring bloom in the North Atlantic Ocean, 47°N, 20°W. *Deep-Sea Res.* 39, 1707–1725.
- Bidigare, R. and M. Ondrusek, 1996: Spatial and temporal variability of phytoplankton pigment distributions in the central equatorial Pacific Ocean. *Deep-Sea Res. II*, 43, 809–833.
- Brink, K., R. Arnone, P. Coble, C. Flagg, B. Jones, J. Kindle, C. Lee, D. Phinney, M. Wood, C. Yentsch and D. Young, 1998: Monsoons boost biological productivity in Arabian Sea. *EOS*, 79, 165, 168–169.
- Chai, F., S. Lindley and R. Barber, 1996: Origin and maintenance of a high nitrate condition in the equatorial Pacific. *Deep-Sea Res. II*, 43, 1031–1064.
- Dugdale, R. and F. Wilkerson, 1998: Silicate regulation of new production in the equatorial Pacific upwelling. *Nature*, 391, 270–273.
- Friedrichs, M. and E. Hofmann, 2001: Physical control of biological processes in the central equatorial Pacific Ocean. *Deep-Sea Res. I*, 48, 1023–1069.
- Honjo, S., J. Dymond, R. Collier and S. Manganini, 1995: Export production of particles to the interior of the equatorial Pacific Ocean during the 1992 EqPac experiment. *Deep-Sea Res. II*, 42, 831–870.
- Honjo, S., J. Dymond, W. Prell and V. Ittekkot, 1999: Monsoon-controlled export fluxes to the interior of the Arabian Sea. *Deep-Sea Res. II*, 46, 1859–1902.
- Honjo, S., R. Francois, S. Manganini, J. Dymond and R. Collier, 2000: Particle fluxes to the interior of the Southern Ocean in the Western Pacific sector along 170°W. *Deep-Sea Res. II*, 47, 3521–3548.
- Jenkins, W., 1988: The use of anthropogenic tritium and helium-3 to study subtropical gyre ventilation and circulation. *Phil. Trans. Roy. Soc.*, 325, 43–61.
- Jenkins, W. and J. Goldman, 1985: Seasonal oxygen cycling and primary production in the Sargasso Sea. *J. Mar. Res.*, 43, 465–491.
- Kim, H.-S., C. Flagg and S. Howden, 2001: Northern Arabian Sea variability from Topex/Poseidon altimetry data: an extension of the U.S. JGOFS/ONR shipboard ADCP study. *Deep-Sea Res. II*, 48, 1069–1096.
- Latasa, M. and R. Bidigare, 1998: A comparison of phytoplankton populations of the Arabian Sea during the Spring Intermonsoon and Southwest Monsoon of 1995 as described by HPLC-analyzed pigments. *Deep-Sea Res. II*, 45, 2133–2170.
- Lee, C., B. Jones, K. Brink and A. Fischer, 2000: The upper-ocean response to monsoonal forcing in the Arabian Sea: seasonal and spatial variability. *Deep-Sea Res. II*, 47, 1177–1226.
- Letelier, R., D. Karl, M. Abbott, P. Flament, M. Freilich and R. Lukas, 2000: Role of late winter mesoscale events in the biogeochemical variability of the upper water column of the North Pacific Subtropical Gyre. *J. Geophys. Res.*, 105, 28, 723–28, 739.
- McGillicuddy, D., A. Robinson and J. McCarthy, 1995: Coupled physical and biological modeling of the spring bloom in the North Atlantic (II): three dimensional bloom and post-bloom processes. *Deep-Sea Res. I*, 42, 1313–1398.
- McGillicuddy, D., A. Robinson, D. Siegel, H. Jannasch, R. Johnson, T. Dickey, J. McNeil, A. Michaels and A. Knap, 1998: Influence of mesoscale eddies on new production in the Sargasso Sea. *Nature*, 394, 263–265.
- McNeil, J., H. Jannasch, T. Dickey, D. McGillicuddy, M. Brzezinski and C. Sakamoto, 1999: New chemical, bio-optical and physical observations of upper ocean response to the passage of a mesoscale eddy off Bermuda. *J. Geophys. Res.*, 104, 15, 537–15, 548.
- Moore, K. and M. Abbott, 2000: Phytoplankton chlorophyll distributions and primary production in the Southern Ocean. *J. Geophys. Res.*, 105, 28, 709–28, 722.
- Murray, J., R. Barber, M. Roman, M. Bacon and R. Feely, 1994: Physical and biological controls on carbon cycling in the Equatorial Pacific. *Science*, 266, 58–65.
- Newton, P., R. Lampitt, T. Jickells, P. King and C. Boutle, 1994: Temporal and spatial variability of biogenic particle fluxes during the JGOFS northeast Atlantic process studies at 47°N, 20°W. *Deep-Sea Res. I*, 41, 1617–1642.
- Robinson, A., D. McGillicuddy, J. Calman, H. Ducklow, M. Fasham, F. Hoge, W. Leslie, J. McCarthy, S. Podewski, D. Porter, G. Saure and J. Yoder, 1993: Mesoscale and upper ocean variabilities during the 1989 JGOFS bloom study. *Deep-Sea Res. II*, 40, 9–35.
- Sarmiento, J., T. Hughes, R. Stouffer and S. Manabe, 1998: Simulated response of the ocean carbon cycle to anthropogenic climate warming. *Nature*, 393, 245–249.
- Siegel, D.A., and D.J. McGillicuddy and E.A. Fields, 1999: Mesoscale eddies, satellite altimetry and new production in the Sargasso Sea. *J. Geophys. Res.*, 104(C6), 13, 359–13, 379.
- Smith, S., 2001: Understanding the Arabian Sea: reflections on the 1994-1996 Arabian Sea expedition. *Deep-Sea Res. II*, 48, 1385–1402.
- Smith, W., R. Anderson, J. Moore, L. Codispoti and J. Morrison, 2000. The U.S. Southern Ocean Joint Global Ocean Flux Study: an introduction to AESOPS. *Deep-Sea Res. II*, 47, 3073–3093.
- Woods, J., 1988: Mesoscale upwelling and primary production. In: *Toward a Theory on Biological-Physical Interactions in the World Ocean*. B. Rothschild, ed. D. Reidel, Dordrecht.
- Yoder, J., S. Ackleson, R. Barber, P. Flament and W. Balch, 1994: A line in the sea. *Nature*, 371, 689–692

Marine Biogeochemical Modeling: Recent Advances and Future Challenges

Scott C. Doney, Ivan Lima, Keith Lindsay and J. Keith Moore
National Center for Atmospheric Research • Boulder, Colorado USA

Stephanie Dutkiewicz
Massachusetts Institute of Technology • Cambridge, Massachusetts USA

Marjorie A.M. Friedrichs
Old Dominion University • Norfolk, Virginia USA

Richard J. Matear
CSIRO Division of Marine Research • Hobart, Australia

Introduction

One of the central objectives of the Joint Global Ocean Flux Study (JGOFS) is to use data from the extensive field programs to evaluate and improve numerical ocean carbon-cycle models. Substantial improvements are required if we are to achieve a better understanding of present-day biogeochemical properties and processes in the ocean and to predict potential future responses to perturbations resulting from human activities. We have made significant progress in this regard and expect even greater strides over the next decade as the synthesis of JGOFS data sets is completed and disseminated to the broader scientific community.

Marine biogeochemical modeling depends inherently upon field data. The data sets from the U.S. JGOFS process studies, global survey and time series programs, together with products derived from satellite-based observations, are invaluable in two ways. They serve as the basis for new and improved mechanistic parameterizations of specific biogeochemical processes. They also provide a resource for evaluating the overall skill of integrated system models through detailed model-data comparisons.

Ocean carbon-cycle models cover a variety of complexities and applications, ranging from simple box models to global four-dimensional coupled physical-biogeochemical simulations and from dedicated research tools to constructs able to generate climate-change projections with direct societal implications. We highlight some recent modeling advances and challenges for the future, drawing on results from the U.S. JGOFS Synthesis and Modeling Project, which are available at <http://usjgofs.who.edu/mzweb/syn->

[mod.htm](#) (see also Doney, 1999). Specific topics covered are phytoplankton production and community structure, interannual climate variability, mesoscale biological-physical interactions, data assimilation, export flux and subsurface carbon cycling, and responses to climate change.

Phytoplankton Production and Community Structure

Primary production in the surface ocean is the base for almost all marine food webs. Biological oceanographers devote considerable effort to developing conceptual and numerical models of the controls on phytoplankton production. Evidence accumulated over the last decade suggests that the micronutrient iron, rather than macronutrients such as nitrogen and phosphorus, governs primary production and phytoplankton community structure, especially the growth of the large diatoms, over much of the world ocean. Shifts between assemblages composed of nano- and pico-sized phytoplankton and ones dominated by diatoms, which are often responsible for seasonal and episodic blooms, affect the production and export of particulate organic carbon (POC), a critical component of the ocean "biological pump" (see Berelson, this issue). Other important groups of phytoplankton include nitrogen-fixing diazotrophs such as *Trichodesmium*, which provide a source of "new" nutrients to the subtropical gyres, and calcium carbonate-forming coccolithophores, which can significantly alter surface-water carbonate chemistry and therefore air-sea fluxes of carbon dioxide (CO₂).

The basic framework for most marine biogeochem-

Ecosystem Model

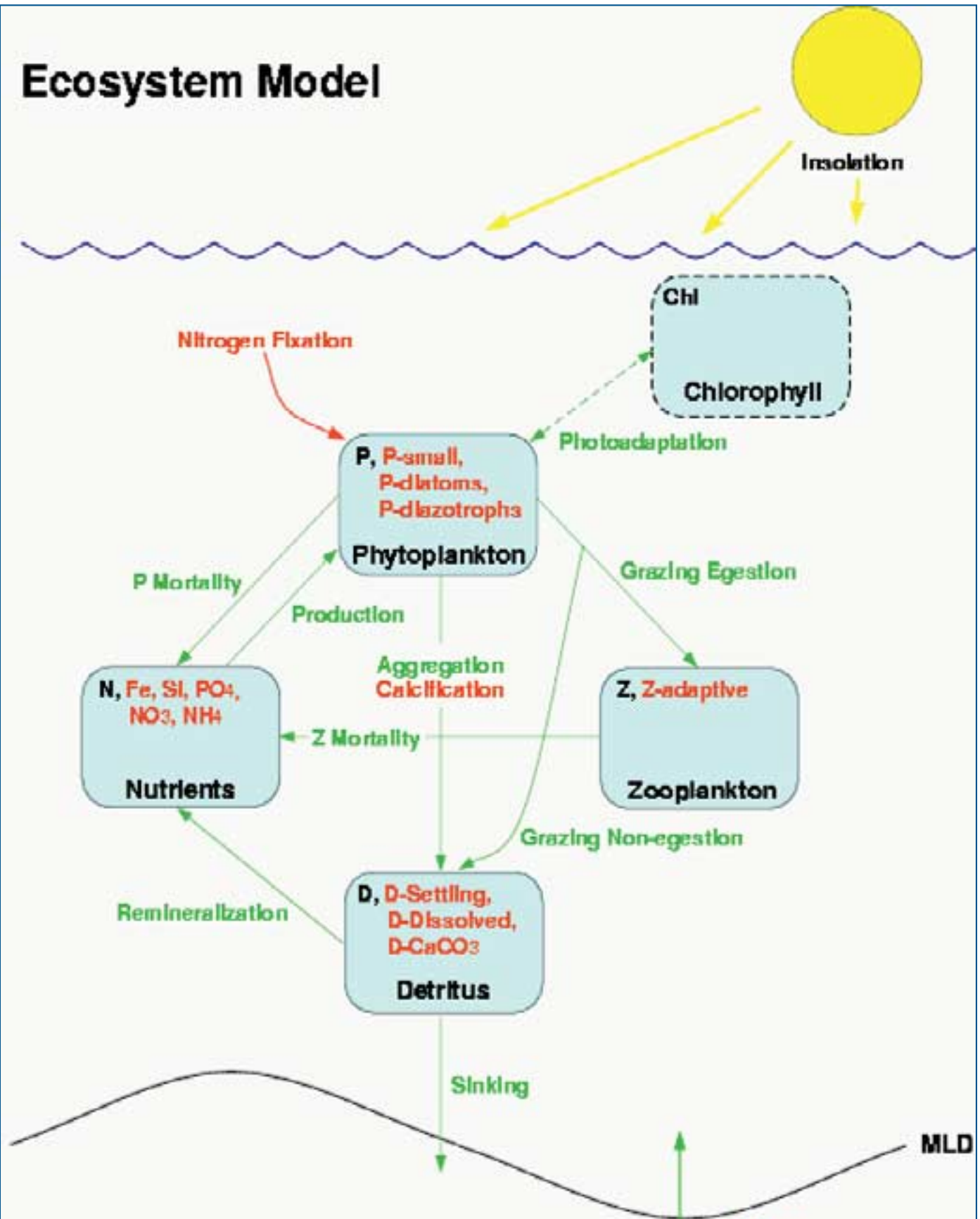


Figure 1. Diagram of a typical marine ecosystem model showing the simulated biomass compartments (boxes) and rates or fluxes (arrows) in terms of the concentration of nitrogen. In red are recent extensions of the model to incorporate multiple nutrient limitation, size structure and planktonic functional groups (Moore et al., 2001).

ical models (Figure 1) has been in use for several decades (Fasham et al., 1990). These models generally aggregate plankton populations into broadly defined trophic compartments (phytoplankton, zooplankton, detritus) and track the flow of a limiting element, such as the concentration of nitrogen or carbon, among the compartments. Biological systems have no analog to the Navier-Stokes equations of fluid dynamics; ecosystems models are by necessity highly empirical, non-linear and full of formulations based on poorly constrained parameters. The various terms for processes such as photosynthesis by phytoplankton, zooplankton grazing or detrital remineralization are calculated using standard, though not always well agreed-upon, sets of empirical functional forms derived either from limited field data or from laboratory experiments. A number of groups are working to expand this genre of model to include new concepts related to iron limitation and biogeochemical functional groups.

For example, Moore et al. (2001) present a global mixed-layer ecosystem model that explicitly accounts for multi-nutrient limitation (nitrogen, phosphorus, silica, iron), picoplankton, diatoms, nitrogen fixation, and calcification. The model has been tested against nine U.S. and international JGOFS time-series and process-study data sets drawn from a wide range of environments as well as with global ocean color data from the Sea-viewing Wide Field-of-view Sensor (SeaWiFS) instrument (see Yoder, this issue).

The marine iron cycle must be included for this model to reproduce accurately the observed high nutrient-low chlorophyll (HNLC) conditions observed in the Southern Ocean, and parts of the subarctic and equatorial Pacific (Figure 2). The atmospheric deposition of mineral dust is an important source of iron for the open ocean, especially near desert regions of North Africa, the Arabian Peninsula, northwest Asia and Australia (Figure 3). Subsurface iron contributes proportionally more in regions of upwelling, such as the equatorial Pacific, and deep winter convection, such as the subpolar North Atlantic and the Southern Ocean. The atmospheric contribution of iron input is generally low in the HNLC areas, which tend to be iron limited during summer months. The model study indicates that primary production in as much as half of the world ocean today may be iron limited.

Two main factors limiting progress on ecosystem modeling are our skill at conceptualizing key processes at a mechanistic level and our ability to verify model behavior through robust and thorough model-data comparisons. The phytoplankton iron limitation story offers an illuminating example. Atmospheric dust/iron deposition estimates vary considerably, by a factor of 10 or more in some areas, and the fraction of iron in dust that is biologically available is not well known. Surface and subsurface ocean iron measurements are limited, particularly from a global modeling perspective, and serious analytical and standardization issues

remain. Organic ligands may play a role in governing both bioavailability and subsurface iron concentrations. Not enough is known about the effect of iron limitation and variability on species competition at generally prevailing low iron levels. The same is true for a host of other processes, including iron release through photochemistry and zooplankton grazing, advection of iron from ocean margin sediment sources and iron remineralization from sinking particles.

Interannual Climate Variability

A key measure of the usefulness of numerical biogeochemical models is their ability to produce accurate descriptions of oceanic responses to natural climate forcing on interannual to interdecadal timescales. Ocean ecosystems exhibit significant variability associated with cyclical climate modes such as the El Niño-Southern Oscillation (ENSO), the Pacific Decadal Oscillation (PDO) and the North Atlantic Oscillation (NAO). The response of ecosystems to physical conditions may be quite nonlinear; in the North Pacific, for example, a major

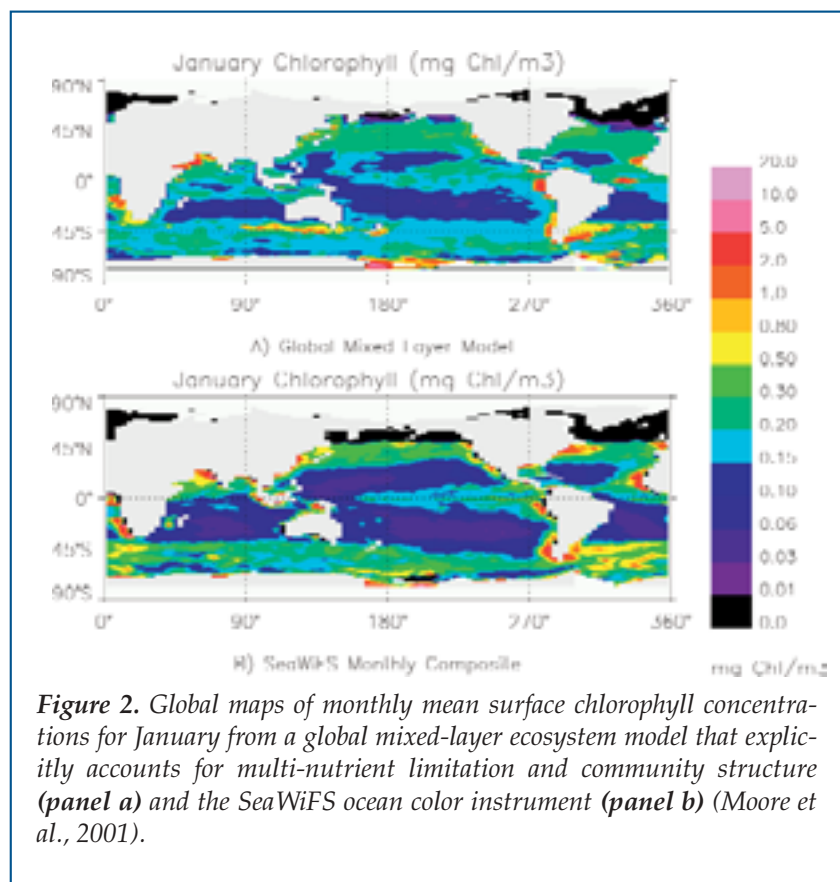


Figure 2. Global maps of monthly mean surface chlorophyll concentrations for January from a global mixed-layer ecosystem model that explicitly accounts for multi-nutrient limitation and community structure (**panel a**) and the SeaWiFS ocean color instrument (**panel b**) (Moore et al., 2001).

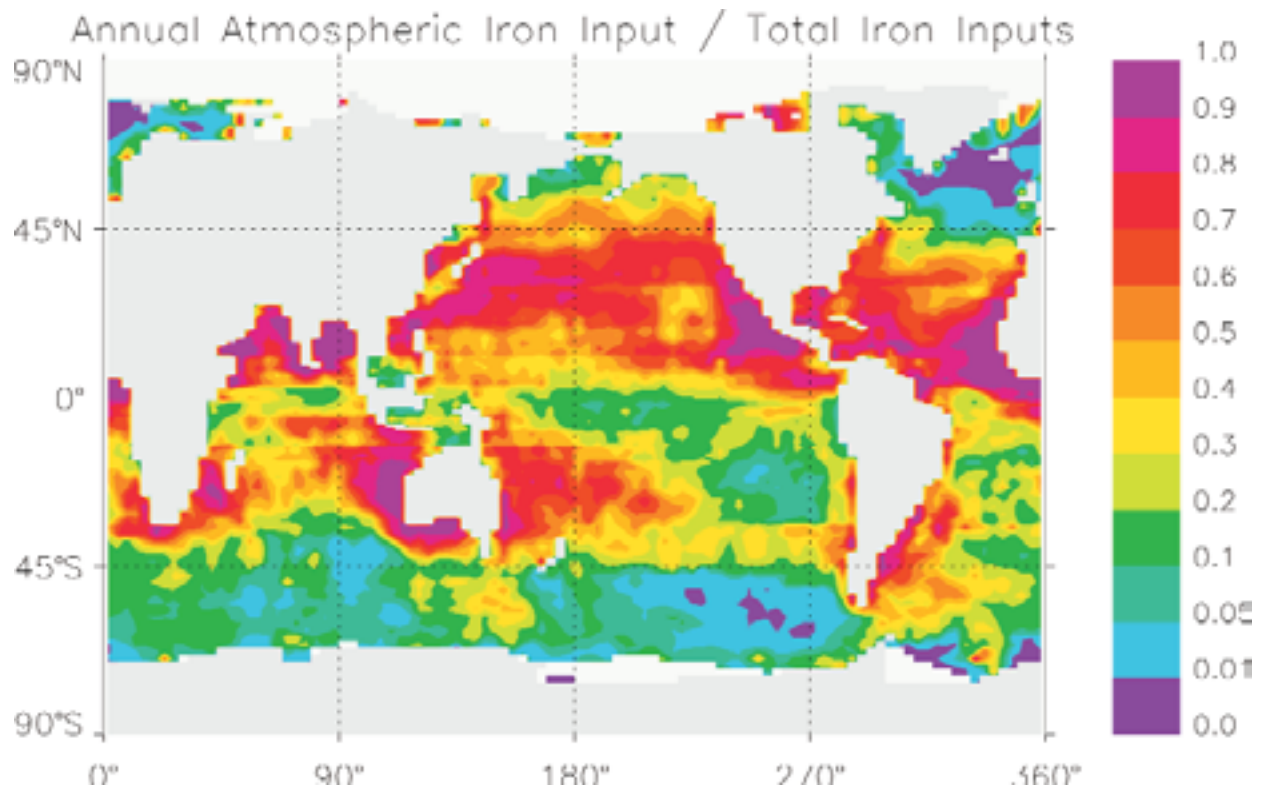


Figure 3. Global modeling simulation of the fractional contribution of atmospheric mineral dust deposition to total inputs of bioavailable iron in the surface ocean (Moore et al., 2001).

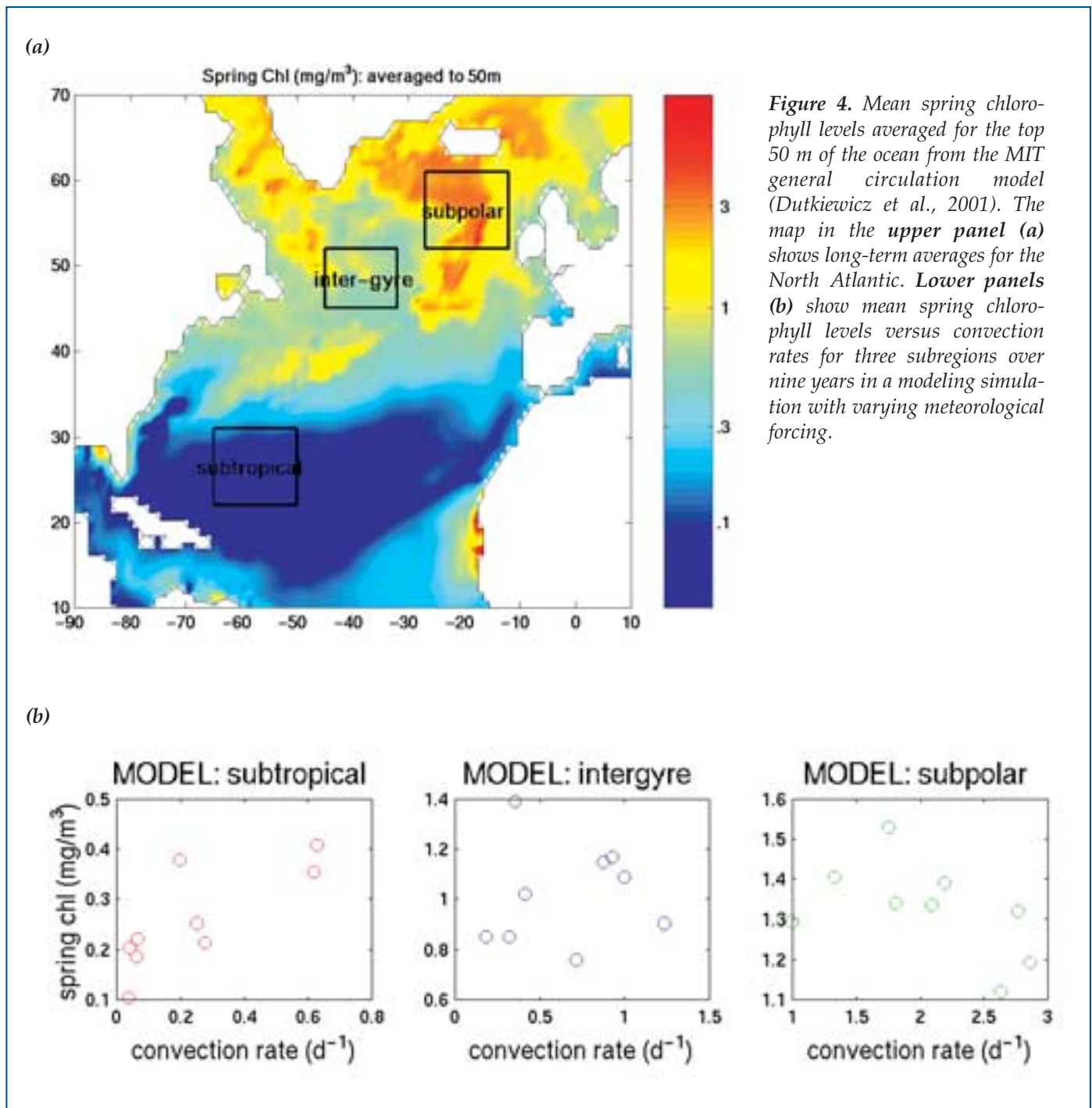
shift in biological regime took place in the mid-1970s in association with the onset of a warm phase of the PDO. Retrospective simulations can help explain the mechanisms that underlie these phenomena and provide clues as to how marine ecosystems could respond to future changes in climate.

Outside of the tropics, variability in boundary-layer mixing that accompanies changes in surface meteorological forcing from storms or winter heat loss affects spring and summer phytoplankton abundances. Simple theoretical models suggest that ecosystem response varies regionally, with increased mixing leading to increased subtropical productivity, which is primarily nutrient limited, and decreased subpolar productivity, which is primarily light limited. The boundaries of the two regimes can be roughly determined by comparing winter mixed-layer depth to the spring critical-layer depth, a measure of phytoplankton light limitation dating back to Harald Sverdrup in 1953.

Using an ecosystem model coupled to the Massachusetts Institute of Technology (MIT) three-dimensional ocean general circulation model, Dutkiewicz et al. (2001) examine this hypothesis in terms of geographical patterns and interannual variability of the spring bloom in the North Atlantic.

Simulations with the coupled model are able to reproduce the gross regional and seasonal distributions of chlorophyll over the basin. The three specific regions selected for investigation are subtropical, subpolar and “inter-gyre,” which includes the convergence of the Labrador and North Atlantic currents (Figure 4). The model simulations use interannually varying meteorological fields to force convection rates and ecosystem responses. Mean annual spring chlorophyll levels respond to variations in convection in a manner broadly consistent with that predicted by the simple conceptual model for the subtropics and the subpolar gyre, although the subpolar response is noticeably weaker. There is no obvious correlation in the model “inter-gyre” box, where other mechanisms such as horizontal nutrient transport may play a more important role (Follows and Dutkiewicz, 2001).

A corresponding diagnostic calculation has been carried out with chlorophyll concentrations derived from three years worth of SeaWiFS data and meteorological analysis from the National Center for Environmental Prediction to see whether the model results described above would be borne out by remote-sensing observations. The subtropical region shows a similarly good correlation between surface chlorophyll and turbulent mixing, estimated from the surface wind



stress and buoyancy fluxes, both between subregions and from year to year. The results of the diagnostic calculation for the subpolar region are less convincing, with essentially no correlation for interannual variability. The changes in chlorophyll predicted by the model that are associated with variations in surface mixing may be counterbalanced by other factors in the subpolar gyre. Relationships among physical forcing, more complex ecosystem interactions and competition among multiple species also must be addressed.

Such modeling studies offer a possible approach to projecting future ecosystem responses under various

climate change scenarios, at least for those regions where the key physical variables can be identified. Coupled ocean-atmosphere model simulations, while differing considerably in their details, generally show warming of the upper ocean and thermocline, weakening of the thermohaline circulation, and increased vertical stratification both in the low latitudes as a result of warming and in the high latitudes as a result of freshening surface waters. One might be so bold as to infer that subtropical production should decrease as nutrients become less available. This inference is contradicted, however, by evidence from the subtropical North

Pacific, where increased stratification associated with a warm phase of the ENSO cycle appears to have stimulated a shift in ecosystem structure toward organisms capable of nitrogen fixation, with resulting increases in primary production and surface chlorophyll levels (see Karl et al., this issue).

Mesoscale Biological-Physical Interactions

The sea is a turbulent medium in which variability on spatial scales of 10 to 200 km and temporal scales of days to weeks is a ubiquitous feature of the physical environment. These mesoscale variations are not typically resolved in ocean circulation models that focus on basin to global scales. New *in situ* measurements and high resolution models are providing evidence that mesoscale variability is a crucial factor governing the structure and functioning of pelagic ecosystems (see McGillicuddy, this issue). Eddies pump nutrients into the euphotic zone, stimulating rates of primary productivity and organic matter export and, potentially, shifts in community composition. The computational demands of basin- to global-scale calculations that resolve eddies accurately are significant; many of the recent advances arise from idealized process-model studies.

Figure 5 presents numerical results obtained with a Princeton Ocean Model simulation for an idealized oligotrophic subtropical frontal zone (Lima et al., 2001). As the front becomes unstable, regions of upwelling and downwelling form along the upstream and downstream sides of meander crests, leading to elevated surface nutrients and primary productivity, particularly on the north side of the front and in cyclonic meanders. Because of strong surface velocities and local patterns of convergence and divergence, regions of biomass accumulation are separated from production, with filaments of high phytoplankton concentration on the southern side of the front and around newly generated cyclonic eddies. The predicted spatial patterns of nutrients, phytoplankton and zooplankton from the model agree well in general with those reported from field observations.

The ecosystem model includes two size classes for both phytoplankton and zooplankton. In undisturbed areas, the smaller phytoplankton are abundant near the surface where nutrient concentrations are low and recycling is high; the larger, diatom-like phytoplankton are most numerous near the subsurface nutrient gradient or nutricline (50–75 m) and contribute disproportionately to new production in the simulation (Figure 5c and 5d). The rise of the nutricline inside cyclonic eddies results in near-surface blooms of both phytoplankton classes, vertical redistribution of the phytoplankton and a shift in the overall community structure towards the larger size class and thus higher export flux. Increased phytoplankton concentrations below 100 m indicate downwelling of near surface waters and an additional export flux associated with the downward advection of living biomass and detritus.

Based largely on such calculations, a semi-quantitative picture is emerging for specific processes and regions. An important next step is to undertake modeling simulations in the submesoscale range (roughly 1 km in space and a few hours in time), where vertical motions can be even stronger. Another is to expand simulations to the basin scale, where interactions with large-scale circulation and biogeography become important. It is also important to develop concerted remote sensing and field programs with data assimilation components to test and evaluate the results.

Data Assimilation

Marine ecosystem models typically include large numbers of poorly known oceanic parameters that are difficult or even impossible to measure with current instrumentation but are essential for numerical models. For example, while primary productivity measurements are common, plankton growth rates are estimated more infrequently, and mortality rates hardly ever. Improvement in consistency between data from field observations and modeling simulations can often be found by using different parameters or model structures. One possibility is to employ data assimilation techniques, which have been successful in fields such as meteorology and physical oceanography. Data assimilation is capable of providing solutions that are consistent with both observations and model equations, given estimated uncertainties. Under certain conditions these techniques provide a means for finding the best-fit or optimized set of parameters for a given model. They therefore may be a crucial part of the development and evaluation of ecosystem models.

Friedrichs (2001) describes a modeling project that focuses on a region of the equatorial Pacific Ocean that is characterized by physical variability on a wide range of time scales. ENSO cycles contribute to interannual variability, tropical instability waves (TIW) produce oscillations on monthly time scales, and equatorially trapped internal gravity waves affect the region on daily and weekly time scales. In order to capture the full range of variability in the region, daily observations of wind velocity, temperature and solar radiation from the Tropical Atmosphere Ocean (TAO) mooring array are used in the modeling simulations to force the ecosystem response. The base simulation adequately reproduces much of the variability in primary production, plankton and nutrient concentrations observed in 1992 during the two time-series cruises of the U.S. JGOFS Equatorial Pacific Process Study (EqPac).

Figure 6 shows time-series results from 50 simulations in which six model parameters (phytoplankton and zooplankton mortality, phytoplankton growth, zooplankton grazing, recycling, and the half-saturation coefficient for iron uptake) are randomly selected to be within a range of ± 30 –50% of their base values. The results clearly demonstrate that even modest changes in these parameters can lead to large differences in simulated fields. The solid line in each panel of Figure 6 is

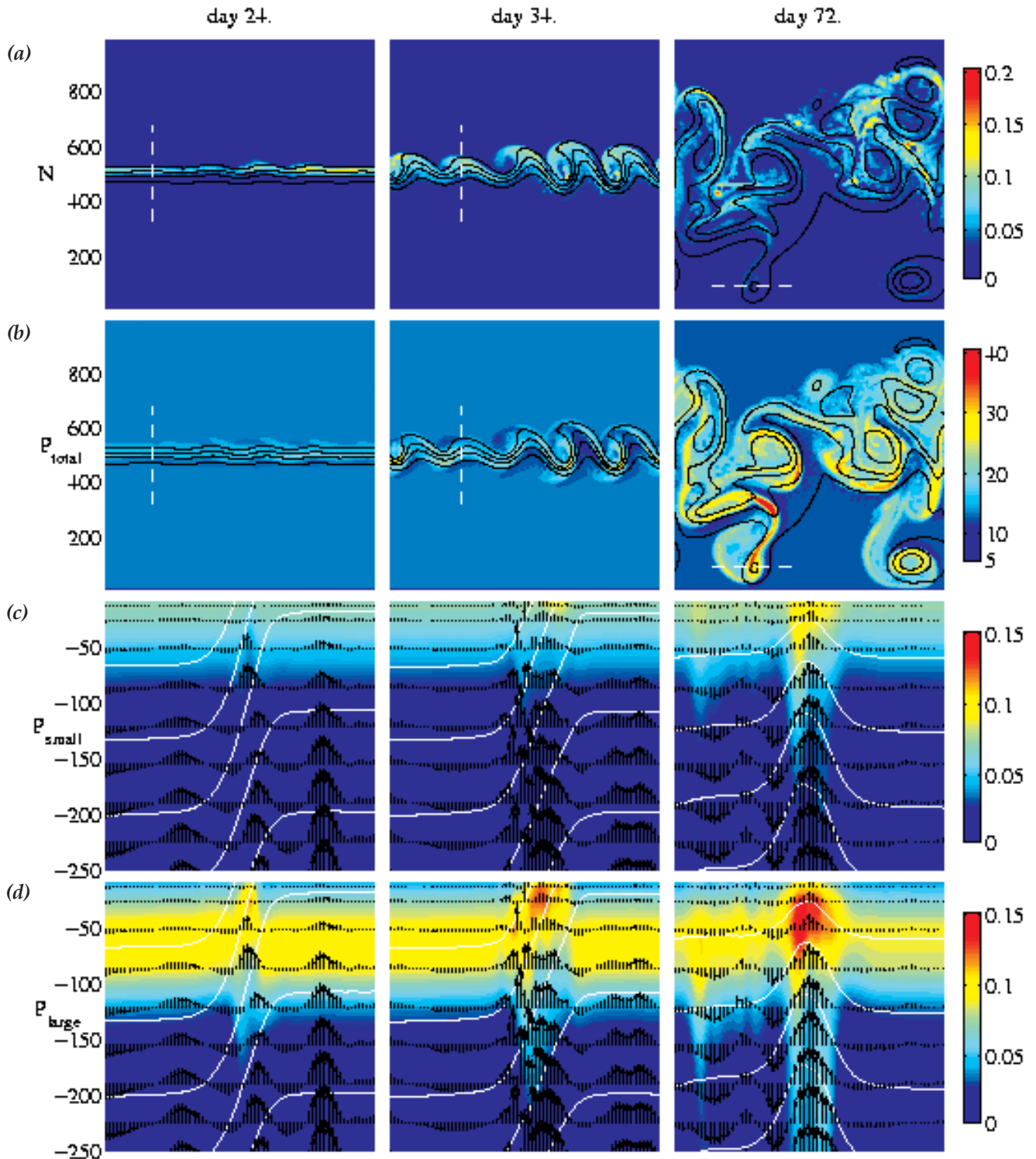


Figure 5. Results from a coupled biological-physical model of an unstable, subtropical front (Lima et al., 2001). (a) Horizontal distribution of dissolved nitrogen at 50 m (mmol N m^{-3}). (b) Horizontal distribution of vertically integrated total phytoplankton inventories (mmol N m^{-2}). The dashed white lines mark the vertical sections (depth on the y-axis) shown in the bottom two rows for (c) small and (d) large phytoplankton biomass (mmol N m^{-3}). Horizontal distances are in km, and vertical distances are in m. Solid lines represent sea-surface elevation in (a) and (b) and isopycnal surfaces in (c) and (d). Black arrows denote direction and magnitude of vertical velocities (m d^{-1}).

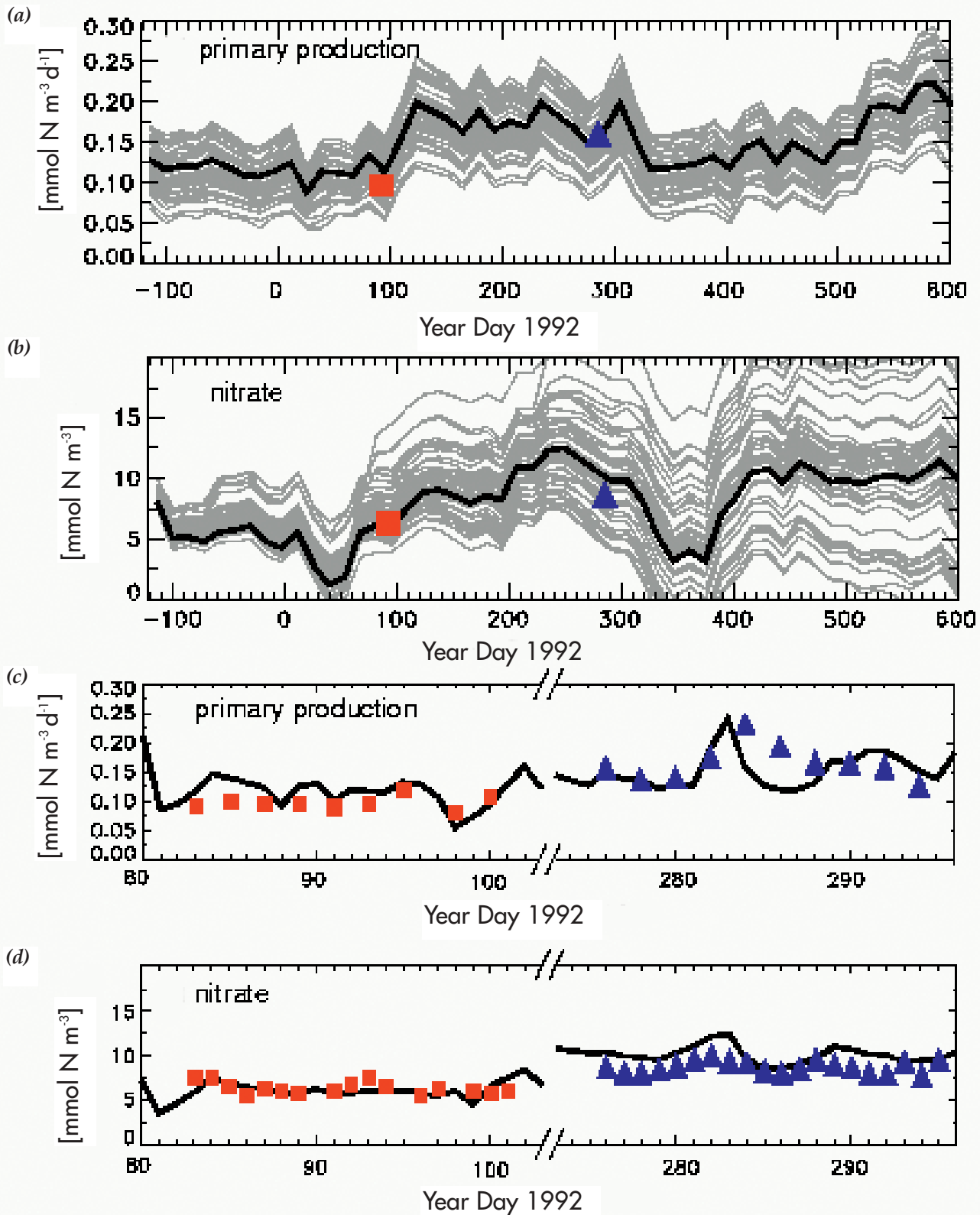


Figure 6. Simulated evolution of primary production and surface nitrate in the equatorial Pacific from a coupled biological-physical mixed-layer model (Friedrichs and Hofmann, 2001). Panels (a) and (b) show an ensemble of 50 cases (each case shown separately as a grey line) with the model parameter values drawn randomly about the base estimates and the parameter set optimized for the first U.S. JGOFS EqPac time-series cruise data (solid line) using an adjoint data assimilation technique (Friedrichs, 2001). The solid symbols represent observations from the two EqPac time-series cruises. Panels (c) and (d) show more detailed model-data comparisons with the EqPac data.

estimated with the optimal parameter set found from the first EqPac time-series cruise using data assimilation techniques.

Using this approach, one can determine objectively whether or not a given model structure is consistent with specific sets of observations. In fact no valid parameter sets are found when either the data from the second EqPac time-series cruise or SeaWiFS ocean color data are assimilated. The model failures are linked to changes in species composition associated with the passage of a TIW in the first case and, in the second, to a brief period of macro-nutrient limitation during the El Niño conditions that prevailed in the region during 1997 and 1998. While not overcoming inappropriate model dynamics, data assimilation can highlight missing processes and guide the reformulation of models.

Many questions remain before data assimilation becomes routine for biological-physical models. For example, the best method for assimilating both physical and biological data simultaneously is still under investigation. Furthermore we currently have far more physical than biological data, though this constraint should lessen in the future as more autonomous *in situ* and remote-sensing methods are developed.

Export flux and subsurface carbon cycling

We do not have as good numbers for the export of organic carbon from surface ocean waters as we do for phytoplankton production. A decade ago, investigators regarded sinking particles as the dominant pathway for the export of organic carbon from the euphotic zone, but a more complex picture has emerged during the JGOFS era (see Ducklow et al., this issue). Vertical migration of zooplankton, mesoscale subduction of living biomass, and the formation and downwelling of dissolved organic matter also contribute to the export flux. Most of the primary production is remineralized (converted back into inorganic form) in the surface layer; the ratio of export to total production varies between 10% and 50%. Export efficiency appears to be highest in cold, productive regions, decreasing in the oligotrophic subtropical gyres both because of the shift in community structure to a system dominated by picoplankton and microzooplankton and increased temperatures, which increase respiration losses at each trophic level (Laws et al., 2000).

Figure 7 presents a map of mean annual organic carbon export in the global ocean from a modeling simulation by Moore et al. (2001). The upper panel shows the sinking particulate component of the export flux, and the lower shows the total flux of biogenic carbon, which also includes export associated with the mixing of semi-labile dissolved organic matter (DOM) to depth (see Hansell and Carlson, this issue). The DOM export in the model accounts for roughly a third of all carbon export from the surface mixed layer. In portions of the mid-ocean gyres and in some high-latitude regions, it exceeds the export via sinking particles.

Almost all of the semi-labile DOM in the model is remineralized in the shallow thermocline.

The partitioning of the export flux of carbon between DOM and sinking particles and the depth and time scales associated with remineralization of sinking material are important determinants of the vertical redistribution of nutrients and carbon in the ocean. Unfortunately, we do not know much about the ecosystem dynamics of the mesopelagic zone, from the base of the euphotic zone to about 1000 m, and most models use empirical particle flux relationships derived from subsurface sediment traps (see Berelson, this issue). Some improvements are underway, such as efforts to link fluxes of organic matter and ballast materials, but more field data at the mechanistic level are clearly needed.

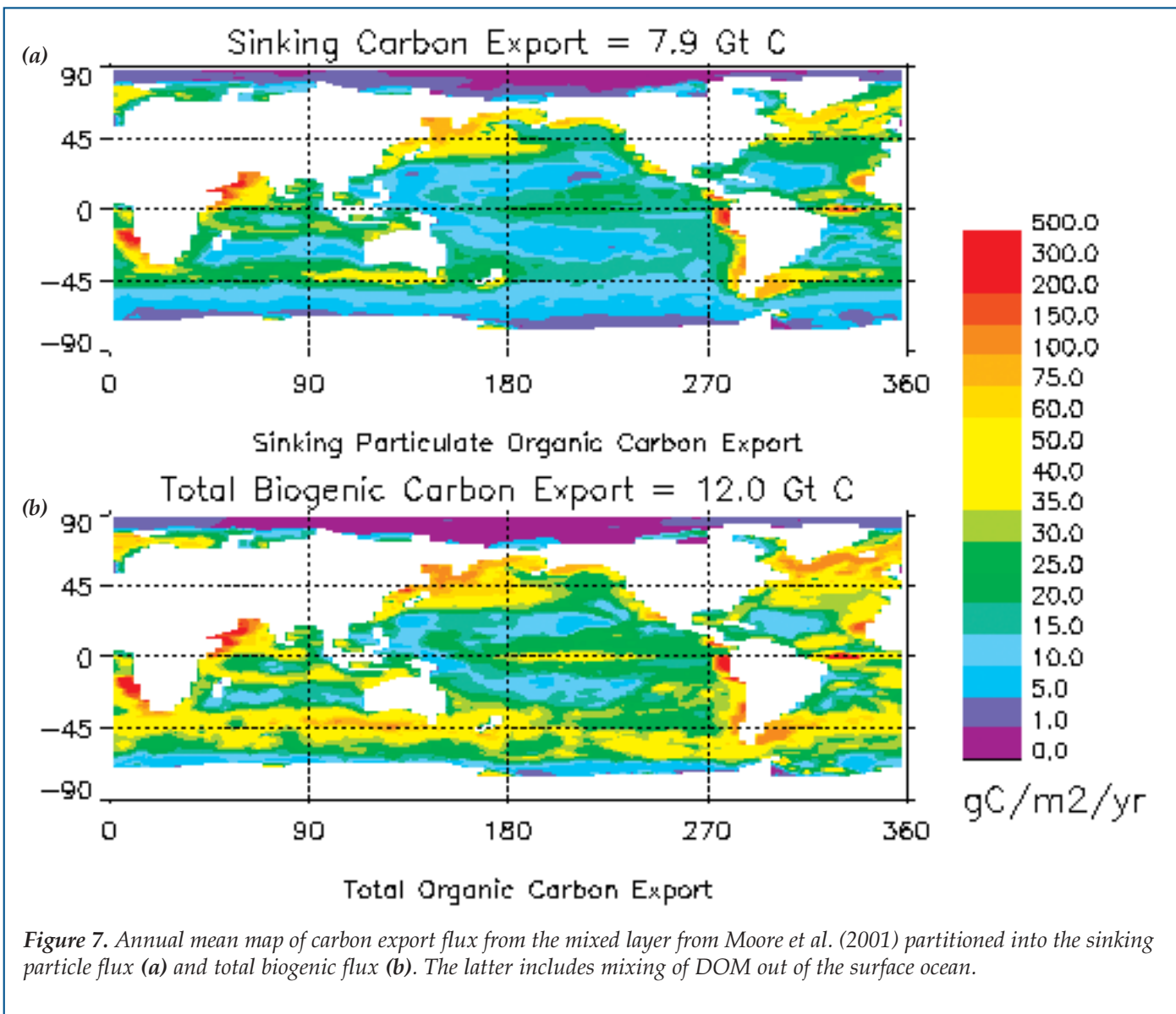
Global three-dimensional ocean carbon-cycle models are now widely used to estimate basin- and global-scale patterns and rates of biogeochemical processes such as export production, remineralization, and the uptake of anthropogenic CO₂ (Maier-Reimer, 1993; see also <http://www.ipsl.jussieu.fr/OCMIP/>). Large-scale data sets of inorganic nutrients, oxygen, dissolved inorganic carbon and hydrography are essential for evaluating such simulations. The JGOFS global survey of CO₂ in the ocean, carried out in cooperation with the World Ocean Circulation Experiment, provides an excellent, high-quality example of what is needed.

Figure 8 shows the distribution of pre-industrial dissolved inorganic carbon (DIC) along north-south transects in the Pacific and Atlantic, determined from both National Center for Atmospheric Research (NCAR) global ocean modeling simulations and observational estimates (Doney et al., 2001). Despite the simplicity of its biogeochemical module, the NCAR model captures many of the large-scale ocean biogeochemical patterns found in the observations. The “biological pump” provides about two-thirds of the increase in DIC from surface to deep waters, and the physical processes of the “solubility pump” provide about one-third. Horizontal gradients in the deep water are determined by a mixture of the thermohaline circulation and the subsurface particle remineralization rate; several of the significant model-data differences can be ascribed, in part, to problems with physical processes in the model.

Future Climate Change

Investigators have incorporated simple marine biogeochemical models in ocean-atmosphere climate simulations to project the effect of the anthropogenic increase in greenhouse gases on the air-sea exchange of CO₂ over the next century (Matear and Hirst, 1999). These simulations suggest that oceanic CO₂ uptake will be reduced as a result of greenhouse warming (Figure 9), providing a positive feedback response to rising atmospheric CO₂.

Three potentially competing mechanisms are involved. First, elevated sea-surface temperatures



decrease the solubility of CO₂ in seawater and thus the capacity to sequester anthropogenic carbon. Second, increased density stratification in the upper ocean and lower meridional overturning rates reduce the transport of anthropogenic CO₂ into the ocean interior. Third, slower ocean circulation rates decrease the supply of nutrient- and carbon-rich water to the upper ocean.

In the Matear and Hirst (1999) simulations, the third factor led to an increase in the overall efficiency of the biological pump, enabling the ocean to absorb more CO₂. The likely responses of biological processes in the ocean to changing climate conditions are not well understood at present, however, and their treatment in current ocean carbon models is quite simplistic. The ongoing JGOFS synthesis will provide the information needed to formulate more realistic models of the present and future behavior of the ocean biological pump and to improve projections of oceanic CO₂ uptake.

In order to develop greater confidence in future projections, it is essential to identify specific climate-change signals from the models that are observable in the real ocean. Model simulations suggest that dissolved oxygen concentrations may be a sensitive early indicator of changes in ocean circulation and warming. Climate change is expected to stimulate a net outgassing of oxygen from the ocean and a corresponding decrease in dissolved oxygen in the ocean. Multi-decadal changes in dissolved oxygen in the Southern Ocean modeled by Matear and colleagues (Matear et al., 2000) agree remarkably well with changes in measured oxygen levels between 1968 and 1996 (Figure 10). Further investigations of dissolved oxygen changes in the ocean are needed to determine their spatial extent and to provide valuable observations to assess climate model projections.

Future Directions

With a few exceptions, the treatment of biological

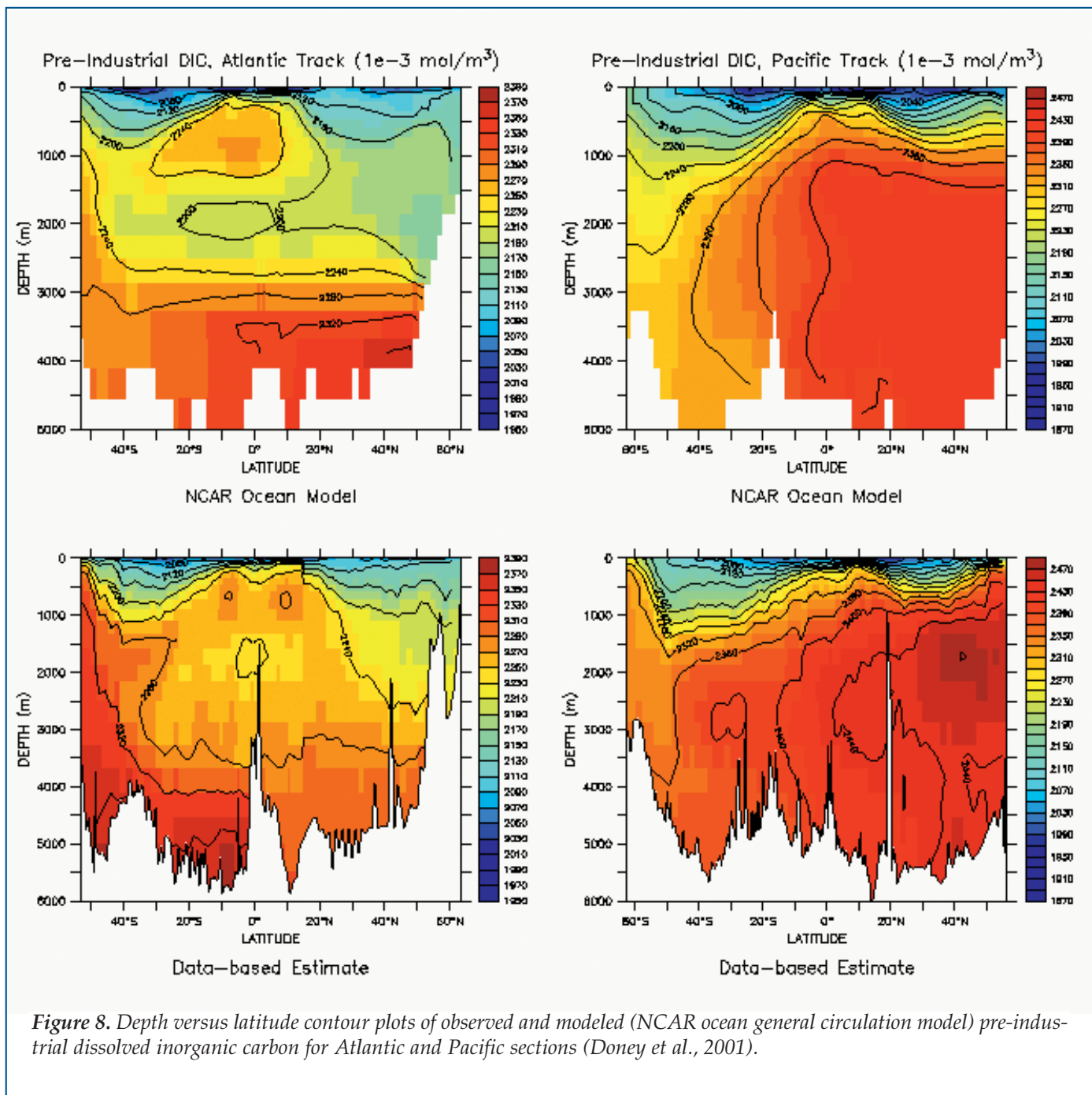


Figure 8. Depth versus latitude contour plots of observed and modeled (NCAR ocean general circulation model) pre-industrial dissolved inorganic carbon for Atlantic and Pacific sections (Doney et al., 2001).

processes and ecosystem structure in global biogeochemical models to date has been rather rudimentary. The next step, already underway, is to combine reasonably sophisticated components for both ecosystem and biogeochemical dynamics in a global modeling framework. The exact form of such models is yet to be determined. But based on the new insights emerging from JGOFS and other recent field studies, one can envision a minimal version covering the basic processes that govern surface production, export flux, subsurface remineralization and the coupling and decoupling of carbon from macronutrients. Important topics that need to be addressed include multi-nutrient

limitation, size structure and trophic dynamics, plankton geochemical functional groups, microbial loop and DOM cycling, subsurface particle transport and remineralization.

Clearly some areas of the field are advancing more rapidly than others, driven primarily by the availability of field observations, particularly by data that elucidate the fundamental mechanisms of the system. Considerable effort has been devoted to understanding processes governing phytoplankton primary production at a number of levels, including molecular biophysics, cellular physiology, community dynamics, seawater bio-optics and remote sensing. Other areas,

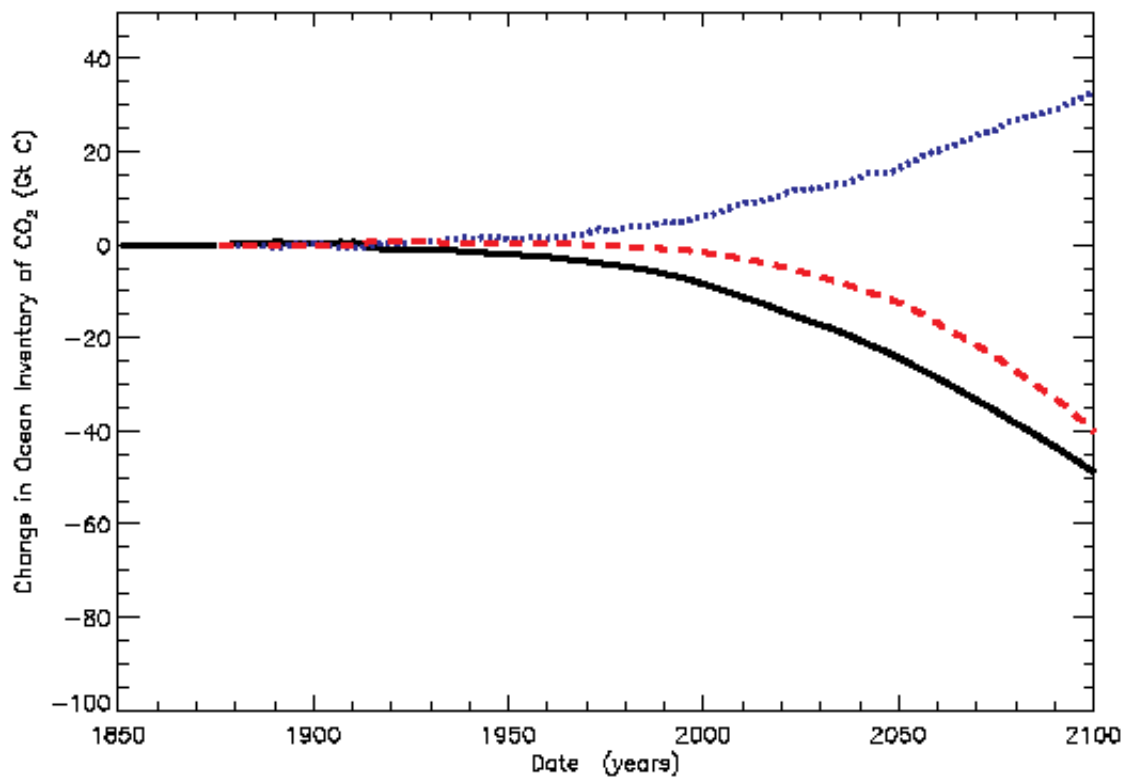
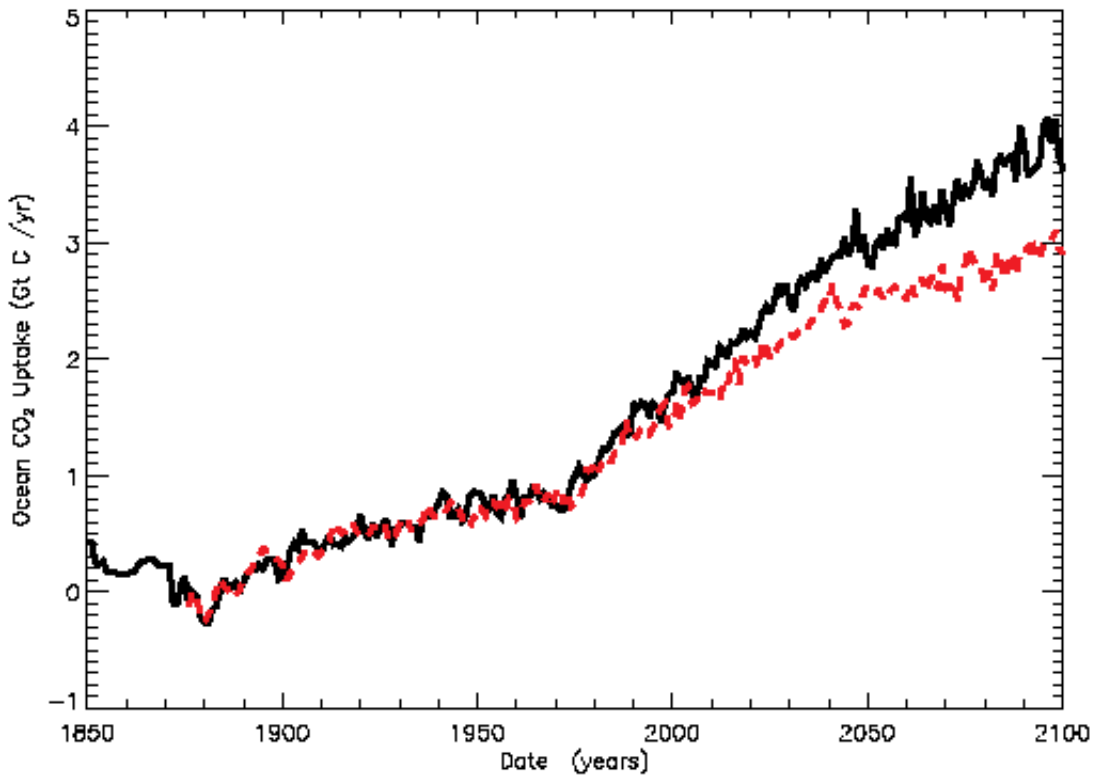


Figure 9. The effect of greenhouse warming on projected oceanic CO₂ uptake over the next century from the CSIRO climate model (Matear and Hirst, 1999). Upper panel shows global oceanic CO₂ uptake for a control case (solid black line) and for a climate-change scenario (red dashed line). Lower panel shows mechanisms driving the cumulative oceanic CO₂ response: elevated sea-surface temperature (black solid line), reduced transport of anthropogenic CO₂ into the interior (red dashed line), and increased efficiency of the ocean biological pump (blue dotted line). The sum of these three curves equals the total change in oceanic CO₂ uptake under the climate-change scenario.

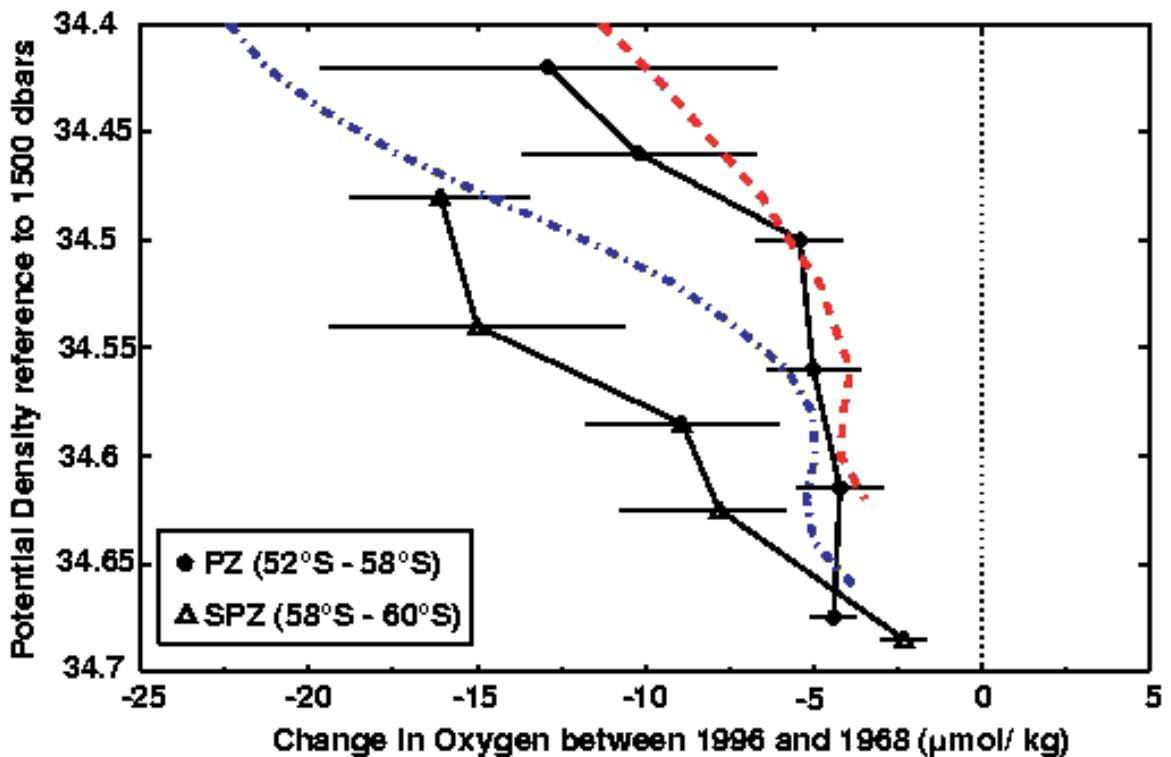
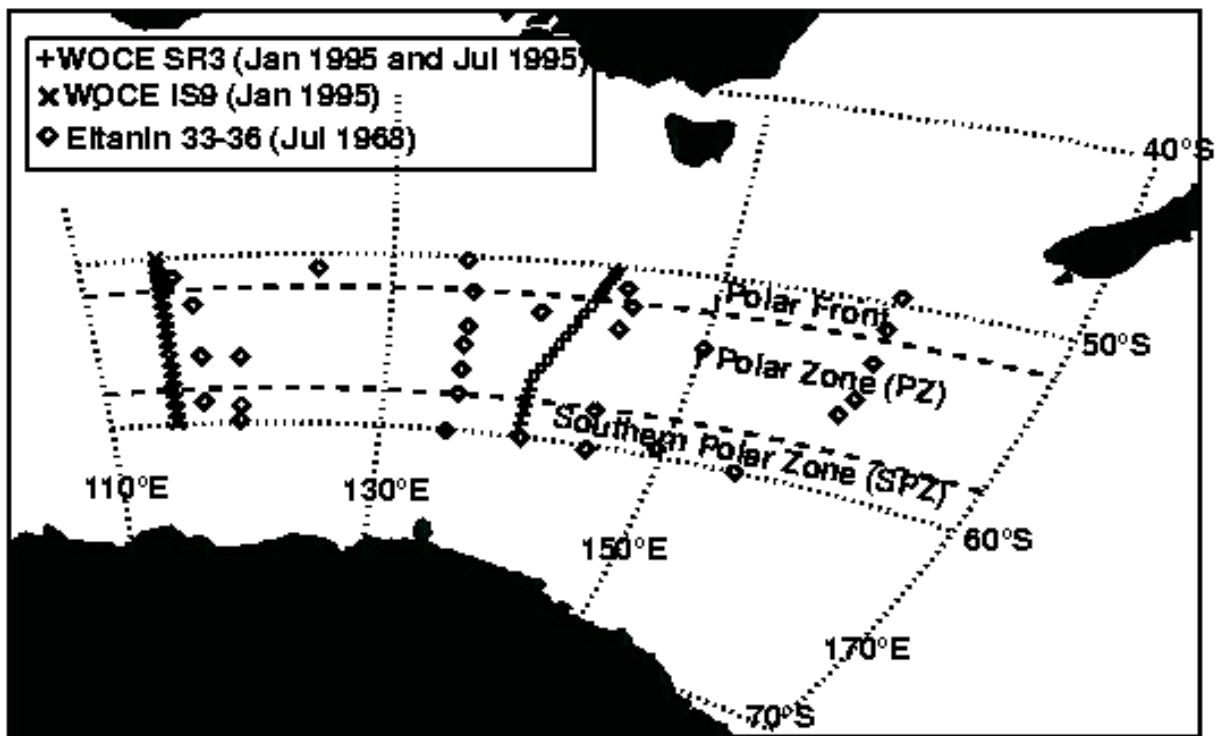


Figure 10. Observed changes in dissolved oxygen between 1996 and 1968 (solid black lines) on potential density surfaces referenced to 1500 dbars in the Polar Zone (PZ), 52°S–58°S, and Southern Polar Zone (SPZ), 58–60°S. The horizontal lines denote the two standard deviation errors. Also shown are the simulated changes in the zonal averaged oxygen (110°E to 170°E) associated with climate change for the 1990–99 period at 59°S (blue dashed line) and 55°S (red dashed line). In the model simulation, the interannual variability in dissolved oxygen was greatest at 33.4, where it was ± 4 mmol kg^{-1} for 55°S and ± 3 mmol kg^{-1} for 59°S. At densities greater than 33.5, the modeled interannual variability in dissolved oxygen was less than ± 1 mmol kg^{-1} . Upper panel shows locations of stations sampled on cruises in 1968 and 1995.

Taking Care Of The Legacy: Data Management In U.S. JGOFS

David M. Glover

*Woods Hole Oceanographic Institution
Woods Hole, Massachusetts USA*

Data management, essential to the success of a large, multidisciplinary scientific enterprise, has been a basic component of the U.S. Joint Global Ocean Flux Study (JGOFS) from the beginning. The planners of the program envisioned two main tasks associated with managing U.S. JGOFS data: the assemblage of a complete, high-quality archive of biogeochemical observations and modeling results that would be readily accessible to the scientific community, and the creation of a flexible and expandable system for providing access to data.

In 1988, with support from the National Science Foundation (NSF), Glenn Flierl, James Bishop, David Glover and Satish Paranjpe began work on an approach to the retrieval, merging and analysis of data stored in a variety of formats and located in different places. This team developed an object-oriented, distributed database system with an interface that permits users to get access to data and "metadata" (information about a data set, such as methodology used) via the world wide web, regardless of the web browser used.

Data management began with the completion of the first JGOFS process study in 1989. George Heimerdinger, northeast liaison officer for the National Oceanic and Atmospheric Administration's National Oceanographic Data Center (NODC), undertook the task of collecting, organizing and distributing U.S. JGOFS data and carrying out quality-control procedures from his office at Woods Hole Oceanographic Institution (WHOI) during the first few years.

An independent U.S. JGOFS Data Management Office (DMO) was set up at WHOI in 1994, and information systems expert Christine Hammond was hired as a full-time data manager. She worked with Flierl and Glover to improve and maintain the database system in addition to overseeing the ongoing work of collecting and organizing the U.S. JGOFS data sets, most of which are stored and served by the DMO. Among her many accomplishments was the creation of a U.S. JGOFS home page, through which users could get access to the steadily growing volume of data from the field programs.

In 2000, Hammond moved to a new position at WHOI, and Glover took over the scientific leadership of the DMO. Cynthia Chandler now acts as system manager and handles the day-to-day operation of the web-based system. David Schneider and Heimerdinger, who returned from retirement to work for the DMO, are responsible for data verification and quality assurance.

Several factors in the development of the DMO have been critical to its mission. The U.S. JGOFS DMO would not have enjoyed the success it has without the unflinching support of the NSF, the U.S. JGOFS Scientific Steering Committee and the investigators. All parties have benefited from the decision of the DMO not to require a fixed format for data submission. Scientists are encouraged to get their data into the DMO, and staff members work with them to get the data into the system.

Equally important was the decision, made at the beginning of the program, to encourage data sharing among investigators as part of U.S. JGOFS data policy. Data were to be made available to all U.S. JGOFS investigators after six months and to the entire scientific community after two years, as required by NSF. The open data policy has enhanced the value of U.S. JGOFS results by encouraging exchanges and intercomparisons.

When the initial development team was working out how users would actually interact with the data system, the powerful idea of using the world wide web as the primary interface was adopted. Any computer user with a web browser of some sort is able to get access to the database without platform-specific code.

Another important early choice was to have a data manager look at the data as they came in. Detection of anomalous data generates a quick call to the originator, and problems are generally solved before anyone makes use of contaminated data.

Finally, the decision to supply data documentation directly linked, as only hypertext can be, with the data themselves has been of great value. Users get not only the data, but also the supporting documentation files when they download data. The information in these documentation files describes methods used, calculations performed on the original data and other forms of metadata information that improve the usability of the data.

One of the new tasks undertaken by the DMO is the support of results from the U.S. JGOFS Synthesis and Modeling Project (SMP). Because of the gridded nature and larger volume of output from modeling studies, the DMO is working with the Live Access Server (LAS) group at the University of Washington and NOAA Pacific Marine Environmental Laboratory (PMEL) in Seattle to provide a visualization and access interface to these results.

Meanwhile, DMO staff members are working on the development of merged data products that combine data objects with com-


mon variables and collection methods to form larger data sets. Currently the DMO is producing both conductivity-temperature-depth (CTD) and bottle merged data objects for the various U.S. JGOFS process studies. These begin at the cruise level and are in due course merged into basin-level objects.

The data scientists leave behind represent their legacy to future generations. Currently all of the originally submitted U.S. JGOFS data are available via the world wide web, as well as some of the newly merged data products that the DMO has been building. With the web interface, users can search, view and download specific "slices" of the data or all of a given data set if they desire.

Some day in the not-so-distant future, U.S. JGOFS and the DMO will come to an end. To ensure the continued availability of U.S. JGOFS data, the DMO plans to produce and distribute a final data product, such as a set of CD-ROMs, that will include all of the field data, the merged data products and a selection of SMP models and results. At the same time, data will be submitted to the NODC, the long-term archive mandated by Congress for oceanographic data. The experts who developed and maintained the U.S. JGOFS data system may go on to support future ocean carbon-cycle research, and the data may be available on the web through these programs. With these various options, U.S. JGOFS data should continue to be available for many years to come.

such as phytoplankton loss rates or the dynamics of mesopelagic ecosystems, have received considerably less attention, not because they are considered less important from a carbon-cycle perspective, but because techniques and measurement systems in these areas are less advanced.

The modeling and synthesis component of U.S. JGOFS came at the end of the program, and with a few notable exceptions, numerical models did not strongly influence the planning for the field studies, either in terms of what was measured or of how the experiments were designed. This lack reflects, in part, the state of modeling a decade ago. But much has changed, and future field programs will require closer, more synergistic relationships between models and observations.

Finally, the recent progress in ocean biogeochemical modeling would not be possible without the treasure trove of JGOFS field data and satellite remote-sensing products now easily accessible in electronic form. U.S. JGOFS has achieved timely, public release of data, including models and modeling simulations, and has provided explicit support for data management, which is neither glamorous nor cheap (see Glover sidebar, this issue). These are major cultural and programmatic advances for our field; they provide lessons that should not be neglected in the future. This is U.S. JGOFS Contribution Number #682. 

References

- Doney, S.C., 1999: Major challenges confronting marine biogeochemical modeling. *Global Biogeochem. Cycles*, 13, 705–714.
- Doney, S.C., K. Lindsay and J.K. Moore, 2001: Global ocean carbon cycle modeling. In: *Ocean Biochemistry: #9 JGOFS synthesis*. M. Fasham, ed., in press.
- Dutkiewicz, S., M. Follows, J. Marshall and W.W. Gregg, 2001: Interannual variability of phytoplankton abundances in the North Atlantic. *Deep-Sea Res. I*, 48, 2323–2344.
- Fasham, M.J.R., H.W. Ducklow and S.M. McKelvie, 1990: A nitrogen-based model of plankton dynamics in the oceanic mixed layer. *J. Mar. Res.*, 48, 591–639.
- Follows, M. and S. Dutkiewicz, 2001: Meteorological modulation of the North Atlantic spring bloom. *Deep-Sea Res. II*, in press.
- Friedrichs, M.A.M., 2001: The assimilation of JGOFS EqPac and SeaWiFS data into a marine ecosystem model of the central Equatorial Pacific Ocean. *Deep-Sea Res. II*, in press.
- Friedrichs, M.A.M. and E.E. Hofmann, 2001: Physical control of biological processes in the central equatorial Pacific Ocean. *Deep-Sea Res. I*, 48, 1023–1069.
- Laws, E.A., P.G. Falkowski, W.O. Smith, Jr., H.W. Ducklow, and J.J. McCarthy, 2000: Temperature effects on export production in the open ocean. *Global Biogeochem. Cycles*, 14, 1231–1246.
- Lima, I.D., D.B. Olson and S.C. Doney, 2001: Biological response to frontal dynamics and mesoscale variability in oligotrophic environments: a numerical modeling study. *J. Geophys. Res.*, submitted.
- Maier-Reimer, E., 1993: Geochemical cycles in an ocean general circulation model: Pre-industrial tracer distributions. *Global Biogeochem. Cycles*, 7, 645–677.
- Matear, R.J. and A.C. Hirst, 1999: Climate change feedback on the future oceanic CO₂ uptake. *Tellus*, 51B, 722–733.
- Matear, R.J., A.C. Hirst and B.I. McNeil, 2000: Changes in dissolved oxygen in the Southern Ocean with climate change. *Geochem. Geophys. Geosystems*, 1, November 21, <http://g-cubed.org/>.
- Moore, J.K., S.C. Doney, J.A. Kleypas, D.M. Glover and I.Y. Fung, 2001: Iron cycling and nutrient limitation patterns in surface waters of the world ocean. *Deep-Sea Res. II*, accepted.

The Role of New Technology in Advancing Ocean Biogeochemical Research

Tommy D. Dickey
University of California • Santa Barbara, California USA

Introduction

The rapid increase in atmospheric carbon dioxide (CO_2) levels has stimulated a growing interest in understanding biogeochemical processes in the ocean and their interactions with the atmosphere. Interestingly, surface CO_2 is also reported to be rising at the Joint Global Ocean Flux Study (JGOFS) ocean time series sites off Hawaii and Bermuda. Potential effects of rising CO_2 levels include increases in global atmospheric and oceanic temperatures, melting of ice caps, sea-level rise and shifts in regional weather patterns, that lead to droughts and floods. One important question concerns our ability to discern natural versus anthropogenic contributions to this rise. Another question concerns the role the ocean plays in the cycling and variability of CO_2 . These and other unanswered questions stimulated the development and execution of JGOFS, a multidisciplinary and international program carried out between 1987 and 2001 by more than 20 nations. JGOFS was designed to study oceanic biogeochemical cycles and their interaction with a changing climate.

On millennial time scales, the ocean dictates the atmospheric concentration of CO_2 . There is an inverse gradient in Dissolved Inorganic Carbon (DIC) in the ocean, such that higher concentrations of DIC are found at greater depths. In contrast, the upper portion of the water column is in overall equilibrium with the atmosphere to first order. This gradient is maintained by two carbon “pumps.” The “solubility pump” depends on the fact that cold water holds more CO_2 than warm water; for example, the solubility of cold, deep water is about twice as great as that of near-surface equatorial water. As a consequence, the net effect of sinking surface waters through thermohaline circulation is to enrich deeper waters in carbon.

The second carbon pump is known as the “biological pump”, and is the primary focus of this review of new technologies and observations (see Ducklow et al., this issue). The biological pump’s process begins with phytoplankton living in the upper or euphotic layer of

the ocean. Phytoplankton take up CO_2 and nutrients to form organic matter. Although much of this organic matter is metabolized and recycled in the surface waters, a significant portion (roughly 10% to 20% but varying greatly over space and time) sinks into the deep ocean before it is remineralized into an inorganic form via the metabolism of microorganisms. Currents and upwelling return CO_2 to the surface of the ocean, but the overall effect of the biological pump is to transport carbon into the deep ocean.

The solubility and biological pumps have significant effects on atmospheric CO_2 levels. The biological pump includes pathways of carbon export to the deeper layers through Dissolved Organic Carbon (DOC) molecules (see Hansell and Carlson, this issue) and Particulate Organic Carbon (POC) matter (see Berelson, this issue). The determination of primary production in the upper ocean is a vital step in quantifying the formation of POC, which is then available for transport via the biological pump. The following paragraphs introduce some of the key concepts regarding primary production in relation to the biological pump, with a focus on its quantification using autonomous measurements from moorings and other platforms.

The biological pump is of interest to researchers studying bio-optics and upper-ocean physics as well as biogeochemistry. Primary productivity and phytoplankton biomass depend on photosynthetic processes, which implicitly involve the availability of light (measured as Photosynthetically Available Radiation or [PAR]) and nutrients such as nitrate, silicate, phosphate, and iron. The spectral quality and intensity of light varies with depth and is important for specific phytoplankton species with special pigmentation or photoadaptive characteristics. Light exposure for individual organisms is affected by variation in physical conditions including mixed layer depth, turbulence and currents, as well as the incident solar radiation, all of which vary in time and space. An important feedback concerns the modulation of the spectral light field

at various depths as phytoplankton concentrations and communities wax and wane. Fundamental measurements and models have been used to estimate primary production (e.g., Behrenfeld and Falkowski, 1997). Such models often use measurements of chlorophyll *a* concentrations and PAR.

Primary production has been estimated for a variety of geographical regions using remote sensing via instruments mounted on satellites. Primary production, $P(z)$, as a function of depth, z , has also been estimated with relatively simple models using chlorophyll *a*, $\text{Chl}(z)$, and $\text{PAR}(z)$ data. In some cases, best estimates or measurements of the chlorophyll *a* specific light absorption coefficient for phytoplankton, $a^*(z)$, and the quantum yield for carbon fixation, $\Phi(z)$, have been utilized as in the following empirical formulation:

$$P(z) = a^*(z) \Phi(z) \text{Chl}(z) \text{PAR}(z) \quad (1)$$

One of the deficiencies of this method is that neither a^* nor Φ is constant in space or time because of changes in community structure and varying light and nutrient stresses.

This review focuses on some of the technological and observational advances achieved primarily during the JGOFS era that are improving our understanding of biogeochemical processes, pools and fluxes in the ocean. It is not comprehensive, but rather highlights a few examples (more references are available at <http://www.opl.ucsb.edu/>). The focus is on *in situ* observations, with a few references to complementary remote sensing data (see Yoder et al., this issue).

The Sampling Problem

Oceanographers must obtain their data from an uncontrolled and often harsh environment. The limits of detection, precision and accuracy of ocean measurements should not be overlooked. It is critically important to obtain large volumes of data because of the vastness and complexity of the ocean and the importance of a large range of time and space scales (Figure 1a) for answering many basic questions. The oceans are naturally dynamic, with large-amplitude periodic and episodic variability that confounds attempts to quantify long-term trends and changes. Recent studies suggest that a few powerful episodic events can often be of far greater importance than small-amplitude, slower variations. JGOFS has characterized, quantified and improved our understanding of ocean processes that affect variability in carbon inventories and carbon fluxes. But insufficient data and undersampling still limit our ability to make further advances in understanding and modeling the biogeochemistry of the ocean. We must find ways to increase massively the variety and quantity of biogeochemical data.

Studies of ocean biogeochemistry necessarily rely heavily on interdisciplinary data sets because of the interdependence of physical, chemical, biological and geological processes. Ideally, the relevant data should

be collected simultaneously and span broad time and space scales to observe processes of interest (Figure 1a). For global climate problems, this means sampling variability that extends over 10 orders of magnitude in space, and even longer in time. Present capabilities for obtaining the necessary atmospheric and physical oceanographic data are relatively well advanced in contrast to those for biogeochemical data. This is not surprising, considering the greater complexity and non-conservative nature of the chemistry and biology of the ocean. Nonetheless, remarkable advances in biogeochemical data collection are being made. New platforms are making it possible to measure certain biogeochemical, bio-optical, chemical and geological parameters on the same time and space scales as physical ones (Figure 1b). Figure 2 shows some examples of data collection platforms, such as moorings, towed vehicles (e.g. SeaSoar), drifters, floats, gliders, and Autonomous Underwater Vehicles (AUVs) now in operation.

Emerging Observational Methods and Results

One of the central goals of JGOFS has been to measure and understand time-varying fluxes of carbon and associated biogenic elements. Regional studies are necessary to sample processes and to develop models for strategic oceanic biomes. All regions experience certain small- and mesoscale processes, especially over short time periods. But the effects of natural phenomena such as monsoons, equatorial longwaves, spring blooms, hurricanes and typhoons, deep convection, El Niño-Southern Oscillation, climatic oscillations and the like vary greatly from one region to another. This section presents examples of applications of new technologies in various regions studied by JGOFS, and provides some highlight results.

JGOFS In The Arabian Sea

The U.S. JGOFS process studies were conducted in the Arabian Sea between 1994 and 1996 (*Deep-Sea Research II*, vols. 45[10–11], 46[3–4, 8–9], 47[7–8]). Before JGOFS, we did not know whether the Arabian Sea absorbs or releases CO_2 into the atmosphere on balance, and upper-ocean physical and biogeochemical responses to monsoonal forcing were undocumented. Arabian Sea field studies employed 1) underway shipboard sampling with Acoustic Doppler Current Profilers (ADCPs) and other instruments, 2) towed instrument systems such as SeaSoar, 3) multiple moorings, and 4) satellite observations for sea-surface temperature and altimetry. Data from satellite-mounted altimeters (Figure 3a), moorings, and towed instrument systems showed important mesoscale processes.

One of the novel aspects of the U.S. JGOFS Arabian Sea study was the deployment of five moorings with meteorological and physical instruments covering a square roughly 55 km on a side (Dickey et al., 1998a). They were located near the axis of the atmospheric

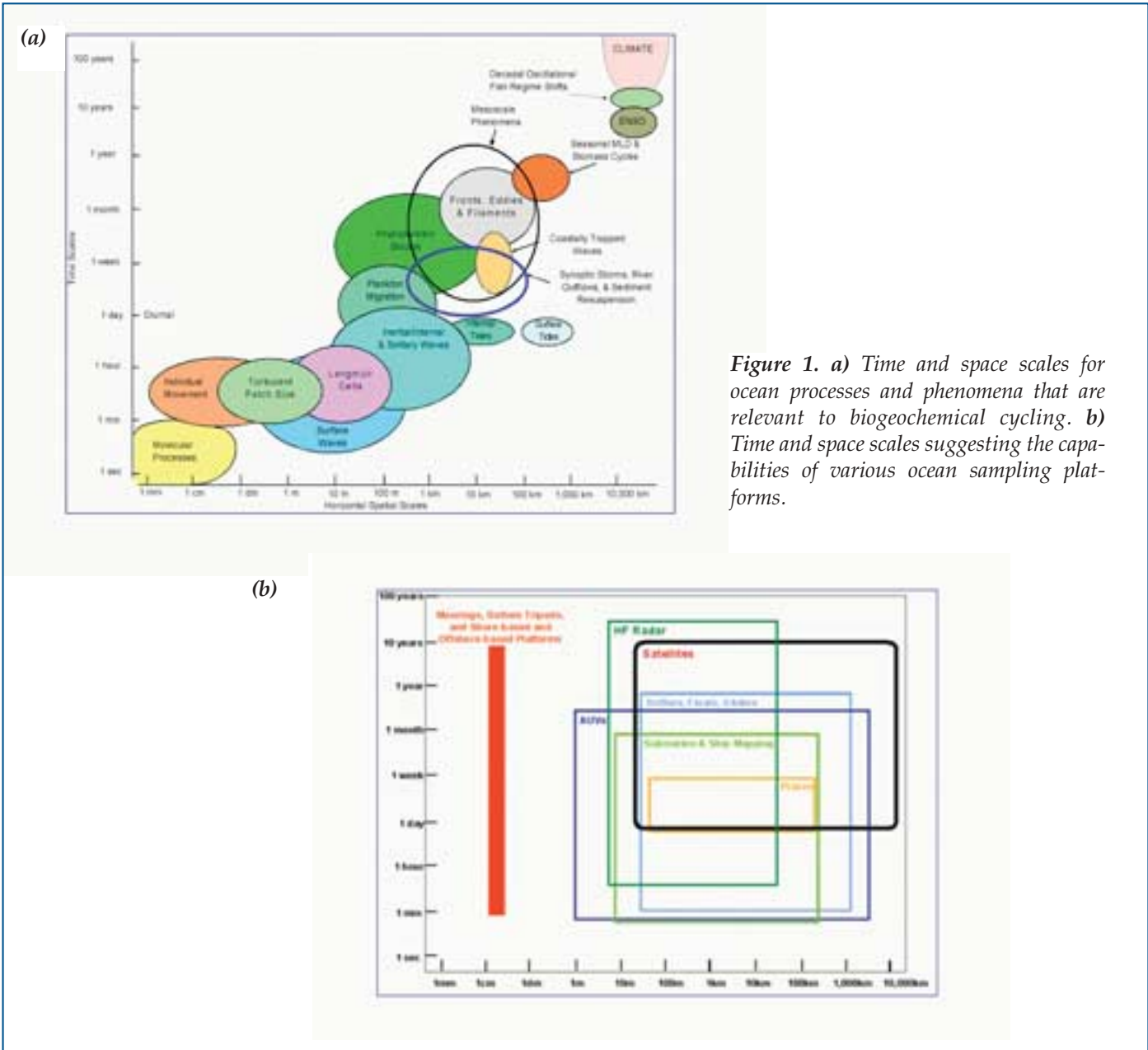


Figure 1. a) Time and space scales for ocean processes and phenomena that are relevant to biogeochemical cycling. b) Time and space scales suggesting the capabilities of various ocean sampling platforms.

Findlater Jet. The central mooring, located at 15°30'N, 61°30'E, carried Multi-Variable Moored Systems (MVMS) at four depths in the upper 80 m of the ocean. Each MVMS (Figure 3b) included a vector-measuring current meter, a thermistor for temperature, a beam transmissometer to measure particle variability as related to primary productivity and particulate organic carbon, a strobe fluorometer to infer chlorophyll *a* concentrations, a scalar irradiance sensor for PAR, an upwelling radiance sensor (683 nm) for natural fluorescence, and a pulsed dissolved oxygen sensor.

An important attribute of the MVMS is that it concurrently measures bio-optical, chemical and physical parameters at sampling intervals of a few minutes for periods of up to 6 months. It thus expands the temporal sampling to capture processes such as internal gravity waves, diel cycling, episodic wind events and phy-

toplankton blooms, mesoscale eddies and associated primary production, and seasonal mixed layer and bloom evolutions. Samples were taken every few minutes with the central mooring's bio-optical, chemical, and physical instruments over an entire annual cycle (October 1994 through October 1995). The array of moorings was designed to quantify the spatial variability associated with the passage of mesoscale and other spatially varying features.

The physical mooring data show that the mixed layer deepens and shoals twice a year (Dickey et al., 1998a). The Northeast (NE) monsoon is characterized by steady northeasterly winds of moderate intensity (6 m/sec), surface cooling and convection, whereas the Southwest (SW) monsoon features strong, persistent southwesterly winds with greater intensity (up to 15 m/sec). The NE monsoon features deeper mixed layers

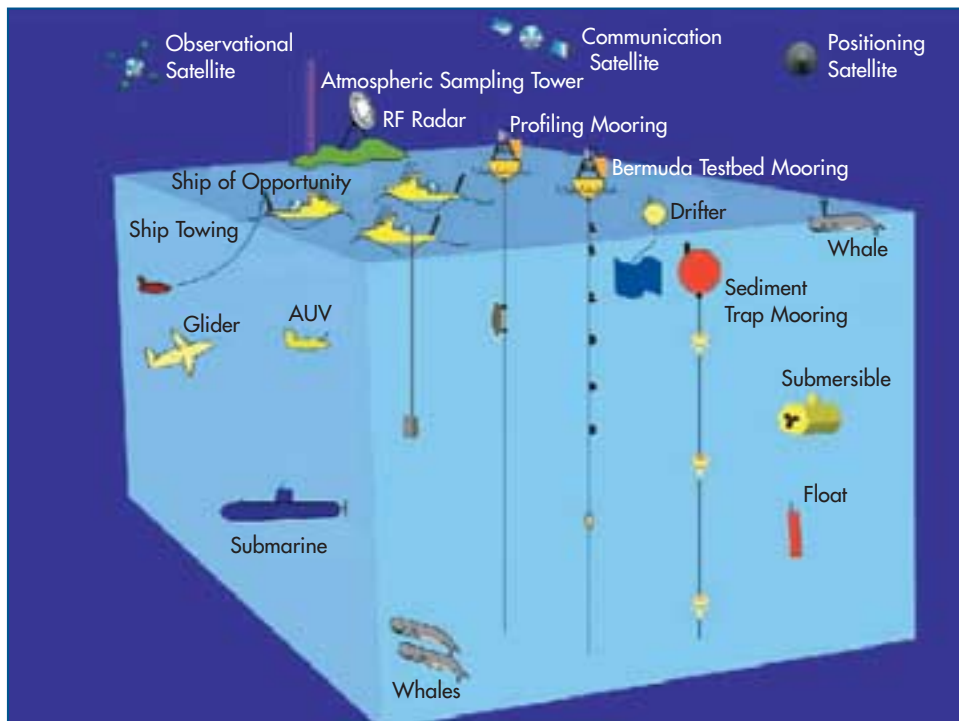


Figure 2. Ocean-observing platforms that can be used to obtain data describing physical and biogeochemical processes in the upper ocean. Many of these platforms have been used during the U.S. JGOFS time-series programs and mooring deployments near Bermuda and Hawaii.

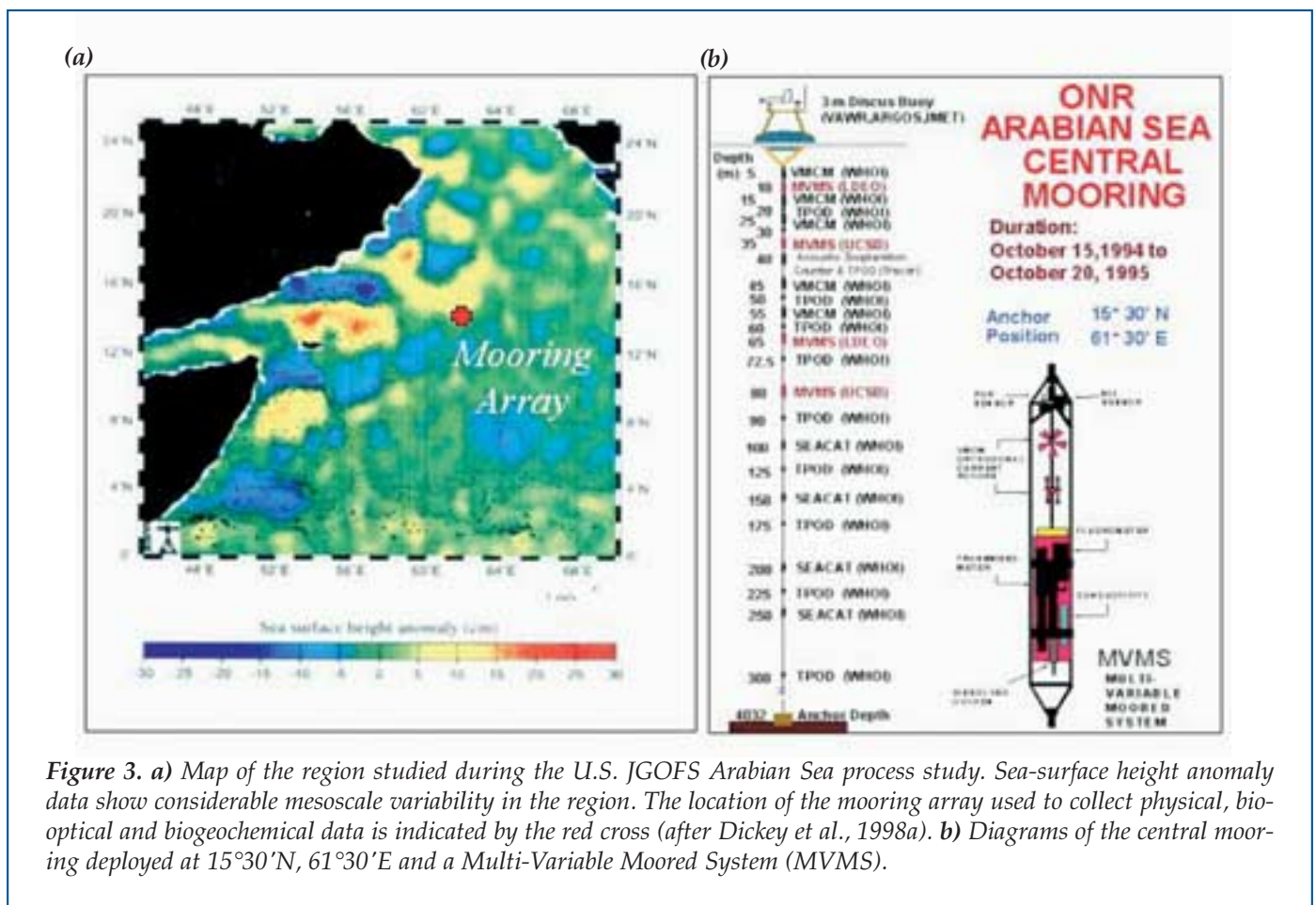


Figure 3. a) Map of the region studied during the U.S. JGOFS Arabian Sea process study. Sea-surface height anomaly data show considerable mesoscale variability in the region. The location of the mooring array used to collect physical, bio-optical and biogeochemical data is indicated by the red cross (after Dickey et al., 1998a). b) Diagrams of the central mooring deployed at 15°30'N, 61°30'E and a Multi-Variable Moored System (MVMS).

(110 m depth) than the SW monsoon (80 m depth) because of convective forcing. The MVMS data show that chlorophyll concentrations and primary production are correlated with the seasonal physical cycle associated with the NE and SW monsoons (Figure 4). A half-yearly cycle in chlorophyll *a* concentrations is an important feature with seasonal blooms that occur late in each monsoon season and into the respective intermonsoon periods. The data show that depth-integrated chlorophyll *a* generally tracks the 1% light level.

One of the more interesting results of the Arabian Sea study was the discovery that mesoscale eddies play such an important role in the evolution of chlorophyll *a* concentrations at the central mooring site (Figure 4). A sediment-trap mooring with serial samplers (see Berelson, this issue) at depths of 0.8, 2.2 and 3.5 km was located approximately 50 km north of the central mooring site by Sus Honjo (WHOI). The combined MVMS measurements of derived primary productivity and sediment trap samples indicate that the timing and amplitudes of phytoplankton blooms associated with seasonal stratification and eddies were strongly correlated (Honjo and Weller, 1997). This correlation suggests relatively rapid (days to weeks) export of organic carbon to the deep ocean. Complementary estimates of the shallow export flux of POC at 100 m were obtained in the Arabian Sea using the recently developed Thorium-234 method. The Thorium-234 data indicated that the single greatest feature of the annual cycle was a basin-wide POC export peak that occurred during the late SW monsoon (Buesseler et al., 1998).

Spatial data were derived from underway ship transects with SeaSoar (Figure 5), ADCP transects and satellite sea-surface temperature and altimetry sensors. SeaSoar, a towed undulating platform, was used by both British and U.S. oceanographers (Lee et al., 2000) in the Arabian Sea. In both cases, suites of physical, bio-optical, chemical and acoustical sensors were interfaced to SeaSoar platforms. The bio-optical and chemical sensors were similar to those deployed on the MVMS packages. In addition, acoustic backscatter data obtained from the ADCPs were utilized to estimate zooplankton biomass and their diel migrations. Multi-frequency acoustic sensors developed by Van Holliday were deployed aboard the SeaSoars to determine zooplankton distributions by size classes.

Spatial and temporal data obtained from these platforms indicate that the region is especially rich in mesoscale features whose origins are probably linked to westward-propagating Rossby waves and coastal filaments and jets that reach far offshore eastward from the Oman coast. Lee et al. (2000) carried out an objective analysis using SeaSoar chlorophyll transect data during the fall intermonsoon of 1995. This analysis emphasizes the power of virtually continuous transect data for resolving patchiness; it also warns of the errors (e.g., aliasing) likely to result from reliance on standard ship-based sampling on coarse grids (>100 km).

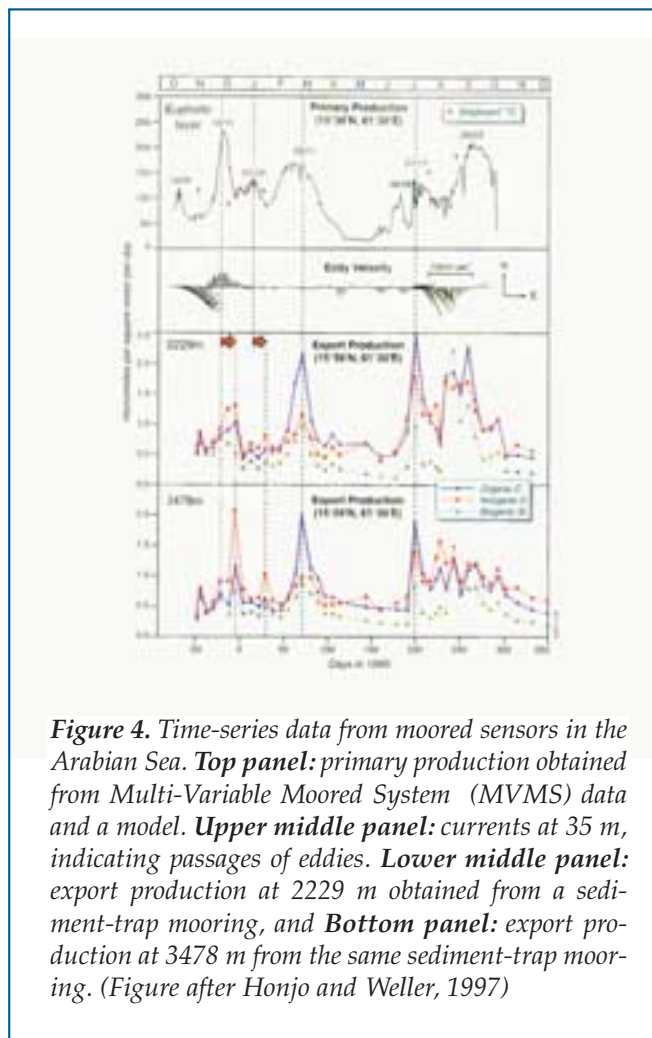


Figure 4. Time-series data from moored sensors in the Arabian Sea. **Top panel:** primary production obtained from Multi-Variable Moored System (MVMS) data and a model. **Upper middle panel:** currents at 35 m, indicating passages of eddies. **Lower middle panel:** export production at 2229 m obtained from a sediment-trap mooring, and **Bottom panel:** export production at 3478 m from the same sediment-trap mooring. (Figure after Honjo and Weller, 1997)

Previous papers describing high-frequency bio-optical data sets have made the same point in the temporal domain (e.g. Dickey, 1991).

Innovations of Two North Atlantic Experiments

The international JGOFS North Atlantic Bloom Experiment (NABE) was carried out in 1989 with a central objective of studying the spring phytoplankton bloom and its associated biogeochemical effects in the North Atlantic, one of the largest transient signals on earth (*Deep-Sea Research II*, 40[1–2], 1993). NABE observations were carried out at seven primary locations between about 18°N and 72°N, roughly along 20°W. A second experiment, The Marine Light in the Mixed Layer (MLML) study, was motivated by the desire to improve the understanding of upper ocean bio-optical variability and bioluminescence as affected by physical forcing at high latitudes (Dickey et al., 1994). MLML was conducted primarily at a site south of Iceland at 59°N, 21°W. Although MLML was not part of NABE, the field studies had several objectives in common and overlapped in time in the spring of 1989. One of the methodological innovations of the NABE and MLML studies was the use of diverse sampling platforms, including ships, aircraft equipped with Light Detection

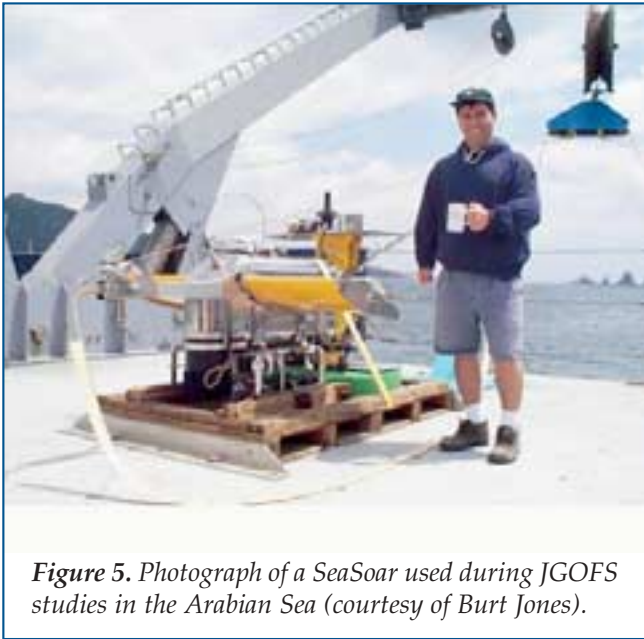


Figure 5. Photograph of a SeaSoar used during JGOFS studies in the Arabian Sea (courtesy of Burt Jones).

and Ranging (LIDAR), drifting sediment traps, a satellite with an altimeter and a multidisciplinary mooring similar to one described above. The collective data sets and models were used to characterize and analyze the temporal and spatial complexities of the spring bloom.

NABE data show that mesoscale eddies and mixed layer variability are important for phytoplankton blooms and ecosystem dynamics (see McGillicuddy, this issue; Dickey et al., 1994). Refinement of techniques for measuring CO_2 at sea, and seasonal and spatial changes in the partial pressure of CO_2 during NABE made it possible to demonstrate links between variability in CO_2 levels and the dynamics of the spring bloom in the North Atlantic (see Feely et al., this issue). Similar advances in seagoing instrumentation were made in the measurement of DOC (see Hansell and Carlson, this issue). In addition, microbial activities were found to be important during the blooms. Moorings at 34°N and 47°N (Sus Honjo) were used to deploy deep sediment traps that captured variability in particle fluxes at various depths.

The MLML field program, carried out from April to June, 1989, and from May to September, 1991, utilized MVMS packages on moorings to obtain high-resolution data over time at eight depths (Dickey et al., 1994). Although the high-latitude location with its high winds and large waves presented a major technological challenge for moored observations, excellent bio-optical and physical time-series data were obtained. The abrupt onset of spring stratification with shoaling of the mixed layer was dramatic (from 550 m to 50 m within 5 days), illustrating the importance of high temporal resolution sampling with moorings. The moored instruments also captured the onset of a phytoplankton bloom, apparently associated with modest near-surface stratification, prior to the major springtime shoaling of the mixed layer and the seasonal spring bloom. An increase in near-surface temperature of

0.2°C accompanied the phytoplankton increase, a change suggested by model studies but previously unobserved because of sampling limitations.

In the MLML field program, the mooring observations were complemented by shipboard profiles and ship tow-yo sections, LIDAR measurements from P-3 aircraft and satellite sea-surface temperature data (Dickey et al., 1994). These data provided context for the mooring data as well as information on horizontal features and scales of variability. For example, the LIDAR data showed that there were patches of high concentrations of chlorophyll a with horizontal scales on the order of 30 km. The NABE and MLML programs represent an early attempt to develop observational strategies for fully three-dimensional, interdisciplinary time-series programs, one of the themes of this review.

The Equatorial Pacific

The JGOFS equatorial Pacific process study took place in 1992, and related studies preceded and followed the main field program (Deep-Sea Research II, 1995: 42[2-3], 1996: 43[4-6], 1997: 44[9-10]). Field experiments were conducted in the central and eastern Pacific from 95°W to 170°W between 10°N and 10°S . The equatorial Pacific is affected by a great variety of physical and climatological processes, including El Niño-Southern Oscillation (ENSO) cycles. It also plays an important role in the global carbon cycle. Estimates suggest that the region supplies roughly one gigaton of carbon (as CO_2) to the atmosphere each year, primarily due to the upwelling of carbon-rich deep water along the equator. The equatorial Pacific is also a High Nutrient-Low Chlorophyll (HNLC) region; its productivity and carbon fluxes are small relative to the supply of nutrients.

The physical dynamics of the equatorial Pacific have become increasingly well understood over the past two decades, largely due to measurements made by the Tropical Atmosphere Ocean (TAO) mooring array. However, understanding of biological and optical variability has been limited because few dedicated ship-based experiments could be performed in such a remote region. In particular, typically only a few biological observations of chlorophyll and primary productivity were made each year prior to JGOFS; hence, these were our only basis for annual estimates of chlorophyll and primary production for the expansive Pacific equatorial waveguide. With this motivation, MVMS packages were installed on the TAO physical mooring at 0° , 140°W for an 18-month period during 1992 and 1993 (Foley et al., 1997). The timing of our sampling period was most opportune as the observations spanned both El Niño and “normal” phases of the ENSO cycle. During the El Niño phase, the mixed layer, the thermocline and a very weak Equatorial Undercurrent (EUC) were deep, at times in excess of 150 m. Kelvin waves with a roughly 60-day period propagated eastward past the site, accompanied by depressions of the thermocline. Time-series measure-

ments of key physical and bio-optical parameters obtained from instruments deployed on the mooring (0° , 140°W) are shown in Figure 6. Light levels were high, but nutrients, including iron, were only elevated in deep waters. As a result, chlorophyll *a* concentrations in the upper layer were low (less than 0.2 mg m^{-3}).

As “normal” conditions returned to the region, Kelvin waves ceased. The thermocline and a strong EUC shoaled, allowing transport of nutrients into the euphotic zone. Westward propagating Tropical Instability Waves (TIW) with periods of roughly 20 days also contributed to large vertical upwelling cycles. TIWs are easily seen in the meridional current records, and appear to be manifest in the time-series data with chlorophyll *a* values double and at times triple those observed during the El Niño period (Figure 6). Importantly, strong, though highly complex, coupling is evident between the physical processes (El Niño, Kelvin waves and TIWs) and the phytoplankton biomass and primary productivity (here roughly proportional to chlorophyll *a*) of the equatorial Pacific.

Passages of TIWs may be envisioned as natural iron enrichment experiments.

Newly developed bio-optical drifters released at the equatorial mooring site provided spatial data as they drifted poleward, enabling estimates of net phytoplankton growth rates. Ship measurements benefited from improved measurement systems for pCO_2 as well as from underway shipboard ADCP data sets. Estimates of export flux of POC were based on the thorium-234 method described earlier. Results of the thorium-234 study indicate considerable spatial and temporal variability in export of organic carbon, which was highest at the equator. They also show that a relatively low percentage of total production ($<5\text{--}10\%$) is exported via sinking particles. The combination of the instrumented TAO mooring array with JGOFS shipboard sampling and sediment traps provided a relatively comprehensive, though coarse, three-dimensional biogeochemical time-series data set for the region.

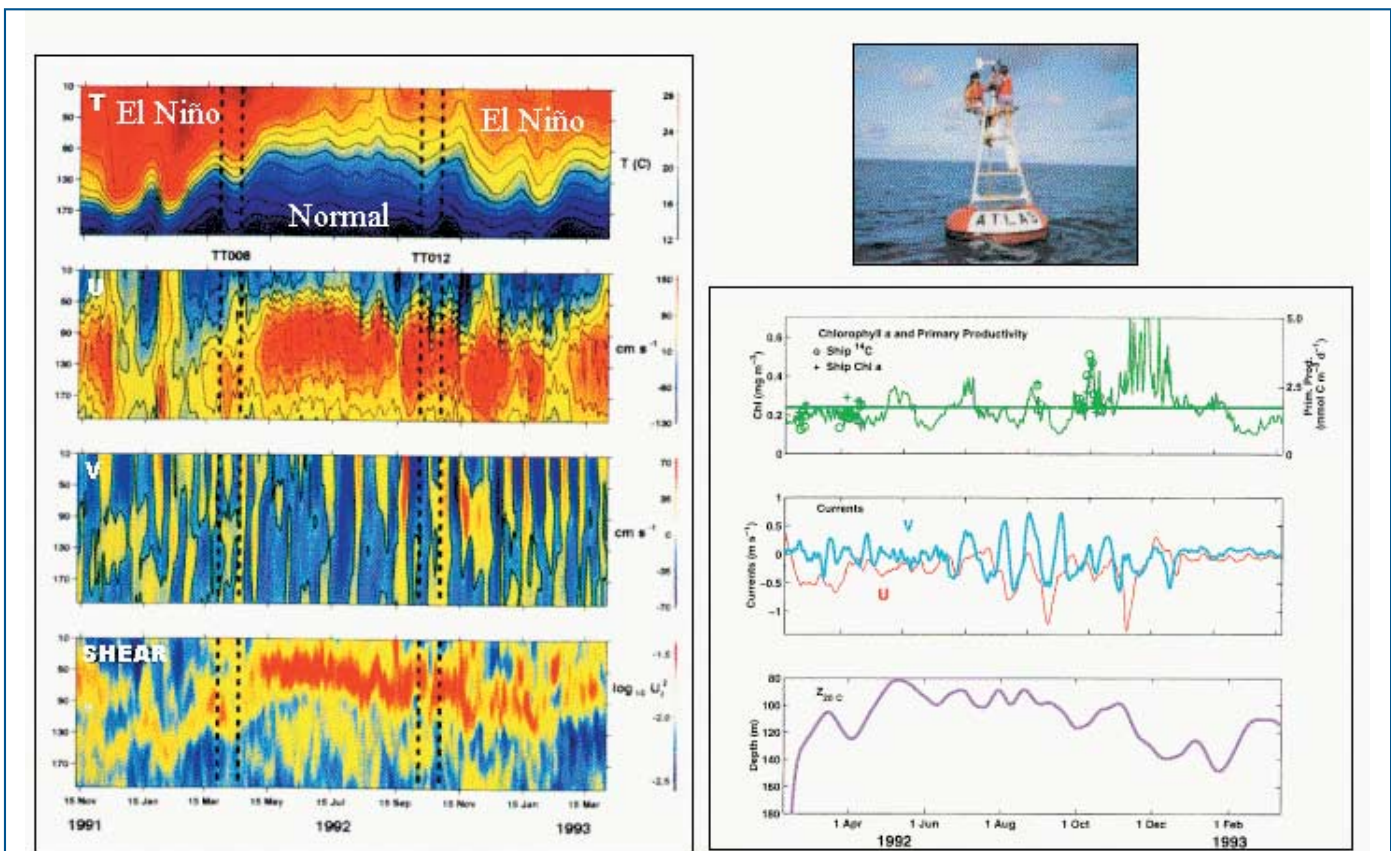


Figure 6. Data collected during the U.S. JGOFS Equatorial Pacific Process Study from a mooring at 0° , 140°W (Foley et al., 1997). **Left, top to bottom:** Time versus depth contour plots of temperature, zonal currents, meridional currents and current shear. Black vertical dashed lines indicate periods of concurrent shipboard sampling at the site. **Right, top to bottom:** ATLAS mooring, chlorophyll *a* and derived primary productivity at 10 m, zonal (red) and meridional (blue) currents at 10 m, and depth of the 20°C isotherm, which deepens during El Niño periods.

The Southern Ocean

The Southern Ocean is generally thought to be one of the most important and sensitive oceanic regions in regard to the carbon budget and climate in general. The Southern Ocean was targeted for study by the JGOFS program because it is likely an ocean of globally significant carbon fluxes, yet it remains a region about which the factors regulating carbon fluxes are less well known (data sparse) than is the case for more readily accessible oceans. Major questions concerning the biogeochemistry of the Southern Ocean remain unanswered: 1) Does the Southern Ocean act as a net source or sink for atmospheric CO₂, 2) What is (are) the limiting factor(s) for primary productivity (note that the Southern Ocean is a high nutrient-low chlorophyll (HNLC) region), and 3) How does biological variability affect the upper ocean's heat budget?

The JGOFS Southern Ocean field studies used many of the sampling platforms and instruments described above; thus only a couple of new sampling methodologies are noted here. The long-awaited Sea Viewing Wide Field-of-View (SeaWiFS) ocean-color instrument, launched in August 1997, provided large-scale information on surface pigments for JGOFS Southern Ocean cruises (see Yoder et al., this issue). Recognizing the importance of capturing migrating frontal features and mesoscale variability, Mark Abbott and his colleagues (2000) deployed an array of 12 moorings, spaced 30 km apart, and equipped with physical and bio-optical sensors in the Antarctic Polar Frontal Zone (APFZ) from November 1997 to March 1998. These moorings differed from others described above in that they were subsurface, relatively lightweight, carried fewer sensors and were relatively easy to deploy and recover under adverse conditions. The mooring array captured a strong spring bloom beginning in December 1997.

The mooring data, together with data sets collected aboard ships, suggest that light levels limit phytoplankton populations initially because of deep mixing. Then silicate concentrations or zooplankton grazing become limiting factors, followed finally by iron limitation. The spring bloom at the polar front in 1997–98 lasted only a few weeks, which supports the argument for the fast sampling rates possible with autonomous moored instruments. The mooring array proved important in a region where both temporal and spatial scales are small.

Bermuda Testbed Mooring and HALE-ALOHA Mooring Programs

The JGOFS Bermuda Atlantic Time-series Study (BATS) and the Hawaii Ocean Time-series (HOT) study, both launched in 1988, have been used to observe, quantify and model temporal changes in the biogeochemical and ecological properties of the subtropical oligotrophic gyres of the North Atlantic and the North Pacific (see Karl et al., this issue; *Deep Sea Research II*, 1996: 43[2–3]; 2001: 48[8–9]). Both of these

programs have relied primarily on shipboard sampling at two- to four-week or longer intervals. But this mode of observation cannot capture important phenomena with time scales from minutes to a month. For this reason, investigators established high-frequency, long-term, autonomous moored sampling programs at both sites. The first was the Bermuda Testbed Mooring (BTM); Tommy Dickey and Dan Frye (WHOI), shown in Figure 7, launched in 1994 at the BATS site (Dickey et al., 1998b; Dickey et al., 2001). A similar mooring, HALE-ALOHA, was established in 1996 at the HOT site (Letelier et al., 2000) by David Karl (University of Hawaii) and colleagues.

These two mooring efforts have clearly demonstrated the importance of events and processes that cannot be captured or resolved by bi-weekly or less frequent shipboard sampling. These events and processes include mesoscale eddies, storms, hurricanes, dust deposition events, rapid shoaling of the mixed layer and transient phytoplankton blooms, inertial oscillations, diel and shorter-term variability in phytoplankton and bio-optical properties, and internal gravity waves. Data from both the BTM and the HALE-ALOHA mooring have documented passages of mesoscale features with high nutrient and phytoplankton concentrations. The BTM time-series data shown in Figure 8 highlight both the passage of a major eddy and its effects on nutrients and phytoplankton biomass in July 1995 and the upper-ocean response to Hurricane Felix, which passed over the BTM in August 1995.

The original aim of the BTM program was to create an opportunity for long-term testing of multidisciplinary autonomous sensors and systems. The BATS site was chosen because of the regular BATS shipboard sampling program and the long-term sediment trap data collected nearby by Werner Deuser and Maureen Conte (WHOI) since 1978. The BTM is used to collect meteorological, physical and bio-optical data every few minutes, including temperature, conductivity, currents, PAR and chlorophyll fluorescence. A complementary project, Ocean-Systems for Chemical, Optical and Physical Experiments (O-SCOPE), has used the BTM to test several proto-type chemical and optical sensors.

Among the systems being tested, as part of the BTM program are newly developed moored bio-optical sensors that include several spectral absorption and attenuation meters (9 to 100 wavelengths over the visible spectrum) for measuring inherent optical properties. Also being tested are spectral irradiance and radiance radiometers (Figure 9a) for measuring apparent optical properties at several wavelengths matched to those sampled by the SeaWiFS ocean color instrument.

Derived data resulting from the BTM program include chlorophyll a concentrations, spectral radiance and irradiance ratios, spectral diffuse attenuation coefficients and spectral water-leaving radiance. The latter data have been used for validation and algorithm development for the SeaWiFS instrument. The BTM data are virtually continuous and provide a large num-

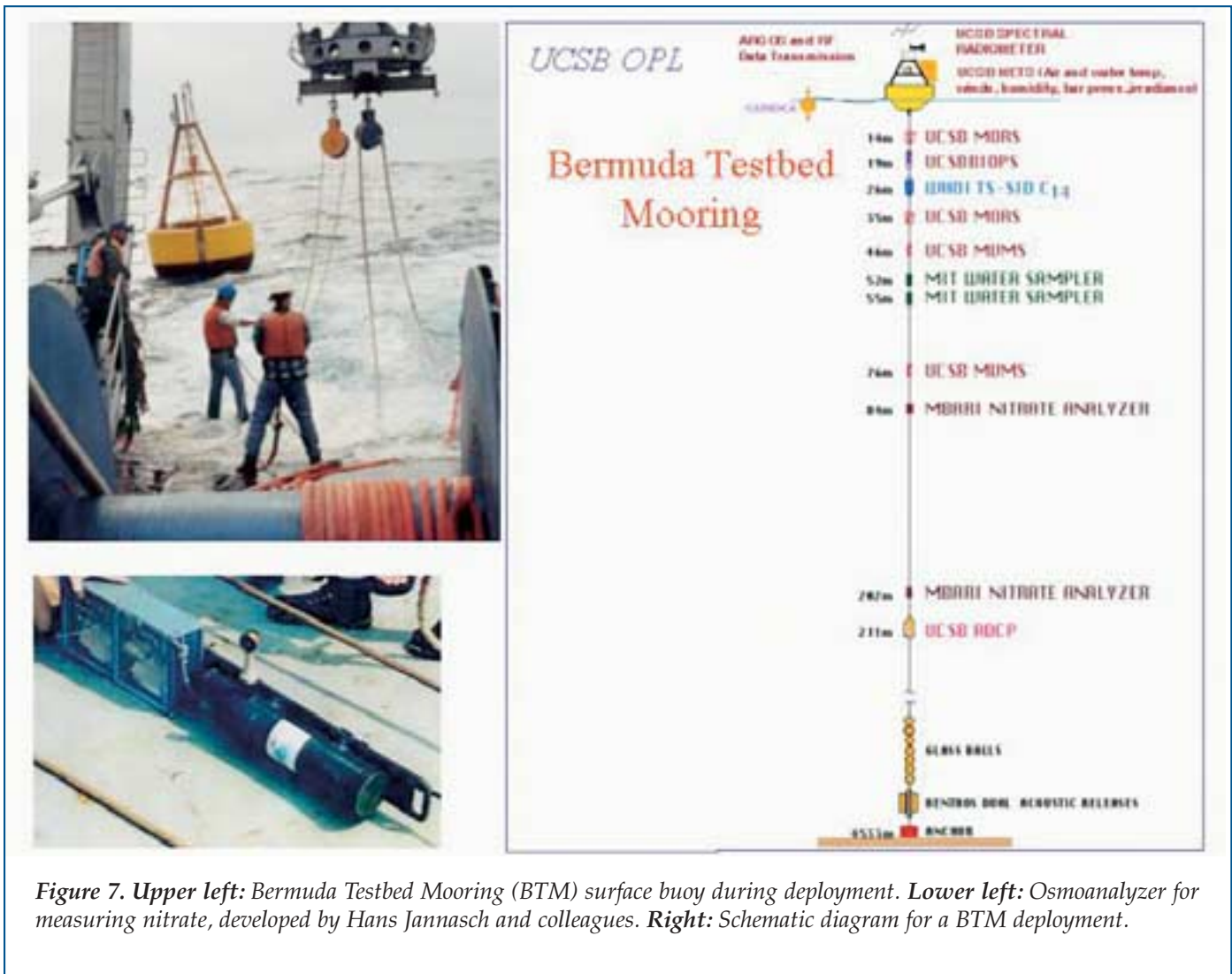


Figure 7. Upper left: Bermuda Testbed Mooring (BTM) surface buoy during deployment. Lower left: Osmoanalyzer for measuring nitrate, developed by Hans Jannasch and colleagues. Right: Schematic diagram for a BTM deployment.

ber of match-ups. The radiometric data are especially important because satellite-based measurements of ocean color are limited to the uppermost ocean layer (roughly one optical depth), and viewing is limited by cloud cover. In addition, data have been collected by other new optical systems tested at the BTM; these systems include a spectral volume scattering function instrument and a spectral fluorometer (6 excitation and 16 emission wavelengths).

One of the major limitations for moored optical systems has been biofouling. Recently copper shutter systems and tubing for pumped systems have been engineered and tested. Results indicate that the duration of deployments can be extended to at least six months (as opposed to three to four months) in oligotrophic waters.

Several new chemical systems and sensors have been deployed on the BTM (Dickey et al., 1998b; Dickey et al., 2001). An *in situ* autonomous sampling colorimetric system, Osmoanalyzer (Figure 7; Hans Jannasch, MBARI), has collected time-series data on nitrate and nitrite concentrations with a 10- or 15-minute sampling interval. The Osmoanalyzer utilizes

osmotic pumps that propel both sample and reagent fluids through a miniature flow-injection manifold. Our understanding of the biogeochemistry of eddies, particularly nitrate injection and subsequent phytoplankton growth, has been improved by data from the Osmoanalyzer as well as the bio-optical and physical data collected with instruments on the BTM (Figure 8).

Four different groups have tested autonomous $p\text{CO}_2$ sampling systems at the BTM (Tokar and Dickey, 2000; Varney, 2000). One of these (called CARIOCA; Liliane Merlirat, University of Paris), which involves a separate buoy tethered to the BTM, has shown variability in $p\text{CO}_2$ on diel and synoptic time scales. A system for measuring the difference between atmospheric and surface-water $p\text{CO}_2$ levels (Gernot Friederich) was tested during a BTM deployment in the summer and fall of 2000. Resulting time-series data suggest that the usual summertime supersaturation of surface-water CO_2 was interrupted during most of July when $p\text{CO}_2$ values returned to near atmospheric levels. During autumn, temperature and $p\text{CO}_2$ decreased in concert. Dissolved oxygen sensors have also been tested.

Investigators have deployed a new Moored *In situ*

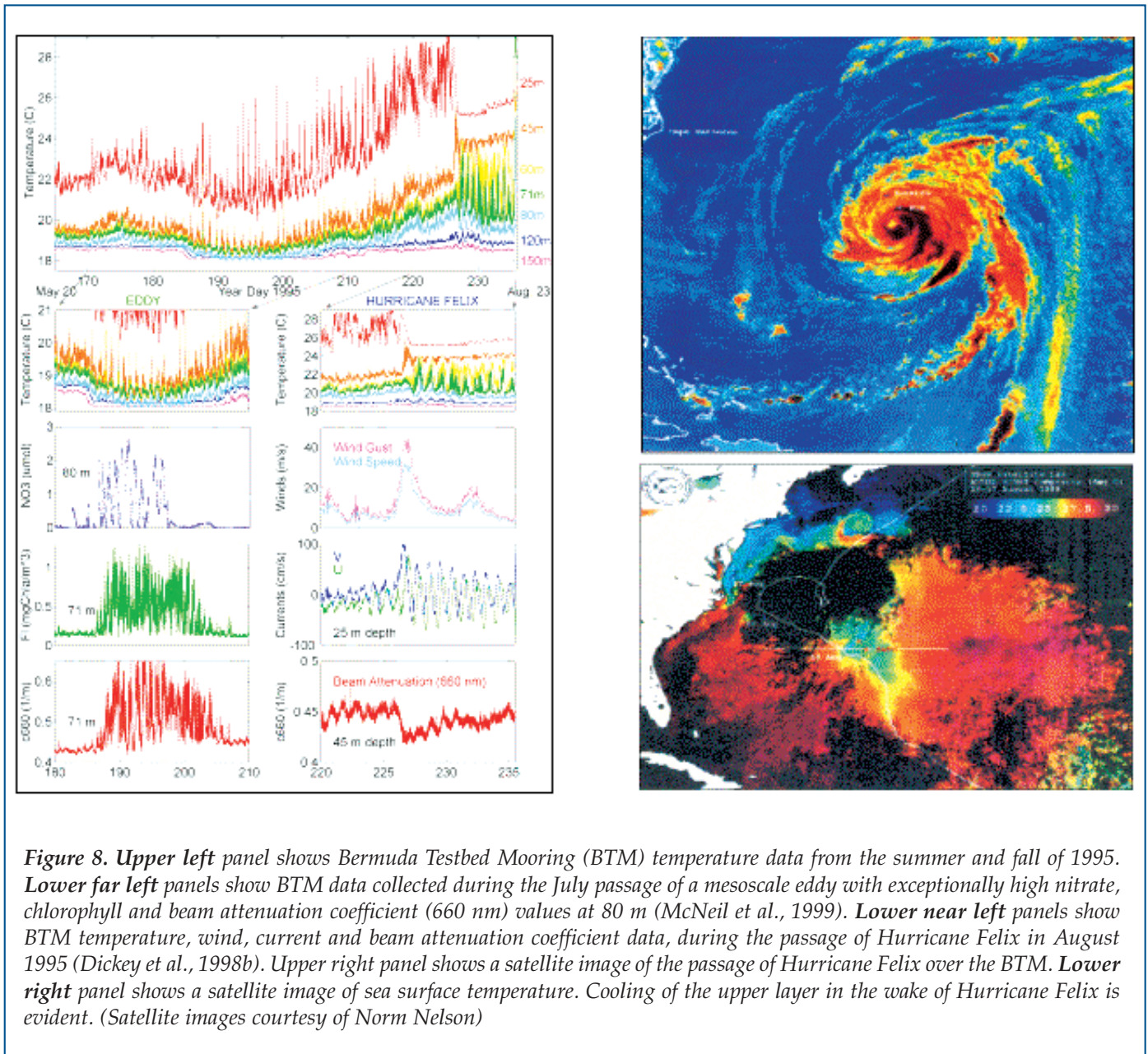


Figure 8. Upper left panel shows Bermuda Testbed Mooring (BTM) temperature data from the summer and fall of 1995. Lower far left panels show BTM data collected during the July passage of a mesoscale eddy with exceptionally high nitrate, chlorophyll and beam attenuation coefficient (660 nm) values at 80 m (McNeil et al., 1999). Lower near left panels show BTM temperature, wind, current and beam attenuation coefficient data, during the passage of Hurricane Felix in August 1995 (Dickey et al., 1998b). Upper right panel shows a satellite image of the passage of Hurricane Felix over the BTM. Lower right panel shows a satellite image of sea surface temperature. Cooling of the upper layer in the wake of Hurricane Felix is evident. (Satellite images courtesy of Norm Nelson)

Trace Element Serial Sampler (MITESS), developed by Edward Boyle (MIT), on both the BTM and HALE-ALOHA moorings. The purpose of the MITESS (Figure 9b) is to track the temporal variability of trace metals in the upper ocean. The system consists of 12 independent sampling modules, made of ultra-high molecular weight polyethylene, mounted on a durable mooring unit. Two MITESS units have been deployed simultaneously from the BTM to increase sampling frequency. Samples are preserved and returned to the laboratory at MIT for analyses. Results from the MITESS and previous sampling at the BTM site indicate that lead concentrations off Bermuda have decreased substantially since restrictions on leaded gasoline were enacted in the United States. Also, MITESS data from both BTM and HALE-ALOHA moorings have shown considerable variability in iron concentrations, apparently relat-

ed to the passage of eddies, transient wind forcing and bloom events (Edward Boyle, pers. comm).

Another instrument deployed from the BTM is the Time-Series Sampler Incubation Device or TS-SID (Figure 9c) that was developed to measure primary production using autonomous carbon-14 (¹⁴C) observations. Simultaneous TS-SID ¹⁴C productivity and bio-optical data have been collected from the BTM and are being used to investigate variability in photosynthetic parameters (a^* and Φ in equation 1) in ongoing work by Craig Taylor (WHOI) and Tommy Dickey. The data sets collected by the BTM and ALOHA-HOST programs have led to exciting discoveries and are being used for several modeling studies.

Data Telemetry

The telemetry of data in near real-time has become



Figure 9. *a*) Photograph of an instrument package before deployment from the Bermuda Testbed Mooring (BTM) with spectral irradiance and radiance, Photosynthetically Available Radiation (PAR), dissolved oxygen and temperature sensors. *b*) Deployment of the Moored In situ Trace Element Serial Sampler (MITESS), a trace metal sampler on BTM (courtesy of Edward Boyle). *c*) Time-series sampler incubation device, developed by Craig Taylor and Kenneth Doherty.



increasingly desirable for many purposes, including data assimilation models for predictions, establishing ground truth for ocean-color sensors aboard satellites, directing observations at sea and warnings to the public of hazardous conditions. Use of fiber-optic and electrical cable data transmission methods is practical for coastal locations, sites near seafloor communication cable junctions or special study areas.

Participants in the BTM project (including Dan Frye, WHOI, and Tommy Dickey) have tested a variety of telemetry systems (Dickey et al., 1998b), including *in situ* systems using acoustic modems and inductive electrical coupling via toroidal pick-ups on the mooring line for transmitting data from subsurface instruments to the BTM surface buoy. Data have been stored in a data-logging system on the buoy for subsequent transmission, either to R/V Weatherbird II for later transmission to land stations, or via satellite (Argos Data Collection System) links to these stations. One of the interesting features of the new system is its two-way communication capability; commands can be sent to the *in situ* instruments. For instance, this system was used at the BTM site as a signal from Monterey, California, was sent to the BTM in order to change an Osmoanalyzer setting.

Two-way communications systems can also be used to change sampling frequencies so that more samples can be taken during passages of eddies or hurricanes. Presently, bandwidth is limited, so that only small subsets of data can be transmitted. This problem should be solved in the next few years, possibly with a constellation of low earth-orbiting communications satellites. Many autonomous ocean sampling platforms are facing the same problem. Scientists from a variety of disciplines want access to data in near real-time from moorings, profiling floats, gliders, AUVs and other ocean platforms.

In addition, the BTM/BATS site was used for testing the Southampton Oceanographic Centre's AUV, Autosub, which included bio-optical sensors (Griffiths et al., 2000), and evaluation of a new neutrally-buoyant sediment trap designed to reduce the effects of hydrodynamic flow interference (Valdes et al., 1997). We anticipate that the BTM and the Hawaii mooring programs will be used in the future for similar studies requiring *in situ* validation of data from sensors deployed on profiling floats, AUVs and gliders.

Future Technologies

Considerable progress has been made in answering the complex questions posed at the beginning of JGOFS, thanks in large part to new instruments and methods of observation. Yet much remains to be learned and explained. The direction of future technologies and observations will be driven by many new questions stimulated by JGOFS studies. Further research is needed to expand scientific knowledge about factors that control primary productivity and nutrient cycles, the efficiency of the biological pump

for different foodwebs, and the roles of physical processes that affect biogeochemical processes. A good starting point for looking toward the future is to reconsider time-space diagrams for processes and platforms (Figures 1a and b). In the next sections, we consider the platforms and then sensors and systems.

Platforms

An important, though ambitious, goal is to develop integrated ocean sampling systems that can collect multidisciplinary time-series data in all three spatial dimensions for the global ocean. The collective platforms illustrated in Figure 2 can, in principal, support observations over a fair portion of the time and space domains illustrated in Figure 1. We have seen an explosive growth in the development and capabilities of autonomous sampling platforms in recent years, including profiling drifters, floats, moorings, AUVs, and gliders. The ARGO program plans to launch 3,000 profiling floats to collect profiles of temperature and salinity as well as Lagrangian current information throughout the global ocean. Plans for time-series moorings, at carefully selected sites, are also underway. Gliders and AUVs are likely to play increasing roles as well. Satellites will provide higher spatial resolution data for more variables including ocean properties like salinity and specific groups of phytoplankton.

The increasing number of ocean platforms is providing oceanographers with unprecedented sampling opportunities. Nonetheless, we cannot yet achieve a continuous spectrum of sampling in time and space, and synoptic observations will remain a problem. The way forward will likely entail the use of diagnostic inverse models and numerical data assimilation models that can be used as "data interpolators" and for ocean predictions. Telemetry of data will be critical, and sophisticated networking of observational systems will be required to optimize sampling.

Sensors and Systems


Because of increased demand for interdisciplinary data, new efforts have begun to capitalize on available platforms for multidisciplinary measurements. Moorings have been especially attractive because of their carrying capacity and the relative ease of getting access to and interpreting data. A number of large instruments with substantial power demands have been adapted for mooring deployment; many were originally developed for laboratory use or vertical profiling from ships. However, many of the present instruments cannot be accommodated on drifters, profiling floats, AUVs or gliders. New questions stimulated by JGOFS and other biogeochemical programs require measurements of even more variables, including those needed for identification of bacteria, phytoplankton and zooplankton, nutrients such as phosphate, silicate and iron, and additional chemical properties such as CO₂, pH and alkalinity.

It is essential that we develop a new class of sensors

and systems. These must be small, inexpensive and have low power requirements. Exciting work is underway to meet these needs. Devices such as in situ flow cytometers, mass spectrometers and DNA analyzers are being developed for deployment on moorings and AUVs. Sensors that use fiber optics are also being developed for several ocean chemical measurements. And “chip-based,” MicroElectroMechanical System (MEMS) and “nano” technologies still await application to oceanographic questions (Tokar and Dickey, 2000). Moored water samplers, such as MITESS, that are capable of preserving samples for long periods of time, will also be needed to provide samples for analyses that cannot be conducted *in situ*.

Summary

The original U.S. JGOFS Long Range Plan envisioned the use of moorings as platforms for autonomous sampling of bio-optical and biogeochemical parameters at the time-series stations and during the process studies. These moorings would be continued as long-term sampling components. At present, JGOFS autonomous moorings measurements are only being made by the BTM program at the BATS site, largely because of previous technological and budgetary limitations. It is imperative that resources for developing and implementing global biogeochemical sampling networks come from a variety of sources or organizations, international as well as domestic. Several of the new sensors, systems, and platforms described earlier are under development or in the hands of just a few researchers. These technologies need to be produced on a commercial scale. Interpretation of many of the signals of these new instruments remains an issue; intensive validation and inter-calibration efforts by scientists are needed.

One interesting benefit of advanced technologies may well be the development of simpler interdisciplinary sampling systems, such as chip-based sensors or nanosensors with automated data processing and telemetry components. These exciting new technologies could greatly benefit all oceanographic programs regardless of their present technical capabilities. Despite the numerous challenges we face, the oceanographic community has never been in a stronger position to make major advances in understanding ocean biogeochemistry. 

Acknowledgements

The present work has benefited greatly from interactions with numerous U.S. and international collaborators and colleagues. My research has been supported by the National Science Foundation, the U.S. Office of Naval Research, the National Aeronautics and Space Administration, the National Oceanic and Atmospheric Administration, the Minerals Management Service and the University of California, Santa Barbara. This is U.S. JGOFS Contribution Number 680.

References

- Abbott, M.R., J.G. Richman, R.M. Letelier and J.S. Bartlett, 2000: The spring bloom in the Antarctic Polar Frontal Zone as observed from a mesoscale array of bio-optical sensors. *Deep-Sea Res. II*, 47[15–16], 3285–3314.
- Behrenfeld, M. and P.G. Falkowski, 1997: A consumer’s guide to phytoplankton primary productivity models. *Limnol. Oceanogr.*, 42[1], 1–20.
- Buesseler, K., L. Ball, J. Andrews, C. Benitez-Nelson, R. Belostock, F. Chai and Y. Chao, 1998: Upper ocean export of particulate organic carbon in the Arabian Sea derived from thorium-234. *Deep-Sea Res. II*, 45[10–11], 2461–2488.
- Dickey, T., 1991: The emergence of concurrent high-resolution physical and bio-optical measurements in the upper ocean and their applications. *Rev. of Geophys.*, 29[3], 383–413.
- Dickey, T., J. Marra, M. Stramska, C. Langdon, T. Granata, R. Weller, A. Plueddemann and J. Yoder, 1994: Bio-optical and physical variability in the sub-arctic North Atlantic Ocean during the spring of 1989. *J. Geophys. Res.*, 99[22], 541–551.
- Dickey, T., J. Marra, R. Weller, D. Sigurdson, C. Langdon and C. Kinkade, 1998a: Time-series of bio-optical and physical properties in the Arabian Sea: October 1994–October 1995. *Deep-Sea Res. II*, 45[10–11], 2001–2025.
- Dickey, T., D. Frye, H. Jannasch, E. Boyle, D. Manov, D. Sigurdson, J.D. McNeil, M. Stramska, A. Michaels, N. Nelson, D.A. Siegel, G. Chang, J. Wu and A. Knap, 1998b: Initial results from the Bermuda Testbed Mooring Program. *Deep-Sea Res. I*, 45, 771–794.
- Dickey, T., D. Frye, J. McNeil, D. Manov, N. Nelson, D. Sigurdson, H. Jannasch, D. Siegel, A. Michaels and R. Johnson, 1998c: Upper-ocean temperature response to Hurricane Felix as measured by the Bermuda Testbed Mooring. *Mon. Wea. Rev.*, 126, 1195–1201.
- Dickey, T., S. Zedler, D. Frye, H. Jannasch, D. Manov, D. Sigurdson, J.D. McNeil, L. Dobeck, X. Yu, T. Gilboy, C. Bravo, S.C. Doney, D.A. Siegel and N. Nelson, 2001: Physical and biogeochemical variability from hours to years at the Bermuda Testbed Mooring site: June 1994–March 1998. *Deep-Sea Res. II*, 48[8,9], 2105–2131.
- Foley, D.G., T.D. Dickey, M.J. McPhaden, R.R. Bidigare, M.R. Lewis, R.T. Barber, S.T. Lindley, C. Garside, D.V. Manov and J.D. McNeil, 1997: Longwaves and primary productivity variations in the equatorial Pacific at 0°, 140°W. *Deep-Sea Res. II*, 44[9–10], 1801–1826.
- Griffiths, G., A. Knap and T. Dickey, 2000: Autosub experiment near Bermuda. *Sea Tech.*, 41[2], 35–46.
- Honjo, S. and R. Weller, 1997: Monsoon winds and carbon cycles in the Arabian Sea. *Oceanus*, 40[2], 24–28.
- Lee, C.M., B.H. Jones, K.H. Brink and A.S. Fischer, 2000: The upper-ocean response to monsoonal forcing in the Arabian Sea: Seasonal and spatial variability. *Deep-Sea Res. II*, 47[7–8], 1177–1226.
- Letelier, R.M., D.M. Karl, M.R. Abbott, P. Flament, M. Freilich, R. Lukas and T. Strub, 2000: Role of late winter mesoscale events in the biogeochemical variability of the upper water column of the North Pacific Subtropical Gyre. *J. Geophys. Res.*, 105[28], 723–739.
- McNeil, J.D., H.W. Jannasch, T. Dickey, D. McGillicuddy, M. Brzezinski and C.M. Sakamoto, 1999: Upper ocean response to the passage of a mesoscale eddy off Bermuda. *J. Geophys. Res.*, 104[15], 537–548.
- Tokar, J.M. and T. Dickey, 2000: Chemical sensor technology: current and future applications. In: *Chemical Sensors in Oceanography*, M.S. Varney, ed., Gordon and Breach Science Publishers, Amsterdam, 303–329.
- Valdes, J.R., K.O. Buesseler, and J.F. Price, 1997: A new way of catching the rain. *Oceanus*, 40[2], 33–35.
- Varney, M.S., ed., 2000: *Chemical Sensors in Oceanography*. Gordon and Breach Science Publishers, Amsterdam, 333 pp.

Challenges and Opportunities for Interdisciplinary Oceanography

Mark R. Abbott

Oregon State University • Corvallis, Oregon USA

U.S. JGOFS has greatly improved our understanding of geochemical fluxes in the ocean and their interaction with biological processes. Moreover, it has nurtured a community of researchers who cross traditional disciplinary boundaries to study the ocean in an integrated manner. The scientific achievements of U.S. JGOFS, documented in this issue of *Oceanography*, are paralleled by achievements in the way oceanographers work together on global-scale questions.

As new programs begin to emerge, it is worthwhile to consider some of the scientific activities necessary for a successful global ocean biogeochemistry program.

- ♦ Modeling is critically important, both to identify critical processes and regions of the ocean and to plan sampling strategies. It must be supported from the beginning of the program and have strong links to the field studies.
- ♦ Long time-series studies with high-quality ocean measurements are essential, given the time scales of ocean variability. Such programs must have strong and continuing scientific collaborations and oversight.
- ♦ International efforts to identify and develop standard reference materials and methods, such as those developed for measuring carbon dioxide in the ocean, are necessary for long-term, global studies.

There are also attributes of program management that are essential to success.

- ♦ It is important to develop a long-term strategy while retaining flexibility to pursue new issues and opportunities as our scientific understanding evolves. Such long-term planning and guidance for projects and expeditions should come from a scientific steering committee.
- ♦ Open data policies encourage collaboration. They are essential for an integrated research program.
- ♦ International partnerships and coordination must be developed for any global-scale program.
- ♦ Interdisciplinary ocean biogeochemistry studies require strong cross-program support within NSF as well as strong multi-agency partnerships.
- ♦ Synthesis of the results from the field programs, modeling projects and remote-sensing observations is essential if we are to obtain the maximum amount of scientific insight. Such synthesis efforts should also take place during the implementation phase of any future ocean biogeochemistry program.

This list is clearly not complete, but the overarching theme is the need to encourage and coordinate interactions among scientists, funding agencies and programs. The questions that we are asking today about the ocean's role in global systems and the predictions that we are striving to make about oceanic responses to environmental change require us to work together. 